Instituto de Bioingeniería
Universidad Miguel Hernández

UNIVERSITAS Miguel Hernández

BRAIN CARBOXYLESTERASES INTERACTING WITH ORGANOPHOSPHORUS COMPOUNDS

Kinetic characterization and approaches to purification and molecular identification

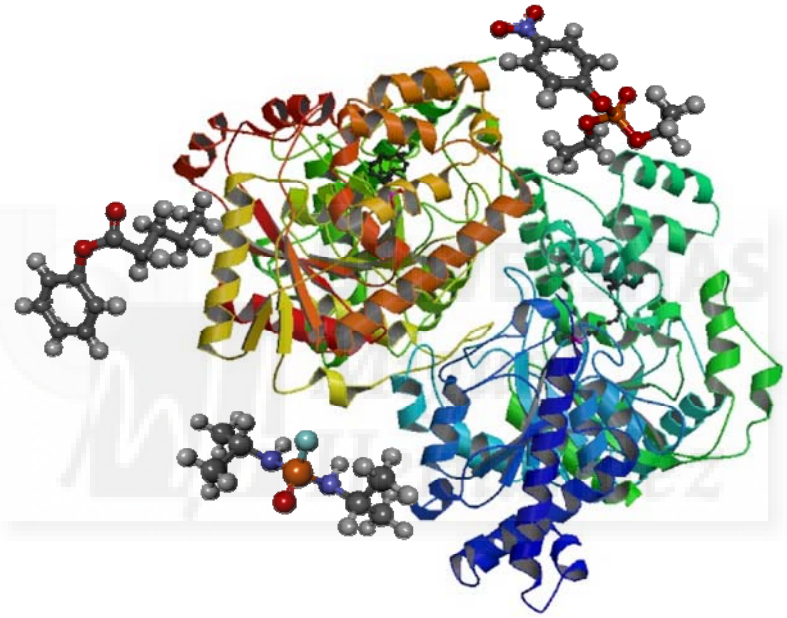

Iris Mangas Nadal

Dirigido por:
Jorge Estévez Domènech
Eugenio Vilanova Gisbert

UNIVERSIDAD MIGUEL HERNÁNDEZ DE ELCHE
Instituto de Bioingeniería
Unidad de Toxicología y Seguridad Química

Diciembre, 2013

UNIVERSITAS
Miguel
Hernández

D. Jorge Estévez Domenech, Doctor en Ciencias Químicas por la Universidad Miguel Hernández de Elche y Profesor Asociado de Toxicología en la Universidad Miguel Hernández de Elche, y

D. Eugenio Vilanova Gisbert, Doctor en Ciencias por la Universidad de Alicante y Catedrático de Toxicología de la Universidad Miguel Hernández de Elche,

CERTIFICAMOS:

Que **Dña. Iris Mangas Nadal**, Licenciada en Farmacia por la Universidad Miguel Hernández de Elche ha realizado bajo nuestra dirección el trabajo de investigación incluido en la memoria de Tesis Doctoral titulada

"Brain carboxylesterases interacting with organophosphorus compounds: Kinetic characterization and approaches to purification and molecular identification "

en la Unidad de Toxicología y Seguridad Química del Instituto de Bioingeniería de la Universidad Miguel Hernández de Elche.

En Elche, 2 de diciembre 2013

Fdo. Dr. D. Jorge Estévez Domenech Fdo. Dr. D. Eugenio Vilanova Gisbert

UNIVERSITAS
Miguel
Hernández

El Dr. **EUGENIO VILANOVA GISBERT,** Catedrático de Toxicología y Director del Instituo de Bioingeniería,

HACE CONSTAR:

Que da su conformidad a la lectura de la tesis doctoral presentada por Iris Mangas Nadal, titulada "**Brain carboxylesterases interacting with organophosphorus compounds: kinetic characterization and approaches to purification and molecular identification**" que se desarrolló dentro del programa de doctorado de Bioingeniería de este instituto de investigación.

Lo firmo en Elche, a instancia de la interesada y a los efectos oportunos, diciembre 2013

EUGENIO VILANOVA GISBERT
Catedrático de Toxicología
Director del Instituto de Bioingeniería

UNIVERSITAS
Miguel
Hernández

"The important thing is not to stop questioning. Curiosity has its own reason for existing. One cannot help but be in awe when he contemplates the mysteries of eternity, of life, of the marvelous structure of reality. It is enough if one tries merely to comprehend a little of this mystery every day.
Never lose a holy curiosity."

-Albert Einstein

UNIVERSITAS
Miguel
Hernández

AGRADECIMIENTOS

Recapitulando la historia de esta aventura que ahora llega a su fin, me doy cuenta de lo afortunada que he sido de poder cumplir un sueño y de que esto ha sido gracias a muchísimas personas que directa o indirectamente han contribuido en el desarrollo de este proyecto. A sí que espero no sólo acordarme de sus nombres, sino haber sabido demostrar lo agradecida que estoy.

En primer lugar quiero expresar inmensa gratitud a mis dos directores de tesis por su absoluta implicación en el proyecto y en mi formación, por aportarme tanto conocimiento, por confiar en mis ideas y valorar mis opiniones y porque sin ellos nada de esto hubiera sido posible. A mi director el Dr Jorge Estévez por enseñarme a moverme en el laboratorio, a analizar juiciosamente los resultados, a ser persistente, estando siempre cerca permitiéndome trabajar a mi ritmo y aprender de mis errores, por las apasionantes discusiones, en definitiva por enseñarme concienzudamente a ser científica. Lo cual no le ha resultado fácil. A mi director el Dr. Eugenio Vilanova por darme la confianza y abrirme las puertas de su laboratorio y por conseguir la financiación que me ha permitido penetrar en el maravilloso mundo de la ciencia, por todas sus enseñanzas y sus sabios consejos que guardo cariñosamente y que espero nunca olvidar. Muchas gracias de corazón, por estar siempre a mano, tanto para resolverme dudas como para ayudarme en todo, ya sea académico o personal.

Mil gracias a mis compañeros de laboratorio, tengo que decir que he disfrutado mucho en estos años trabajando con todos ellos y espero que el futuro nos depare muchas aventuras científicas por compartir. Quiero agradecer especialmente su ayuda al Dr Miguel Ángel Sogorb, por su plena disposición a ayudar en cualquier cosa, contribuyendo y echando una mano en el desarrollo del trabajo experimental e intelectual de esta tesis. Al Dr. David Pamies, por ser un gran compañero y amigo, por transmitirme su pasión por la ciencia y por escucharme, aconsejarme y apoyarme en los momentos más duros. A mis queridas compañeras y amigas Mónica y Eva, por estar siempre dispuestas a ayudarme en todo y porque gracias a su apoyo, sus consejos, sus ánimos, su amistad y sus risas este tiempo ha sido divertido. A la Dra Carmen Estevan, por todo lo que hemos compartido juntas y escucharme y animarme con mis experimentos. A Jose María, por ser un gran profesional y ayudarme enormemente en el laboratorio en los momentos más complicados. A Roberto, por llenar el laboratorio de cantos y alegría y por todo su cariño. Al resto de compañeros por ayudarme siempre que lo he necesitado, a Mª Cruz, Óscar, Lucía, Carolina, Encarna…Y a todos ellos no sólo por ser compañeros excelentes sino por haberse convertido en grandes amigos en estos años.

Quiero agradecer al Dr. Héctor Candela, compañero del área de genética su brillante ayuda en el análisis bioinformático de este trabajo.

I would like to express my deepest gratitude to Dr. Palmer Taylor, from University of California-San Diego for accepting me in his laboratory, for all his support and help in the experiments of this project; for his confidence and trust on me and for his valuable comments and suggestions. I consider working in his group an honor. I cannot find words to express my gratitude to Dr. Zoran Radic for his kind willingness to help me with everything in my stay in San Diego; for his great effort, his enthusiasm and inspiration in the research. It gives me great pleasure in acknowledging the help of all my coworkers at Dr. Taylor´s lab in UCSD; I want to thank especially their help in the experiments and research of this work to Edzna, Limin, John, and Aracely. I want to especially thank to Dr. Tanos Franca, for teaching me the wonderful world of the computational biology (lhe agradeço muito).

I want to thank to Dra. Komives and Dr. Ghassemian from the Proteomics facility of UCSD for their brilliant help in the mass spectrometry experiments of this work.

Quiero dar las gracias a mi familia porque ellos son lo que más quiero, a mi padre Guillermo, porque soy quien soy todo gracias a él, por educarme en los verdaderos valores y enseñarme lo realmente importante -a no dejarme llevar por las apariencias y a ser siempre yo misma, afrontar la vida con valor y una gran sonrisa- y por ser un claro ejemplo de esfuerzo y superación. A mis preciosos hermanos Zaira y Daniel y mi sobrino Darío, porque la vida sin ellos no sería tan bonita y porque a ellos les he quitado el tiempo para realizar este trabajo. A mis abuelitos, Zótico y Mercedes, a mis tíos Estrella, Richard y Lorenzo, que aunque no nos vemos mucho sé que están ahí para lo que haga falta.

Quiero dar las gracias de corazón a mis amigos por su cariño, su energía, sus risas y abrazos, por escucharme, aconsejarme y animarme, especialmente a mi mejor amiga Angela -por estar siempre y porque sé que siempre va a estar-; a Pedro -por ser un gran apoyo durante muchos años sin el cual no hubiera sido posible este trabajo. A Yasmina, Ricardo, Laura, Xavi, Antonio, Alex, Irene, Gabi, Eric y Tiffany, millones de gracias por estar ahí durante este tiempo cuando os he necesitado, habéis sido un gran apoyo.

Dedicado a mi padre Guillermo, mi maestro
y a mis hermanos Zaira y Daniel
con profundo amor

UNIVERSITAS
Miguel
Hernández

Abstract

TITLE: "BRAIN CARBOXYLESTERASES INTERACTING WITH ORGANOPHOSPHORUS COMPOUNDS: kinetic characterization and approaches to purification and molecular identification"

Organophosphorus compounds (OPs) are a large, diverse class of chemicals used for several purposes (pesticides, warfare agents, flame retardants, ectoparasiticides, investigation drugs, etc.). They induce several neurotoxic disorders: (i) acute cholinergic toxicity caused by covalent organophosphorylation of acetylcholinesterase; (ii) organophosphate-induced delayed neuropathy (OPIDN) caused by the inhibition and subsequent aging of the membrane protein called neuropathy target esterase (NTE); (iii) chronic neurobehavioral and neuropsychological consequences have been associated with a low-medium level of exposure to OP, which cannot be explained with known targets; (iv) potentiation of neuropathy, whose molecular target is not identified, is caused by some esterase inhibitors (potentiators) when they are administered following a low dose of neuropathic OPs .

Potentially, many enzyme systems can interact with specific OPs. Most of the known targets of OPs have been found in the serine esterases family. Kinetic models have been developed and applied to detect OPs binding esterases in complex biological preparations. Here, some esterases have been detected using phenyl valerate as a substrate, and they have been kinetically discriminated with mipafox (OIPDN inducer), paraoxon (non inducer) and phenylmethyl sulfonyl fluoride (potentiator of OPIDN). The study was performed using soluble and membrane fractions of chicken brain, the animal model of OPIDN. The existence of at least seven esterase components with varying kinetic behaviors was deduced. Four are membrane-bound (**EPα, EPβ, EPγ** and **EPδ)** and three are cytosolic (**Eα, Eβ** and **Eγ**). One of them, **EPγ** is attributed to the protein NTE given its kinetic properties. **EPγ** is the only esterase component known for which toxicological and biological roles have been identified, and it is molecularly and genomically characterized. The role of the other six esterase components remains unknown, but they might contain one or various enzymes with similar kinetic properties. However their interactions with the inhibitors reveal that they can be related with OPs neurotoxicity. Components **Eα** and **EPα** might play a role in toxicity and detoxication in the low-level long-term exposure of organophosphate compounds because they are highly sensitive and can be spontaneous reactivated after paraoxon inhibition. Components **Eβ** and **EPβ** may play a role in OPIDN potentiation because they are sensitive to PMSF and resistant to mipafox. Moreover, preexposure to PMSF, paraoxon or mipafox at non inhibitory

concentrations in components **Eα** and **Eγ** diminishes sensitivity to mipafox, PMSF or paraoxon, suggesting an irreversible modification of sites other than the catalytic center by inhibitors. These interactions may be relevant for interpreting the potentiation phenomenon and for understanding the neurotoxic effects of multiple exposures to xenobiotics.

Thanks to this work, we have established appropriate criteria for prepare a protocol to simply test a routine analysis of all the phenyl valerate esterases components in chicken brain. A soluble chicken brain fraction was selected as raw material to separate toxicologically relevant target proteins. A fractionation method of the soluble esterase components was developed by multistep high-performance semipreparative chromatography. The soluble chicken brain fraction was separated into three different fractions in size exclusion chromatography. Then ion exchange chromatography of all these fractions was applied. Enriched fractions with the enzymatic components of interest were obtained. Different chromatographic profiles were obtained when the same separation procedure was carried out with samples pretreated with mipafox, suggesting that treatment with mipafox modifies the ionic properties of a wide range of proteins.

High specific activity was obtained for component **Eα** in one of the fractions. This fraction was chosen to do a preliminary protein identification test by liquid chromatography tandem mass spectrometry. Indeed 259 proteins were identified in the sample according to the genomic chicken data, which demonstrates that the samples obtained in the fractionation procedure are appropriate for proteomic analysis. Using a bioinformatics approach, a cholinesterase precursor was found to be a potential target to bind to OPs as it is the only one of the 259 proteins that possesses the specific sequence for being potential serine esterase according to the genomic data. However, we cannot discard that any of the other proteins present in the sample could be responsible for the enzymatic activity.

The molecular identification of the whole group of enzymes responsible for phenyl valerate esterase activity and the interaction with inhibitors is a long-term objective of our laboratory, and the results of this work are useful for ongoing purification and molecular identification studies.

Resumen

TITULO: "CARBOXILESTERASAS DE CEREBRO QUE INTERACCIONAN CON COMPUESTOS ORGANOFOSFORADOS: Discriminación cinética y aproximaciones a su purificación e identificación molecular"

Los compuestos organofosforados (OPs) constituyen un amplio grupo de compuestos químicos utilizados con diversos fines (plaguicidas, agentes de guerra, retardantes de llama, ectoparasiticidas, medicamentos en investigación, etc.). Los OPs pueden causar varios efectos neurotóxicos: (i) la toxicidad colinérgica aguda debida a la organofosforilación de la enzima acetilcolinesterasa, (ii) la neuropatía retardada inducida por organofosforados (OPIDN) causada por la inhibición y posterior envejecimiento de la enzima esterasa diana de neuropatía (NTE), (iii) efectos neuroconductuales y neuropsicológicos crónicos se han asociado con una exposición a dosis medio-bajas de OPs, que no se puede explicarse con las moléculas diana conocidas; (iv) la potenciación de OPIDN , cuya molécula diana se desconoce.

Potencialmente, muchos sistemas enzimáticos podrían interaccionar con los OPs. La mayoría de las moléculas diana de los OPs se han encontrado en la familia de enzimas serina esterasas. Recientemente se han desarrollado los modelos cinéticos que permiten la detección de esterasas que se unen a OPs en preparaciones biológicas complejas donde se dan distintas reacciones concomitantemente y hay varios sistemas enzimáticos. En este trabajo, se han detectado las esterasas de cerebro de pollo (de las fracciones solubles y de membrana) que hidrolizan fenilvalerato esterasa. Éstas se han discriminado cinéticamente con los inhibidores mipafox (inductor de OPIDN), paraoxon (no inductor) y PMSF (potenciador de OPIDN). Se han caracterizado siete componentes esterásicos con diferentes comportamientos cinéticos. Cuatro son de mebrana (**EPα , EPβ, EPγ** y **EPδ**) y tres son citosólicos (**Eα, Eβ** y **Eγ**). **EPγ** se atribuye a la enzima NTE dado sus propiedades cinéticas, éste es el único componente detectado para el cual se han identificado roles toxicológicos y biológicos, y esta molecularmente y genómicamente caracterizado. El papel toxicológico y biológico de los otros seis componentes se desconoce, además cada uno podría estar formado por una o varias enzimas con propiedades similares. Sin embargo, las interacciones observadas con los inhibidores revelan que puedan estar relacionados con la neurotoxicidad de OPs. Los componentes **Eα** y **EPα** podrían desempeñar un papel en la toxicidad a bajas dosis y largo plazo de OPs, debido a su alta sensibilidad y a que pueden ser espontáneamente reactivados después de la inhibición con paraoxon. Los componentes **Eβ** y **EPβ** podrían jugar un papel en la potenciación de OPIDN ya que son sensibles a PMSF y resistentes a mipafox. Además se ha

observado en los componentes **Eα** y **Eγ** que la exposición a concentraciones no inhibitorias a los inhibidores disminuye la sensibilidad al mipafox, PMSF o paraoxon. Esto sugiere una modificación irreversible de los inhibidores en otro sitio de unión al del sustrato. Estas interacciones podrían ser pertinentes para interpretar fenómenos de potenciación y en la comprensión de los efectos neurotóxicos de exposiciones a múltiples xenobióticos. Gracias a esta discriminación cinética se ha establecido un ensayo sencillo que permite la discriminación de todos los componentes enzimáticos.

Se ha desarrollado un método de semifraccionamiento de los componentes esterásicos en la fracción soluble de cerebro mediante varias etapas en cromatografía preparativa de alta resolución. Mediante el cual la fracción soluble de cerebro de pollo se separó en tres fracciones diferentes por cromatografía de exclusión molecular. Cada una de estas fracciones se separo posteriormente en más de cinco por cromatografía de intercambio aniónico se obtuvieron fracciones enriquecidas con los componentes enzimáticos de interés toxicológico. Cuando el mismo procedimiento de semifraccionamiento se llevó a cabo con muestras pretratadas con mipafox se obtuvieron perfiles cromatográficos diferentes, sugiriendo que el tratamiento con mipafox modifica las propiedades iónicas de un amplio número de proteínas.

Se obtuvo una alta actividad específica para el componente **Eα** en una de las fracciones, en la que se realizó un ensayo preliminar de identificación de proteínas por espectrometría de masas. Se identificaron 259 proteínas en la muestra de acuerdo con los datos genómicos, demostrando que las muestras obtenidas en el procedimiento de fraccionamiento son apropiadas para el análisis proteómico. Mediante un análisis bioinformático de la lista de proteínas se encontró la enzima butirilcolinesterasa como potencial diana de los efectos cinéticos observados en esa fracción, ya que es la única de las 259 proteínas que posee potencial actividad esterásica. Sin embargo no puede descartarse que cualquiera del resto de proteínas presentes en la muestra pudiera ser responsable de la actividad enzimática.

La identificación molecular de todo este grupo de enzimas responsables de la actividad fenilvalerato esterasa y de la interacción con los inhibidores es un objetivo a largo plazo de nuestro laboratorio y estos resultados están siendo aplicados en actuales estudios de purificación e identificación molecular.

Abbreviations

2-AG	2-arachidonyl glycerol
AAP	aminoantipirine
ABPP	activity based protein profiling
ACh	acetylthiocholine
AChE	acetylcholinesterase
AD	alzheimer´s disease
AFMID	arylformamidase
APH	acylpeptide hydrolase
BuChE	butyrylcholinesterase
CarbEs	carboxylesterases
CB1	cannabinoid receptor type 1
CB2	cannabinoid receptor type 2
ChEs	cholinesterases
CNS	central nervous system
DBDCVP	dibutyl-2,2-dichlorovinyl phosphate
DEAE	diethylaminoethyl-cellulose
DFP	diisopropylfluorophosphate
DFPase	diisopropyl-fluorophosphatase
EDTA	ethylenediaminetetraacetic acid
FAAH	fatty acid amide hydrolase
FP	fluorophosphonate
GABA	aminobutyric acid
FP	fluorophosphonate
GABA	aminobutyric acid
Glu	glutamic
HDCP	O-hexyl O-2,5-dichlorophenyl phosphoramidate,
His	histamine
HPLC	high performance liquid chromatography
Km	Michaelis constant
LC	liquid chromatography
lysoPC	lysophosphatidyl choline

mAChRs	muscarinic receptors of AChE
MAFP	muscarinic receptors of AChE
MAGL	monoacyl glycerol lipase
MALDI-TOF MS	matrix-assisted laser desorption/ionisation-time of flight mass spectrometry
NADPH	nicotinamide adenine dinucleotide phosphate-oxidase
NEST	sterasic domain of Neuropathy Target Esterase
NTE	neuropathy target esterase
OP	organophosphates
OPCW	Organization for the Prohibition of Chemical Weapons
OPIDN	organophosphorus induced delayed neuropathy
OPs	organophosphorus compounds
PMSF	phenylmethylsulfonyl fluoride
PNS	peripheral nervous system
PON1	paraoxonase 1
PPA	1-phenylacetic acid;
PTEs	phosphotriesterases
PV	phenyl valerate
S9B	1- (saligenin cyclic phosphor)-9-biotinyldiaminononane
SD	standard Desviation
Ser	serine
SNTE	soluble neuropathy target esterase
TCEP	tris (2-chloroethyl) phosphate
TCPP	tris (1-chloro-2-propyl) phosphate
TDCPP	tris (1,3-dichloro-2-propyl) phosphate
TOCP	tri-o-cresyl phosphate
Tyr	tyrosine
USDA	United States Department of Agriculture
WHO	World Health Organization

Index

Index of Tables

N page

Index of Figures

UNIVERSITAS
Miguel
Hernández

1. INTRODUCTION:

State of the art in organophosphorus toxicity

UNIVERSITAS
Miguel
Hernández

1.1. ORGANOPHOSPHORUS COMPOUNDS (OPs)

Organophosphorus compounds (OPs) are a large and diverse class of chemicals. The first organophosphate (OP), tetraethyl phosphate, was synthesized by Philippe de Clermont in France in 1854. OP esters were discovered as toxicants for people in 1932, when Lange and Kruger described the synthesis of dimethyl and diethyl phosphofluoridate, and noted that inhalating their vapors produced dimness of vision and a choking sensation. In 1937, Schrader synthesized OP for I. G. Farbenindustrie to be used as pesticides, and one of the earliest was parathion, which is still used (Gupta., 2006). Before World War II their priority passed from pesticides to chemical warfare agents, and considerably more toxic OPs were synthesized (tabun, sarin and soman), followed by VX. Since then an estimated several thousand OPs have been synthesized for various purposes. During the second half of the twentieth century, OP esters became very popular worldwide because organochlorine pesticides were found to persist in the environment, which posed serious health risks to humans, animals, and to the environment as a whole (Satoh and Hosokawa., 2000).

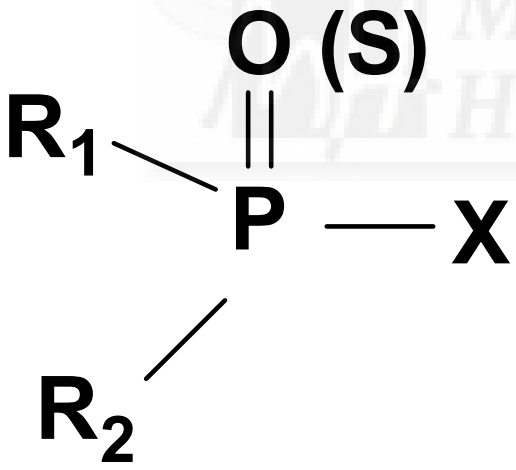

Figure 1.1. General chemical structure of organophosphorus compounds. R1 and R2 are commonly alkyl or aryl groups. Group X is the leaving group and could be a variety of groups.

Essentially, OPs are esters of phosphoric acid with varying combinations of oxygen, carbon, sulfur, or with nitrogen attached**.** OPs are esters of phosphoric acid and its derivates. The general chemical structure of an organophosphate **(Figure 1.1)** comprises a central phosphorus atom (P) and the characteristic phosphoric (P=O) or thiophosphoric (P=S) bond. Symbol X represents the leaving group, which is replaced (by nucleophilic substitution) with the oxygen of the residue at the protein active site. There are at least 13 types of Ops, which are presented in **Table 1.1**. The OPs that derive from phosphoric or phosphonic acid possess anticholinesterase activity, unlike those that are derivates of phosphinic acid (Gupta., 2006). Many OPs are used as pesticides; most are insecticides, but others are herbicides, fungicides, nematicides or plant growth regulators (Lowit., 2006). For many decades, OPs have been major insecticides in terms of their number and market share. They were the first highly effective and systemic ones, and moved throughout plants to protect even the growing tip from sucking insect pests for several days or weeks. The selective toxicity of OPs pesticides is based on specificity differences in AChE targets, more rapid detoxification in mammals than in insects, and the use of proinsecticides undergoing preferential activation in insects as compared with mammals. Their easy biodegradation and low environmental persistence are coupled with toxic effects, which are more likely due to acute rather than chronic exposure (Casida and Quistad., 2004; 2005).

The amount of OPs pesticides in use is declining, especially in developed countries. Since 1997, there has been a market shift from OPs and carbamates to neonicotinoids, accompanied by a distinct trend toward a variety of non neuroactive insecticides. However, their importance will probably continue for decades since they are effective and inexpensive (Casida and Durkin., 2013). For example, the amount of organophosphate insecticides used has dropped by more than 60% since 1990, from an estimated 85 million pounds in 1990 to 33 million pounds in 2007 in the Unites States. OPs have accounted for about 35% of the insecticides used in the latest year of analysis, 2007. Despite the number of compounds acting as other targets having increased in the last three decades, OPs and methylcarbamates, and their AChE target, remain at the top of the list numbers among commercial insecticides (Casida and Durkin., 2013; Grube et al., 2011).

OPs have also evolved into principal chemical warfare agents **(Table 1.1)** and since the 1980s, they have been used in wars and by dictators and terrorists. Unfortunately, there are currently extensive stockpiles, which is a continuous threat worldwide (Marrs et al 1996). On March 20, 1995, a terrorist attack using sarin occurred in the Tokyo subway, when 12 people died and more than 5000 were injured (Suzuki et al., 1995; Masuda et al., 1995). Between 1942 and 1945 about 12,000 tones of tabun were produced. At the end of World War II, the Allies seized

large quantities of this nerve agent. Up until the end of this war, Schrader and his co-workers synthesized about 2000 new organophosphorus compounds, including sarin in 1938. The third of the "classic" nerve agents, soman, was first produced in 1944. The Organization for the Prohibition of Chemical Weapons (OPCW) estimates that as of September 30, 2010, there were nearly 30000 metric tons of nerve agents undestroyed, and that these numbers did not include the stockpiles of non member states that had neither signed nor acceded to the Chemical Weapons Convention.

Furthermore, halo alkyl phosphates are used as flame retardant, as for example tris (1,3-dichloro-2-propyl) phosphate (TDCPP), tris (2-chloroethyl) phosphate (TCEP), and tris (1-chloro-2-propyl) phosphate (TCPP). These compounds do not possess anti-AChE activity. TCEP is used as flame retardant additives in flexible plastic products, such as polyurethane and polyisocyanurate foams, carpet backing, flame retardant paints, resins and adhesives. These compounds can be released to the environment and are toxic to aquatic organisms (Gupta., 2006). OPs are also used as anthelmintics and ectoparasiticides in veterinary medicine. The OP echotiophate has been used in medicine for glaucoma and, for many years, the OP trichlorfon (metrifonate) has been used to treat mild and moderate Alzheimer´s disease (AD) and as an investigation drug (Taylor., 2001; Karczmar., 1998; Casida and Quistad., 2004).

Table 1.1. Types of Organophosphates.

Types of Organophosphate	Chemical structure	Examples
PHOSPHATES		
O,O' dialquil-phosphate	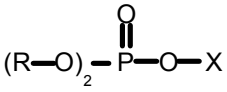	chlorfenvinphos, dichlorvos, monocrotophos, Tri-o-cresyl phosphate
THIOPHOSPHATES		
O,O' dialquil phosphorothioates	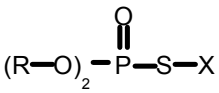	amiton, omethoate
O,O'-dialquil thiophosphates	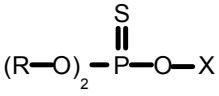	bromophos, chlorpyrifos, diazinon
phosphorodithioates	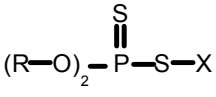	methidathion,malathion, dimethoate, disulfoton,

Types of Organophosphate	Chemical structure	Examples
O-alquil, S-alquil phosphorothioate	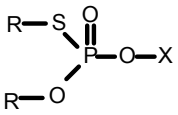	profenofos, trifenophos
O-alquil, S-alquil phosphorodithioate	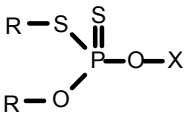	protiophos, sulprophos
PHOSPHOROMIDATES O' dialquil phosphoramidate	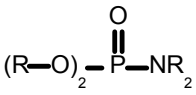	cruformato, fenamiphos
O-alquil, S-alquil phosphorothioamidate	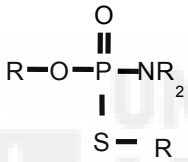	methamidophos
O,O' dialquil phophorothioamidate	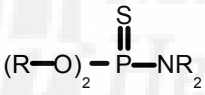	isofenphos
PHOSPHONATES	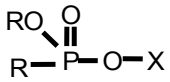	triclorphon
PHOSPHOROFLUORIDATES	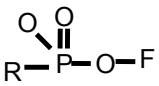	diisopropyl phosphorofluoridate (DFP)
PHOSPHONOFLUORIDATES	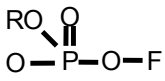	cyclosarin, sarin, soman (*) Chemical warfare agents
phosphonothioate	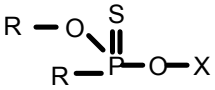	leptophos
PHOSPHINATES	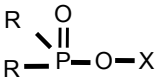	gluphosinate

1.2. BIOTRANSFORMATION OF OPs

1.2.1. Main biotransformation reactions of OPs

Figure 1.2 shows the biotransformation of OPs. These biotransformation reactions can be classified into two types: (1) toxic activation, when the product of the reaction is more soluble in water and more reactive; (2) detoxication reactions, when the product is less toxic (Sogorb and Vilanova., 2006).

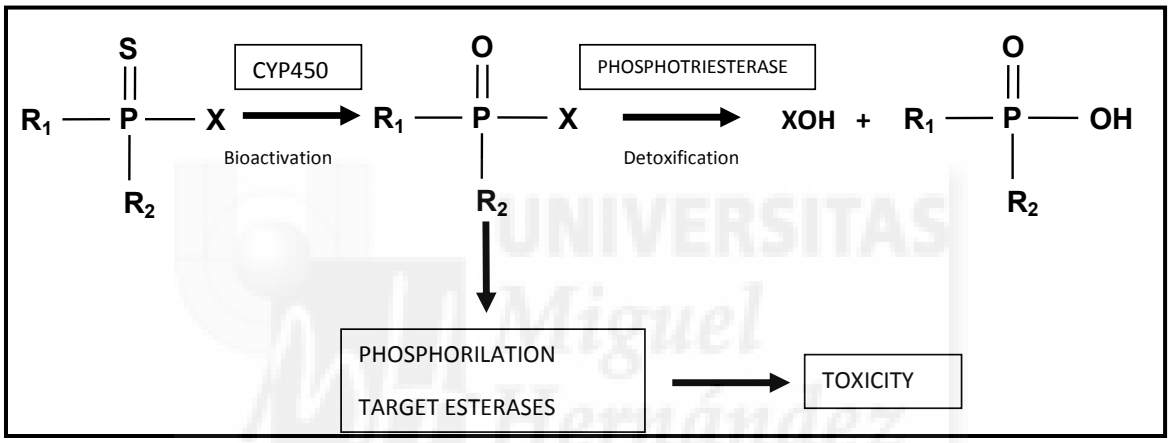

Figure 1.2. Main scheme for the metabolism of insecticide OPs.

1.2.2. Toxicokinetics of OPs

The ADME (administration, distribution, metabolism, excretion) of organophosphates has been studied in both animal and human species (Poet et al., 2004). OPs can easily cross lipid bilayers, such as alveolar and dermal membranes, because of their lipophilic characteristic (WHO., 1986a; Sogorb and Vilanova., 2006). These chemicals can enter the body after exposures of different sources; i.e., ingestion of pesticide residues in food, or accidental and intentional ingestion of insecticides; while dermal exposure represents the principal route, particularly during the mixing, loading and application of insecticides, or from skin coming into contact with contaminated surfaces (Knaak et al., 1993). Likewise, inhalation is also plausible while spraying pesticides. Based on the bioavailability for a given OP and exposure route, once the compounds have been absorbed a systemic dose of the parent compound will enter the

circulation. OPs are generally well-distributed in tissue thought the body, especially in fatty tissues. These compounds do not usually bioaccumulate due to fast biodegradation (Sogorb et al., 2004). The same property, their lipophilicity, determines slow urine excretion. More stable degradation metabolites are readily excreted in urine and offer the potential utility as biomarkers of exposure (WHO 1986b; Colosio et al., 2002; Iverson et al., 1975). Based on the detection of low levels of metabolites in urine in human populations, there is sound evidence for widespread, but low-level, exposures (Aprea et al., 1999).

1.2.3. OPs activation and detoxication routes and enzymes

Although the portal of the entry metabolism has been localized, the bulk of metabolic activation and detoxification reactions occur in the liver (Sultatos et al.,1994). Most insecticides are formulated in the form of phosphorothionates because they are more stable than the corresponding oxon forms, such as parathion, chlorpyrifos and diazinon. Once the phosphorothioate (with reduced capability to phosphorylate esterases) has been absorbed in the organism, the compound is bioactivated through desulfurative oxidation to become the phosphorothioate in the corresponding oxon form, with a high capability to phosphorylate esterases (bioactivation in **Figure 1.2**). Phosphorothioates and oxonphosphates can be detoxified by several biotransformation reactions.

Phosphorothioate might also undergo bioactivation, a detoxication through an O-dearylation reaction, while the phosphate form can be detoxified through either oxidative dealkylation or hydrolysis (Sogorb and Vilanova, 2006).

The O-dearylation reaction of phosphorothioate OPs is catalyzed by cytochrome P450 and its yields alkyl phosphates, alkyl phosphorothioate, plus the corresponding alcohol.

O-dealkylation is catalyzed by microsomal oxygen and NADPH-dependent enzymes, and it involves hydroxylation at the α-carbon atom of an alkyl group.

Hydrolysis yields more polar compounds, which hare not capable of phosphorylating esterases. The main enzymatic systems involved in the hydrolysis of OPs are phosphotriesterases, carboxylesterases and glutathione-S-transferases (Jokanovic., 2001).

Aldridge and Reiner (1972), classified esterases according to their reactions with OPs: A-esterases, or arylesterases, are those which hydrolyze OPs, but are not inhibited by them and B-esterases, which are inhibitors for both serine hydrolases and substrates. The A-esterases

group is formed mainly by phosphotriesterases (PTEs) and B-esterases are carboxylesterases (CarbEs). PTEs are classified by the International Union of Biochemistry as EC 3.1.8. They are widely spread on the phylogenetic scale and are strongly expressed in the serum and liver of mammals, while levels are barely detectable in birds (Sogorb et al., 1996; Vilanova and Sogorb., 1999; Sogorb and Vilanova., 2002). The two best-understood OP-detoxifying enzymes are PTEs: paraoxonase, which hydrolyzes many OPs, (Costa et al., 1990) and diisopropylfluorophosphatase (DFPase), which acts on diisopropylfluorophosphate (DFP) and other fluorophosphates.

CarbEs are classified by the International Union of Biochemistry as EC 3.1.1. CarbEs can act as scavengers to protect against OPs, facilitated by spontaneous reactivation after OP inhibition. Insecticide-hydrolyzing esterases are generally better characterized in insects in relation to resistance than in mammals. Resistance to OP insecticides in several insect species is associated with changes in carboxylesterases activity.

These enzymes are expressed in the endoplasmic reticulum of many mammalian tissues. Mammalian CarbEs play key roles in the metabolism of a good number of drugs and of xenobiotics (Satoh and Hosokawa., 1998). They all possess an amino acid residue of serine in the active center of the enzyme. This serine is the target of the irreversible phosphorylation by OPs which, in some cases, is the cause of toxic effects (such as NTE or AChE). In others however, these inhibitions do not apparently cause toxic effects and such reactions must be considered a detoxication reaction since each molecule of the enzyme is capable of scavenging one molecule of OP from the media (Sogorb and Vilanova., 2002, 2006; Vilanova and Sogorb., 1999). This detoxication system is much less efficient than hydrolysis by PTEs because each CarbE is able to capture only one molecule of OP and it is not an enzymatic cycle.

The role of human serum albumin in OPs detoxication was reported in 1984 (Ortigoza-Ferago et al., 1984). More recently, studies have reported OPs -chlorpyrifos-oxon, diazoxon, O-hexyl O-2,5-dichlorophenyl phosphoramidate (HDCP), paraoxon, soman- to hydrolyze by albumins of different species (Sogorb et al., 1998, 1999; 2008; Li et al., 1995). The hydrolysis mechanism is based on the phosphorylation of Tyr-411 (Sogorb et al., 1998; Li et al., 2007). This residue is reversibly acetylated during hydrolysis and its efficacy is based on the large number of albumin molecules present in the organism and not in its high catalytic efficacy.

The final balance between activation routes (oxidative desulfuration) and deactivation routes (O-dearylation, O-dealkylation, and specially hydrolysis by PTEs) will become a determinant in species´ susceptibility to the toxic effect of OPs. Interactions between different pathways of metabolism (activation-detoxication) are especially important when evaluating mixtures of

pesticides that involve a secondary chemical which changes the toxicokinetics of the pesticide as a result of its increased activation or decreased detoxification, followed by enhanced or reduced toxicity, respectively (Hernández et al., 2013). In some cases, concurrent multiple OP exposure may lead to a potentiating effect which is based on the interference exerted by one compound on the detoxification process of the others through metabolic inhibition. Such an effect has been observed in Pakistani applicators after handling malathion contaminated with isomalathion (Baker et al., 1978).

1.3. NEUROTOXICITY OF OPs

Neurotoxicity of OPs has been extensively documented in accidental human poisonings, epidemiological studies and animal models. It is clear that OPs can produce several distinct neurotoxic effects depending on the dose, frequency of exposure, type of OP, and the host factors that influence susceptibility and sensitivity. Some of them have mechanistic and molecular target identified and others not. These effects include acute cholinergic toxicity, the intermediate syndrome and organophosphorus-induced delayed neuropathy (OPIDN). Recent years have witnessed the recognition of additional developmental neurotoxicity, of persistent signs of chronic neurotoxicity (involving neurobehavioral, neuropsychiatric, cognitive and neuromuscular functions) and of a disruption of cannabinoid system (**Table 1.2**).

Table 1.2. Neurotoxic effects and symptoms observed after OPs exposure.

Effect	Mainly symptoms	Molecular target	OPs implicated
Cholinergic crisis	Headache, numbness of extremities, vomiting, miosis, weakness, muscular fasciculations, flaccid paralysis, respiratory difficulty, cardiac arrhythmias.	***AChE***	All of them, non the alkyl phosphates
Intermediate syndrome	Moderate proximal limb paralysis, weakness	***AChE***	Most of them
OPIDN	Flaccid weakness of the distal limb muscles, especially in the legs	***NTE***	Inducers of OPIDN: chlorpyrifos, dichlorvos, isofenphos, methamidophos, mipafox, trichlorfon, trichlornat, triaryl phosphates and phosphamidon/mevinphos (in humans)
Potentiation of OPIDN	Enhancement of OPIDN at doses non neuropathic	***Not identified***	NTE inhibitors (inducers and non-inducers)
CNS long term neurotoxicity	Neurobehavioral, neuropsychiatric, cognitive, sensory-motor	***Not identified***	Soman, chlorpyrifos, sarin, etc.
Developmental neurotoxicity	Neurodevelopmental effects have been observed in animal outcomes	***Not identified***	Mainly chlorpyrifos
Disruption of the cannabinoid system	In vitro observations	***FAAH, MAGL***	Mainly chlorpyrifos

1.3.1. Cholinergic crisis, acute toxicity

The mechanism by which OPs elicit their mainly toxic effect is the inhibition of the enzyme acetylcholinesterase (AChE), which is the molecular primary target of these compounds. The primary mechanism of action of OPs through AChE inhibition was first described by DuBois with parathion (DuBois., 1948; DuBois et al., 1949) and currently the mechanism from the inhibition of AChE to the development of the symptoms is well documented (reviewed in **Section 2.2**).

Sufficient AChE inhibition within the synapse prevents the efficient breakdown of ACh molecules, leading to an accumulation of acetylthiocholine (ACh) in the synaptic region and the persistent stimulation of cholinergic receptors on postsynaptic cells. Under normal conditions, this shift to enhanced cholinergic receptor activation leads to functional signs and symptoms of cholinergic toxicity (Ecobichon., 1996; 2010). Effects of AChE inhibition have been well-documented and involve changes mainly in the peripheral nervous system (PNS), but also in autonomic and central nervous system (CNS) functions. Signs and symptoms of OP poisoning can be divided into three broad categories: muscarinic effects, nicotinic effects and CNS (**Table 1.3**). Levels of nerve AChE inhibition of approximately over 70% lead to ACh to accumulate in synaptic clefts of neuromuscular junctions, which causes neuromuscular block and respiratory failure in severe cases. Inhibition of brain or neuromuscular AChE activity to the extent of 70-90% is usually lethal.

Table 1.3. Effects of acetylcholine receptor over-stimulation following acute exposure to OPs

Receptor	Clinical Signs
Muscarinic receptors	Diarrhea, urinary incontinence, miosis, bradycardia, bronchoconstriction, bronchorrhoea, hypotension, increased gastrointestinal motility, abdominal cramps, miosis and hypersalivation
Nicotinic receptors	Hypertension, tachycardia, fibrillation, fasciculation, striated muscle necrosis
Both central muscarinic and nicotinic and nicotinic receptors	Tremor, loss of movement co-ordination, seizures, central depression of respiration, coma death

1.3.2. Intermediate syndrome in organophosphate poisoning

The intermediate syndrome refers to health effect observed in patients who survive acute high-level exposure to OP nerve agents. A delayed intermediate syndrome affecting muscles, expressed as weakness, which can occur days following recovery from severe acute affects and it is reversible over days or weeks has been reported is some people exposed to OPs.

Signs and symptoms include moderate proximal limb paralysis beginning 1-4 days after recovery from the acute effects (Karalliedde et al., 2010). In 1987, Senanayake and Karalliedde in a landmark paper reported 10 patients who developed facial, proximal limb, and respiratory muscle weakness. Several patients reported before the recognition of intermediate syndrome by Senanayake and Karalliedde (1987) can in retrospect be related to this syndrome. The largest cohort was probably presented by Wadia et al., (1972) for diazinon poisoning. The pathogenesis of intermediate syndrome was unclear and the question arose whether or not intermediate syndrome bore a separate structure-activity relationship (Karalliedde et al., 2010).

Some reports describing delayed neuromuscular effect in mice exposed to sarin vapor may actually be more related to the intermediate syndrome than to OPIDN (Brown and Brix., 1998). Nonetheless, the intermediate syndrome's exact mechanism is not understood. The effect is likely to be due to the excessive accumulation of acetylcholine at the neuromuscular junction that occurs with high-level exposure leading to prolonged transmitter-receptor interaction (Karalliedde and Henry., 1993).

Manifestation of intermediate syndrome correlates with the severity of acute toxic reaction from exposure to any OP nerve agent-specifically, to prolonged inhibition of acetylcholinesterase activity at the neuromuscular junction and synaptic impairment of neuromuscular transmission and it is not toxicologically related to delayed neuropathy or OPIDN.

1.3.3. Organophosphorus induced delayed neuropathy (OPIDN)

Early in 1930, around 50,000 people were paralyzed in a poisoning epidemic in southern U.S.A. It was known by the 1960s that the poisonings arose from adulteration of Jamaica ginger extract, a popular source of alcohol during the Prohibition era, with tri-o-cresyl phosphate (TOCP). Later in 1959, 10000 Moroccans who ingested TOCP-contaminated cooking oil, and 600 Indians who consumed contaminated rapeseed oil in 1988, also became ill (Travers., 1962; Ehrich and Jortner., 2001). The paralysis of several British workers engaged in the manufacture

of mipafox, a new candidate organophosphorus insecticide, made it clear that the ability of TOCP to cause OPIDN was not unique, and this finding spurred the start of still-continuing investigations into the mechanism of this syndrome (Davison., 1953).

OPIDN is a neurodegenerative condition that affects nerves with long fiber tracts in both the CNS and the PNS, and is characterized by an axonopathy of long sensorimotor axons in peripheral nerves and spinal cord (Davis and Richardson., 1980). Some OPs called OPIDN inducers or neuropathic have been found to induce OPIDN, which is characterized by delayed onset of extended periods of ataxia and upper motor neuron spasticity arising from single or repeated exposure to OPs. Compounds that have been reported to cause OPIDN in humans are: chlorpyrifos, dichlorvos, isofenphos, methamidophos, mipafox, trichlorfon, trichlornat, triaryl phosphates and phosphamidon/mevinphos (Moretto and Lotti., 2006).

OPIDN is now the best understood delayed syndrome of OP esters. OPIDN symptoms usually appear 2 or 3 weeks after a single dose, depending on the kinetic characteristic and the dose of the compound. Initially, the usual complaint is cramping muscle pain in the lower limbs, followed by distal numbness and paresthesia. Progressive weakness then occurs, together with depression of patellar and Achilles reflexes. When severe symptoms and signs of neuropathy appear in the arms and forearms, a physical examination reveals wasting and flaccid weakness of the distal limb muscles, especially in the legs (Moretto and Lotti., 1998). Functional recovery occurs with time in less severe cases, with most distal involvement and sparing of spinal cord axons. Otherwise spastic ataxia may be permanent. The very few cases of OPIDN reported in young individuals indicate that they recover completely, even from severe lower and upper limb involvement (Senanayake., 1981; Goldenstein et al., 1988).

The mechanism proposed for OPIDN is a multistep hypothesis, as shown in **Figure 1.3**. However the exact mechanism it is not completely understood. Although NTE inhibition and aging (**Figure 1.4**) are a necessary antecedent to OPIDN, the precise relationship between NTE and OPIDN has not yet been defined as it is not understood the function of NTE neither its inhibition as it is explained in **Section 2.2**. It has been proposed that the association with NTE inhibition may be an epiphenomenon (Winrow et at., 2003).

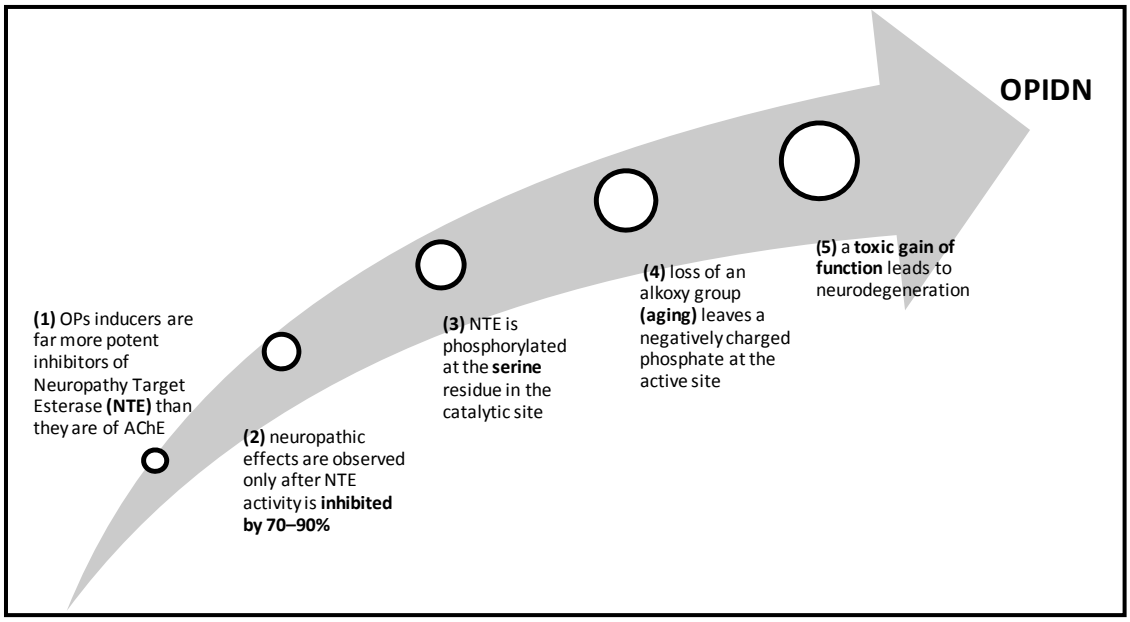

Figure 1.3. Multistep hypothesis of the mechanism of OPIDN.

1.3.4. Protection against OPIDN

The protection effect against OPIDN is observed if some NTE inhibitors are dosed before neuropathic OP. This effect is detected when carbamates, phosphinates, and sulfonyl halides are administered to hens at doses that block (inhibit) more than 30-40% of NTE before a high neuropathic dose of a neuropathic OP ester (Johnson and Lauwerys., 1969; Johnson and Read,. 1991).

The protection effect to OPIDN is related to the inhibition of NTE. Pretreatment of experimental animals with reversible inhibitors of NTE prevents OP-induced inhibition and aging and protects exposed subjects from OPIDN (**Figure 1.4**). It is necessary the inhibition of a 30-40% of NTE to protect the animal. NTE, inhibited by these compounds, does not undergo the aging reaction, and consequently protects against further phosphorylation by an inducer.

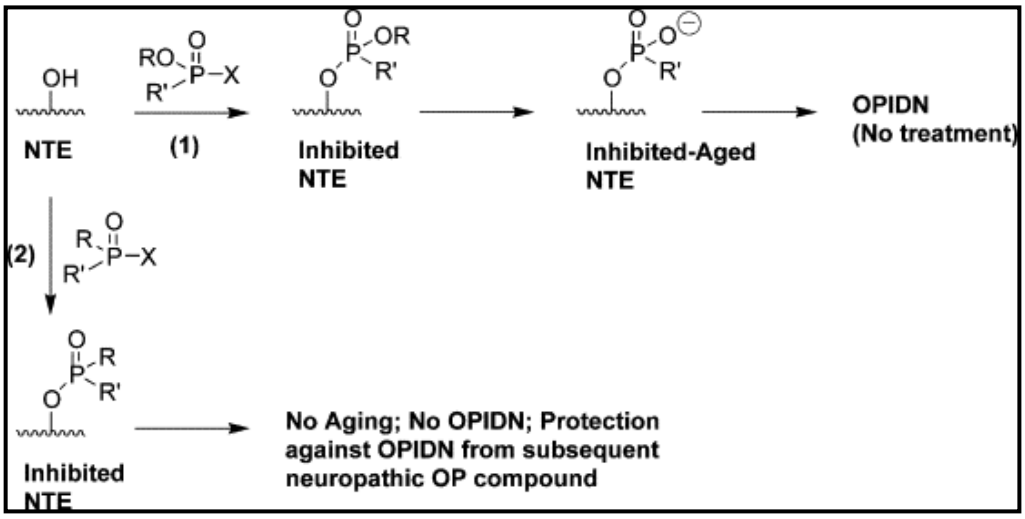

Figure 1.4. Inhibition and aging of neuropathy target esterase (NTE) are both required to produce OPIDN; inhibition of NTE without aging protects against OPIDN. Pathway (1): NTE inhibition by an ageable phosphinate proceeds rapidly to aging and then to OPIDN after 8–21 days. Pathway (2): NTE inhibition by a non ageable phosphinate does not produce OPIDN. However, non ageable NTE inhibitors are not biologically inert: they protect against OPIDN from subsequently administered neuropathic OP compounds by blocking their inhibition and via the aging of NTE. Adapted from Richardson et al., (2013).

1.3.5. The promotion/potentiation of OPIDN

OPIDN is enhanced when some non neuropathic esterase inhibitors (OPs, sulfonyl fluorides and carbamates) are dosed after a low non neuropathic dose of a neuropathy inducer. This effect was first observed in hens when phenylmethylsulfonyl fluoride (PMSF) was administrated after mipafox or DFP, and it was called potentiation (Pope and Padilla., 1990). Lotti and coworkers reported similar observations in hens treated with chlorpyrifos (Lotti et al., 1991) and they called it “promotion” since an order of dosing (first exposure to an “inducer” or initiator, and afterward to the “promoter”) is needed. The in vivo potentiation/promotion effect of PMSF and other potentiators has been widely assayed in chicken (Pope et al., 1993; Moretto et al., 2001; Peraica et al., 1991). Cases of promotion of OPIDN in humans have not been reported, nor has the phenomenon been observed outside a laboratory.

Since promotion is nonspecific, other toxic axonopathies (i.e., 2,5-hexanedione) (Moretto et al., 1992) and traumatic nerve lesions (Moretto et al., 1993) were promoted by PMSF. Potentiation appears to be an interesting laboratory model to investigate neurological disorders (Milatovic et al., 1997).

Despite all the efforts made, neither the mechanism or the target for promotion is unknown. It is likely that potentiation involves a separate mechanism from that of the initial lesion because, according to the bibliography, retrograde axonal transport is selectively impaired during OPIDN development and its reduction precedes the onset of morphological and clinical signs (Lotti et al., 1987). However it has been shown that PMSF does not further impair retrograde axonal transport when used to promote a dose of dibutyl-2,2-dichlorovinyl phosphate (DBDCVP), which causes moderate OPIDN in chicken (Moretto et al., 1992; Lotti., 2002). Neuropathological studies after OPIDN promotion have shown that the types of lesion observed did not differ from those observed in typical OPIDN. Moreover brain regions (brainstem and cerebellum) were not affected, indicating that degeneration does not affect areas which are not typically involved in OPIDN (Pope et al., 1993; Moretto et al., 2001). A number of observations has led to the hypothesis that promotion might directly affect the compensation/repair mechanism(s) of the nervous system (Lotti., 2002). Promotion is less effective in chicks where compensation-repair mechanisms are more efficient. The minimum promoting dose of PMSF in chicks (90 mg/kg sc) was much higher than in hens (5 mg/kg sc) (Peraica et al., 1993), which suggests a relationship with compensation/repair mechanism(s) that abates with age.

It has been reported that, given the chemical nature of promoters, all the promoters identified to date are NTE inhibitors, the molecular target has to be a esterase similar to NTE, but not NTE and is therefore likely to hydrolyze the same substrate – i.e., phenyl valerate –(Aldridge., 1993; Moretto et al., 1994; Céspedes et al., 1997).

Recently, studies have been done with another substrate, phenyl benzoate, which was assayed because it was poorly hydrolyzed by NTE, but extensively by enzymes which are not sensitive to non promoters, such as mipafox, but are sensitive to promoters such as PMSF. However, this attempt failed because none of these esterases was associated with clinical effects (Moretto el al., 2007). Other non neuropathic NTE inhibitors, such as phenyl-N-methyl-N-benzyl-carbamate and phenyl-n-pentyl-phosphinate, n-butyl sulfonyl fluoride, S-ethyl hexahydro-1H-azepine- 1-carbothioate (molinate), S-4-chlorobenzyl diethylthiocarbamate (thiobencarb) and O-(2-chloro-2,3,3 trifluorocyclobutyl) O-ethyl Spropyl phosphorothioate (KBR-2822), have also been found to promote OPIDN (Lotti et al., 1991; Johnson and Read., 1993; Moretto et al., 1994; Osman et al., 1996; Moretto et al., 2001). However, other inhibitors of esterases, but not of NTE (such as paraoxon and other sulfonyl fluorides), do not promote OPIDN when administered at the maximum tolerated doses. Dose-response relationship studies have shown that the level of NTE inhibition by neuropathic OPs to initiate OPIDN is much lower when PMSF was administered afterward (i.e., 30-40%) and promotion is

not observed when animals are protected by PMSF after inhibiting all the NTE (Lotti et al., 1991; Osman et al., 1996).

1.3.6. Long term central nervous system neurotoxicity

Long term CNS toxicity related to OPs exposure was first reported when, returning from the Gulf War in 1991, thousands of soldiers exhibited a variety of signs and symptoms of neurological deficits (i.e., attention deficits, memory difficulties and sleep disorders) that were referred as Gulf War illnesses. Despite intentional exposure to pyridostigmine, exposure to low levels of OPs nerve agents has been associated with these effects (McCauley., 2006; RAC report., 2008).

In recent decades, an increasing number of epidemiological studies have suggested that exposure of people to repeated doses of low-medium levels of OPs can produce long term neurological and neurobehavioral effects, that affect the CNS to a greater extent than the PNS (COT report., 1999, Colosio et al., 2009; Brown and Brix., 1998; Parrón et al., 1996; Roldán-Tapia et al., 2006). These effects have also been observed in military personnel, farm workers (Bazylewicz-Walczak et al., 2005; Roldán-Tapia et al., 2005; 2006; Mackenzie Ross et al., 2008), sheep dippers exposed to OPs (Dunn., 2002), and pilots exposed to contaminated air with OPs (Mackenzie Ross et al., 2008). Similar symptoms have also been reported after the acute exposure to the OP sarin during the terrorist attack of Tokyo in 1995 (RAC report., 2008).

Now there is no doubt that almost every person in the world is exposed to low levels of OPs. Most of the population has measurable levels of OPs metabolites in urine: Barr and colleagues (2004) reported that 50% of individuals in US have measurable levels of the OPs metabolite dialkyl phosphate and 71% of the OPs metabolite dietylphosphate. The USDA reported in 2006 that approximately 73% of fresh fruits vegetables, 61% of processed foods and 66% of drinking water in the US contained detectable levels of OPs (USDA., 2005).

Observations in epidemiological studies

Different symptoms and signs have been observed in various studies and are reviewed in **Table 1.4**. The phenomenon called as chronic OP-induced neuropsychiatric disorder (Jamal et al., 1997) can include the following effects:

(1) **neuropsychiatric effects**: depression, fatigue, anxiety, irritability, emotional state problems, etc.

(2) **cognitive effects**: attention deficits, reduced visuomotor, perceptual and constructive abilities, verbal learning, speed of processing, memory problems, fatigue and muscle strength, and altered reflexes, etc.
(3) **neurobehavioral deficits**: lower scores in digit span, digit symbol and vigilance tasks
(4) **sensory-motor functions altered**: motor coordination, balance, postural, visual acuity, auditory, olfactory, etc.

Several studies have been done in population exposed to OPs, some of them are reviewed in **Table 1.4**. Despite the number of studies and several reviews on this topic having been published, the authors have reached conflicting conclusions (Colosio et al., 2009; Rohlman et al., 2011, Ross., 2013; Prueitt et al., 2011). Behavior and psychiatric functions are a very complex system made up of several different functions and biochemical activities, which have to be studied based on a very complex approach in which different tests are performed (Colosio et al., 2009). Distinct approaches have been adopted in epidemiological studies by different researchers with varying results, which complicates the task of comparing studies.

In 2009, Colosio and colleagues reviewed 24 papers published on human neurobehavioral effects of organophosphorus and carbamates pesticides up to May 1st 2008. They concluded that 13 studies yielding positive or uncertain results (for the cognitive function), there were 22 (for the psychomotor function), 11 (for the sensory-motor function) and 11 (for psychological function impairment). In 46% of the positive studies, severe acute poisoning was previously reported. Exposure levels were measured only in five studies, and very often several limits were found in the studies, such as: limited number of studies and compounds addressing significant differences. The most recent review is that done by Mackenzie Ross and colleagues in 2013. They did a meta-analysis to quantify and evaluate data published in 14 studies with more than 1600 participants occupationally exposed to long-term low-levels of OPs, defined as repeated or prolonged exposure to doses that do neither produce recognized clinical symptoms of acute toxicity nor require medical evaluation or intervention. They concluded that there is sufficient evidence in these studies to accept the hypothesis. More they reached the conclusion that the majority of well-designed studies found a significant association between low-level exposure to OPs and impaired neurobehavioral function which is consistent, small to moderate in magnitude, and is concerned primarily with cognitive functions, such as psychomotor speed, executive function, visuospatial ability, working and visual memory.

Table 1.4. Long term central nervous system neurotoxicity observed in some recent epidemiological studies in people exposed to low-moderate doses of OPs.

Reference	Observations	Country	Biochemical exposure levels
Srivastava et al. (2000)	Neuropsyquiatric, neurobehavioral effects and motor alterations symptoms in 59 Indian workers exposed to different chemicals during the manufacture of 'quinalphos'	**India**	Mean blood AChE levels in the exposed and in control group were not different
Mackenzie Ross., (2008)	Neuropsyquiatric, neurobehavioral effects in a cohort with 27 pilots exposed to engine oil with OPs	**UK**	not measured
Farahat et al. (2003)	Neuropsyquiatric and neurobehavioral effects in 52 pesticides applicators. A longer duration of work with pesticides was associated with lower performance on tests	**Egypt**	Serum AChE was significantly lower in the exposed group than in the control
Kamel et al. (2003)	Farm work was associated with poor performance on four neurobehavioral tests in 288 farm workers	**USA**	Not measured
Roldán-Tapia et al., 2005 ***Roldán-Tapia et al., 2006***	Neuropsychological dysfunctions and emotional disturbances in 40 exposed farm workers measuring cumulative exposure as a number of years working with pesticides	**Spain**	No relationship with plasma BuChE inhibition as a measure of recent exposure.
Abdel Rasoul et al., 2008	functional cognitive effects with increased years of exposure to OP pesticides in children applicators of pesticides	**Egypt**	lower AChE activity was also measured

However, what does not come over clearly are the exact exposure conditions, and controversial results have been reported (Farahat et al., 2003; Kamel et al., 2003; Rohlman et al., 2011; Roldan-Tapia et al., 2005). Thus, although overt intoxication with anti-ChEs may elicit long-term, subtle changes in neurologic functions, the potential for low-level exposures that lead to chronic neurological changes is even less uncertain and a matter of diverse opinion. At this point, the question arises as to whether or not these effects are caused in doses below those causing acute toxicity or AChE inhibition. Long-term exposure to low or moderate levels of OP pesticides does not cause clinically overt cholinergic toxicity (Romana et al., 2001). However, most studies done into the biochemical measure of cholinesterase activity over time provide no data on this aspect. Ray and Richards (2001) reviewed the data until 2001, and they

proposed that any chronic effects of low-level exposures are likely to occur through a mechanism that is independent of AChE inhibition. Jamal et al., (2002) reviewed epidemiological and experimental studies published until 2002 of chronic effects of OPs with or without previous acute cholinergic episodes.

Moreover, the majority of studies have primarily found associations in the occupational setting and very few studies have looked for chronic neurologic effects beyond the occupational setting. A recent ecological study conducted in Spain in a general population and a large sample size (n=17429) indicated a higher prevalence and greater risk for certain neurodegenerative diseases (Alzheimer`s disease, Parkinson`s disease) and suicide attempts in populations living in areas with high use of pesticides, most of which are carbamates and OPs. However, ecological bias and other types of confounders preclude etiological interpretations (Parrón et al., 2011.).

Observations in experimental studies

Experimental data on low-medium doses of OPs neurotoxicological outcomes in animals are abundant, but relatively few have dealt with long-term exposures. In the review of Jamal and coworkers, five published experimental studies were found where chronic OP neurotoxicity was observed with subclinical exposure in primates, rhesus, mice and rats (Jamal et al., 1997).

Most of the reports in the literature deal with repeated exposures to OPs, which are as short as 5 days as and are rarely longer than 3 months (Moser et al., 2007), and almost all the studies used chlorpyrifos or its metabolite chlorpyrifos oxon as OP pesticides. Animal experiments studying asymptomatic exposure to OP have found various effects on physiological and behavioral functions (Scremin et al., 2003; Mach et al., 2008). **Table 1.5** presents some of these more recent studies and some of the neurotoxic effects observed.

Table 1.5. Low-medium doses of central nervous system neurotoxicity observed in some animal studies.

Reference	Observations	Animal
Terry *et al.*, 2003	Hippocampus-dependent learning and memory effects of repeated subclinical chlorpyrifos exposure	**Mice**
Mamczarz et al., 2010	Anxiety-and related behavior neurotoxicity in an acute exposure to a sub-lethal dose of soman have been related with an	**Guinea pigs**
Oswal et al., 2013	Potent long-term effect on the monoaminergic neurotransmitter systems after low dose of sarin, with no signs of cholinergic toxicity or cell death, has been reported to have	**Mice**

1.3.7. Developmental neurotoxicity

The information available on the capability of OPs to cause neurodevelopmental toxicity is contradictory. Since many in vivo studies have reported such effects on exposures to the OPs chlorpyrifos and scant work has been done on other OPs, neurodevelopmental effects of exposure to chlorpyrifos have been studied with different approaches in epidemiological studies (Mars et al., 2010; Young et al., 2005; Eskenazi et al., 2007) and have obtained different results.

Neurodevelopmental effects have been observed in animal outcomes and some gene alterations in cells studies (Estevan et al., 2013). Most of these studies indicate doses causing decreases in brain AChE, while other studies report effects at dose levels which do not cause apparent AChE inhibition (Eaton et al., 2008; Middlemore et al., 2010). Indeed, Slotkin and colleagues (2006) have suggested that there is a complete dichotomy between the systemic toxicity of OPs and their capability to cause developmental neurotoxicity. These data indicate that it is necessary to assess the risk of exposure to chlorpyrifos during development (Ostrea et al., 2002).

In their recent review of human and animal data, Prueitt and collegues concluded that chlorpyrifos exposure and neurodevelopmental effects in the absence of acetylcholinesterase inhibition in the brain are not plausible in humans, and that the associations observed are most likely to be attributed to alternative explanations (Prueitt et al., 2011). Thus there is not enough evidence in the literature as to whether these effects are specific of chlorpyrifos or are general of OPs, and if they are plausible without inhibition of cholinesterase. Along these lines,

explaining the molecular mechanism of these effects is an important research task in current OPs toxicity studies and different approaches have been used as in vitro studies of embryotoxicity (Estevan et al., 2013).

1.3.8. Disruption of the cannabinoid system

The cannabinoid system consists of the CB1 and CB2 G protein–coupled cannabinoid receptors in the CNS and the PNS, respectively, and two endocannabinoid ligands, anandamide and 2-arachidonyl glycerol (2-AG), which are biosynthesised as required and degraded by serine hydrolases fatty acid amide hydrolase (FAAH) and monoacyl glycerol lipase (MAGL), respectively. Endocannabinoids are neuromodulators that influence a variety of neurological processes throughout both the PNS and the CNS (Pope et al., 2010). They regulate the release of a variety of neurotransmitters, including ACh, dopamine, glutamate, GABA and others in a brain-regional manner. This system is involved in appetite, pain, synaptic plasticity, mood and the psychoactive effects of cannabis. OPs have demonstrated to be able to disrupt this system in various ways.

Furthermore in order to inhibit serine hydrolases FAAH and MAGL, OPs block (a) CB1 site(s) (Deutsch et al 1997). Ex vivo studies with mouse brains indicate that OPs inhibit FAAH much more than CB1 and that these targets generally appear to be less important in poisoning than AChE and NTE-LysoPLA (Quistad et al., 2001; Segall et al., 2003).

Indeed, a number of studies have also reported the inhibition of hippocampal ACh release by endocannabinoids (Degroot et al., 2007). A proposed mechanism is: (1) OPs inhibit AChE and (2) ACh accumulation in a brain-regional manner activates CB signaling, which could modulate the degree of ACh.

Chemicals that can enhance CB signaling have been seen to reduce the functional and neurobehavioral signs of toxicity in rats following OP anticholinesterase exposure (Nallapeni et al., 2006; 2008). Similar cholinergic toxicity and AChE inhibition have been observed after the acute treatment of CPF in mice CB1(-/-) and the wild type. However, chlorpyrifos significantly reduces hippocampal ACh release ex vivo in both, but significantly more so in CB1(-/-) (Baireddy et al., 2011). However, current OP insecticides normally used do not appear to pose any cannabinoid-related toxicity problems and further research is ongoing in other directions. Selective and reversible carbamate FAAH and MAGL inhibitors have been designed for pain relief purposes (Long et al., 2009).

UNIVERSITAS
Miguel
Hernández

2. BACKGROUND:

Approaches for detecting molecular targets of OPs

UNIVERSITAS
Miguel
Hernández

2.1 GENERAL VIEW OF PROTEIN TARGETS OF OPs

2.1.1. Cholinesterase and non cholinesterase targets of OPs

The molecular primary target of OPs is AChE. This primary mechanism of action of OPs through AChE inhibition was discovered by DuBois (1948).

Currently it is clear the role of AChE inhibition in mediating toxicity following acute exposures to OP pesticides, but there is increasing evidence that others molecular targets molecules have to be responsible of OPs neurotoxicity. There is a lack of a good correlation between certain behavioral affects and the magnitude and regional selectivity of AChE inhibition and the brain (McDaniel and Moser., 2004).

There is sufficient bibliographical evidence to support the view that OPs also have other noncholinergic targets

1) OPIDN is unrelated to anti-ChE effects; it is clear the relationship between NTE inhibition and OPIDN.

2) The AChE knockout mouse display no AChE activity in any tissue and is supersensitive to OP toxicity (Xie et al., 2000; Duysen et al., 2001; 2002; Lockdridge et al., 2005) and it has been proposed that the target could be BuChE, although this has not been proven.

3) Secondary target effects that are not specific of AChE inhibitors were observed in zebra fish (Behra et al., 2004).

4) Different OP pesticides cause different degrees of toxicity despite similar levels of AChE inhibition (Moser., 1995; Pope., 1999).

5) There is no correlation between AChE inhibition and the disposition of [^{3}H]-soman, [^{3}H]-DFP and [^{3}H]-sarin in the brain; this suggests that in the hypothalamus, targets other than AChE bind to OP (Little et al., 1988).

6) Low doses of OP inhibitors produce distinct effects that depend on the identity of the OP (Moser., 1995).

7) Low levels of chlorpyrifos impaired cognitive function without significantly inhibiting AChE activity and without down regulating cholinergic receptors in rats (Jett et al., 2001).

8) Biotinylated OP FP-biotin labels at least 12 proteins in mouse plasma at doses without cholinergic effects (Peeples et al., 2005).

9) The current strategies adopted to treat acute OP toxicity include early interventions using the anticholinergic agent atropine (to block muscarinic AChE receptor activation), cholinergic re-activators and anticonvulsant drugs, such as

benzodiazepines (Slotkin et al., 2008), do not prevent delayed neurotoxicity from developing.

Many protein systems have the potential to interact with specific OP pesticides and several proteins have been observed to covalently bind to OP in experimental assays *in vitro,* and some of them in *in vivo* experiments. However, the toxicological relevance of these secondary targets (molecular targets not related to their pesticidal activity) is not clear (Lockridge and Schopfer., 2006). Linking these sets of proteins that bind to OP pesticides of toxicological relevance are future research directions and will be useful to help understand the low-dose long-term neurologic and cognitive effects of OP (Lockdridge and Schopfer., 2006; Costa., 2006).

2.1.2. Methods and approaches to identify molecular targets

Several lines of research have been studied in different groups of enzymes as potential targets of OPs, and most have focused on serine hydrolases (see **Section 2.2**). Recently, increasing interest is being shown in the disruption of the cannabinoid system associated with behavioral effects (Long and Cravatt., 2011). Different methods have been used to recognize OP-sensitive enzymes to:

1) Assay the established enzymes (AChE, BuChE, chymotrypsin and arylformidase AFMID) for sensitivity to DFP or other OPs. They were found to vary in OP-sensitivity to OP from nanomolar to high micromolar ranges (Casida and Quistad., 2004; Aldridge and Reiner., 1972).

2) Label tissue preparations with OP inhibitors for target isolation and identification by protein sequencing. This was used for NTE, AFMID and acylpeptide hydrolase (APH).

3) Direct assessment of enzymes activity and inhibition by traditional substrate analysis, using phenylvalerate as a substrate and different OPs as inhibitors (these targets are explained in **Section 2.6**; Sogorb et al., 1994; Escudero et al., 1997; Estévez et al., 2011; Estévez et al., 2012).

4) Create a method that develops the reaction with FP-biotin or an analog to introduce the phosphoryl substituent and biotin for isolation with avidin (Liu et al.,1999; 2001). An important improvement of this method has been introduce with the modern chemoproteomic platform ABPP, Activity-based protein profiling) (Kam et al., 1993), which examines the functional state of serine hydrolases using a fluorophosphonate reactive group conjugated to a spacer arm and analytical handle (rhodamine or biotin), has demonstrated useful for this porpoises in serine hydrolases (Barglow and Cravatt., 2007; Cravat t et al., 1996; Casida and Quistad., 2004; Casida and Quistad., 2005;

Nomura et al., 2008; Nomura and Casida., 2011). This had led to a recent surge of new candidate targets.

Moreover there is increasing evidence to suggest that proteins other than serine hydrolases and other residues can interact with OPs. Tyrosine and lysine residues may provide alternative OP binding sites and may be relevant for numerous proteins. In 1998, Sogorb and colleagues demonstrated that the Tyr-411 of albumin is phosphorylated by HDCP in chicken serum (Sogorb et al., 1998). Recently, it has been suggested that these interactions might be relevant in numerous proteins; e.g., of the neuronal cytoskeleton that exhibits an altered phosphorylation status (Lockdridge et al., 2010), while mass spectrometry approaches have been used to detect the binding of chlorpyrifos oxon, dichlorvos, diisopropylfluorophosphate (DFP) and sarin to human serum albumin. This suggests that this approach might form the basis of a prognostic test of the response to exposure (Li et al., 2007). Similar outcomes were obtained for human transferrin (Li et al., 2009). The covalent interaction of chlorpyrifos with tyrosine residues in tubulin, the core protein of microtubules, has been also observed by mass spectrometry (Grigoryan et al., 2008; 2009).

Final remarks

The importance of performing further proteomics analyses of OP-treated cells and organisms has been emphasized, and will no doubt they will reveal other potential targets of OPs interactions and will help to establish the way in which different OPs affect neural forms and functions. These kind of molecular studies are required to characterize novel OPs targets and their role in toxicity, which can help establish the molecular basis of OP-induced neurodegeneration more fully.

The safety of the continued use of OPs in agriculture and their potential extended use in medicine depend on understanding the relevance of not only AChE inhibition, but also of all these secondary potential targets in the health effects of acute and long-term exposures (Casida and Quistad., 2004). However, currently most safety evaluations of OP insecticides are based on the premise that AChE inhibition is the principal action for both acute and chronic toxicity of individual compounds or mixtures (Casida and Quistad., 2005).

2.2. SERINE-HYDROLASES AS TARGETS OF OPs TOXICITY

The serine hydrolase superfamily is one of the largest and most diverse enzyme classes in mammalian proteomes and it plays key roles in all cells and organisms. Members of this family display serine hydrolase activity: (1) contain a conserved serine hydrolase motif, GXSXG/A, where the serine is the active site that is used for the hydrolysis of substrates and (2) they have an alpha-beta hydrolase fold; which is characterized by a β-sheet core of five to eight strands connected by α-helices to form a α/β/α sandwich showed in **Figure 2.1**. The members of the superfamily alpha-beta hydrolase were defined by structural homology and diverged from a common ancestor based on during evolution structural similarity is preserved much longer than sequence similarity (Lenfant et al., 2013).

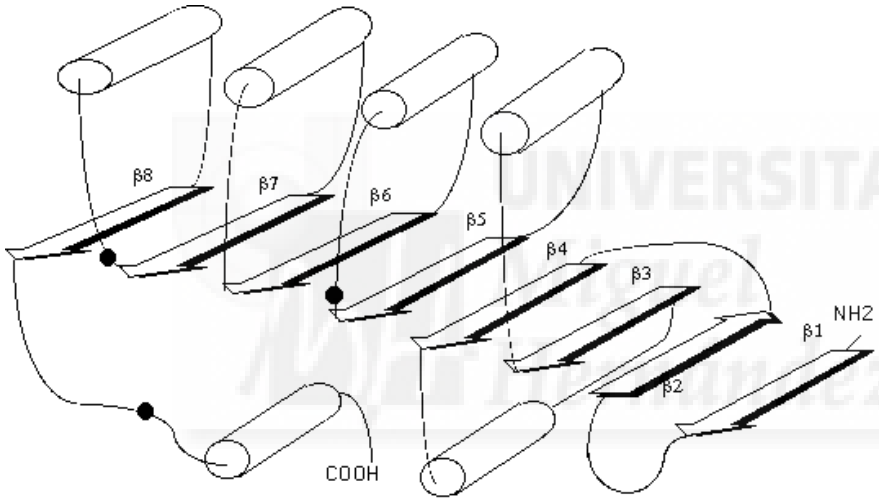

Figure 2.1 Schematic diagram of the α/β hydrolase fold (from Ollis et al., 1992).

There are a wide range of families of hydrolytic enzymes with different substrate specificities, together with other proteins with no recognized catalytic activity. In the enzymes the catalytic triad residues are presented on loops, of which one, the nucleophile elbow, is the most conserved feature of the fold. Of the other proteins, which all lack from one to all of the catalytic residues, some may simply be 'inactive' enzymes while others are known to be involved in surface recognition functions (Lenfant et al., 2013).

There is a long list of potential OP targets in the alpha-beta hydrolase fold superfamily. There are more than 200 just in the serine hydrolases enzyme group in humans, based on genomic evidence. Obviously, this apparent number will change when further knowledge is acquired.

Currently, most of them remain mostly or completely uncharacterized (Long and Cravatt., 2011).

Any serine hydrolase could be sensitive to OPs due to the nucleophilic nature of the serine residue present in these hydrolytic enzymes (Pope., 1999; Pope., 2006). Around 50 catalytic serine hydrolases have been recognized as potential targets of Ops, but only a few of them have been thoroughly studied. The toxicological relevance of known OP targets is established from observations made with humans (AChE, BuChE and NTE), studies into mice (carboxylesterases, lysophospholipase and platelet-activating factor acetylhydrolase) and hen eggs (arylformidase or kynurenine formidase). In safety evaluations, knowledge about known OP targets must be balanced against the major gaps there are in our current understanding because more serine hydrolases are essentially unknown as far as OP targeting and relevance are concerned (Casida and Quistad., 2005).

A few serine hydrolases have been thoroughly studied for their interest in considering OPs toxicology (**Figure 2.2**). Some are membrane-bound (AChE, NTE, and FAAH), while others are cytosolic (BuChE, AFMID, APH).

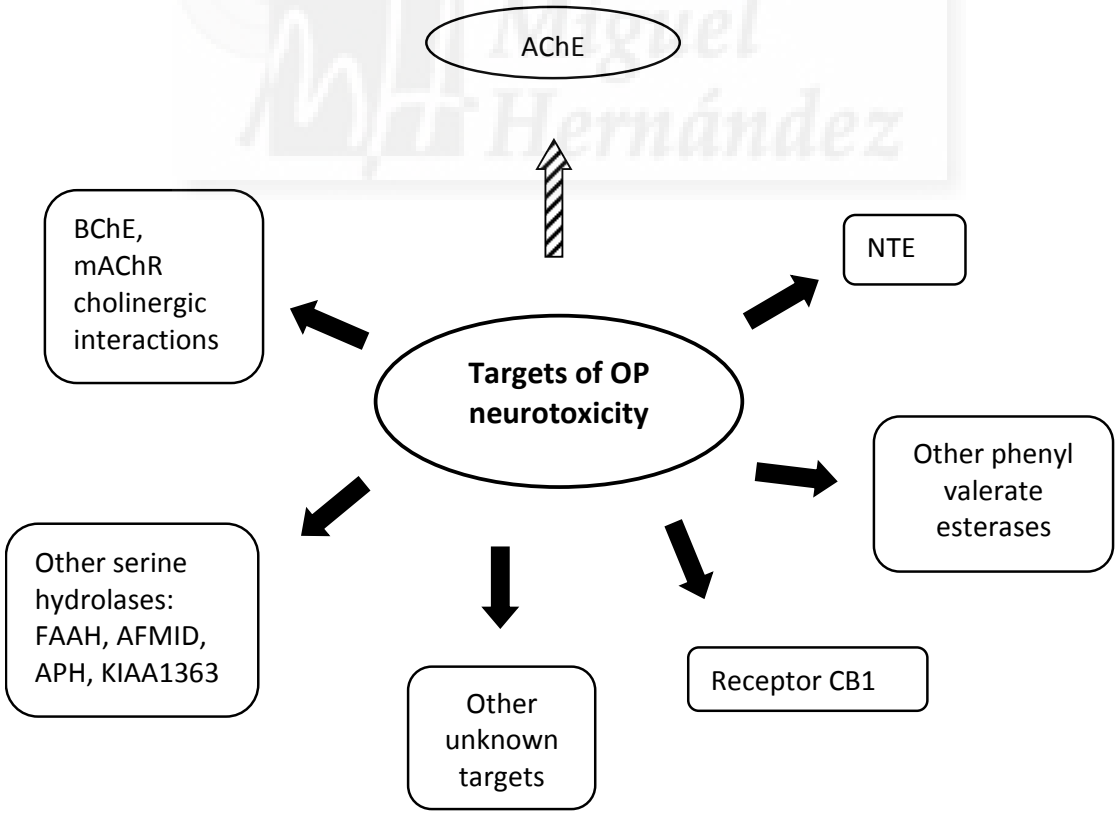

Figure 2.2. Some targets of organophosphorus compounds

Cholinesterases, AChE and BuChE

Cholinesterases are enzymes that are serine hydrolases which hydrolyze the breakdown of acetylcholine (ACh); **Figure 2.2**. Vertebrates are known to have two cholinesterases, acetylcholinesterase (AChE; EC 3.1.1.7) and butyrylcholinesterse (BuChE, EC 3.1.1.8). These two cholinesterases have been differentiated historically on the basis of their substrate selectivity, which has been related from differences in acyl pocket structures (Harel et al., 1992; Kovarik et al., 2003). AChE is known to play a critical role in the termination of ACh action at synapses and neuromuscular junctions, whereas the exact function(s) of BuChE remain(s) unclear. For both, different posttranscriptional forms (isoenzymes) are found, while six different forms have been observed for acetylcholinesterase: globular monomer, dimer and tetramer; tailed tetramer, double tailed tetramer and triple tailed tetramer. Monomer and disulfide-linked dimmer forms may be soluble or attached to a membrane by a glycophospholipid, whereas tetramer forms may be soluble, lipid-linked to membranes or attached to a collagen triple helix.

Numerous potential roles for BuChE or pseudocholinesterase have been suggested, which range from the metabolism of lipoproteins (Kutty and Payne., 1994) to cell adhesion (Tsigelny et al., 2000), a physiological function in thymus (Sanchez-Del-Campo et al., 2007), the etiology of certain neurodegenerative diseases and it is known to be involved in the breakdown of certain drugs, including muscle relaxant drugs (Darvesh et al., 2003).

Inhibition of AChE leads to the accumulation of ACh at synapses and neuroeffector junctions (**Figure 2.3**), which in turn leads to a range of symptoms known as cholinergic crisis, that are explained in **Section 1.3.1**.

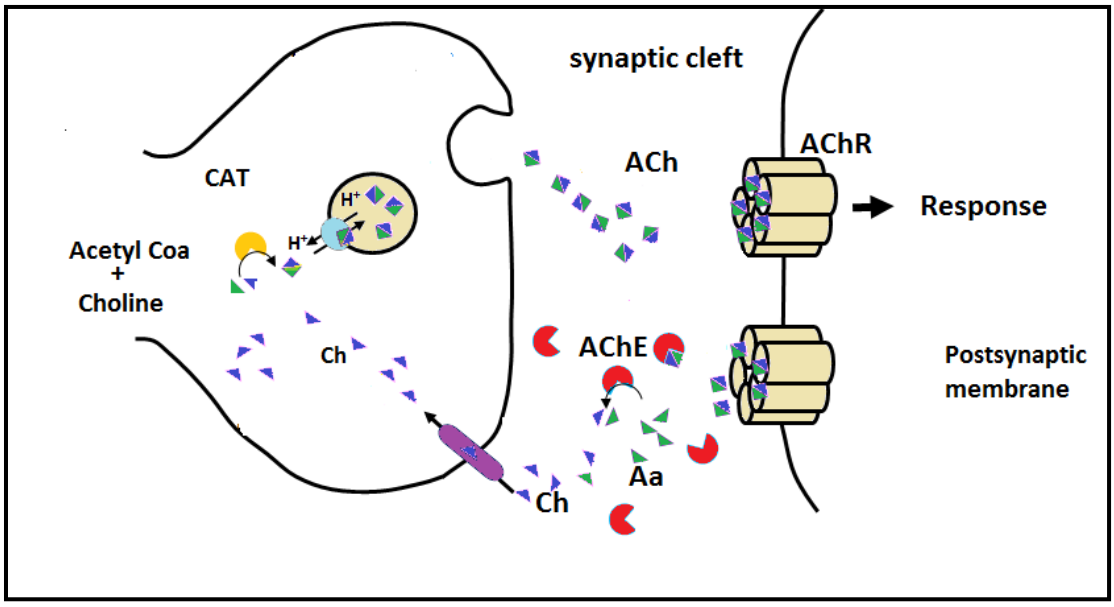

Figure 2.3. AChE function in the synapsis

OPs inactivate cholinesterases by phosphorylating the serine hydroxyl group located at the active site. The active center of AChE was identified and the gene encoding the enzyme wassequenced in 1986 for the enzyme from fish Torpedo californica (Schumacher et al., 1986). Five years later, the first three-dimensional structure of a cholinesterase was solved (Sussman et al., 1991). In the present-day, 170 three-dimensional structures of AChE are available, with 68 for BuChE.

Figure 2.4 represents the crystal structure and the active center of aged phosphonylated acetylcholinesterase inhibited by sarin active center of Tc AChE, as observed by X-Ray crystal structures of aged phosphonylated acetylcholinesterase: nerve agent reaction products at the atomic level (Millar et al., 1999). Phosphorylation occurs by loss of an OP leaving group and by the establishment of a covalent bond with the serine of the so-called catalytic triad of AChE (Gibney et al., 1990). Of the approximately 50 serine residues found in cholinesterases sequences, only one is directly involved and essential in catalysis, Ser200. The Ser200 is conserved in 124 of the 125 AChE available sequences. Residues His440 and Glu327 have been identified as the remaining two elements of the catalytic triad (**Figure 2.4**). Substitution of His440 Gln in T. californica AChE yielded an inactive protein (Gibney et al., 1990; Radic and Taylor., 2006). This reaction results in the formation of a transient intermediate complex that partially hydrolyzes with the loss of the Z substituent group, leaving a stable, phosphorylated and largely unreactive inhibited enzyme that can be reactivated at only a very slow rate. The reactivation of phosphorylated AChE can be accelerated by certain compounds that are more nucleophilic than water, such as pralidoxime [N-methyl.(2-hydroxyaminoformylpyridinium)chloride] or obidoxime (bis[4-

hydroxyaminomethylpyridinium] ether dichloride), and by other experimental reactivators, such as HI-6 [1-(2-hydroxyiminomethyl-1-pyridinium)-1-(4-carboxyaminopyridinium) dimethyl ether hydrochloride] or TMB4 [1,1´-trimethylene bis(4-(hydroxyimino)-methyl) pyridinium dibromide];(Rousseaux and Dua., 1989).

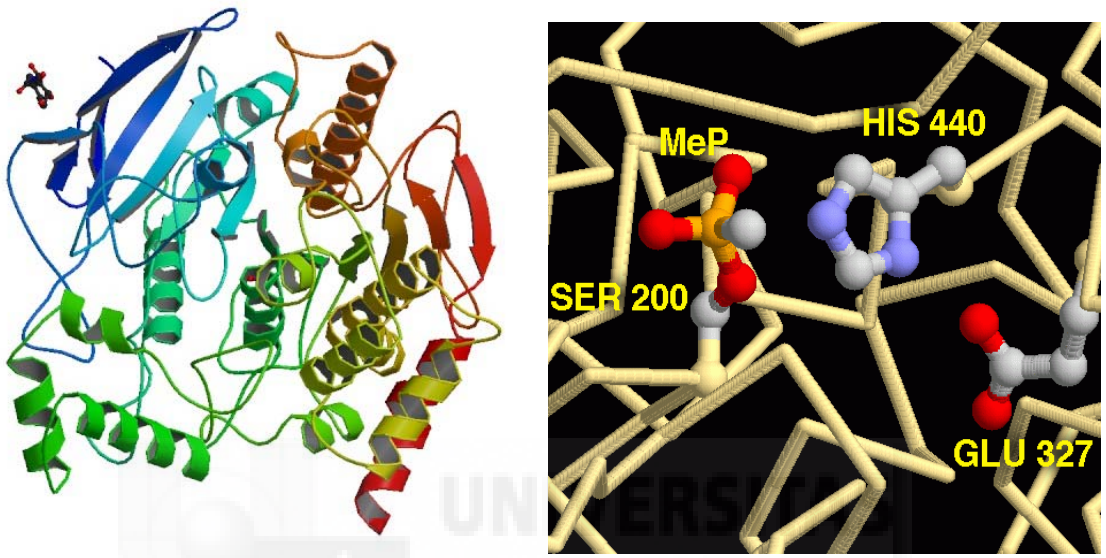

Figure 2.4. Crystal structure and representation of the active center of aged phosphonylated AChE inhibited and aged by sarin. Obtained from Protein Data Base (Millar et al., 1999).

Several OP esters have the ability to bind strongly to the active site of cholinesterases to produce an irreversibly inhibited enzyme by a mechanism known as aging through the loss of an alkyl group from the phosphyl alkoxy substituent. The remaining negatively charged monophosphylate ester of serine is resistant to reactivation by nucleophilic oximes (Aldridge and Reiner., 1972). The specific molecular events that lead to aging are not known with certainty and resistance to reactivation has been attributed, at least in part, to two possible mechanisms. The first is an aging-induced change of the inhibited enzyme, resulting in increased stability. The second, aged ChEs, may electrostatically repulse oximes as a result of the negatively charged oxygen of the monophosphylate moiety and the negatively charged Glu100 (Masson et al., 1997).

The role of the OP structure in AChE inhibition has been studied intensively. Systematic studies with paraoxon (diethyl p-nitrophenylphosphate) and similar substituted phenyl phosphates have shown that their anticholinesterase activity is a direct function of their alkaline hydrolysis rates, which reflects phosphorus reactivity (Fukuto., 1990).

The deletion of AChE in Drosophila through mutagenesis results in embryonic lethality (Greenspan et al., 1980). Yet AChE-/- mice survive over 1 year when fed on a liquid diet, thereby providing a unique model for studies into the cholinergic system and its importance in OPs toxicity (Xie et al., 2000, Duysen et al., 2002). Mice suffer from pulsating paws, pinpoint pupils, body tremors, a film of white mucus on eyes when handled, and lack of grip strength (Duysen et al., 2002, Duysen et al., 2001). BuChE is an obvious candidate to take over in mice lacking AChE. BuChE activity is the same in various tissues of wild-type and nullizygous mice (Li et al., 2000). It is thought that BuChE may hydrolyze excess Ach as the postsynaptic membrane or that it may be involved in a presynaptic modulatory step of the Ach release process. It seems that BuChE is essential to survival peripherally, but not centrally, in AChE-/- mice (Chatonnet et al., 2003). However, AChE-deficient mice still suffer from cholinergic symptoms, so not enough Ach is being hydrolyzed.

Although BuChE inhibition by these compounds has not been shown to result in a specific adverse event, BuChE is considered to represent an important non enzymatic pathway for the detoxification of anticholinesterase compounds, and is often used as a biomarker of OP exposure.

BuChE was the first secondary target in OP poisoning to be recognized and continues to be of interest as a way to monitor OP exposure by determining plasma activity inhibition. It is generally more sensitive to OP esters than AChE. Ethephon inhibits plasma BuChE with no apparent ill effects on mice, rats, dogs and humans (Haux et al., 2002, Haux et al., 2000). Animals with inhibited BChE are of enhanced sensitivity to succinylcholine, mivacurium and aspirin (Sparks et al., 1999). The potency of cocaine in humans and lethality in mice are enhanced by OP pesticide BuChE inhibition (Herschman et al., 1991, Hoffman et al., 1992). The functions of BuChE will be better understood when it is possible to study BChE-deficient mice, but it is already evident that it serves as a possible peripheral target in OP poisoning and as a scavenger in reducing OP toxicity. It has been well-established that cholinesterases, particularly BuChE, are associated with the pathogenesis and progression of AD (Guillozet et al., 1997; Darvesh et al., 2003).

NTE, lysophosphatidyl choline hydrolase

NTE was discovered in the late 1960s by M.K. Johnson (Johnson., 1969a; 1969b) thanks to his quest to identify the target protein for the initiation of OPIDN, a central-peripheral distal axonopathy. NTE was originally identified as a set of sites in chicken brain homogenates which either reacted with radiolablled di-isopropylfluorophosphate (DFP) or hydrolyzed a phenolic ester: the portion of the labeling or esterase activity, which was resistant to a non neuropathic OP, but sensitive to a neuropathic one, was defined as NTE (Johnson 1969a; 1969b; 1977). NTE is monitored operationally as that esterase activity which hydrolyzes the artificial substrate phenyl valerate (PV), which is resistant to the non neuropathic OP ester paraoxon, 40 μM, 20 min, pH 8.0, and is sensitive to the neuropathic OP ester mipafox, 250 μM, 20 min, pH 8.0, (Johnson 1969a). The next step was to add an ester instead of a radiolabeled neuropathic OP compound to the paired samples which had been preinhibited differentially with neuropathic OP compounds or neuropathic, plus non neuropathic OP compounds. The initial substrate choice was phenyl phenylacetate (PPA). Titration of radiolabeling by preincubating brain homogenates with neuropathic OP compounds correlated with the titration of PPA esterase activity, and the inhibition kinetics of the neurotoxic protein, or ”neurotoxic esterase”, exhibited the characteristics of a single enzyme. The further refinement of the assay yielded phenyl valerate (PV) as the substrate of choice (more specific than PPA and yields a higher proportion of total esterase activity; Johnson., 1974).

Decades after its operational definition as an esterase activity that remains after differential inhibition by neuropathic and non neuropathic inhibitors, a physiological function of NTE was sought. NTE was purified by Glynn in 1994 (Glynn et al., 1994) and its encoding gene was identified (Glynn et al., 1998; 1999). Now we know that NTE (E.C. 3.6.2) is the mammalian homolog of the Drosophila gene swisscheese and is an integral membrane enzyme of around 150 KDa that is anchored to the endoplasmic reticulum by an N-terminal transmembrane domain. NTE is the 6th member of a 9-protein family called patatin-like phospholipase domain-containing proteins, PNPLA1–9. NTE is a large protein comprising 1327 amino acid residues with its active site residue at Ser966. Mutagenesis studies have indicated that the catalytic site might be a triad consisting of Ser966 and two aspartames, Asp960 and Asp1086 (Atkins and Glynn., 2000; Li et al., 2003; Kienesberger et al., 2009). There is a transmembrane domain near the N-terminus that anchors the protein to the endoplasmic reticulum membrane, and three homologous tandem domains to cyclic nucleotide-binding proteins, suggesting a possible regulatory or signal transduction role. PNPLA 6 is highly expressed throughout the brain, peripheral nerve and some cells (Pamies et al., 2010). A truncated form of PNPLA 6 (NTE), containing the esterase domain, has been shown to hydrolyze phospholipids and lysophospholipids (Glynn., 2005).

Studies have shown that the knockout of NTE is embryonic lethal (Winrow et al., 2003), probably due to impairment of vasculogenesis in the placenta (Moser et al., 2004), and when localized to the hippocampus, it gives vacuolation of neuronal bodies and dendrites (Akassoglou et al., 2004). A peak in gene expression has been demonstrated in the early cell differentiation stage (Pamies et al., 2010). NTE(+/-) mice survive, but exhibit increased sensitivity to an acute effect of OP compounds, which is distinct from OPIDN. Diminished NTE activity in mice links OP exposure to hyperactivity (Winrow et al., 2003), but not necessarily to attention deficit disorder in humans (Casida and Durkin., 2013). Conditional knockout of CNS NTE leads to neurodegeneration (Akassoglou et al., 2004; Read et al., 2009; 2010), demonstrating that the absence of NTE protein and its associated enzymatic activity in this scenario can precipitate neurological disease. It has been shown that either genetic or chemical inactivation of NTE activity in mice causes axonal damage and leads to the accumulation of phosphatidylcholine (Read et al., 2009). However, the impairment of these functions is not critical to induce neuropathy since non neuropathic compounds inhibit this activity.

Recently our group silenced Pnpla6 in embryonic bodies of mice and a microarray analysis of the whole genome was done; 545 genes were modified 96 h after silencing, which revealed alterations in multiple genetic pathways, such as cell motion and migration, vesicles regulation and cell adhesion, which confer mechanistic support to in vivo observations. Altered pathways impair the formation of respiratory, neural and vascular tubes to cause the observed deficiencies in nervous and vascular systems development (Pamies et al., 2013). Moreover, mutations have been discovered in the catalytic domain of NTE that are linked to a form of motor neuron disease which resembles hereditary spastic paraplegia (Rainer et al., 2008; Rainer et al., 2011). This subset of motor neuron diseases has been named NTE-motor neuron disorder, which involves a slow-developing motor axonopathy, attendant muscle wasting and paralysis with similarities to OPIDN.

Most of the work done to date on NTE has focused on its catalytic function as an esterase, and more recently as a phospholipase and lysophospholipase. Future studies should extend the scope of work to encompass the cyclic nucleotide-binding domains and their possible role in the regulation of NTE or its interacting partners, which have yet to be defined (Richardson et al., 2013).

KIAA1363 protein

KIAA1363, an acetyl monoakyl glycerol ether hydrolase, has been established as the primary brain detoxifying enzyme for chlorpyriphos oxon (Nomura et al., 2005). KIAA1363 null mice demonstrate that KIAA1363 partially protects brain AChE from in vivo inhibition by CPO. KIAA1363 knock-out mice were also found to be more sensitive to intraperitoneally administered chlorpyrifos and parathion than wild mice (Nomura et al., 2006; Nomura et al., 2008). KIAA1363 first appears on a list of predicted proteins based on the human genome (Nagase et al., 2000). KIAA1363 is a membrane-bound protein of about 50 KDa that plays a regulatory role in ether lipid metabolism.

MAGL (monoacylglycerol lipase) and FAAH (fatty acid amide hydrolase)

ABPP and substrate hydrolysis assays reveal that some OPs are MAGL and FAAH inhibitors that act at 0.1-1 nM in vitro and at 1-10 mg/kg in vivo (Nomura and Casida., 2011, Pope., 2006). MAGL was characterized first in adipose tissue, which is important for fat mobilization (Segall et al., 2003), and subsequently in the brain, and is involved in 2-AG hydrolysis for endocannabinoid inactivation. It is a membrane-bound cytosolic protein with a suggested alpha/beta hydrolase fold, a GXSXG motif, a typical catalytic triad (S122-D239-H269). The OP sensitivity of FAAH was first shown with methyl arachidonylfluorophosphonate (MAFP) and the rat brain enzyme (IC50 =2.5 nM) (Deutsch et al., 1997). FAAH hydrolyzes the endocannabinoid arachidonyl ethanolamide (anandamide) and the endogenous sleep-inducing agent oleamide (Nomura et al., 2008). The behavioral effects of some OPs have suggested the possible involvement of the cannabinoid system, while it has been discovered that serine hydrolases FAAH and MAGL are sensitive to chlorpyrifos and profenofos in vivo in mice (Nomura et al., 2008; Nomura and Casida., 2011).

AFMID, kynurenine formamidase

AFMID (arylformamidase), also known as kynurenine formamidase, is a 303-amino-acid serine hydrolase protein belonging to the AFMID family. Many OPs and a few methylcarbamates are avian teratogens; that is, they induce severe developmental abnormalities, including malformation of lower extremities (micromelia) and abnormal feathering when injected into chicken eggs on incubation days 4-6 (Roger et al., 1964, Seifert et al., 1981). The biochemical target has been defined by three observations in chicken eggs (Seifert et al., 1981). First, nicotinic acid, nicotinamide, and metabolic precursors partially to completely protect against or ameliorate abnormalities (Roger et al., 1964). Second, the severity of teratogenic signs is correlated with a lowering embryo NAD level (Proctor et al., 1975). Finally, the primary lesion

is an inhibition of AFMID (Moscioni et al., 1977). AFMID in birds and mammals is very sensitive to many OPs diazinon, diazoxon, and monocrotophos and some methylcarbamates. Potential OP teratogenesis is much more prominent in birds than mammals, partly because embryogenesis in birds requires yolk tryptophan conversion into nicotinic acid, unlike a dietary vitamin source in mammals (Seifert et al., 1981).

APH, Acylpeptide hydrolase

APH is the most sensitive enzyme in the rat brain to phosphorylation by [3H] DFP. APH hydrolyzes the N-terminal-acetylated amino acid residue on peptides and its activity is inhibited by the OPs (chlorpyrifos, methyloxon, dichlorvos and DFP) with IC50=18-119 nM (6-10-fold greater sensitivity as compared to AChE; Richards et al., 2000). APH is not an alternate target for OP acute lethality since <40% is inhibited in AChE-/- . However the effects of long-term in vivo APH inhibition remains unknown, although it has been proposed as a possible target of pharmacological significance for cognitive-enhancing drugs (Richards et al., 2000).

Other serine hydrolases

In addition to these above considerations, The ABPP analysis of the brain proteome from chlorpyrifos oxon and IDFP-treated mice shows that chlorpyrifos oxon inhibits ABHD3, an acyl-amino acid-releasing enzyme (AARE), carboxylesterase-N (CE-N), and hormone-sensitive lipase (HSL), while IDFP inhibits all these targets, plus ABHD6 OP-detoxifying hydrolases (Nomura et al., 2008).

2.3. OTHER NON SERINE ESTERASE TARGETS

2.3.1 Mitochondrial enzymes

Several studies have suggested that OP exposure can result in structural changes and impairment in the activity of a range of key mitochondrial enzyme activities such as succinate deshydrogenase, NADH dehydrogenase and cytochrome oxidase (Masoud et al., 2009). It has been observed that OPs can disrupt metabolism, mitochondrial membrane organization and respiratory activity, leading to apoptotic cell death in cultured neurons.

2.3.2. Muscarinic receptors, other cholinergic components

Muscarinic receptors (mAChRs) are G-protein-coupled receptors of five subtypes (M1, M2, M3, M4 and M5). OPs have several mAChR-mediated effects in vivo in rats or guinea pigs. Rat heart M2 and brain mAChRs are sensitive to many OP anticholinesterases at 1-100 nM (Bomser and Casida., 2001; Howard et al., 2007). Heart and brain M2/M4 mAChRs are sensitive to OPs in vitro and in vivo by direct action and as an indirect response to elevated ACh levels. M2 are the primary subtypes in the heart that regulate muscle contraction. The muscarinic effects of ACh can be blocked by atropine, which therefore serves as an antidote for OP poisoning. It is difficult to evaluate and to interpret the toxicological relevance of these muscarinic effects because of the coupling to complex signal transduction systems (Bomser and Casida., 2001).

2.4. PHENYL VALERATE ESTERASES THAT INTERAC WITH OPs

2.4.1. Serine protein target of OPs detected as phenylvalerate esterase

Identifying an enzyme merely by its behavior toward inhibitors is a long way from understanding its catalytic capacity or physiological function. However is an alternative approach to solve these difficulties (Johnson 1969a) and is a useful method to follow the activity during protein purification methods. In 1963, Ramachandran and colleagues separated numerous liver esterases after unselective labeling by [32P] DFP (Ramachandran et al., 1963). In 1964, Aldridge showed that there were several esterases in chicken central nervous tissue that are inhibited by low concentrations of phenyl saligenin phosphate and DFP, which hydrolyzed the phenyl ester 1-phenylacetic acid (Poulsen and Aldridge, 1964; Aldridge, 1964). Johnson identified a fraction of the phosphorylation site of [3H]DFP in the hen brain as the target of OPIDN in 1969.

Phenyl valerate is a carboxylic ester that has been used as a substrate to detect NTE and other OPs sensitive esterases. It has also been utilized as a substrate of other esterases such as fungal enzyme proteinase K (EC 3.4.21.14) (Borhan et al., 1996).

Other carboxylesterases that hydrolyze phenyl valerate and that are sensitive to OPs have been observed by adopting the same operational criteria used to discriminate NTE. Distribution of Phenyl valerate esterase activities sensitive to OPs was measured in brain, spinal cord and sciatic nerve in homogenate, soluble and particulate fractions in chicken (Escudero et al., 1997a; 1997b). Afterward, the discrimination of sensitive components in chicken brain, spinal cord and sciatic nerve in soluble fractions was done with paraoxon (as a non neuropathic OP model), mipafox (as a neuropathic OP model) and PMSF (as a model of the inhibitor potentiator of neuropathy; Céspedes et al., 1997). To discriminate NTE from other PVases, two different assays were designed: a concurrent assay where paraoxon and mipafox together were incubated with the test compound (DFP, PMSF, or DFP), and a sequential assay where each inhibitor was added after the one before (Vilanova et al., 1999). These early studies were able to discriminate at least four different carboxylesterases components in the brain membrane, six in the membrane spinal cord, six in the membrane sciatic nerve, three in the soluble brain fraction, five in the soluble spinal cord and four in the soluble fraction of chicken sciatic nerve. The interest shown in esterases of the chicken nervous system using phenyl valerate as a substrate stems from studies into OPIDN and promotion (Céspedes et al., 1997).

2.4.2. Two different NTE forms

Whole brain has been the tissue assayed in most species to find NTE. NTE activity was first assayed with Johnson´s differential assay, also called a "conventional" or concurrent assay (inhibition by 40 µM paraoxon or by 40 µM paraoxon, plus 50µM mipafox, respectively, for 40 min at 25ºC using phenyl valerate as a substrate). Chemnitius and colleagues used a slightly modified version of Johnson´s assay (the sequential assay), in which paraoxon was removed by centrifugation and then mipafox was added. Using this approach, Chemnitius and colleagues kinetically determined two isoenzymes in hen brain with NTE activity and they called them (NTEA and NTEB) using homogenized brain in 1983. However they were unable to identify these two isoenzymes by the conventional assay (Chemnitius et al., 1983). NTEA (was around 20% of NTE activity) and it was inhibited at a faster rate by mipafox than the major specie NTEB. In 1985, Carrington and Abou-Donia suggested that this discrepancy of apparent two forms of NTE was an artefact that can be explained due to a reversible interaction of paraoxon to NTE (Carrington and Abou-Donia., 1984; Carrington and Abou-Donia., 1985).

2.4.3. Spontaneous reactivation

A comparison of the concurrent and reverse-sequential inhibition protocols has shown that paraoxon brings about marked interferences in the interaction of mipafox and other test compounds with S-NTE (Barril and Vilanova., 1997). These interferences have been explained to be a spontaneous reactivation after paraoxon inhibition on some phenyl valerate esterases when paraoxon is removed. Between 65% and 100% of the phenyl valerate esterase activity of chicken peripheral nerve was spontaneously reactivated (Barril et al., 1999; Estévez et al., 2011), as was almost 100% of phenyl valerate esterase activity in chicken serum (Garcia-Pérez et al., 2003) after removing the paraoxon progressively. This reactivation of paraoxon-inhibited PVase activity is an important, practical consequence: the use of paraoxon as a tool for discriminating irrelevant esterases has been deemed inappropriate to discriminate paraoxon irreversibly resistant and mipafox sensitive esterases.

2.4.4. Soluble NTE-like enzymatic activities: SNTE1 and SNTE2

NTE has been considered a membrane-bound protein obtained mainly in the microsomal fraction. The subcelullar distribution of NTE with no solubilization additive in different chicken nervous system tissues was studied and NTE activity was found in the soluble form using the same operational criterion of around 2% in chicken brain. The subcellular distribution of NTE

activity in the sciatic nerve was very different than in the brain (Vilanova et al., 1990). Following centrifugation, 50% of activity was found in the supernatant, and this activity was called S-NTE (Vilanova et al., 1990; Tormo et al., 1993). SNTE was also found in cats and rats (Tormo et al., 1993).

Later, total phenyl valerate esterase activity from the soluble peripheral nerve fraction was distributed into three separate peaks when subjected to gel filtration chromatography via Sephacryl S-300. Two of them fitted the operational criteria of NTE, and the NTE activities within these peaks were termed S-NTE1 (V0 peak) and S-NTE2 (100 KDa peak) (Escudero et al., 1995). A similar pattern was obtained, but with a lower proportion of SNTE2 in the spinal cord soluble fraction, but in the brain, only one peak containing S-NTE1 was obtained (Escudero et al., 1997). SNTE1 was deduced to be NTE partly solubilized from membranes at a higher pH. Two observations support this hypothesis: (1) SNTE1 activity decreased when the different nervous tissues were homogenized and centrifuged at pH 6.8 instead of pH 8; (2) SNTE1 (4.7μM) sensitivity to mipafox was comparable to the NTE sensitivity found in particulate fractions (5.5-7.7 μM; Vilanova et al., 1999). Afterward a second purification step in HPLC was done by weak anion exchange chromatography (Protein-Pak DEAE 8HR 10 MM). The fractions containing greater specific activity were collected and a 96-fold purification for total PVase activity and a 218-fold for SNTE2 were achieved (Escudero et al., 1997).

The toxicological meaning of these enzymatic activities, operationally called soluble NTE, remains unknown.

2.4.5. Phenyl valerate esterases other than NTE are sensitive to organophosphates in chicken sciatic nerve

Chicken sciatic nerve soluble fraction has been demonstrated to contain a high level of PVase activity, 1432±131 nmol phenol/min/g fresh tissue, n=7 (Gargía-Pérez et al., 2003). An automatable microassay method was developed and optimized to measure NTE and totalphenyl valerate esterase activities in a simple assay using the automated workstation Biomek 1000. This system can be used to measure enzymatic activities in tissues with very limited activity or availability or when a large number of samples has to be processed, and it reduces the time of manual assays. This method can also be used to measure enzymatic activities which yield phenols and chlorophenols as reaction products, and to assay phenyl valerate esterase activity of hen sciatic nerve: three PVase activities have been defined: activity A (total PVase activity), activity B (paraoxon-resistant PVase activity), activity C (PVase activity resistant to 40 μM paraoxon and 250 μM mipafox; Escudero et al., 1997a).

Using an adapted method of this microassay kinetic studies were performed on the total phenyl valerate esterase in soluble fraction of chicken sciatic nerve using the following inhibitors: mipafox, as a inducer of OPIDN (Estévez et al., 2004), paraoxon as a non-inducer of OPIDN (Estévez et al., 2011), PMSF, as a protector/promoter of OPIDN (Estévez et al., 2011) and S9B, the inhibitor model used to identified and isolated NTE (Estévez et al., 2011). High sensitive esterase activity was detected at the level of nanomolar.

This kinetic analysis has validated a method to assay such enzymatic activities in complex multienzymatic systems where different kinetic reactions are concomitant. These model equations and kinetic reactions are reviewed in Section 3. Furthermore, new mathematical processing for the kinetics of esterases inhibition by OPs consisted in the direct 3D fitting of residual PVase activity versus not only inhibition time, but also inhibitor concentration has been developed. This three-dimensional method permits all the data to be used in one step to obtain an overall estimation of the influence of low and high inhibitor concentrations simultaneously, as well as low and high inhibition times. The model was validated against a multi-step approach in which each parameter was obtained under "the best" condition to prove the consistency of the applied model's appropriateness (Estévez et al., 2004).

Mipafox for up 180 min inhibited 85% of PVase activity (Table 2.2). The kinetic behavior deduced from inhibiting peripheral nerve soluble PVases with mipafox was compatible with the existence of at least three independent enzymatic entities: E2= 47.8% and E1=36.6% with k2= $2.6 \cdot nM^{-1}$ min^{-1} and k1= 0.28 nM^{-1} min^{-1}, respectively, with the third being resistant to the highest mipafox concentration used with an amplitude of 15.6% (Estévez et al., 2004).

When using ***paraoxon*** as an inhibitor up to 200 nM up to 180 min, almost 90% of the phenyl valerate esterase activity of the soluble fraction of chicken peripheral nerve was inhibited (**Table 2.2**. mipafox column). Kinetic behavior was compatible with a resistant component, R=22%, and also with two highly sensitive enzymatic entities, E1=37 and E2=41%, the corresponding second-order rate constants of inhibition, k1= $1.8 \cdot 10^{-3}$ nM^{-1} min^{-1} and k2= $5.1 \cdot 10^{-3}$ nM^{-1} min^{-1}, respectively. Spontaneous reactivation was observed after removing the inhibitor by ultrafiltration up to a level of 60% in around 180 min. The kinetic model also allowed to establish the spontaneous reactivation constants for the two components kr1= 0.428 min^{-1} and kr2= 0.011 min^{-1}, respectively (Estévez et al., 2011).

S9B, a biotinylated OP, 1- (saligenin cyclic phosphor)-9-biotinyldiaminononane, which has been used for the detection, labeling and isolation of NTE, was used to inhibit the complete PVase activity of chicken sciatic nerve. Nanomolar concentrations of S9B inhibited PVase activity totally and three sensitive enzymatic entities were discriminated with E1=33, E2=52 and

E3=15%, indicating NTE-like esterases. The corresponding second-order rate constants of inhibition were k1= 116·nM^{-1} min^{-1}, k2= 1.6·nM^{-1} min^{-1} and k3= 0.28·nM^{-1} min^{-1}, respectively. The first component was spontaneously reactivated with the second-order rate constant of inhibition, k1r= 0.0054 min^{-1}. These kinetic studies allowed a kinetic model to be validated in which the "ongoing inhibition" or inhibition during the substrate reaction time (**Section 3.6** and **3.7**) has been considered (Estévez et al., 2009).

PMSF is the sulfonylfluoride inhibitor model protector/potentiator of OPIDN. This compound is spontaneously hydrolyzed in Tris pH 8.0 solutions (James., 1978), so it progressively disappears and the inhibition rate lowers until it stops when the inhibitor concentration comes close to zero. Another kinetic model is required when the esterase inhibition and the spontaneous hydrolysis of PMSF are considered to occur simultaneously (**Section 3.6** and **3.7**). The best-fitting model was compatible with a resistant component (E3=16.5–18%) and with two sensitive enzymatic entities (E1 and E2, both of 41%). The corresponding second-order rate constants of inhibition (*ki*=12.04·10^{-5} and 0.54·10^{-5} nM^{-1}·min^{-1}, respectively) and the chemical hydrolysis constant of PMSF (*kh*=0.0919 min^{-1}) have been simultaneously estimated using this kinetic model (Estévez et al., 2012).

When globally considering all the data, three different phenyl valerate esterase components were discriminated in the soluble fraction of chicken peripheral nerve using four inhibitors (paraoxon, mipafox, PMSF and S9B*)*. Chicken sciatic nerve PVases activity was highly sensitive to all the inhibitors. Consistently, the same number of components and similar relative amplitudes were found in the different experiments done with the four inhibitors. The consistency of the results of all the experiments has been considered an appropriate internal validation of the methodology. **Table 2.1** offers the kinetic parameters with the inhibitors model. It has been suggested that these esterases may play potential roles in toxicity and/or detoxication during low-dose long-term exposure to organophosphorus compounds, which warrants further research (Barril et al., 1999; Garcia et al., 2003; Estévez et al., 2011). These highly sensitive enzymes, if compared with other esterases such as NTE (Milatovic et al., 1997), might be related with the OPIDN potentiation effect, and this phenomenon may prove significant to improve our understanding of the potential neurotoxicological consequences of the exposure to environmental pollutants that are not regarded as neurotoxicants (Estévez et al., 2012).

Table 2.1. Phenyl valerate esterase enzymatic components in the soluble fraction of chicken peripheral nerve soluble fraction and serum.

TISSUE	Amplitude	Paraoxon I50 (30 min)	Mipafox I50 (30min)	PMSF I50 (30min)	S9B I50 (30min)
Peripheral nerve(*)					
E1	33-42%	0.24-0.26 nM (r)	69-71 nM	6.8-17 µM	0.20 nM (r)
E2	41-52%	6-12 nM (r)	11-12 nM	0.58-0.77µM	5 nM
E3	10-22%	R	R	R	83 nM
Serum (#)					
E1	36-37%	0.43 nM (r)	110 nM	no data	no data
E2	72-75%	13.7 nM (r)	3.6-4 nM	no data	no data
E3	5.0-5.6%	R	R	no data	no data

(*)Extracted from (Estévez et al., 2012); (#) Extracted from (García-Pérez et al., 2003); ***(r)*** *the component is spontaneously reactivated after removing the inhibitor.*

2.4.6. Semifractionation of phenyl valerate esterases that are sensitive to OPs in chicken sciatic nerve

The profile of phenyl valerate esterase activity was semifractionated by two preparative chromatography steps: first exclusion molecular chromatography, where two peaks of phenyl valerate esterase activity were separated and called S1 and S2; second, anionic exchange chromatography, where activity was separated into six peaks called S1Q1 and S1Q2 from S1; and S2Q1, S2Q2, S2Q3 and S2Q4 from S2. S1-Q1 contained mainly E1; S2-Q1 and S2-Q2 activity, which was mipafox-sensitive with a mixture of the two components (E1+E2), while S2-Q3 and S2-Q4 contained mainly resistant activity (E3, **Table 2.1**). It was concluded that the different kinetic components in the soluble fraction are actually due to several molecular entities that can be separated by preparative chromatography (Estévez et al., 2004). However, it was not possible to separate a fraction which contained activity corresponding to just one enzymatic component

2.4.7. Phenyl valerate esterases other than NTE are sensitive to organophosphates in chicken serum

Chicken serum has been demonstrated to contain a high level of PVase activity, 1347±65 nmol phenol/min/ml serum, n=8 (Gargía-Pérez et al., 2003). Kinetic inhibition studies were performed in this tissue with paraoxon and mipafox ,and reversibility of inhibition was studied with chicken serum. Phenyl valerate esterase activity was extremely sensitive to paraoxon and mipafox (**Table 2.1**) at the nanomolar concentration level, and some fractions were lower than nanomolar, at around 100 times lower than AChE or NTE. Moreover this activity extensively shares similarities with the previously reported properties for the soluble fraction of chicken peripheral nerve (**Table 2.1**). After paraoxon inhibition, a 100%recovery of the activity was observed after removing paraoxon by ultrafiltration, and activity was not recovered after mipafox inhibition. These phenyl valerate esterases of serum have been proposed to be biomarkers of low levels of OP exposure because of their greater sensitivity to OP as compared with AChE inhibition, and the PVases of serum well reflect the inhibition of peripheral nerve system-based soluble esterase by compounds with potential clinical monitoring and in *in vivo* experimental studies. Inhibition of serum esterases has been proposed as a non destructive biomarker of biomonitoring the exposure of wild fauna (García-Pérez et al., 2003; Estévez et al., 2011).

2.5. SUMMARY AND REMARKS

OPs are a large, diverse class of chemicals that has been used for several purposes (pesticides, warfare agents, flame retardants, ectoparasiticide, etc.). Despite the reduced amount of OPs pesticides being used, currently OPs continue to be one of the most important classes of insecticides. The cast majority of the world's population has been exposed to low-medium levels of OP. Moreover, some are used for other industrial purposes and as an investigation drug to treat Alzheimer´s disease.

OPs can cause several neurotoxic disorders: acute cholinergic toxicity caused by the covalent organophorylation of AChE; OPIDN caused by the inhibition and subsequent aging of the membrane protein NTE, whose mechanism is not completely understood; long-term neurobehavioral and neuropsychological consequences have been associated with low-medium levels of exposure to OP in an increasing number of epidemiological and animal studies, which cannot be explained by known targets; the potentiation of neuropathy is a neurotoxic effect caused by some esterase inhibitors, including some OPs and other compounds like PMSF, whose neurotoxicity is enhanced when potentiators are administered to hens following a low dose of a neuropathic OPs.

Many enzyme systems have the potential to interact with OPs, and elucidating the nature and functional significance of the OP-sensitive pool of esterases in the CNS is an important research task. Kinetic models have been developed and applied to detect OP-binding enzymes in complex biological preparations. These models consider multi-enzymatic systems with inhibition, spontaneous reactivation, chemical hydrolysis of inhibitor and ongoing inhibition (inhibition during the substrate reaction time).

In this work, the phenyl valerate esterases of chicken brain have been studied. The kinetic behavior of these esterase components has been discriminated with mipafox (as an OPs model inducer of OIPDN), paraoxon (as an OPs model non inducer of neuropathy) and phenylmethyl sulfonyl fluoride (as an inhibitor model potentiator of neuropathy). Kinetic interactions with different inhibitors have also been studied. A fractionation method has been developed by preparative chromatography, and enriched fractions have been obtained with enzymatic components of interest. Finally, Tandem Mass Spectrometry has been used to identify the complexity of the sample, while potential proteins have been detected in the most toxicologically interesting sample.

3. METHODS:

Comments on the materials and methods used in the experimental studies

UNIVERSITAS
Miguel
Hernández

3.1. INTRODUCTION TO THE COMMENTS TO THE MATERIALS AND METHODS USED IN THE EXPERIMENTAL STUDIES

All the details of the materials and methods used in the work described in this report have been explained in the methods sections of published articles or in the non published data section. By globally considering this work, three different approaches have been used: (1) kinetic studies with one or more than one inhibitor in soluble and membrane fractions of chicken brain (**Mangas et al., 2011; 2012a; 2012b; 2013a**) using the automatable workstation Biomek 2000; (2) protein separation methods **(Mangas et al., 2013b**) and (3) proteomics analysis by Tandem Mass Spectrometry **(unpublished data).**

3.2. BIOLOGICAL PREPARATIONS

Tissue preparation: Broiler chicken brains (n=8-25, depending on the experiment) were obtained from a commercial slaughtering house immediately after animals were killed and they were kept in cold (0-5ºC) homogenization buffer until use. They were homogenized in a Polytron homogenizer (Kinematica Gmbh, Germany) using a PTA 10S head (70% power, 3x30 seconds) at a concentration of 200 mg fresh tissue/ml in the same buffer.

Subcellular fractionating: The homogenized tissue was centrifuged at 1000xg for 10 min (4ºC) to precipitate debris and nuclei. The supernatant was centrifuged at 100000xg for 60 min to obtain a precipitate consisting of the mitochondrial and microsomal fractions (membrane brain fraction) and a final supernatant or a cytosol component (soluble brain fraction). Supernatant soluble fractions were discarded or used for other purposes. Membrane brain fractions were resuspended in buffer at the same concentration of the membranes from 200 mg fresh tissues per mL. Samples were frozen to conserve them in liquid nitrogen and were diluted at the appropriate concentration for use in the kinetic assays (**Figure 3.1**).

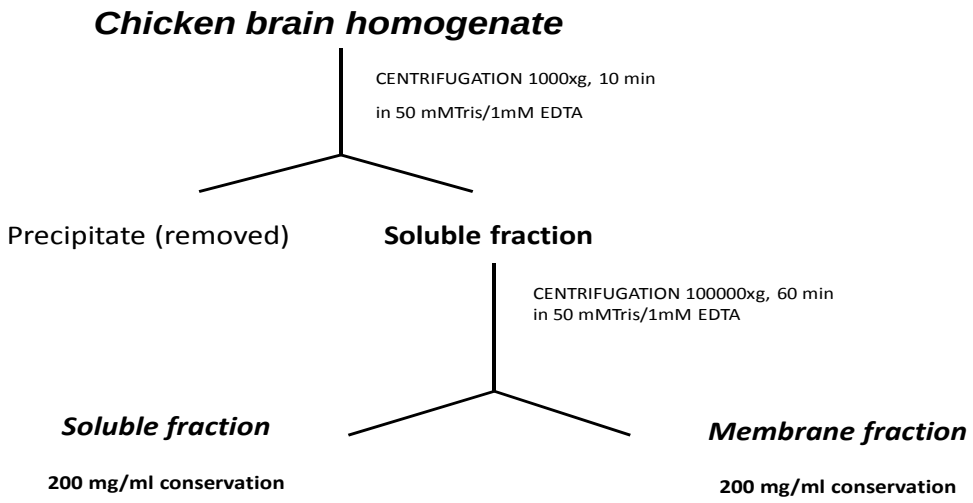

Figure 3.1. ***Subcellular fractionating method of chicken brains.***

3.3. COMPOUNDS TESTED

In the present work, the whole group of phenyl valerate esterases in chicken brain was kinetically characterized with three models of esterase inhibitors: paraoxon, mipafox and PMSF. This biological material seems to be the most appropriate to identify target esterases since it has been used employed for assaying OP-delayed neuropathy, it is the model in which the neuropathy potentiation phenomenon is usually studied, and it is also a sensitive animal model to cholinesterase effects of OPs.

PARAOXON

Paraoxon, diethyl 4-nitrophenyl phosphate (**Figure 3.2**), has been chosen because it is the OP non-inducer inhibitor model of OPIDN used in the NTE assay (Johnson., 1974). It is the active metabolite of the OP pesticide parathion and it is a representative compound of the diethyl-OP group of pesticides (Worek et al., 2012). Parathion was developed by Farben in the 1940s and it is still being used in many countries as an insecticide, primarily on fruits, cotton, wheat, vegetables and nuts. Its acute toxicity is: for rat: LD50 oral (M): 13 mg/kg; (F): 3.6 mg/kg and an oral dose of 3-5 mg/kg is reported to be usually fatal to humans (FAO report., 1969).

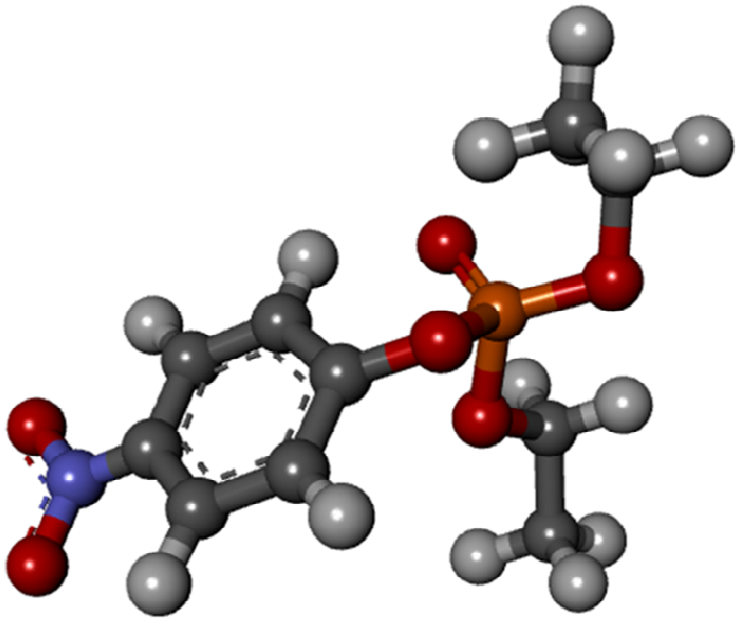

Figure 3.2 Molecular structure of paraoxon. Molecular structure of paraoxon, diethyl 4-nitrophenyl phosphate constructed in Accelrys Discovery Studio software (Accelrys Software Inc., 2013 Discovery Studio Modeling Environment, Release 4.0, San Diego).

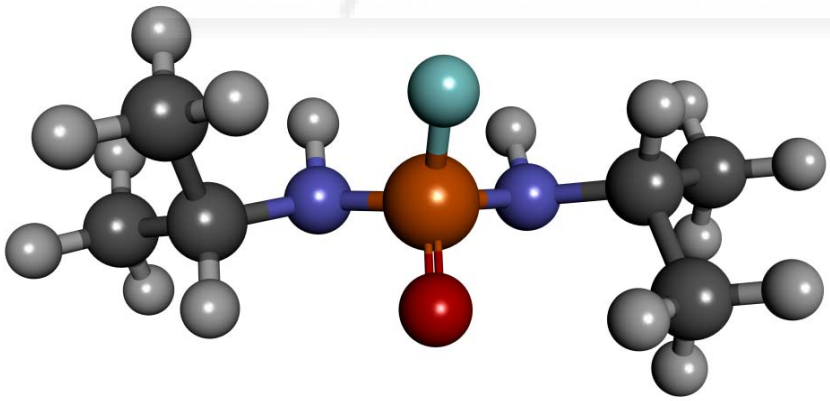

Figure 3.3. Molecular structure of mipafox. Molecular structure of mipafox, N, N¢-diisopropylphosphorodiamidofluoridate constructed in Accelrys Discovery Studio software. software (Accelrys Software Inc., 2013. Discovery Studio Modeling Environment, Release 4.0, San Diego).

MIPAFOX

Mipafox, N, N¢-diisopropylphosphorodiamidofluoridate, **Figure 3.3**, has been chosen because it is the OP inhibitor model inducer of OPIDN used in the NTE assay. Mipafox was invented and commercialized as an insecticide by Merck (The Merck Index., 1983). However, it was withdrawn from market in 1973 as it was suspected to cause the paralysis of two operators (Spencer, 1973). After this unfortunate event, it has been employed only as an investigative chemical for OPIDN studies since then it was the inhibitor model used in the NTE assay.

PMSF

Phenylmethylsulfonyl fluoride (PMSF), **Figure 3.4**, is an irreversible inhibitor of serine proteases, such as trypsin, chymotrypsin and thrombin. It causes sulfonylation of active-site serine residues. PMSF also inhibits most cysteine proteases, and inhibits metalloproteases and aspartic proteases. It is a widely used fatty acid amid hydrolase (FAAH) inhibitor for the pretreatment of brain membrane preparations when testing CB1 receptor activity. PMSF is the inhibitor model of the potentiation-protection of neuropathy.

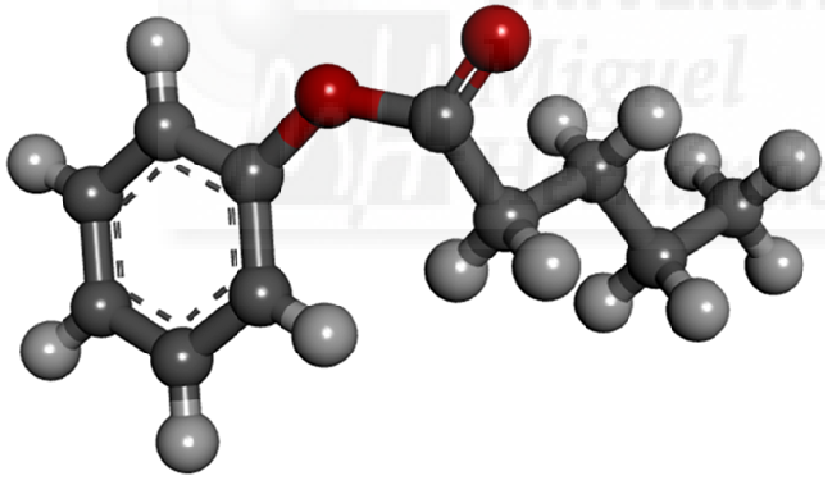

Figure 3.4 Molecular structure of phenylmethylsulfonyl fluoride. Molecular structure of **phenylmethylsulfonyl fluoride** constructed in Accelrys Discovery Studio software. software (Accelrys Software Inc., 2013. Discovery Studio Modeling Environment, Release 4.0, San Diego).

3.4. ESTERASE ACTIVITY AND PHENYL VALERATE AS SUBSTRATE

Phenyl valerate (**Figure 3.5**) has been chosen as a substrate because it appropriately detects esterases that are sensitive to Ops, such as NTE (Aldridge. 1993). Esters and thioesters of the general formula RC(O)XR´, with varying R, X and R´, were firstly synthesized for carboxylesterases, juvenile hormone esterase and neuropathy esterase (Walter., 1984). The hydrolysis of phenyl esters can be determined spectrophotometrically by measuring the released phenol with 4-aminoantipyrine and potassium ferricyanide (Seifert and Wilson., 1994). Phenyl valerate was the elected substrate for NTE (Johnson., 1974) because it has long since been used to discriminate other carboxylesterases in chicken tissues (Vilanova et al., 1990; Garcia-Perez et al., 2003; Estévez et al., 2009). Furthermore, it has been proposed that the target of potentiation could be found among phenyl valerate esterases (Moretto et al., 2007).

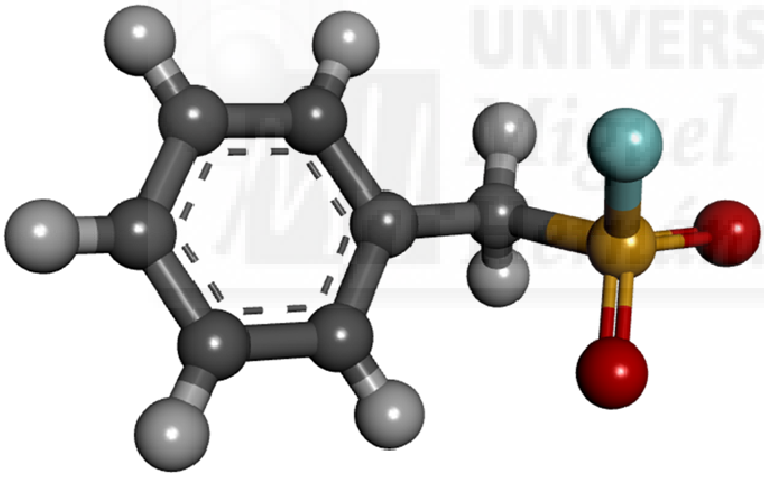

Figure 3.5 Molecular structure of phenyl valerate construted in Discovery Studio Accelrys Software Inc., 2013 Discovery Studio Modeling Environment, Release 4.0, San Diego).

3.5. KINETIC EXPERIMENTAL STUDIES

Figures 3.6 depicts the general assay, and the inhibition strategy involves performing experiments by preincubating the biological preparation to be studied at several inhibitor concentrations (I) for different inhibition times (t). Activity is measured by adding substrate at the end of the inhibitor preincubator time during a fixed time, normally 10 min. Residual activity (E) can be plotted in a bidimensional (2D) plot creating a plot of E versus t for each inhibitor concentration or by plotting all the data in a three dimensional (3D) plot of E versus t and I.

Various experiments can be performed: a fixed time inhibition experiment, a time-progressive inhibition experiment and spontaneous reactivation experiment. Different equations (in **Section 3.6**) can be used to analyze the data by fitting the model equation to the data and estimating the kinetic parameter of the model that best fits the experimental data. The selection of the appropriate model can be deduced by considering: (1) previous system data; (2) the general profile of the inhibition curve, and mainly (3) the quantitative statistical criteria by applying an F-test to establish the best fitting model. The Sigma Plot computing software allows to define the equation, to establish restrictions and the initial parameters, and to successfully fit non linear model equations (Estevez et al., 2004) using the Marquardt-Levenberg algorithm. The estimated parameters are the kinetic parameters of the model equation applied; the statistic F-test should be applied to establish the most statistically appropriate model equation.

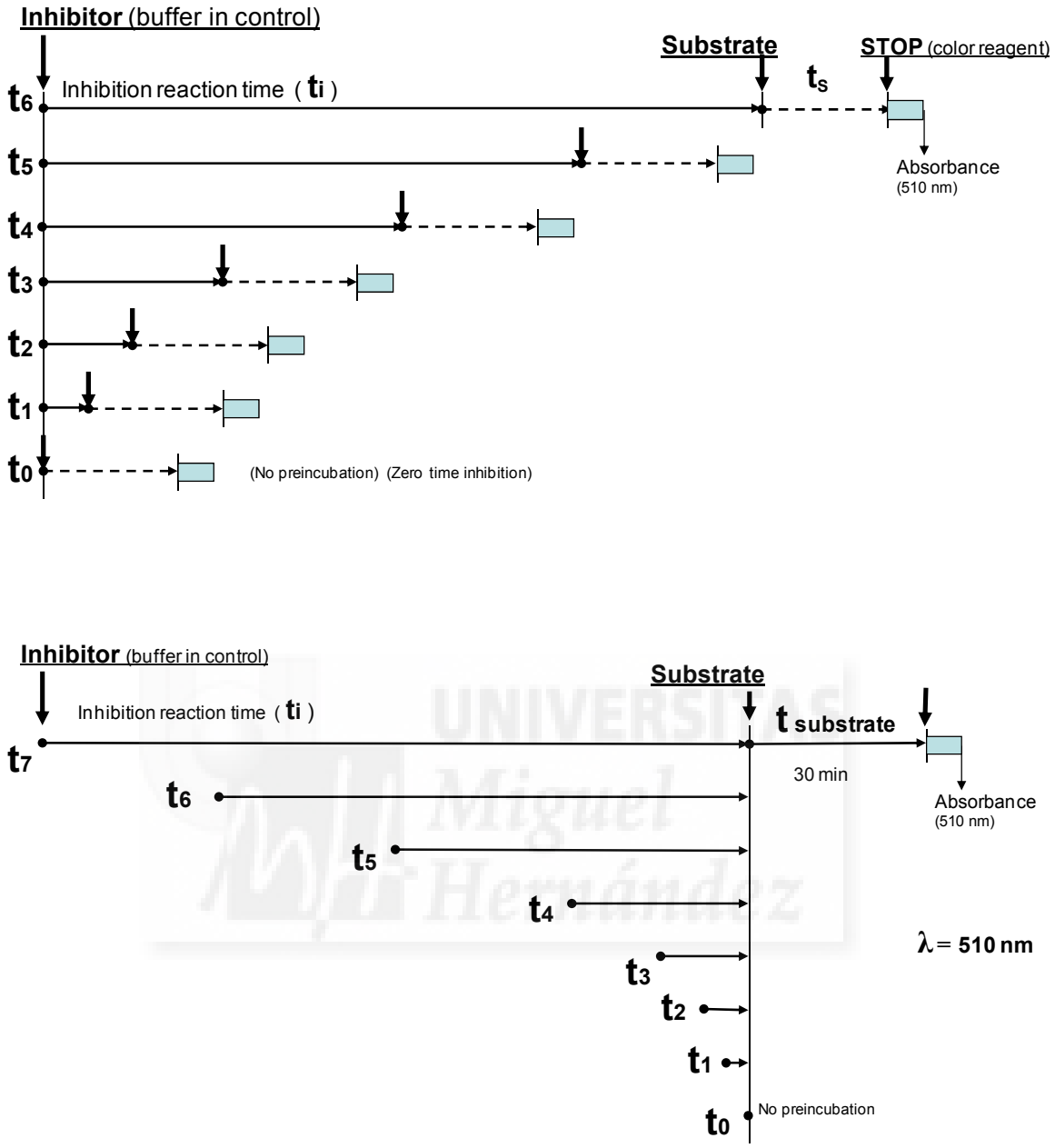

Figures 3.6. Two typical time course strategies of the inhibition experiment. The enzyme preparation is pre-incubated with the inhibitor during the inhibition time and then the substrate is added to measure residual enzymatic activity (substrate incubation time, ts; Estévez and Vilanova 2009). After a constant substrate reaction time has passed, the reaction is stopped, color is developed and absorbance is measured (adapted from Estévez and Vilanova., 2009).

3.6. KINETIC REACTIONS AND MODELS FOR THE INHIBITION OF ESTERASES BY OPs

3.6.1. Reactions for the covalent inhibition of esterases by OPs

Type-B esterases catalyze the hydrolysis of the carboxylester substrate by a reaction which involves the formation of a covalent acyl-enzyme intermediate with the release of the "leaving group" (**Figure 3.7**. Reaction 1). OPs exert their mechanism of toxicity by the covalent organophosphorylation of esterases, the phosphoryl-enzyme is very slowly cleaved, or not at all, and the enzyme remains inhibited. However with the carboxyl ester substrate, the catalytic circle is completed with the subsequent hydrolysis of the acyl group and the recovery of the active enzyme, which becomes available to initiate the next catalytic circle (**Figure 3.7.** Reaction 2) (Aldridge and Reiner., 1972). In some cases, the recovery by spontaneous reactivation may occur at a significant speed (Barril et al., 1999; Sogorb et al., 2002; Carr and Chambers., 1996; Hovanec et al., 1977; Skrinjaric-Spoljar et al., 1973) and may be forced by nucleophilic reagents such as fluoride or oximes for cholinesterases (**Figure 3.7**. Reaction 3; **Figure 3.8**). In some cases, the phosphoryl enzyme undergoes a dealkylating reaction called 'aging' (Vilanova et al., 1987; Worek et al., 2007). The negative charge of the 'aged' phosphoryl enzyme is more stable and is not reactivated, either spontaneously or by a reactivating agent. Operationally, the presence of a covalent inhibition is detected by a time-progressive inhibition, which may be used to monitor the proportion of enzyme that has been phosphorylated, and which remains active, by plotting residual activity versus time of the preincubation with the inhibitor. The potency of inhibitors and the properties of the interaction may be quantified by kinetic rate constants and the I50 value (the concentration causing 50% inhibition (Estévez and Vilanova., 2009).

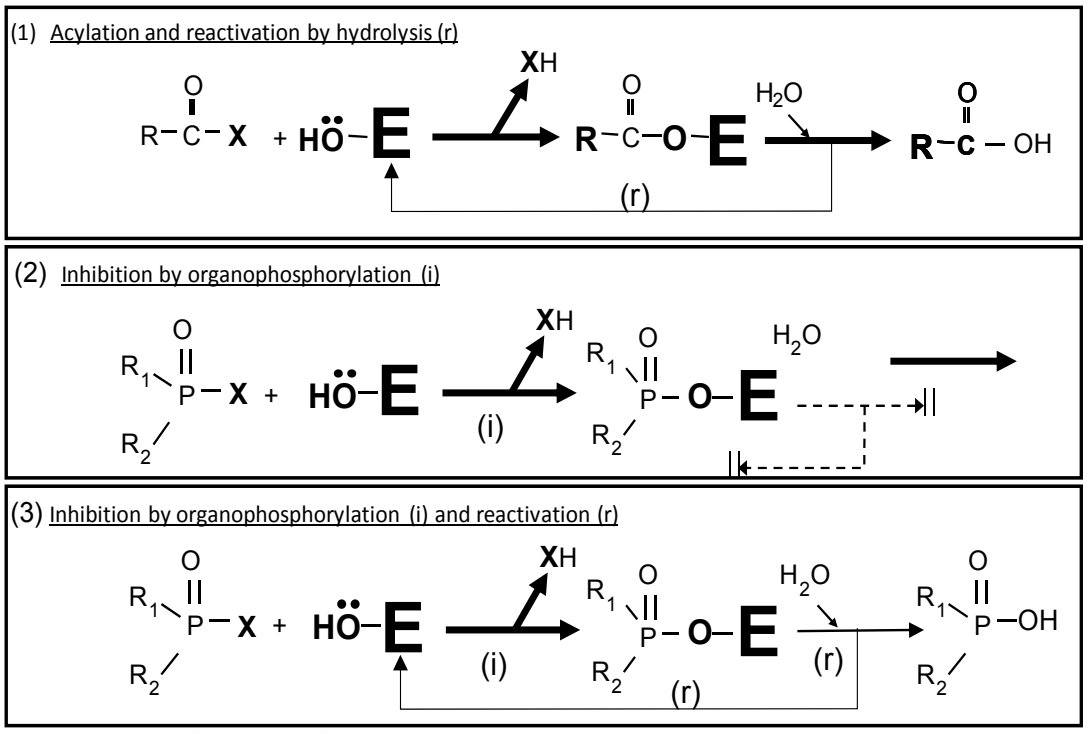

Figure. 3.7. Mechanism of reaction of an esterase. (1) Hydrolysis with the substrate; (2) Inhibition by a reaction with OPs and (3) Inhibition by a reaction with OPs and spontaneous reactivation (adapted from Estévez and Vilanova., 2009).

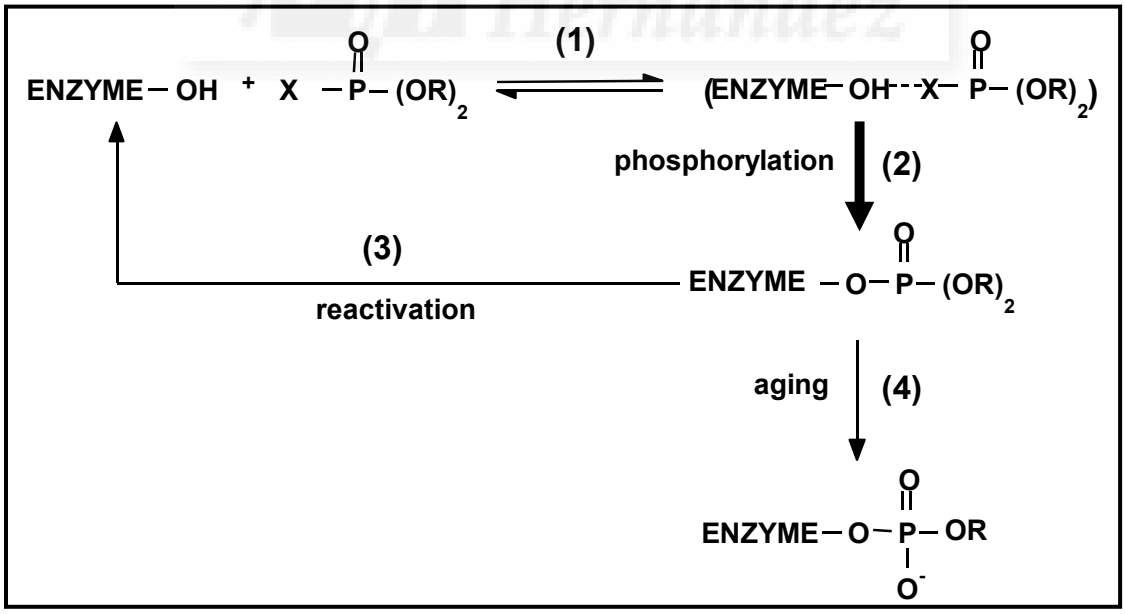

Figure 3.8. Reaction of inhibition (i), reactivation (r) and aging (a) of a type-B esterase (E-OH) by organophosphorus compounds.

3.6.2. Kinetic models and model equations for the phosphorylation of esterases

Molecular reactions

The molecular reactions which occurred upon the organophosphorylation of esterases (the inhibition reaction in **Figure 3.8**) are as follows:

$$E + PX \rightleftharpoons [E\cdots PX] \longrightarrow E\text{-}P + X$$

or

$$E + I \rightleftharpoons [E\cdots I] \longrightarrow E\text{-}P + X$$

In cases of inhibition by xenobiotic inhibitors (as OP), the observed kinetic behavior is usually the equivalent to a mechanism with the first-order molecular reaction (Estévez and Vilanova., 2009) because the formation of a Michaelis-like complex [E-P•••X] is not kinetically relevant because: (1) the solubility of the inhibitor is low and, therefore, a sufficient inhibitor concentration cannot be reached; (2) affinity is low, as the inhibitor is not the natural ligand; and (3) the phosphorylation reaction is faster than the binding reaction. Consequently, the reaction is presented as follows:

$$E + I \xrightarrow{ki} E\text{-}P + X$$

The kinetic equation can be derived as follows:

Approach: $I >> E_0$; $I \approx I_0$ (the inhibitor concentration is much higher than the enzyme and does not change significantly while the experiment lasts). Consequently the bimolecular reaction between the enzyme and inhibitor becomes a reaction in which the active enzyme concentration (E) is the only dependence variable with the inhibition time, while the rate of inhibition or the disappearance of the active enzyme is:

$$vi = dE/dt = -ki \cdot E \cdot I = -a \cdot E$$

$$dE = -ki \cdot E \cdot I \cdot dt \quad \text{and} \quad dE/E = -ki \cdot I \cdot dt$$

By integrating this differential equation from t = 0 (E = E_0) to t = t, it follows that:

$$\mathrm{Ln}\ (E/E_0) = -ki \cdot I \cdot t$$

from which the exponential equation is deduced:

$$E = E_0 \cdot e^{-ki \cdot I \cdot t}$$

Classical linear models

If only a single esterase is measured in a preparation, kinetic behavior may be linearized by plotting Log (% Activity) versus time (fixed inhibitor concentration) or versus inhibitor concentration (fixed inhibition time). This linearization has been the basis of classical kinetic studies using graphic procedures, which have proved useful for understanding and analyzing time-progressive and fixed-time inhibition curves (**Figure 3.9**; Aldridge and Reiner., 1972; Vilanova et al., 1987). It has been applied mainly to fixed-time inhibition curves (Chemnitius and Zech., 1983; Vilanova et al., 1987; Chemnitius et al., 1993). This classical approach involves linearized equations used to analyze data graphically or by simple calculations. For this purpose, enzyme activity is expressed as a percent (E% Activity; **Figure 3.9**), and the equation is converted into a decimal logarithmic equation as follows:

$$\%\ \mathrm{Activity} = 100 \times E/E0 = 100 \times e^{-ki \cdot I \cdot t}$$

$$\mathrm{Log}\ \%\ \mathrm{Activity} = 2 - \mathrm{Log}\ (e) \cdot ki \cdot I \cdot t$$

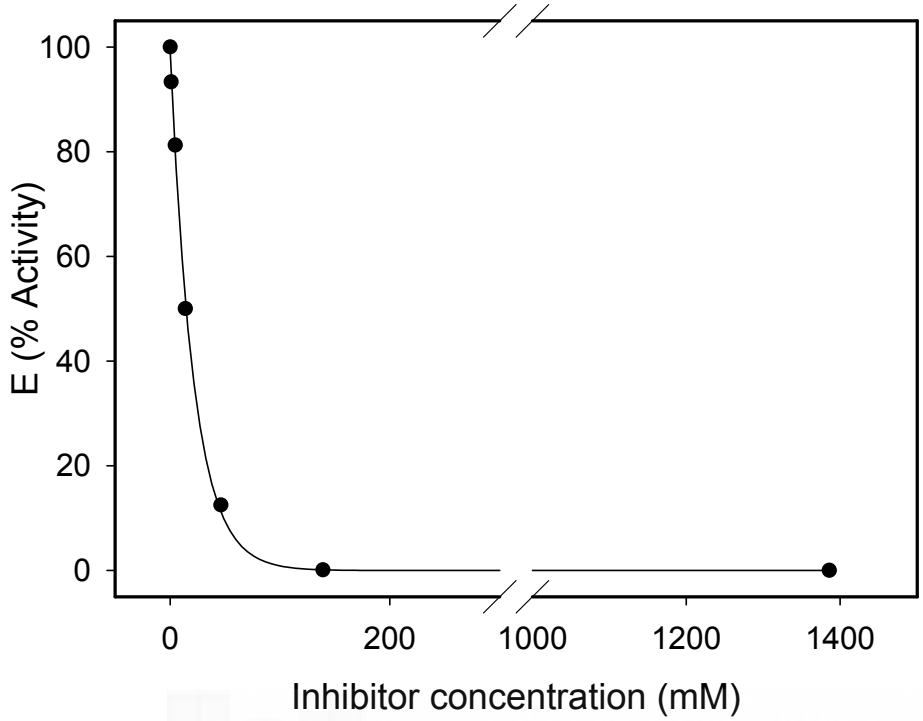

Figure 3.9. Typical inhibition of a single sensitive enzyme at a fixed time of inhibition (30 min). This plot represents a theoretical case case with ki = 500 M−1·min−1, whose activity versus inhibitor concentration is plotted for seven inhibitor concentrations (I = 0, 1, 4.6, 13.9, 46.2, 139 and 1385 µM) at 30 min of inhibition time. Adapted from Estévez and Vilanova., 2009.

Under normal testing conditions, the inhibitor concentration may be several orders of magnitude higher than the enzyme concentration. For one set of experimental points with the same inhibitor concentration, I may be considered constant for the experiment time and may be included in a constant: We can define $ki = k' \cdot I$ and then:

$$\text{Log \% Activity} = 2 - \text{Log (e)} \cdot \text{k}' \cdot \text{t}$$

Hence a linear relationship is deduced, and by plotting Log (%Act) versus time (t) for each constant inhibitor concentration, a straight line is observed (**Figure 3.10**). A linear regression analysis may then be applied to the experimental data either graphically or numerically. By applying a linear regression, from the slope, the k´ value is estimated, from which the second-order kinetic constant ki may be deduced: $ki = k' \cdot I$

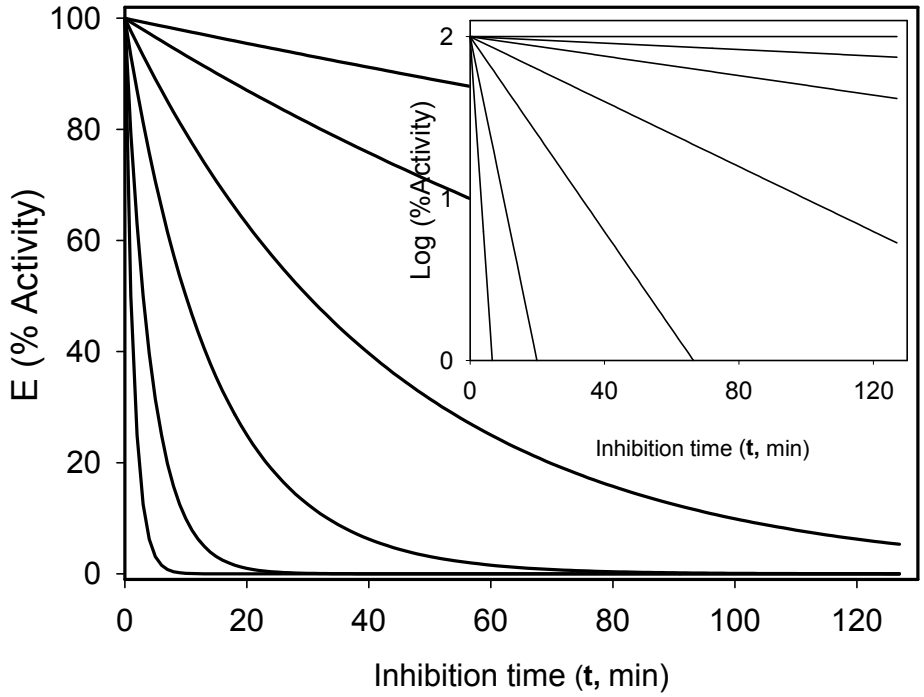

Figure 3.10. Typical kinetics of inhibition of a single sensitive enzyme. This plot represents a theoretical case with ki = 500 M−1·min−1 which correspond to an I50 (30 min) of 46.21 µM for seven inhibitor concentrations (I = 0, 1, 4.6, 13.9, 46.2, 139, 1386 µM). In the insert, a lineal logarithmic representation is shown. Adapted from Estévez and

3.6.3. Model equations and experimental approaches for complex situations

More complex situations can be considered as follows:

i. systems contain several enzymes, including a resistant part
ii. systems with a significant spontaneous reactivation
iii. systems with inhibition during the substrate time or hydrolysis of the inhibitor
iv. systems where the inhibitor is chemically hydrolyzed

In that cases the simplified previously approach described with linear equation (**Figure 3.10**) is not possible, and the plot of Log (% activity) versus time or versus the inhibitor concentration is not linear (**Figures 3.11; 3.12; 3.13**). In such cases a non-linear regression method must be applied to analyze data (Estévez and Vilanova., 2009).

i. Systems contain several enzymes

In a biological preparation, esterase activity may contain several sensitive enzymatic fractions (E1, E2, E3, etc.) as well as resistant components (R). Each sensitive component follows an equivalent exponential behavior to the equation in **Section 3.5.2**. After an inhibition time (t), residual activity (E) is the sum of all the enzymatic residual activities (Estévez and Vilanova., 2009). When there is a resistant fraction for a different inhibitor concentration, tendency with time should be asymptotic to the same residual levels (R) and should correspond to the fraction of total activity that is resistant to inhibition (R, **Figure 3.11**). This residual activity may be 0% of the total activity if all the activity is sensitive.

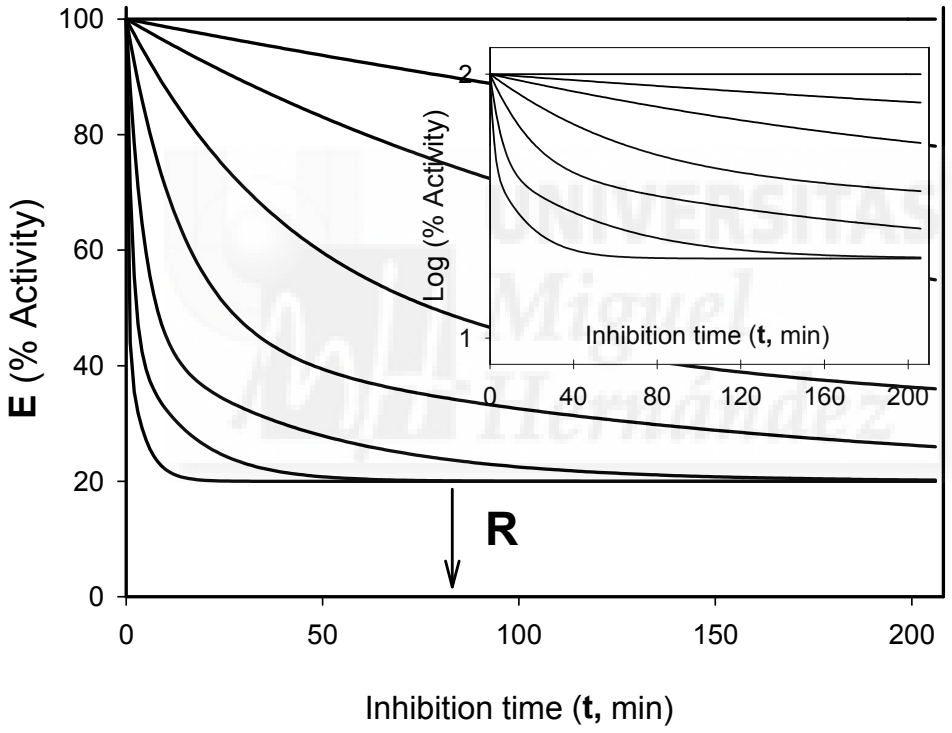

Figure 3.11. Typical kinetics of inhibition of a single sensitive enzyme. This plot represents a theoretical case with ki = 500 M−1·min−1, which corresponds to an I50 (30 min) of 46.21 µM for seven inhibitor concentrations (I = 0, 1, 4.6, 13.9, 46.2, 139, 1386 µM). The insert shows a lineal logarithmic representation . Adapted from Estévez and Vilanova., 2009.

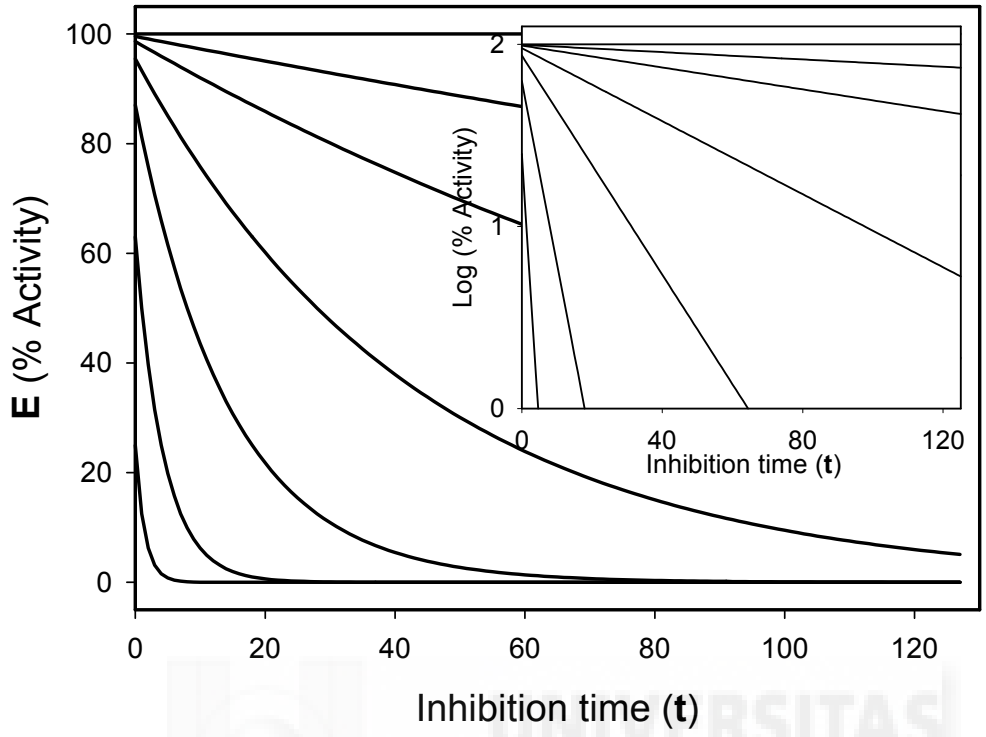

Figure 3.12. Example of kinetic behavior with ongoing inhibition. A case is plotted with the same kinetic constant as that of **Figure 3.10** for a single enzyme, but with significant ongoing inhibition with a ka=0.001 μM^{-}

ii. *Systems with ongoing inhibition*

The detection and analysis of inhibition in the presence of a substrate is needed to establish Detecting and analyzing inhibition in the presence of a substrate is necessary to establish the appropriate model equations in the time-progressive inhibition data evaluation (Estévez et al., 2010). If ongoing inhibition affects the kinetic inhibition data, the % of activity at the zero inhibition time will lower along with the inhibitor concentration in the progressive inhibition experiment (**Figure 3.12**).

Exponential decay models are used to fit the data of the % of activity versus the inhibitor concentration at the zero-time during the progressive inhibition experiment. The general model equation to fit these data is as follows:

$$E = E1_0 \cdot e^{-ka'1 \cdot I} + E2_0 \cdot e^{-ka'2 \cdot I} + \ldots + R$$

where parameters ka'1, ka'2, ka'n represent the apparent first-order kinetic constants of inhibition observed during the substrate reaction time, and $E1_0$, $E2_0$ represent the % of activity and the enzymatic component affected by the ongoing inhibition effect (Estévez and Vilanova., 2009; Estévez et al., 2010).

i. Systems with spontaneous reactivation

The spontaneous reactivation valuation made at the time of the experiments is necessary, and for this purpose, spontaneous reactivation after the inhibition experiment is required after removing the inhibitor a many organophosphates have high spontaneous reactivation rates with esterases such as paraoxon.

If spontaneous reactivation affects the kinetic inhibition data, the residual activity over a long time will not have the same value, rather a plateau of the steady stage at which the inhibition speed is the same as the reactivation rate (Estévez and Vilanova., 2009; **Figure 3.13**).

ii. Systems with a significant spontaneous chemical hydrolysis of the inhibitor

Binding sensitive esterases is not usually considered significant to modify inhibitor concentrations if tested at initial levels from nanomolar or micromolar concentrations upward, as individual sensitive active proteins are within the picomolar or femtomolar concentrations.

However, another kinetic model is required when the spontaneous hydrolysis of the inhibitor is significant, as in esterases inhibition with PMSF (Estévez et al., 2012). The inhibition and spontaneous hydrolysis of the inhibitor have to be considered in a kinetic model. In this case, the progressive inhibition curves would tend to reach a ''plateau'' and do not converge at the same point, even though no spontaneous reactivation would be detected, due to the progressive disappearance of the inhibitor. The inhibition rate lowers until it stops when the inhibitor concentration comes close to zero (Estevez et al., 2012).

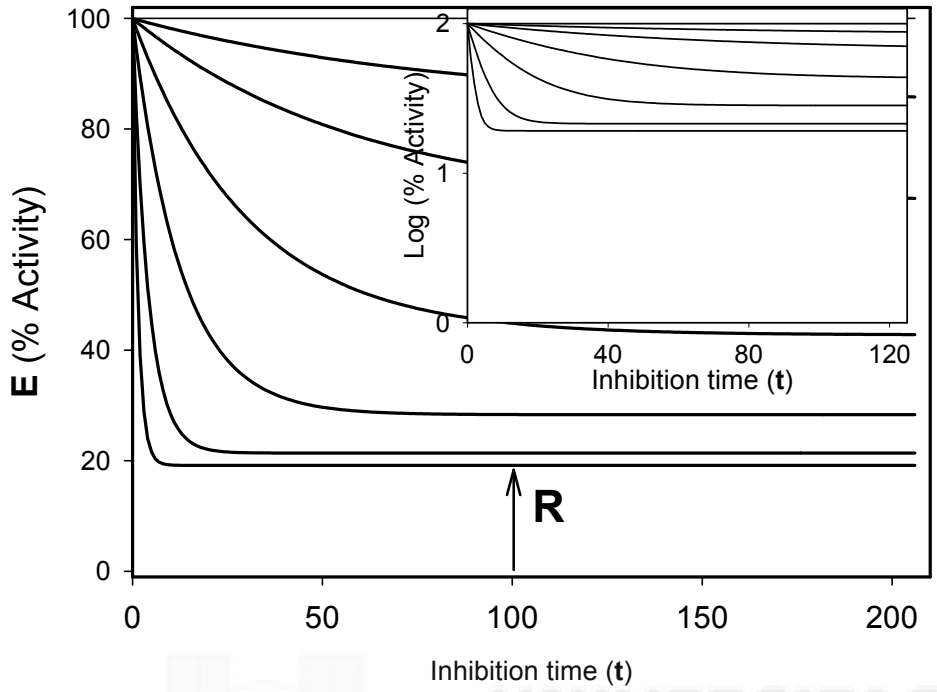

Figure 3.13. Example of kinetic behaviour with spontaneous reactivation simultaneously. A theoretical case is plotted with one sensitive and one resistant component with the following parameters values: sensitiveenzymatic component : 82%, inhibition constant ki=100 M^{-1} min^{-1}, spontaneous reactivation constant kr=0.01 min^{-1}, for inhibitor concentrations I=0.0, 23.1, 69.3, 231.0, 693.0, 2310.0, 6931.0 µM

3.6.4. Review of the kinetic model equations

The general model equation for *inhibition* without spontaneous reactivation is as follows when n enzymatic components are present:

$$E = E1_0 \cdot e^{-(k1 \cdot I \cdot t)} + E2_0 \cdot e^{-(k2 \cdot I \cdot t)} + E3_0 \cdot e^{-(k3 \cdot I \cdot t)} + \ldots + En_0 \cdot e^{-(kn \cdot I \cdot t)} + R$$

If *spontaneous reactivation* is observed for one of the enzymatic components, the general model is as follows:

$$E = \left\{ \left[(kr1 \cdot E1_0) \Big/ (k1 \cdot I + kr1) + (k1 \cdot I \cdot E1_0) \Big/ (k1 \cdot I + kr1) \right] \cdot e^{-(k1 \cdot I \cdot kr1 \cdot t)} \right\} + E2_0 \cdot e^{-(k2 \cdot I \cdot t)} + R$$

If spontaneous hydrolysis has to be considered, then the general model is so as follows:

$$E = E1_0 \cdot e^{\left(e^{-kh \cdot t} - 1\right) \cdot \frac{k1}{kh} \cdot I_0} + E2_0 \cdot e^{\left(e^{-kh \cdot t} - 1\right) \cdot \frac{k2}{kh} \cdot I_0} + R$$

If *ongoing inhibition* (inhibition during the substrate reaction time) is significant, exponential factor $[e^{-ka' \cdot I}]$ or $e^{\left(-k'a \cdot I_0 \cdot e^{-(kh \cdot t)}\right)}$ has to be included to correct the "ongoing inhibition" during the substrate reaction (Estévez et al., 2010; Estévez and Vilanova., 2009). When ongoing inhibition is significant the general model equation is as follows:

$$E = [e^{-(ka' \cdot I)}] \cdot E1_0 \cdot e^{-(k1 \cdot I \cdot t)} + E2_0 \cdot e^{-(k2 \cdot I \cdot t)} + E3_0 \cdot e^{-(k3 \cdot I \cdot t)} + \ldots$$

$$\ldots + En_0 \cdot e^{-(kn \cdot I \cdot t)} + R$$

If *spontaneous hydrolysis* has to be considered, then the general model was as follows:

$$E = E1_0 \cdot e^{\left(-ka'1 \cdot I_0 \cdot e^{-(kh \cdot t)}\right) \cdot e^{\left(e^{-kh \cdot t} - 1\right) \cdot \frac{k1}{kh} \cdot I_0}} + E2_0 \cdot e^{\left(-ka'2 \cdot I_0 \cdot e^{-(kh \cdot t)}\right) \cdot e^{\left(e^{-kh \cdot t} - 1\right) \cdot \frac{k1}{kh} \cdot I_0}} + R$$

In all the mathematical models, k1, k2, k3, …, kn are the second-order inhibition constants, kr1 is the reactivation constant, ka represents the apparent first-order kinetic constants of inhibition observed during the substrate reaction time, kh is the kinetic constant of the spontaneous chemical hydrolysis of the inhibitor, $E1_0$, $E2_0$, $E3_0$,…, En_0 and R are the proportion (amplitude) of enzymatic components E1, E2, E3, En, … and R, respectively.

For the purpose of obtaining a coherent result in the interactive computing estimation, some restrictions were applied:

(1) All the parameters (rate constants and amplitudes) must have positive values (>0).

(2) Component 1 is the most sensitive, therefore k1>k2, k2>k3.

(3) The following complementary restriction is also applied: $E1_0+E2_0+E3_0+R=100\%$.

Model equations are fitted to the experimental inhibition data by a non linear computerized method based on the least squares principle using version 8 of the Sigma Plot software (Systat Software Inc., Chicago, USA). The same software was used to apply an F-test in order to compare the different tested kinetic models with a view to identifying the best fitting model.

The results are expressed by giving the values of the kinetic parameters for each component, including:

- ✓ The exponential kinetic constant ($M^{-1} \cdot min^{-1}$)
- ✓ The proportions/amplitudes of each component (% of activity)
- ✓ The I_{50} values (30 min): concentration to achieve a 50% inhibition of each component, deduced from the kinetic model.

3.7. PHENYL VALERATE ESTERASE ASSAYS

3.7.1. General phenyl valerate inhibition procedures

The standard procedure of all phenyl valerate esterase activity assays was performed automatically in the Biomek 2000 and was programmed by the workstation's software. The standard microassay was: a 20-µl volume containing buffer solution or inhibitor was added to 1-ml microtubes. Then 200 µl of the diluted enzyme preparation (Tris buffer in blanks) were added. The mixture was incubated at 37ºC for the desired (preincubation) time. In those experiments with more than one inhibitor, before this step, a 20-µl volume of the inhibitor was added and incubated for the corresponding time. After this time, 200 µl of substrate phenyl valerate in water at a concentration of 1.34 mg/ml were added. The mixture was incubated at 37ºC for 10 min to run the enzymatic reaction. The reaction was stopped by adding 200 µl of 2% SDS/0.5 mg/ml aminoantipiryrine solution. Then 50 µl of ferricyanide were added. After mixing and waiting 5 min, a 300-µl volume from each microtube was transferred to a 96-well microplate, and absorbance was read at 510 nm. The data were recorded by the microplate reader and were processed. Then graphic adjustments were made with the Sigma Plot software (Systat Software Inc, Chicago, USA) for Windows. **Figure 3.14** shows a scheme of the procedure's timing. The results were expressed as % of activity (E/E_0 x 100) over the control without an inhibitor, and are plotted versus either time (t) or inhibitor concentration (I), or both in a 3 D plotting.

*Kinetic studies in the **soluble** fraction of chicken brain.* The following studies were performed:

- Fixed-time inhibition (30 min) with different concentrations of: Paraoxon, mipafox and PMSF.
- Reactivation kinetics by dilution after inhibition with : Paraoxon, mipafox and PMSF.
- Time-progressive inhibition experiment with different concentrations of: Paraoxon, mipafox and PMSF.

*Kinetic studies in the **membrane** fraction of chicken brain.* The following studies were performed:

- Fixed-time inhibition (30 min) with different concentrations o: Paraoxon, mipafox and PMSF.

- Reactivation kinetics by dilution after inhibition with: Paraoxon and mipafox.
- Time-progressive inhibition experiment with different concentrations of: Paraoxon, mipafox and PMSF.

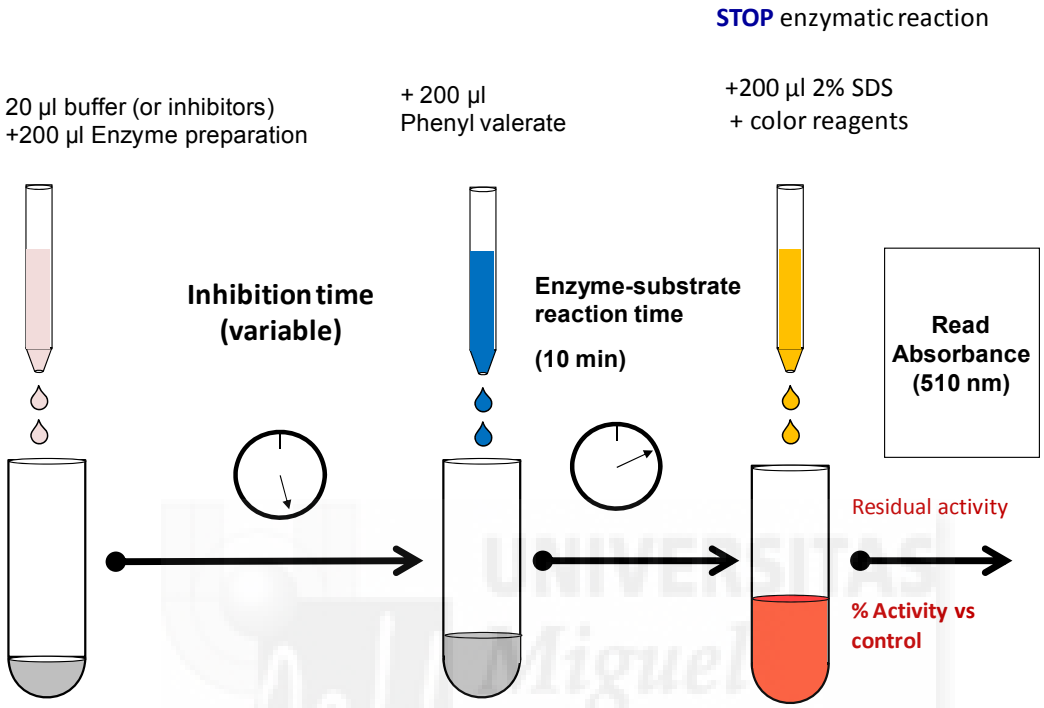

Figure. 3.14. General microassay method procedure. The complete standard procedure was done automatically as programmed by the workstation's software

3.7.2. Kinetic studies of the interaction with more than one inhibitor in soluble and in membrane fractions of chicken brain

The complete standard sequential inhibition assays procedure was performed automatically in the Biomek 2000, as programmed by the workstation's software. A modification in the standard microassay in **Section 3.7.1** was taken by adding one or various steps of inhibition before. **Figure 3.15** shows the scheme for inhibition with two different inhibitors.

*Kinetic studies with more than one inhibitor in the **soluble** fraction.* The following studies were performed:

- Paraoxon progressive inhibition in samples preinhibited with 100 µM mipafox

- PMSF progressive inhibition in samples preinhibited with 20 nM mipafox.
- Mipafox inhibition (30 min) in samples preinhibited with 10 µM paraoxon.
- Mipafox inhibition (30 min) in samples preinhibited with 10 µM paraoxon plus 10 µM PMSF
- Mipafox inhibition (30 min) in samples preinhibited with different PMSF concentrations.
- Paraoxon inhibition (30 min) in samples preinhibited with 4000 µM PMSF
- Reactivation kinetics by dilution after inhibition with paraoxon in samples preinhibited with 2000 µM PMSF

*Kinetic studies with more than one inhibitor in the **membrane** fraction.* The following studies were performed:

- Concurrent NTE assay: inhibition with 40 µM paraoxon versus inhibition with 40 µM paraoxon, plus different concentrations of mipafox for 30 min.
- Sequential NTE assay after removing paraoxon by ultrafiltration
- Mipafox fixed-time inhibition in the samples preinhibited with 20 µM PMSF.
- PMSF fixed-time inhibition in the samples preinhibited with 20 µM mipafox.

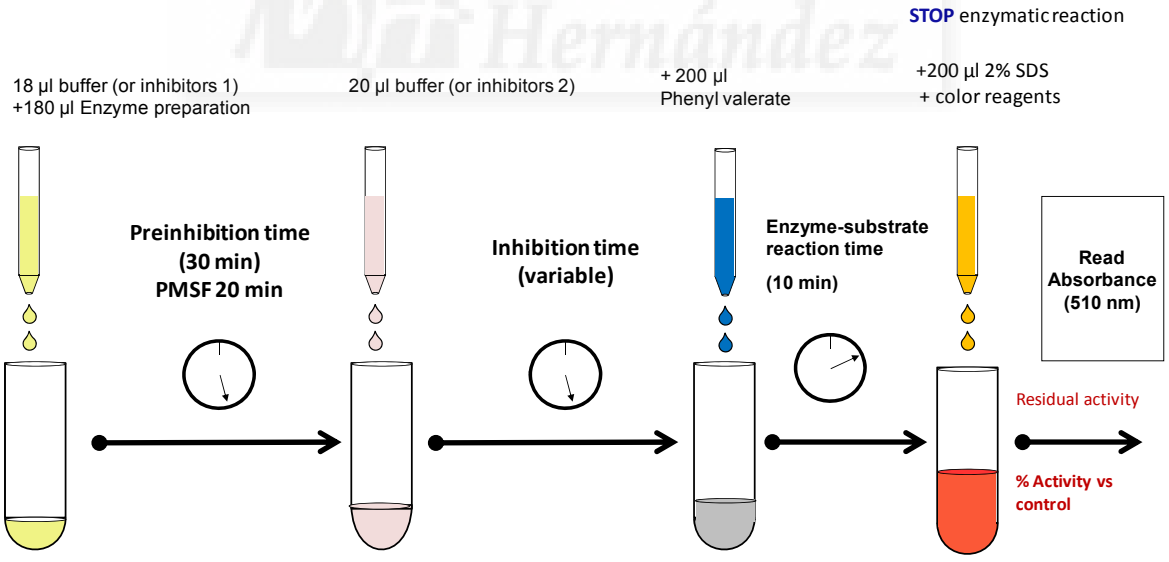

Figure 3.15. General microassay method procedure for inhibition assays with two inhibitors.

3.8. PROTEIN SEPARATION STUDY

3.8.1 Ultrafiltration for protein concentration

A volume of up to 15 ml was filtered through Ultracel-Amicon Ultra-15 (Millipore Corporation, Spain) filters, with a pore size of 3 kDa or 10 kDa. This was centrifuged at 4000×g at 4ºC for the time required to concentrate samples to the volume required. The PVase activity recovered in the concentrated solution after the ultrafiltration of the soluble fraction from sciatic nerves at pH 8 was >98% and the recovered protein measured by the Bradford method was around 70-80%.

3.8.2. Fractionation procedure

Semipreparative high performance liquid chromatography was performed in a UFLC Shimadzu equipped with a fraction collector at 4ºC as follows:

Size exclusion chromatography was performed at 4°C in a 300 x 7.8 mm BioSep-SEC-s3000 (part no: 00H-2146-KO), balanced with 50 mM Tris buffer at pH 7.5. Fifty consecutive injections of 200 µl were made during the molecular exclusion chromatography procedure, which was eluted in the column with 50 mM Tris /1 mM EDTA pH 7.5 buffer at a flow rate of 1 ml/min, and 30 x 0.5 ml fractions were obtained for each injection. The subfractions corresponding to the 50 consecutive chromatograms were collected and accumulated in the same tubes. Absorbance at 280 nm was recorded continuously, while protein and enzymatic activities were measured in each subfraction.

The dead volume was determined by the elution volume of dextrane blue (VD', = 5, 489 ml). The elution volume of potassium ferricyanide (Ver = 11, 304 ml) was used to calculate the inclusion volume (Vi = Ver - V, = 5, 815 ml). The column was calibrated using standard proteins (Gel Filtration Markers Kit-Sigma Aldrich for proteins to 29 KDa to 700 KDa): bovine serum albumin (66,000 kDa); yeast alcohol dehydrogenase, (150,000 kDa); β-amylase sweet potato, (200,000 kDa); Blue dextran (2,000,000 kDa); Carbonic bovine erythrocytes anhydrase (29,000); bovine thyroglobulin, (669,000 kDa). Molecular weights were calculated by making comparisons with a calibration curve using standard proteins (MW-GF-1000 Kit, Sigma Chem. Co.) and plotting the log (MW) versus distribution coefficient (kd). Behaviour within the molecular weight range used was linear, with a correlation coefficient of 0.994.

The ion exchange chromatography of the samples obtained from the molecular exclusion chromatography was performed at 4°C in a 75 x 7.8 mm BioSep-DEAE-PEI (part no: CHO-1680), balanced with 50 mM Tris buffer pH 7.5. A 2-ml volume from the previous fractionation step was eluted in the column with 50 mM Tris /1 mM EDTA pH 7.5 buffer at a flow rate of 1 ml/min. Samples were eluted at the 1 ml/min1 flow rate. A stepwise gradient with 0.5 M NaCl was optimized per sample applied, subfractions of 1.2 ml were collected at 4ºC and the subfractions corresponding to two consecutive chromatograms accumulated in the same tubes. Absorbance at 280 nm was recorded continuously, while protein and enzymatic activities were measured in each subfraction.

3.9. TANDEM MASS SPECTROMETRY STUDY

Protein samples obtained in the separation study were diluted in TNE (50 mM Tris pH 8.0, 100 mM NaCl, 1 mM EDTA) buffer and where transporter in cold to the Biomolecular/Proteomics Mass Spectrometry Facility in University of California-San Diego where tryptic digestion and proteomic study was performed by LC-MSMS. Materials and Methods used for this purpose are explained in **Section 6.2**, unpublished results.

4. GLOBAL SUMMARY OF THE RESULTS AND DISCUSSION

UNIVERSITAS
Miguel
Hernández

4.1. AIMS.

Justification

Organophosphorus compounds (OPs) are a large and diverse class of chemicals that have been, and continue to be, used for various purposes and cause several neurotoxic disorders; some of these effects cannot be explained with known molecular targets. Many esterases with key biological roles have the potential to interact with OPs. Kinetic models have been developed to detect OPs binding esterases in complex biological preparations.

Overall objective

To improve knowledge on the esterases targets of organophosphorus compounds, on the bases of kinetic experimental data with inhibitors models of neurotoxic effects and of protein purification, as well as molecular identification approaches in chicken brain.

Specific objectives

1. To develop an automatable microassay method of enzymatic measurements of phenyl valerate esterase enzymatic activity in the Workstation Biomek 2000 (Beckman Instruments).

2. To characterize quantitatively the kinetic behavior of phenyl valerate esterases in soluble and in membrane fractions of chicken brain. Including the following parameters:

- number of enzymatic components
- inhibition rate constant
- spontaneous reactivation rate constant
- spontaneous hydrolysis of the inhibitor rate constant
- inhibition during the reaction with the substrate

For this purpose, the following inhibitors were used:

- paraoxon (non inducer of neuropathy)
- mipafox (inducer of neuropathy)
- phenyl methyl sulfonylfluoride (potentiator of neuropathy)

3. To discriminate the entire group of phenyl valerate esterase enzymatic components in soluble and membrane fractions of chicken brain.

4. To propose a practical assay to discriminate all the esterase components by a simple inhibition procedure in soluble and membrane fractions.

5. To study the kinetic interactions by exposure to low non inhibitory concentrations to one inhibitor and to measure sensitivity to others in the phenyl valerate esterase components discriminated among the different inhibitors in chicken brain soluble and membrane fractions.

6. To develop and apply a fractionation method for isolating the enzymatic components of toxicological interest using high-performance chromatography by semipreparative molecular exclusion chromatography and by semipreparative ion exchange chromatography. To analyze the enzymatic components, fraction activities and the effect of inhibition with an OP in the protein chromatography profiles.

7. To identify and analyze the proteins present in at least one toxicological interesting fraction using Tandem-Mass Spectrometry and to identify potential targets of the OPs binding in the serine esterase enzyme family.

4.2. OPTIMIZATION OF THE AUTOMATABLE MICROASSAY OF PHENYL VALERATE ESTERASES *(results unpublished, Section 6.1)*

An automatable microassay for phenyl valerate esterase activity using the Biomek 2000 workstation was developed in order to perform all the kinetic experiments of the following sections. **Section 6.1** shows assay linearity with tissue concentration and enzymatic activity assay linearity with time incubated at 37ºC **(Figure 6.1, 6.2** and **6.3).**

This automation was necessary to reduce the manual assay time, to increase the reproducibility of the kinetic experiments and it allowed to perform experiments in a short time with little tissue and to use fewer reagents, including OPs.

4.3. SOLUBLE PHENYL VALERATE ESTERASES INHIBITION WITH PARAOXON, MIPAFOX AND PMSF

In a soluble fraction of chicken brain Kinetic experiments were done with paraoxon and mipafox (published in ***Mangas et al., 2011***) and PMSF (published in ***Mangas et al., 2012b***). The reference numbers of the tables and figures in this section correspond to those reference numbers in the publications.

4.3.1. Paraoxon kinetic behavior (*Mangas et al., 2011)*

Three different kinetic experiments were done in the soluble brain fraction with the inhibitor paraoxon: fixed-time inhibition, spontaneous reactivation and progressive inhibition. The best model equation obtained to fit the data according to the F-test is shown in each section with the kinetic parameters obtained for each experiment (**Table 1**).

- *A fixed-time inhibition experiment* with paraoxon at a concentration from 1 nM to 40 µM, as shown in **Figure 1**. The best fitting model was that in which three enzymatic components were discriminated, two were sensitive to paraoxon and one was resistant.
- A s*pontaneous reactivation experiment* with paraoxon at the 40 nM and 1000 nM concentrations, 40 nM to inhibit only the most sensitive component and 1000 nM to inhibit both the sensitive components. More than 12% of activity was time-progressive and spontaneously reactivated after diluting 10 times (**Figure 2**). Mathematical models for reactivation were applied to the data by considering the residual paraoxon concentration of 4 nM after diluting.

- *The ongoing inhibition* during the substrate reaction was evaluated by plotting residual activity with the different paraoxon concentration at 0 time of inhibition (**Figure 3, plot B**). This effect was around 8% of activity with the highest concentration, and it corresponded to the most sensitive component.
- A progressive inhibition experiment was done with paraoxon 0, 40, 250, 1000 and 7000 nM for times of up to 180 min at 37ºc (**Figure 3, plot A**). A 3D model was used to fit the data by plotting % activity versus time versus paraoxon concentration (**Figure 4**) to consider all the data simultaneously.
- *Conclusions of kinetic studies with paraoxon*: More than 90% of phenyl valerate esterase activity was extremely sensitive to paraoxon in a time-progressive manner, suggesting covalent irreversible phosphorylation. Kinetic behavior was coherent with two sensitive esterase components, 21% and 71% and I50 (30 min) of 11 and 1216nM respectively and a resistant component of 8% of the activity; where the most sensitive one was spontaneously reactivated and it was affected by the ongoing inhibition effect.

4.3.2. Mipafox kinetic behavior (*Mangas et al., 2011)*

Three different kinetic experiments were done in the soluble brain fraction with the inhibitor mipafox: fixed-time inhibition, spontaneous reactivation and progressive inhibition. The best model equation obtained to fit the data according to the F-test is shown in each section with the kinetic parameters obtained for each experiment (**Table 2**).

- *A fixed-time inhibition experiment* with paraoxon at a concentration from 1 nM to 75 µM, as shown in **Figure 5**. The best fitting model was a model in which three enzymatic components were discriminated.
- A s*pontaneous reactivation experiment* with mipafox at a concentration of 10 nM and 6000 nM, 10 nM to inhibit only the most sensitive component and 6000 nM to inhibit both the sensitive components. No spontaneous reactivation was observed in any experiment (**Figure 6)**
- *The ongoing inhibition* during the substrate reaction was evaluated by plotting residual activity with the different mipafox concentrations at 0 time of inhibition (**Figure 7, plot B**). This effect was more than 20% of activity with the highest concentration and corresponded to the most sensitive component.
- A progressive inhibition experiment was done with mipafox 0, 10, 100 nM and 80 and 100 µM for times of up to 180 min at 37ºc (**Figure 7, plot A**). A 3D model was used to fit the data by plotting % activity versus time versus paraoxon concentration (**Figure 8**) to consider all the data simultaneously.

- *Conclusions of kinetic studies with mipafox*: Around 25% of phenyl valerate esterase activity was sensitive to mipafox in a time-progressive manner, suggesting covalent irreversible phosphorylation. Kinetic behavior was coherent with two sensitive esterase components, 11% and 5% and I50 (30 min) of 4 and 3398 nM respectively and a practically resistant component of 84% of the activity; where the most sensitive one was affected by the ongoing inhibition effect and a practically resistant component of 84% of the activity.

4.3.3. PMSF kinetic behavior (*Mangas et al., 2012b)*

Three different kinetic experiments were done in the soluble brain fraction with the inhibitor PMSF: fixed-time inhibition, spontaneous reactivation and progressive inhibition. The best model equation obtained to fit the data according to the F-test is shown in each section with the kinetic parameters obtained for each experiment (**Table 1**).

- *A fixed-time inhibition experiment* with PMSF at a concentration from 1 nM to 1000 µM, as shown in **Figure 1**. The best fitting model was a model in which three enzymatic components were discriminated.
- A s*pontaneous reactivation experiment* with PMSF at a concentration of 500 and 1000 µM, 500 µM to inhibit only the most sensitive component and 1000 µM to inhibit both sensitive components. No spontaneous reactivation was observed in any experiment (**Figure 2**).
- *The ongoing inhibition* during the substrate reaction was evaluated by plotting residual activity with the different PMSF concentrations at 0 time of inhibition (**Figure 3, plot B**). This effect was more than 20% of activity with the highest concentration and corresponded to the most sensitive component.
- A progressive inhibition experiment was done with PMSF 0, 20, 70, 300 and 1000 µM for times of up to 75 min at 37ºC (**Figure 3, plot A**). A 3D model was used to fit the data by plotting % activity versus time versus paraoxon concentration (**Figure 3, plot C**) to consider all the data simultaneously.
- *Conclusions of kinetic studies with PMSF*: More than 70% of phenyl valerate esterase activity was sensitive to PMSF in a time-progressive manner, suggesting covalent irreversible sulfonylation. Kinetic behavior was coherent with two sensitive esterase components of 61% and 11%, with I50 at 20 min of 70 and 447 µM, respectively and a third resistant component of 28%. The estimated constant of the chemical hydrolysis of PMSF was kh = 0.23 min−1 and the most sensitive component was affected by the ongoing inhibition effect.

4.3.4. Discrimination of components with mipafox to those with paraoxon, a sequential inhibition experiment (*Mangas et al., 2011).*

Preincubation with 100 µM mipafox was performed to inhibit both the components sensitive to mipafox according to kinetic data with mipafox. Afterward, a progressive inhibition experiment was performed with paraoxon (0, 600 and 2000 nM), as shown in **Figure 9 (*Mangas et al., 2011*)**. This experiment allowed relating those phenyl valerate esterases sensitive to mipafox with those sensitive to paraoxon.

The resistant fraction to 100 µM mipafox was inhibited completely by paraoxon and it had the kinetic constant of component E2 for paraoxon. Based on these data it is concluded that E2 for paraoxon is the resistant component (R) to mipafox.

Other sequential inhibition assays were done in soluble fraction which are described in **Section 4.5**.

4.3.5. Global analysis to discriminate esterase components in soluble fraction

Three enzymatic components were discriminated using paraoxon, three using mipafox and three using PMSF as inhibitors. The detected amplitudes were similar with all the inhibitors. This observation allows the identification of components with paraoxon, and of those with mipafox and PMSF. Moreover, the sequential experiment using paraoxon and mipafox confirm this hypothesis as mipafox-resistant activity shows the expected properties of E2 with paraoxon. **Table 4.1** provides the three esterase components discriminated, called **Eα, Eβ** and **Eγ (Table 3, *Mangas et al., 2012b*)**

Eα is around 11-28% of activity in soluble fraction. It is highly sensitive to either paraoxon (I50, 30min=9-11 nM) and mipafox (I50, 30min=4 nM), and it is spontaneously reactivated after paraoxon inhibition ***(Mangas et al., 2011).*** This component has a greater or similar sensitivity to other serine hydrolases known as targets of OPs in nervous tissues: e.g., (1) Hen brain AChE, paraoxon I50, 30 min of 28 nM and mipafox of 5373 nM, (Kemp and Wallace., 1990).

The global analysis of the kinetic interactions with **Eα** suggest that **Eα** might play a role in toxicity in the low-level long-term exposure of organophosphate compounds, and may be relevant in chronic exposure or in OPs detoxication in relation to spontaneous reactivation after paraoxon inhibition ***(Mangas et al., 2012b).***

Eβ is 61-84% of phenyl valerate esterase activity in soluble fraction and is sensitive to paraoxon (I50, 30min=1216 nM) and PMSF (I50, 30min=70 μM). However it is resistant to mipafox at micromolar concentrations.

According to its kinetic behavior, the molecular target of potentiation can be found among esterases **Eβ** as it is sensitive to PMSF and is resistant to mipafox. This component is likely to be involved in the potentiation of the OPIDN effect, which further isolation and molecular characterization assays will help elucidate. Sequential inhibition assays show that no kinetic interactions were observed at other sites in component **Eβ.**

Eγ is 5-11% of activity and is also the so-called S-NTE (Vilanova et al., 1990). **Eγ** fits the operational criteria of NTE by being NTE-like (40 μM paraoxon-resistant and with I50 (30 min) with mipafox of 3.3-6.0 μM, which is comparable to the value obtained by the Johnson membrane-bound protein, I50 (30 min) = 4.7 μM with mipafox (Johnson, 1982). **Eγ** is also sensitive to PMSF, as is NTE, with I50, 20 min=447 μM, is less sensitive than the NTE-membrane bound enzyme value of 100 μM for 30 min obtained by Milatovic et al., (1997).

An enzymatic activity like NTE in soluble esterases called S-NTE1 has already been defined by Escudero and coworkers, in a brain soluble fraction, with I50 (30 min) 5.2 μM. Fraction S-NTE1 was proposed to be a membrane-bound NTE form, solubilized at pH 8.0 and not at pH 6.8. (Escudero et al., 1997). Gambalunga and colleagues (2010) suggested that the potentiation target is embraced in a separated fraction by molecular exclusion chromatography of soluble phenyl valerate esterases of hen sciatic nerve, called peak V0. This soluble esterase fraction forms part of S-NTE, which was first described by Escudero and coworkers. It has been found in brain, spinal cord and sciatic nerve soluble esterases (Escudero et al., 1997).

Final remarks about the kinetic discrimination of soluble esterases

Further purification, isolation and molecular studies will be needed to elucidate the toxicological and biological meaning of all of these kinetic interactions in these esterase components. At this point, questions arise as to whether these esterase components are known protein targets of OPs or if they are novel protein targets; if each esterase component corresponds to one protein or to a mixture. It seems plausible that esterase activity corresponds to one major enzyme in any of the components as behavior with the different inhibitors is the same for the whole percentage of activity. The kinetic data of this work will be useful in defining the search of target esterases in further isolation and molecular studies to identify these target proteins, to evaluate the potency of inhibitors, and to design prevention and therapy strategies (Sogorb et al., 2004; Worek et al., 2004, 2007).

Table 4.1. Discrimination of the three esterase enzymatic components in soluble brain fractions by globally considering all the experiments with paraoxon, mipafox and PMSF.

	Amplitude of the component	PARAXON I50 (30 min) #	MIPAFOX I50 (30min) #	PMSF I50 (20min) *
Eα	11-28%	9-11 nM (r)	4 nM	R
Eβ	61-84%	1216 nM	R	70 µM
Eγ	5-11%	R	3398 nM	447 µM

(r) Spontaneous reactivation; R= Resistant to the highest tested concentration
From ***Mangas et al., 2011***
* From ***Mangas et al., 2012b***

4.3.6. Proposed simplified method for monitoring esterase components in soluble fraction

A protocol for a simple test of a routine analysis of all the phenyl valerate esterases components in soluble chicken brain is a practical conclusion drawn from the kinetic data obtained. Mipafox was selected as the inhibitor model because there was no spontaneous reactivation after its inhibition and it remained stable during the inhibition assay.

Figure 4.1 shows the proposed simplified assay, and three different conditions are defined:

- ✓ **Activity A** was measured as total phenyl valerate esterase.
- ✓ **Activity B** was measured as phenyl valerate esterase activity resistant to 25 nM mipafox for 30 min at 37ºC.
- ✓ **Activity C** was measured as activity resistant to 25 µM mipafox for 30 min at 37ºC.

The esterase components were estimated as follows.

- ✓ **Component Eα** calculated as the difference of (A-B) activities.
- ✓ **Component Eβ** calculated as activity C.
- ✓ **Component Eγ** calculated as the difference of (B-C) activities.

This simplified assay with discriminating mipafox concentration (0, 25 nM and 25 µM) is a useful tool for toxicological testing *in vivo* and for the routine analysis to discriminate the main esterase components in a soluble fraction. This simplified assay was applied to monitor the subfractions in the separation and purification by the high-performance chromatography method described later.

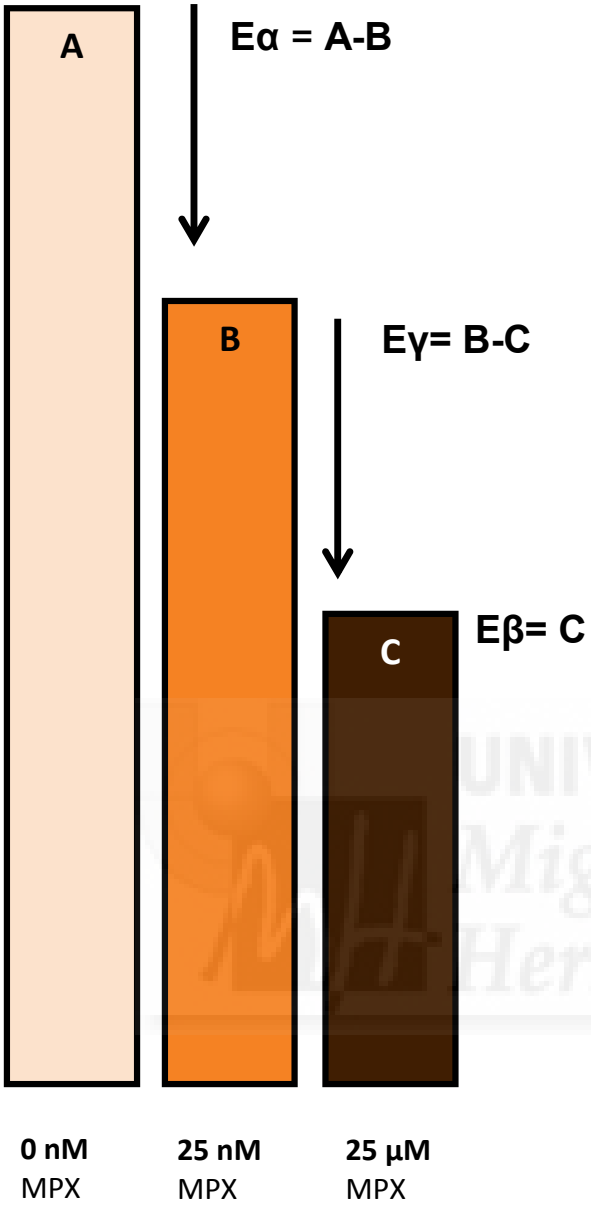

Figure 4.1. Discriminating assay with mipafox of the phenyl valerate esterase components in soluble fraction of chicken brain. A simple test with selected critical discriminating inhibitor concentrations allowed to discriminated the three different enzymatic activities in a soluble fraction: **(A)** was measured as total phenyl valerate esterase; **(B)** was measured as phenyl valerate esterase activity resistant to 25 nM mipafox for 30 min at 37ºC; and **(C)** was measured as activity resistant to 25 µM mipafox for 30 min at 37ºC. The percentage of the each esterase component is estimated as: Eα= (A-B), Eβ = C and Eγ =(B-C).

4.4. MEMBRANE PHENYL VALERATE ESTERASES INHIBITION WITH PARAOXON, MIPAFOX AND PMSF

In membrane fraction of chicken brain kinetic experiments were done with paraoxon and mipafox (published in ***Mangas et al., 2012a***) and PMSF (published in ***Mangas et al., 2013a***). The reference numbers of the tables and figures in this section correspond to those reference numbers in the publications.

4.4.1.Paraoxon kinetic behavior (*Mangas et al., 2012a)*

Three different kinetic experiments were done in membrane brain fraction with the inhibitor paraoxon: fixed-time inhibition, spontaneous reactivation and progressive inhibition. The best model equation obtained to fit the data according to the F-test is shown in each section with the kinetic parameters obtained for each experiment (**Table 1**).

- *A fixed-time inhibition experiment* with paraoxon at a concentration from 1 nM to 40 µM, as shown in **Figure 1**. The best fitting model was a model where three enzymatic components were discriminated.
- A s*pontaneous reactivation experiment* with paraoxon at a concentration of 40 nM and 1000 nM, 40 nM to inhibit only the most sensitive component and 1000 nM to inhibit both sensitive components. More than 4% of activity was time-progressive and spontaneously reactivated after diluting. Mathematical models for reactivation were applied to the data by considering the residual paraoxon concentration of 4 nM after diluting.
- *The ongoing inhibition* during the substrate reaction was evaluated by plotting residual activity with the different paraoxon concentrations at 0 time of inhibition (**Figure 2, plot B**). This effect was around 8% of activity with the highest concentration and corresponded to the most sensitive component.
- A progressive inhibition experiment was done with paraoxon 0, 40, 250, 1000 and 7000 nM for times of up to 180 min at 37ºc (**Figure 2, plot A**). A 3D model was used to fit the data by plotting % activity versus time versus paraoxon concentration (**Figure 2, plot C**) to consider all the data simultaneously.
- *Conclusions of kinetic studies with paraoxon*: Around 70% of phenyl valerate esterase activity was extremely sensitive to paraoxon in a time-progressive manner, suggesting covalent irreversible phosphorylation. Kinetic behavior was coherent with two sensitive esterase components, 8% and 38%, with I50 at 30 min of 15 and 1540 nM, respectively and a third resistant component of 54%; where the most sensitive

component it is spontaneously reactivated and is affected by the ongoing inhibition effect.

4.4.2.Mipafox kinetic behavior (*Mangas et al., 2012a)*

Three different kinetic experiments were done in membrane brain fraction with the inhibitor mipafox: fixed-time inhibition, spontaneous reactivation and progressive inhibition. The best model equation obtained to fit the data according to the F-test is shown in each section with the kinetic parameters obtained for each experiment (**Table 2**).

- *A fixed-time inhibition experiment* with mipafox at a concentration from 1 nM to 250 µM, as shown in **Figure 3**. The best fitting model was a model where three enzymatic components were discriminated.
- A s*pontaneous reactivation experiment* with mipafox at a concentration of 40 nM and 8000 nM, 40 nM to inhibit only the most sensitive component and 8000 nM to inhibit both sensitive components. No spontaneous reactivation was observed in any experiment.
- *The ongoing inhibition* during the substrate reaction was evaluated by plotting residual activity with the different mipafox concentrations at 0 time of inhibition (**Figure 4, plot B**). This effect was around 10% of activity with the highest concentration and corresponded to the most sensitive component.
- A progressive inhibition experiment was done with mipafox 0, 200, 800, 3500 and 8000 nM for times of up to 180 min at 37ºc (**Figure 4, plot A**). A 3D model was used to fit the data by plotting % activity versus time versus paraoxon concentration (**Figure 4, plot C**) to consider all the data simultaneously.
- *Conclusions of kinetic studies with mipafox*: Around 60% of phenyl valerate esterase activity was sensitive to mipafox in a time-progressive manner, suggesting covalent irreversible phosphorylation. Kinetic behavior was coherent with two sensitive esterase components, 5% and 39%, with I50 at 30 min of 29 and 6601 nM, respectively and a third resistant component of 56%; where the most sensitive component is affected by the ongoing inhibition effect.

4.4.3. PMSF kinetic behavior (*Mangas et al., 2013a)*

Two different kinetic experiments were done in membrane brain fraction with the inhibitor PMSF: fixed-time inhibition and progressive inhibition. The best model equation obtained to fit the data according to the F-test is shown in each section with the kinetic parameters obtained for each experiment (**Table 1**).

- *A fixed-time inhibition experiment* with PMSF at a concentration from 1 to 1000 µM, as shown in **Figure 1**. The best fitting model was a model where three enzymatic components were discriminated.
- *The ongoing inhibition* during the substrate reaction was evaluated by plotting residual activity with the different PMSF concentrations at 0 time of inhibition (**Figure 2, plot B**). This effect was around 60% of activity with the highest concentration and corresponded to two enzymatic components. Despite PMSF not being a potent inhibitor, Inhibition during the substrate reaction was significant in this case and it affected two enzymatic components. This could be related to the fact that it needed higher concentrations at PMSF in the PMSF inhibition experiments due to its spontaneously chemical hydrolysis, and because PMSF cannot be blocked by the presence of the phenyl valerate. These constants have to be considered to be operational empiric constants, and not real kinetic constants (Estévez and Vilanova., 2009). Carrington and Abou-Donia (1986) also used a similar deduced exponential factor to analyze the effect of inhibition during the substrate reaction time.
- A progressive inhibition experiment was done with PMSF 0, 10, 25, 75, 150, 250, 400 and 1000 µM for times of up to 180 min at 37ºC (**Figure 2, plot A**). A 3D model was used to fit the data by plotting % activity versus time versus PMSF concentration (**Figure 2, plot C**) to consider all the data simultaneously.
- *Conclusions of kinetic studies with PMSF*: Around 75% of phenyl valerate esterase activity was sensitive to PMSF in a time-progressive manner, suggesting covalent irreversible phosphorylation. Kinetic behavior was coherent with two sensitive esterase components entities representing 44 and 41 %, with I50 (20 min) of 23 and 138 µM, respectively, where both were affected by the ongoing inhibition effect and a resistant fraction of 15 % of activity. The estimated constant of the chemical hydrolysis of PMSF was also calculated (kh = 0.28 min−1).

4.4.4. Discrimination of NTE in the sequential assay versus the concurrent assay

This study was published in ***Mangas et al., 2012a***. The reference numbers of the tables and figures in this section correspond to those in the publication.

In order to distinguish the potential delayed neuropathy target or NTE (phenyl valerate esterase activity resistant to 40 µM paraoxon and sensitive to 250 µM of mipafox), two NTE assays were done: the sequential NTE assay, where paraoxon was removed before adding mipafox (**Figure 5A**) by ultrafiltration, and a concurrent assay, where paraoxon was not removed. Two NTE (paraoxon-resistant and mipafox-sensitive) esterase components were present using the sequential NTE assay by removing paraoxon before incubating with mipafox. However, there was only one NTE (paraoxon-resistant and mipafox-sensitive) component in the assay without removing paraoxon (**Figure 5B**). This work has proved that component **EPα** can be spontaneously reactivated, so it appears in the sequential NTE assay after removing paraoxon.

Discrepancies between the sequential and concurrent NTE assays were previously reported in 1983 (Chemnitius et al., 1983): Similar results were reported by Carrington and Abou-Donia (1985) and by Chemnitius et al., (1983). This mechanism was explained considering that inhibition by paraoxon of hen brain particulate NTE shows kinetics that are compatible with the formation of a reversible intermediate complex between the enzyme and the inhibitor (Carrington and Abou-Donia., 1986). This work proves that the discrepancy in the methods can be explained as being the result of spontaneous reactivation after paraoxon inhibition. The results of this work confirm that paraoxon is not the most appropriate tool to discriminate potential targets of neurotoxicity in a membrane fraction of brain as some fraction can be spontaneously reactivated.

4.4.5 Sequential inhibition experiments with mipafox and PMSF

This study was published in ***Mangas et al., 2013a***. The reference numbers of the tables and figures in this section correspond to those in the publication.

In the kinetic experiments with PMSF, only three phenyl valerate esterase components were discriminated. However a four-esterase component appeared when the NTE assays were done using paraoxon and mipafox. The sequential inhibition experiments with two inhibitors were required to establish the equivalence of the components detected herein with PMSF with those previously discriminated with paraoxon and mipafox. Two experiments were done:

Preincubation with 6 µM mipafox was performed to inhibit component **EPα** and part component **EPγ** (NTE), according to the kinetic data with mipafox in ***Mangas et al.2012a***. Afterward, a fixed-time inhibition experiment was performed with PMSF (**Figure 3B**). The best model to fit the PMSF fixed-time inhibition data was a model with two sensitive components and a resistant one. fixed-time inhibition data was a model with two sensitive components and one resistant one. These components display similar sensitivities to EP1 and EP2 with PMSF (**Table 1, Mangas et al., 2013a**) and the resistant component is resistant to PMSF and mipafox.

A second experiment was done by preincubation with 20 µM PMSF to inhibit part of components **EPβ** and **EPγ** according to the kinetic data with PMSF in **Table 1**. Afterward, a fixed-time inhibition experiment was performed with mipafox (**Figure 3A**). The best fit to the mipafox inhibition data was a model with two sensitive components and a resistant one. These components have displayed similar sensitivities to **EPβ** and **EPγ** (Mangas et al. 2012a).

Therefore, the two sensitive components discriminated with PMSF (EP1 and EP2) correspond to components **EPβ** and **EPγ**, which are discriminated with paraoxon and mipafox, while the PMSF-resistant component (R) should correspond to components EPα (inhibited by 6 µM mipafox), plus EPδ (resistant to mipafox and PMSF).

4.4.6. Global analysis discriminating esterase components in membrane fraction

When globally considering all the previous kinetic studies, including the sequential experiment data with PMSF-mipafox, four enzymatic components were discriminated in membrane brain fractions (**Discussion section, Figure 4, *Mangas et al., 2013a***) according to their sensitivity to paraoxon, mipafox and PMSF, and are called **EPα**, **EPβ**, **EPγ** and **EPδ** (**Table 4.2**)

EPα represents a small proportion of phenyl valerate esterase activity, of 4-8% of activity in the membranes. It is a highly sensitive to both paraoxon (I50, 30min=15-43 nM) and mipafox (I50, 30min=29nM), and it is spontaneously reactivated after paraoxon inhibition (***Mangas et al., 2012a***). However **EPα** is resistant to PMSF inhibition, therefore unlike to be the target of potentiation. It is more sensitive to both paraoxon and mipafox than chicken NTE -paraoxon resistant to 40 µM and mipafox sensitivity of 5-7 µM- (Johnson., 1982). **EPα** sensitivity is in the same order of sensitivity as other serine hydrolases known as targets of OPs: E.g. (1) Hen brain AChE, paraoxon I50, 30min of 28 nM and mipafox of 5373 nM (Kemp and Wallace., 1990). It is spontaneously reactivated after paraoxon inhibition. Hence, it appears as a second NTE component in the sequential NTE assay when paraoxon is removed, so it cannot be ruled out as a potential target of OPIDN according to the operational definition of NTE.

The global analysis of the kinetic interactions with **EPα** suggest that may be relevant in chronic exposure in relation to spontaneous reactivation after paraoxon inhibition (***Mangas et al., 2012a***). **EPα** could also be related with the detoxication of OPs because of its spontaneously reactivation, therefore acting as B-esterase catalytic scavenger.

EPβ represents a 38-41% of phenyl valerate esterase activity in membrane, is sensitive to both paraoxon with I50, 30min=1540 nM (***Mangas et al., 2012a***) and PMSF with I50, 30min=144 µM (***Mangas et al., 2013a***). However, it is resistant to mipafox at micromolar concentrations.

According to its kinetic behavior, the molecular target of potentiation could be found among the esterases in **EPβ** component as it is sensitive to PMSF and resistant to mipafox (***Mangas et al., 2013a,*** **Discussion section**). Other no-NTE phenyl valerate esterases were studied as potential targets of potentiation of OPIDN in homogenized chicken brain and sciatic nerve, I50 (30 min) with PMSF was 50 µM, and sequential assays were done with mipafox or DFP, followed by PMSF (Moretto et al., 2007).

EPγ corresponds to NTE according to its kinetic characteristics and is the only esterase component of these discriminated in this work for which a toxicological role has been identified. Already, in 1954 Aldridge proposed the phosphorylation of an esterase as the primary target of mechanism of OPIDN. NTE was discovered as a result of the search to identify the target protein for OPIDN by kinetic identification in 1969 by Johnson (Johnson., 1969a; 1969b). Currently, it has been molecularly and genomically characterized (Glynn. et al., 1999). Since 1969, NTE has been operationally monitored as that esterase activity which hydrolyzes the artificial substrate phenyl valerate, which is resistant to the non neuropathic OP ester paraoxon (40 µM, 20 min, pH 8.0) and is sensitive to neuropathic OP ester mipafox (50 µM, 20 min) (Johnson 1969a). **EPγ,** 39-48% of activity in membranes, has a I50 (30 min)= 5.3-6.6 µM mipafox, which is comparable to the value obtained by Johnson for the membrane-bound protein, which had I50 (30 min) = 4.7 µM mipafox (Johnson., 1982). It is also sensitive to PMSF with I50 (20 min)=138 µM, which is also comparable to the value obtained by Milatovic and colleagues for NTE with I50 (30 min) =100 µM for 30 min (Milatovic et al., 1997).

Kinetic data for **EPγ** component allow to validate the method used in this work to discriminated enzymatic components and to obtain kinetic parameters for enzymatic complex situations (more than one enzymatic component with different properties).

After its kinetic identification, NTE was purified by Glynn in 1994 (Glynn et al., 1994) and its encoding gene identified (Glynn et al., 1998; Glynn et al., 1999). Studies have shown its

molecular structure (Li et al., 2003) and its distribution in tissues and cells (Escudero et al., 1997). Nonetheless, the relationship of NTE and OPIDN has been established and the inhibition and aging of NTE are considered to be the initiation event of OPIDN. Currently, the biological function of NTE is not completely understood and some questions in OPIDN-NTE molecular toxicology remain to be answered. Yet the most important ones are: What are the exact events occurring after NTE inhibition and aging and before the clinical signs of OPIDN? Why do susceptible animals, such as humans, cats and hens, display the OPIDN signs after being exposed to neuropathic OP, while rodents like mice, rats, and rabbits are reluctant? What is the function of NTE in non neural tissues and cells? (Wu and Chang, 2006). The organophosphates used to establish the multistep hypothesis of OPIDN have multiple targets and it has been proposed that the association with NTE inhibition may be an epiphenomenon (Winrow et al., 2003). Now there is some evidence for its physiological function: NTE knockout of NTE is embryonic lethal (Winrow et al., 2003), probably due to the impairment of vasculogenesis in the placenta (Moser et al., 2004), yet when localized to the hippocampus, it gives vacuolation of neuronal bodies and dendrites (Akassoglou et al., 2004). However studies continue to focus on understanding the functional roles of some of its domains (Richardson et al., 2013).

EPδ represent around 10% of phenyl valerate esterase activity in membranes and it is a resistant phenyl valerate esterase component to all the inhibitors concentrations tested.

Purification, isolation and molecular studies will be needed to elucidate the toxicological and biological meaning of all of these esterase components.

Table 4.2. Discrimination of the four esterase enzymatic components in membrane brain fraction by globally considering all the experiments with PMSF, mipafox and paraoxon.

	Amplitude of the component	**PARAXON** I50 (30 min) #	**MIPAFOX** I50 (30min) #	**PMSF** I50 (20min)*
membrane				
EPα	4-8 %	15-43 nM(r)	29 nM	R
EPβ	38-41 %	1540 nM	R	138 µM
EPγ	39-48 %	R	6601 nM	23 µM
EPδ	10 %	R	R	R

(r) Spontaneous reactivation; R= Resistant to the highest tested concentration.
 # From Mangas et al., 2012a* From Mangas et al., 2013a

4.4.7. Proposed simplified method for monitoring the esterase components in membrane fraction

A protocol for simply testing in routine analysis of all the phenyl valerate esterases components in membrane chicken brain is a practical conclusion of the obtained kinetic data. Mipafox was selected as the model inhibitor because no spontaneous reactivation occurred after its inhibition and it remained stable during the inhibition assay.

Figure 4.2 shows the proposed simplified assay, and four different conditions are defined:

- ✓ **Activity A** was measured as total phenyl valerate esterase.
- ✓ **Activity B** was measured as phenyl valerate esterase activity resistant to 120 nM mipafox for 30 min at 37ºC.
- ✓ **Activity C** was measured as activity resistant to 25 µM mipafox for 30 min at 37ºC.
- ✓ **Activity D** was measured as the activity resistant to 25 µM mipafox + 600 µM PMSF for 30 min at 37ºC.

The esterase components were estimated as follows:

- ✓ **Component EPα** calculated as the difference of (A-B) activities.
- ✓ **Component EPβ** calculated as the difference of (C-D) activities.
- ✓ **Component EPγ** calculated as the difference of (B-C) activities.
- ✓ **Component EPδ** calculated as activity D.

This kinetic assay will be needed for further purification and fractionation assays in order to molecularly identify these esterases.

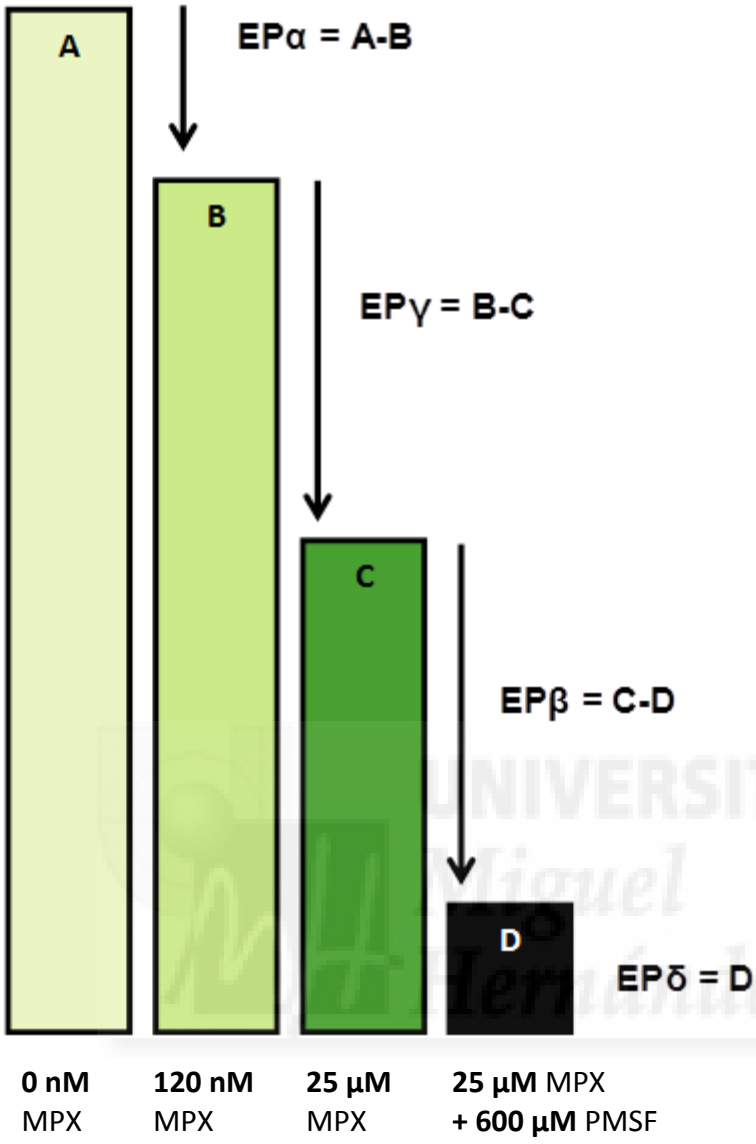

Figure 4.2. Discriminating assay of the four phenyl valerate esterase components in membrane fraction of chicken brain. A simple test with a four discriminate inhibitor concentrations in a membrane fraction: (**A**) was measured as total phenyl valerate esterase; (**B**) was measured as activity resistant to 120 nM mipafox for 30 min at 37ºC; (**C**) was measured as activity resistant to 25 µM mipafox for 30 min at 37ºC; and (**D**) was measured as activity resistant to 25 µM mipafox + 600 µM PMSF for 30 min at 37ºC. The percentage of the each esterase component is: **EPα** =(A-B), **EPβ** =(C-D), **EPγ** = (B-C) and **EPδ**=D

4.5. KINETIC STUDIES WITH MORE THAN ONE INHIBITOR, STUDY OF THE INTERACTION AMONG INHIBITORS

Sequential inhibition assays are defined as experiments where samples were preinhibited with an inhibitor. After a preinhibition time, residual activity was used to study kinetic inhibition with the other inhibitor. Sequential inhibition experiments with more than one inhibitor were done in order to confirm the discrimination of the components (explained in **Sections 4.3.4** and **4.4.4** and **4.4.5**) and to study if any of the components change their sensitivity to the other inhibitor in soluble and membrane fractions.

4.5.1. Kinetic interactions among inhibitors in the soluble fraction

The following effects related to the interaction with the inhibitors in soluble fraction were studied by sequential inhibition experiments:

- If the sensitivity of component **Eβ** changes to paraoxon after preincubation with 100µM mipafox
- If the sensitivity of any of the components **Eβ** or **Eγ** change to PMSF after preincubation with 20 nM mipafox
- If the sensitivity of component **Eγ** changes to mipafox after preincubation with paraoxon, with PMSF, or with both concurrently.
- If the sensitivity of component **Eα** changes to paraoxon or to mipafox after preincubation with PMSF

For these purposes, the following sequential experiments in soluble fraction were done:

i. *Paraoxon progressive inhibition in soluble fraction preinhibited with 100 µM mipafox, component* **Eβ** *(*explained in **Section 4.3.4**)

The resistant fraction to mipafox was inhibited completely by paraoxon and it had the kinetic constant of Eβ. From these data, it is concluded that sensitivity of **Eβ** to paraoxon is not affected by mipafox preincubation, neither when mipafox is still in the assay.

ii. *Mipafox inhibition (30 min) in soluble fraction preinhibited with different PMSF concentrations (**Figure 4** and **Table 2** in **Mangas et al., 2012b**)*

Fixed-time inhibition experiments (for 30 min at 37ºC) with different concentrations from 0.1 nM to 250 µM mipafox were done on residual phenyl valerate esterase activity after preincubation with 0, 1, 10, 50, 150 or 4000 µM of PMSF for 20 min. Moreover, a sample was incubated with the product of the chemical hydrolysis of PMSF 2000 µM for 40 min at 37ºC. The resistant activity to the PMSF concentrations and the kinetic parameters of the best fitting model of the mipafox inhibition data for each experiment are shown in ***Table 2, Mangas et al., 2012b***.

The best fitting model (according to the F-test) in the soluble fraction preinhibited with 0 and 5 µM of PMSF were the models with two sensitive enzymatic entities (which correspond to the properties of the components **Eα** and **Eγ**) and one resistan (**Eβ).** The best fitting model (according to the F-test) in the soluble fraction preinhibited with 10, 50 and 150 µM consisted in one sensitive enzymatic entity (**Eα)** and a resistant one (which included **Eβ,** plus part of **Eγ)**. The best fitting model (according to the F-test) in the soluble fraction preinhibited with 4000 µM consisted in one sensitive enzymatic entity (**Eα).**

The partial preincubation with PMSF of the soluble fraction affected the sensitivity to mipafox of the residual activity of components **Eα** and **Eγ** (***Table 2, Mangas et al., 2012b***). Eα became less sensitive to mipafox when the preparation was preincubated with PMSF, while **Eγ** became less sensitive after preincubation with 5 µM PMSF, and totally resistant to mipafox after preincubation with 10 µM, or more (***Mangas et al., 2012b***).

*iii. Paraoxon inhibition (30 min) in the soluble fraction preinhibited with 4000µM PMSF, component **Eα** (**Figure 5** and **Table 2** in **Mangas et al., 2012b**)*

A fixed-time inhibition experiment (for 30 min at 37ºC) with different concentrations from 0.1 nM to 40 µM paraoxon was done on residual phenyl valerate esterase activity after preinhibition with 4000 µM PMSF for 20 min, component (data shown in **Figure 5, Mangas et al., 2011**).

The resistant activity to PMSF, (**Eα**), was 18% and the best fitting model with paraoxon according to the F-test was a model with one sensitive component with an estimated I_{50} (30 min) of 185 nM. These results imply that sensitivity of Eα to paraoxon diminishes after preincubation with 4000 µM PMSF by changing paraoxon I50 (30 min) from 9-11 nM to 185 nM.

iv. Reactivation kinetics by dilution after inhibition with paraoxon in soluble fraction preinhibited with 2000µM PMSF, component ***Eα.***

A spontaneous reactivation assay after inhibition with 100 nM paraoxon was done for up to 150 min the resistant fraction to 2000 µM PMSF, component *Eα*. No spontaneous reactivation of ***Eα*** after inhibition with paraoxon was observed. Hence, ***Eα*** lost the spontaneous reactivation capacity previously observed after preincubation with PMSF.

v. PMSF progressive inhibition in soluble fraction preinhibited with 20 nM mipafox, components ***Eβ*** *and* ***Eγ*** *(**Estévez et al., 2013**)*

A progressive inhibition experiment (for up to 20 min at 37ºC) with 0, 20, 70, 300 or 1000 µM PMSF was done on residual phenyl valerate esterase activity after preinhibition with 20 nM mipafox for 30 min at 37ºC. (***Figure 2, Estévez et al., 2013***). The ongoing inhibition during the substrate incubation effect was analyzed (***Figure 2B, Estévez et al., 2013***) and it was significant. A 3D fit was applied to the data (***Figure 2, plot C, Table 2, Estévez et al., 2013***) by plotting % activity versus time versus paraoxon concentration to consider all the data simultaneously. Two sensitive components of 88.3% and 10.4%, and a resistant one of 1.3%, were estimated according to the best fitting model (according to the F-test).

Eβ showed a similar inhibition constant and a I50 value to the **Eβ** not preincubated, but the **Eγ** inhibition constant with mipafox was one order of magnitude lower with a I50 value more than a 10-fold higher than the I50 of the **Eγ** component that was not preincubated, although a similar proportion was observed (***Table 2, Estévez et al., 2013***).

vi. *Mipafox inhibition (30 min) in the samples preinhibited with 10µM paraoxon or with 10µM paraoxon and 10µM PMSF* ***(Estévez et al., 2013**)*

A soluble fraction was preincubated with 10 µM paraoxon to inhibit **Eα** and **Eβ** and residual activity, and **Eγ** was incubated with 10, 100 or 250 µM of mipafox (**Table 4, Estévez et al., 2013**). The observed inhibition was much lower than that expected for the properties deduced for **Eγ** in the non preincubated samples.

Similar experiments were done with 10 µM paraoxon and 10 µM PMSF. **Eα** and **Eβ** were both inhibited, while residual activity, **Eγ**, was incubated with 10, 100 or 250 µM of mipafox. Once again, the inhibition observed after further incubation with mipafox showed less inhibition than expected (***Table 4, Estévez et al., 2013***). However in this

second experiment, more inhibition of component **Eγ** was reached as compared with the experiment when only paraoxon was used.

The interaction between paraoxon or PMSF and mipafox in the active center was not expected because the concentration of the paraoxon or PMSF was lower (25-fold lower) than the higher mipafox concentration used.

vii. *Conclusions of the kinetic interactions studies in soluble fraction*

The sensitivity of components **Eα** and **Eγ** of the soluble esterases changed after preincubation to another inhibitor with no change noted in their phenyl valerate esterase activity, which contrasts to what happened in **Eβ** and in the membrane esterases. The partial preincubation with PMSF of the soluble fraction affected sensitivity to mipafox of the residual activity of components **Eα** and **Eγ** (***Table 2, Mangas et al., 2012b***). **Eα** became less sensitive also to paraoxon when the preparation was pre-incubated with PMSF (Table 2, Mangas et al., 2012b). **Eγ** became less sensitive to mipafox after preincubation to either paraoxon or PMSF (Table 4, Estévez et al., 2013).

The instability of PMSF is an advantage when used in sequential assays. PMSF disappeared from the medium in around 15 min without disturbing further studies. So it is clear that the inhibitor was not present in the assay. Furthermore, the observed alterations by preincubation with PMSF were not apparently related with the degradation products of PMSF, such as the hydrolyzed product of PMSF, and DMSO did not affect the activity of any component's sensitivity to mipafox (***Table 2, Mangas et al., 2012b***).

It is concluded that PMSF can interact covalently with **Eα**, and **Eγ** at a concentration that does not inhibit esterase activity. This effect changed the sensitivity to mipafox and paraoxon of **Eα** and the sensitivity to mipafox of **Eγ**. Paraoxon can interact covalently with **Eγ** at a concentration that does not inhibit esterase activity. Mipafox can interact covalently with **Eγ** at concentrations that not inhibit esterase activity.

4.5.2. Kinetic interactions among inhibitors in the membrane fraction

Kinetic studies with two inhibitors, paraoxon and mipafox or PMSF and mipafox, were done in a membrane fraction in the sequential inhibition experiments explained in **Section 4.3.4**.
Three experiments were performed:

i. *Discrimination of NTE in the sequential assay versus the concurrent assay* (***Mangas et al., 2012a***)

These experiments allowed to study if the sensitivity of any of the components **EPα, EPγ** or E**Pδ** changes to mipafox after preincubation with 40 µM paraoxon.

ii. *Mipafox fixed-time inhibition in a membrane fraction preinhibited with 20 µM PMSF* (***Mangas et al., 2013a***).

This experiment allowed to study if the sensitivity of any of the components **EPα, EPβ, EPγ** or **EPδ** changes to mipafox after preincubation with 20 µM PMSF.

iii. *PMSF fixed-time inhibition in a membrane fraction preinhibited with 20 µM mipafox* (**Mangas et al., 2013a**)

This experiment allowed to study if the sensitivity of any of the components **EPβ, EPγ** or **EPδ** changes to PMSF after preincubation with 20 µM mipafox.

iv. *Conclusions of the kinetic interactions studies in membrane fraction*

There is no evidence to suggest any changes in the sensitivity of these components to mipafox after preincubation with paraoxon and PMSF or of the esterase components to PMSF after preincubation with mipafox in membrane fraction.

Similar studies have been done by Vicedo and coworkers (1993), but these authors studied the interaction of PMSF and DFP in brain membrane NTE activity inhibition. No alteration in the inhibition kinetics of DFP for residual activity was observed after preincubation with PMSF, and vice versa.

It is highlighted that one interaction was not methodologically possible to study: if preincubation to mipafox affects PMSF sensitivity in **EPα** because of its highly sensitivity to mipafox.

4.5.3. Molecular implications of changes in sensitivity observed in soluble components

The strong modifications of sensitivity to another esterase inhibitor in soluble esterases of chicken brain (explained in **Section 4.5.1**) suggest that inhibitors can interact permanently at other sites than the site where phenyl valerate is hydrolyzed.

Preinhibition did not seem to significantly alter the reaction with the substrate because the estimated proportions of the components did not alter. According to these data in components **Eα** and **Eγ,** it is plausible that sites other than the active center binding with the substrate are present and can be inhibited by paraoxon, mipafox and/or PMSF. This covalent binding to the "second site" does not affect the phenyl valerate hydrolysis rate, but affects the inhibition rate of other esterase inhibitors. This different binding rate to the second inhibitor, but not to phenyl valerate, might be related to a structural change in the protein that does not affect phenyl valerate hydrolysis given the different sizes of the molecules.

Figure 4.3 shows an enzyme-inhibitor-substrate two sites binding model by way of example for the interactions observed with PMSF-mipafox in component **Eγ.** Where site 1 is the phenyl valerate catalytic site (**Figure 4.3, 1**). When an inhibitor bind to site 1 phenyl valerate esterase activity is inhibited, as by mipafox (**Figure 4.3, 2**). PMSF can bind to both sites, at high concentrations both sites are inhibited (**Figure 4.3, 3),** however at low concentration only site 2 is ocuped and phenyl valerate is hydrolyzed at the same rate (**Figure 4.3, 4),** however mipafox binding rate is lower (**Figure 4.3, 5).**

Several early studies provided evidence that some inhibitors of AChE, the esterase for which more molecular and structural data exist, can influence steady-state parameters by associating with a remote allosteric site from the active center (Changeux, 1966; Roufogalis and Quist, 1972; Robaire and Kato, 1974). However in this case, the catalysis of substrate acetylthiocholine was affected. This second site of AChE is now referred to as the peripheral anionic site. The peripheral site of AChE has been well mapped by mutant studies and by X-ray crystallography. The inhibitors of this second site have been shown to inhibit catalysis through a combination of steric blockades of ligands entering and leaving the gorge, and by an allosteric alteration of catalytic triad conformation and efficiency. However, currently the function of these second sites of AChE is not clear and non catalytic functions of AChE have been suggested (Inestrosa *et al*., 1996; Johnson and Moore, 1999; Soreq and Seidman, 2001). Peripheral site ligands have been demonstrated to accelerate AChE inhibition by some organophosphates, such as paraoxon or haloxon (Radic and Taylor., 2001). A peripheral site

has been also proved in human BuChE (Macdonald et al., 2012), but X-ray crystallographic data are still lacking.

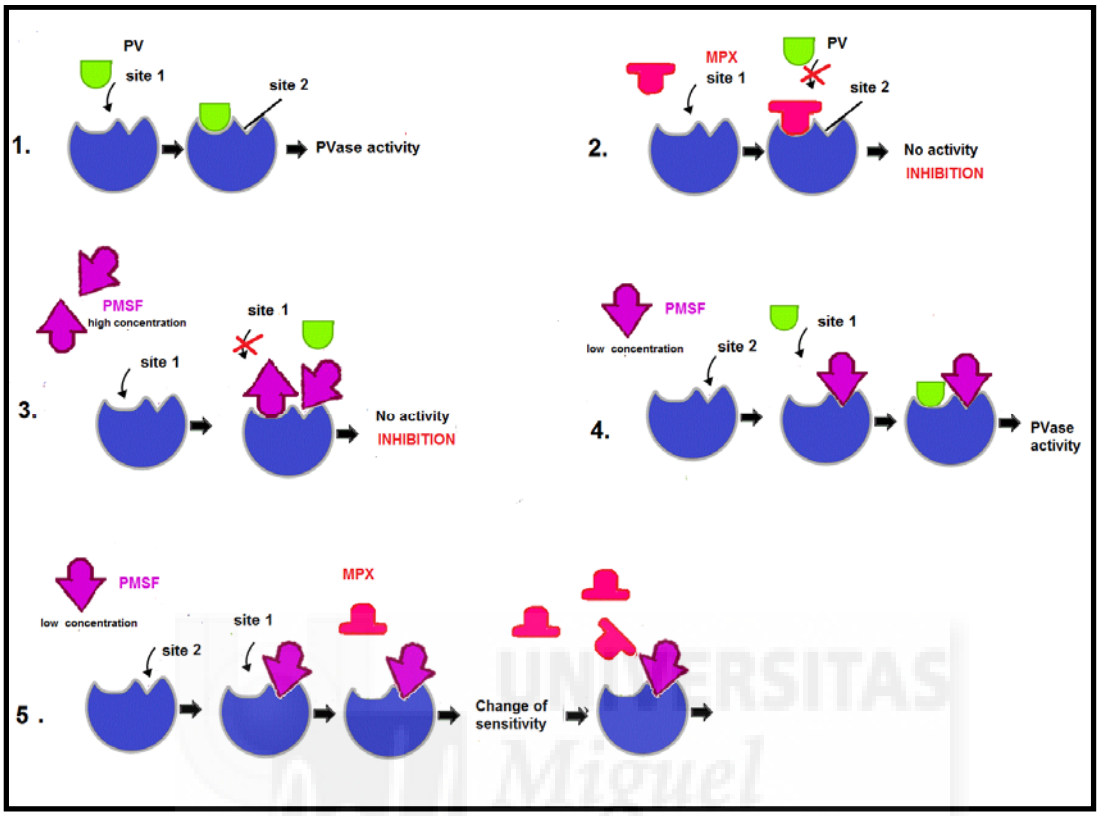

Figure 4.3. The enzyme-substrate binding model if two centers are present, by way of example for the interactions of Eγ. 1. Phenyl valerate binds to the catalytic site (site 1). **2**. Where site 1 is the phenyl valerate catalytic site. Mipafox binds to the catalytic site and there is no esterase activity. **3.** PMSF at high concentration binds to both sites. **4** and **5.** PMSF at low concentration binds to site 2 and phenyl valerate is hydrolyzed at the same rate, but mipafox binding rate is lower.

In this work, alterations of sensitivity occurred at low concentrations, at which esterase activity is not modified. The sensitivity of component **Eγ** to another inhibitor can be modify by nanomolar concentrations of mipafox, or micromolar of PMSF or paraoxon. Sensitivity of component **Eα** to another inhibitor can be modified with a few micromolars of PMSF.

Such interactions will have to be considered in the potentiation of OPIDN studies (***Mangas et al., 2013b; Estévez et al., 2013***). The potentiation effect appears when some esterase inhibitors (non neuropathic) are dosed after a low non neuropathic dose of a neuropathy inducer. PMSF has been reported to modify the sensitivity of components **Eα**, and **Eγ**, and these modifications can be related to the potentiation of the OIPDN effect (***Mangas et al., 2013b; Estévez et al., 2013***).

Such interactions have to be also considered in *in vivo* exposures to multiple esterase inhibitors (e.g., OPs pesticides and methylcarbamates) because preexposure to a low concentration can modify the response to the next exposure to another inhibitor. These molecular reactions highlight the possibility that exposure to an environmental toxicant may not affect the hydrolysis of the substrate. So no biological function can be modified, but the response to another environmental toxicant can. It has to be taken into account that carboxylesterases are enzymes that play key roles in the metabolism and that esterases inhibitors are common xenobiotics present in the environment (Satoh and Hosokawa., 1998). The results from this research have to be considered by understanding the molecular toxicological processes in exposure to mixtures of neurotoxicants.

4.6. FINAL REMARKS OF THE MOLECULAR AND TOXICOLOGICAL IMPLICATIONS THAT THE RESULTS OF THE KINETIC EXPERIMENTS HAVE

In the present work, the analysis of the kinetic data allowed us to characterize the whole group of phenyl valerate esterases in chicken brain with paraoxon, mipafox and PMSF. Carboxylesterases, and other serine hydrolases of brain, have received special attention to search for targets of the neurotoxic effects of OPs (AChE, BuChE, NTE, etc.). The target protein of OPIDN (NTE) was first found among esterases of chicken brain membranes (Johnson., 1969, 1982).

This work provides evidence that most of the esterases that hydrolyze phenyl valerate are highly or quite sensitive to one or several of these inhibitors. **Table 4.1** and **Table 4.2** show the kinetic parameters obtained with the three inhibitors. Knowledge of the kinetic behavior of esterases of the chicken brain with these inhibitor models is essential to be able to identify and to purify potential targets proteins (of OPIDN, of potentiation of OPIDN, and other neurotoxic effects of OPs) in order to evaluate the potency of inhibitors, and to design prevention and therapy strategies (Sogorb et al., 2004; Worek et al., 2004; 2007).

Susceptible components, associated inhibition constants and spontaneous reactivation constants are determined by applying the strategy and kinetic models previously described by Estévez and Vilanova (2009). These kinetics models have been previously used to discriminate sensitive esterases in chicken peripheral nerve (Estevez et al., 2004; 2009; 2011; 2012). With the present work, these kinetics models are applied in soluble and membrane complex tissues where different enzymatic components are present and distinct kinetic reactions are concomitant: spontaneous reactivation (***Mangas et al., 2011; Mangas et al., 2012a***), ongoing inhibition (***Mangas et al., 2011: 2012a; 2012b; 2013a***), chemical hydrolysis of the inhibitor (***Mangas et al., 2012b; 2013a***). The number of enzymatic components is the same as the different inhibitors, and the estimated kinetic parameters for each inhibitor are comparable in different kinds of experiments. These observations may be considered an internal validation of both the consistency of the results and the applied kinetic model. These kinetic models can be applied to discriminated esterases that are sensitive to OPs or to other inhibitors of esterases, such as carbamates and sulfonyl fluorides in other tissues and other species. This simple procedure has been demonstrated to be a useful tool to identify potential biomarkers of toxicity or exposure to OPs.

This characterization deduces the existence of seven esterase components with varying kinetic behaviors (**Table 4.1**.). Three of them are cytosolic (called **Eα, Eβ** and **Eγ, *Mangas et al., 2011; Mangas et al., 2012b***) and four are membrane-bound enzymes or group of enzymes (called

EPα, EPβ, EPγ and **EPδ**). Susceptible components and the associated kinetic parameters are determined by applying the strategy and kinetic models previously described by Estévez and Vilanova (2009).

The molecular identification of the proteins responsible for these enzymatic esterase components is a long-term objective of our group. So far, the only one identified is **EPγ,** NTE, which corresponds to the protein lisophosphatidyl choline hydrolase, codified by the gene pnpla6. For the other six components, molecular identification remains unknown and is under study.

4.7. FRACTIONATION OF PHENYL VALERATE ESTERASE COMPONENTS IN SOLUBLE CHICKEN BRAIN FRACTION

This study is submitted for publication in ***Mangas et al., 2013b*** (submitted paper). The reference numbers of the tables and figures in this section correspond to those in the publication.

To elucidate the functional significance of the OP-sensitive pool of esterases in chicken brain, protein fractionation and isolation method/s is/are needed. Indeed, our general interest lies in all the esterases that are able to interact with OPs and/or PMSF.

In this work, a soluble fraction of chicken brain was selected as the raw material to separate toxicologically relevant target proteins because: (1) soluble esterases have been shown to be more sensitive to OPs in this work; (2) the kinetic interactions among the inhibitors have been observed in soluble esterases and in non membrane esterases that can be related to their toxicological relevance; and (3) the enzymatic activity of interest can be followed during the fractionation procedure in soluble esterases without the addition of detergent, which is needed to dissolve proteins of interest and to keep membrane proteins in solution during purification.

In this work, the esterase components that are sensitive to OPs in the soluble fraction of chicken brain have been fractionated by several fractionation procedure steps. **Figure 4.4.** shows the final fractionation strategy. Afterward, an analysis of the same fractionation procedure was done with the esterase activity of the soluble fraction inhibited by mipafox (***Mangas et al., 2013b***).

4.7.1 Fractionation procedure of soluble esterases of chicken brain

In this work, a HPLC separation method was developed using native protein purification methods. To monitor the fractionation procedure, the protein profile at 280 nM, protein measure by the Bradford method (Bradford., 1976), esterase activity and the proportion of the enzymatic components discriminated were measured during the procedure in all the fractions onteined (***Mangas et al., 2013b***).

Figure 4.4 shows a diagram of the fractionation procedure, while **Tables 1** and **2** in ***Mangas et al., 2013b*** provide the purification values for each enzymatic component. The preparation scheme can be described as consisting mainly in three steps:

1. Subcellular fractionation: ultracentrifugation and ultrafiltration.
2. Size exclusion semipreparative high-performance chromatography.
3. Ion exchange semipreparative high-performance chromatography.

4.7.2. Subcellular fractionation by ultracentrifugation and ultrafiltration.

Broiler chicken brains (n=15) were obtained from a commercial slaughterhouse immediately after animals were killed and were kept in cold (0-5ºC) homogenization buffer until use. They were homogenized at a concentration of 200 mg of fresh tissue/ml in the same buffer and were centrifuged at 100,000xg for 60 min to obtain the soluble fraction of chicken brain. Samples were frozen in liquid nitrogen before use.

A volume of up to 15 ml of defrosted sample was introduced into a Ultracel-Amicon Ultra-15 to concentrate the biological material at a concentration corresponding to 1600 mg of fresh tissue/ml. The PVase activity in this tissue was 574 nmol/min g of fresh tissue and this tissue underwent the chromatography procedure (***Mangas et al., 2013b***).

4.7.3. Size exclusion chromatography step

Figure 3 shows the fractionation proteins profile by molecular exclusion chromatography. Total phenyl valerate esterase activity (A activity) showed three main peaks, the activity profile of **Eα** showed just one peak, the activity profile of **Eβ** was distributed along the three peaks, while **Eγ** activity showed just one peak. Subfractions were pooled as follows: Fraction S1: (from 4.50 ml to 6.00 ml Ve; total volume of 75 ml), containing mainly activity **Eα** and **Eβ**; Fraction S2: (from 6.01 to 8.50 ml Ve; total volume of 125 ml), containing mainly activity **Eβ**; Fraction S3: (from 8.51 ml to 9.00 ml Ve; total volume of 25 ml), containing mainly activity **Eβ** and **Eγ** and fraction S4: (from 9.01 to 15 ml Ve), without enzymatic activity. **Table 1** (***Mangas et al., 2013b***) shows the purification characteristics of fractions S1, S2, S3 and S4.

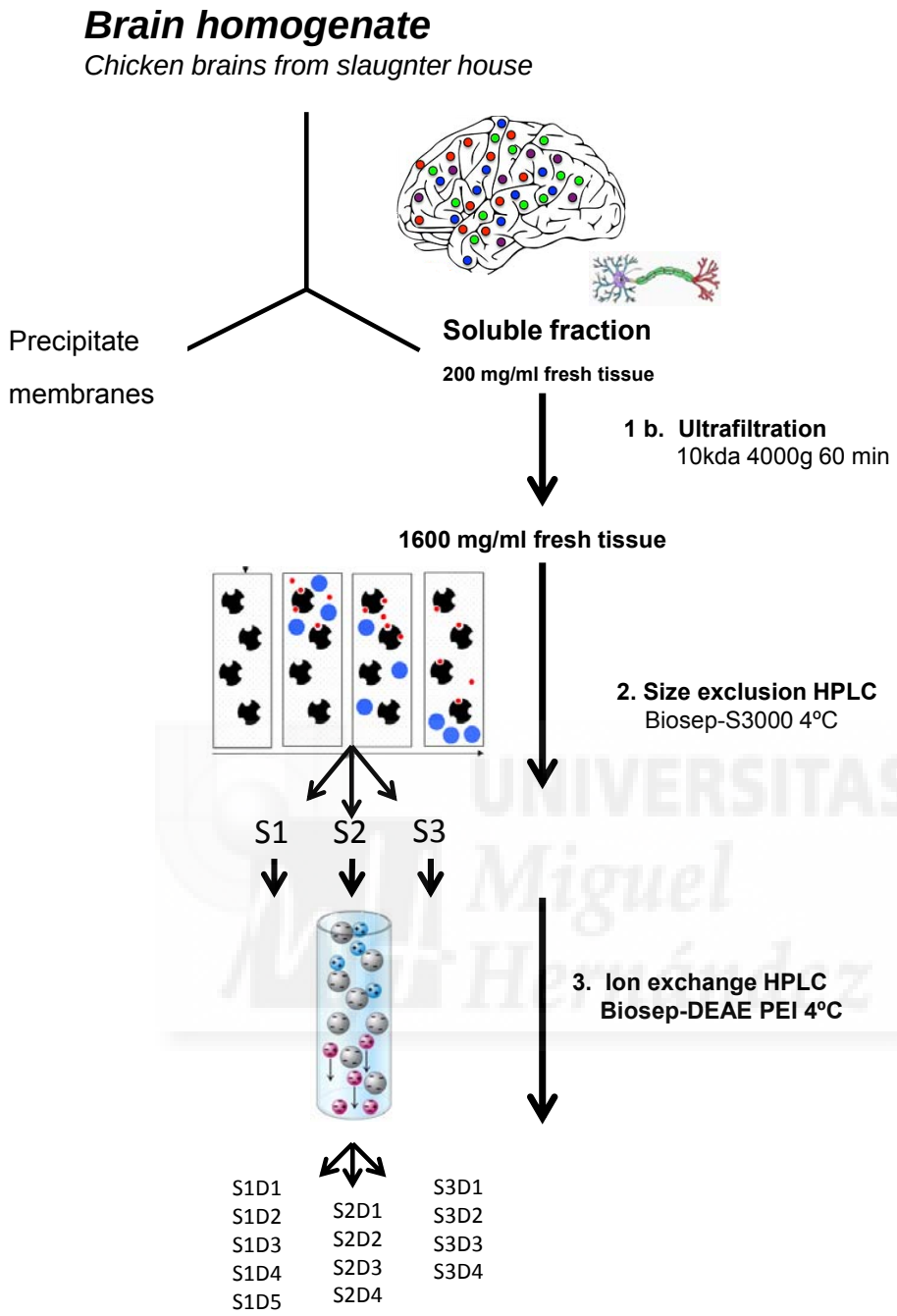

Figure 4.4. Fractionation procedure of soluble phenyl valerate esterases of chicken brain. A 80-ml volume of soluble brain fraction (at a concentration of 200 mg of fresh tissue/ml) **(1)** was defrosted 37ºC and **(2)** concentrated by ultrafiltration with 10 kDa Millipore filters at 4ºC up to 3.5 ml (corresponding to ~ 1600 mg of the original fresh tissue per milliliter). High-performance liquid chromatography was performed in an UFLC Shimadzu equipped with a fraction collector at 4ºC, as follows: ***(3)*** *Molecular exclusion chromatography* was performed at 4°C in a 300 x 7.8 mm BioSep-SEC-s3000. Fifty consecutive injections of 200 µl were performed and eluted in the column with 50 mM Tris /1 mM EDTA pH 7.5 buffer at a flow rate of 1 ml/min, and 30 x 0.5 ml subfractions were obtained for each injection. After the analysis, the subfractions containing esterase activity were pooled in three fractions, called S1, S2 and A3. Each fraction underwent *Ion exchange chromatography* in a 75 x 7.8 mm BioSep-DEAE-PEI.

4.7.4 Fractionation by ion exchange chromatography

Each fraction obtained in the previous step was underwent into the ion exchange chromatography procedure (***Mangas et al., 2013b***) and the proteins profile at 280 nm, proteins quantity by Bradford (Bradford., 1976), total phenyl valerate esterase activity and enzymatic components were followed during the procedure.

The fraction S1 profile results are provided in **Figure. 4**, the fraction S2 profiles in **Figure 5** and the fraction S3 profiles in **Figure 6**. **Table 2** shows the purification characteristics of each fraction obtained.

S1 was separated in the S1D1 fraction (Ve=2.73-3.93 ml), containing most of the total phenyl valerate esterase activity, 98% of activity corresponded to component **Eα**; the S1D2 fraction (Ve=14.-20.73 ml), containing the activity of components **Eα** and **Eβ**; the S1D3 fraction (Ve=20.74-26.73 ml), containing a mixture of the three components, and the S1D4 fraction (Ve=26.74-35.14 ml, containing a mixture of the three components.

S2 was separated in: the S2D1 fraction (Ve=2.73-5.13 ml), containing mainly activity **Eα**; the S2D2 fraction (Ve=17.73-18.33 ml), containing mainly Eα and a little **Eβ**; the S2D3 fraction (Ve from 21.93 ml to 31.53 ml), containing mainly **Eβ**. The S2D4 fraction (Ve= 31.53-47.13 ml), containing mainly **Eβ**. The majority of PVase activity was recovered in fractions S2D3 and S2D4, but mainly **Eβ**.

S3 was separated in: S3D1 (Ve= 1.53 -3.93 ml), containing a mixture of Eα and Eβ; S3D2 (Ve=15.93-19.53 ml), containing a mixture of the three components); S3D3 (Ve=19.53-21.93 ml), containing mainly Eγ and the S3D4 fraction (Ve from 21.93 ml to 26.73 ml), containing mainly Eγ. The majority of total activity was recovered in fractions S3D1, mainly **Eα**, and in fraction S3D4, mainly **Eγ**.

4.7.5. Chromatography of the samples inhibited and not inhibited by mipafox

A fractionation procedure was carried out with a preincubated soluble fraction of chicken brain with 25 µM mipafox for 30 min at 37ºC in order to inhibit components **Eα** and **Eγ**.

No difference in separation by size was observed between the chromatogram of the samples inhibited and the controls (**Figure 7**). However, different profiles were noted in the separation by ion exchange chromatography (**Figure 8**). Specifically, the chromatograms of fractions S2

and S3 gave a significant different chromatography profile of absorbance at 280 nm after inhibition with mipafox.

4.*7.6.* Molecular implications of the fractionation results

The soluble chicken brain fraction was separated into three different fractions of phenyl valerate esterase activity during the size exclusion chromatography; these fractions were pooled at 4ºC, conserved and called S1, S2 and S3. The recovery yield of protein and enzymatic activity was around 100%, and the chromatography procedure was high reproducible in more than 50 chromatograms. The majority of activity was recovered in S2 (around 60% of activity), with 30% recovered in S1 and 15% in S3, and the recovered protein yields were similar (19% in S1, 58% in S2 and 10 in S3). Fraction S1 contained a mixture of **Eα** and **Eβ**, fraction S2 comprised mainly **Eβ**, while fraction S3 included a mixture of **Eγ** and **Eβ**. The ion exchange separation method of all these fractions allowed us to obtain 13 fractions with activity with the distinct kinetic behavior with OPs. Different results were obtained when the same separation procedure was carried out with samples pretreated with mipafox. These results may suggest that treatment with mipafox modifies the ionic properties of a wide range of proteins in fractions S2 and S3.

We were unable to completely separate any of the esterase components in a unique fraction. Moreover, the purification factors of components **Eβ** and **Eγ** in the obtained fractions were poor. It is concluded that several molecular entities with phenyl valerate esterase activity are able to bind to OPs in the soluble fraction, which means that molecular characteristics are apparently responsible for the complexity of the chromatography separation profile: a wide range of proteins interacting with OPs in brain, different isoforms with the same kinetic behavior or a different oligomer complex of varying sizes (with several retention times in the gel filtration chromatography), but with the same kinetic behavior.

However, a 260 purification factor was obtained for component **Eα** in fraction S1D1 (**Table 2**). Moreover this fraction possesses only the activity corresponding to component **Eα** according to its inhibition with mipafox. It has around a 50% of total activity **Eα** in the soluble fraction. This fraction was chosen to do a preliminary protein identification test by Tandem Mass Spectrometry.

4.8. TANDEM MASS SPECTROMETRY APPROACH TO STUDY A FRACTIONATED SAMPLE (unpublished results).

4.8.1. Proteome profile of fraction S1D1

Fraction S1D1 was selected to analyze and test the proteomic analysis because: (1) it is the obtained fraction with the highest purification factor (more than 26-fold higher than the next fraction); (2) this fraction contains only one type of phenyl valerate esterase activity: activity **Eα**, the highest; (3) component **Eα** seems to be very toxicologically interesting according to kinetic experiments because it is highly sensitive and may have more than one catalytic center that interacts with OPs and PMSF.

From the S1D1 fraction obtained during chromatography, 259 proteins with multiple peptide details were identified from the 2818 peptides found to have a 5% FDR (False Discovery Rate) based on the LCMSMS analyses.

This study with fraction S1D1 demonstrated that the samples obtained in the fractionation procedure are appropriate for further proteomic analyses.

4.8.2. Search for potential targets of the organophosphorus bound in the list of proteins

This list of proteins was compared with the list of all the serine hydrolases in the proteome of chicken (Gallus gallus) in NCBI database and with the list of alfa/beta hydrolases in ESTHER database. Of the 259 proteins identified, only one met the criterion of being a serine hydrolase and a alfa/beta hydrolase, the protein called “cholinesterase precursor”. Cholinesterase precursor of Gallus gallus, gi 453828, was identified with 19.9% coverage and six peptides of the protein were identified. Further studies are required to identify if the phenyl valerate esterase activity of S1D1 is due to this protein. However, there is evidence to suggest that proteins other than serine hydrolases and other residues, such as tyrosine and lysine, can interact with OPs and that perhaps these phenyl valerate esterases are from another family of proteins. Further work is needed to perform the complete physical isolation and biochemical characterization of these enzymatic entities.

5. PUBLICATIONS

UNIVERSITAS
Miguel
Hernández

Toxicology and Applied Pharmacology 256 (2011) 360–368

Contents lists available at ScienceDirect

Toxicology and Applied Pharmacology

journal homepage: www.elsevier.com/locate/ytaap

Kinetics of the inhibitory interaction of organophosphorus neuropathy inducers and non-inducers in soluble esterases in the avian nervous system

Iris Mangas, Eugenio Vilanova, Jorge Estévez *

Unidad de Toxicología, Instituto de Bioingeniería, Universidad Miguel Hernández de Elche, Avda. Universidad s.n. ES-03202, Elche (Alicante), Spain

ARTICLE INFO

Article history:
Received 25 February 2011
Revised 3 May 2011
Accepted 4 May 2011
Available online 12 May 2011

Keywords:
Organophosphorus
Esterases
Spontaneous reactivation
Inhibition
Neurotoxicity
Kinetic

ABSTRACT

Some published studies suggest that low level exposure to organophosphorus esters (OPs) may cause neurological and neurobehavioral effects at long term exposure. These effects cannot be explained by action on known targets. In this work, the interactions (inhibition, spontaneous reactivation and "ongoing inhibition") of two model OPs (paraoxon, non neuropathy-inducer, and mipafox, neuropathy-inducer) with the chicken brain soluble esterases were evaluated. The best-fitting kinetic model with both inhibitors was compatible with three enzymatic components. The amplitudes (proportions) of the components detected with mipafox were similar to those obtained with paraoxon. These observations confirm the consistency of the results and the model applied and may be considered an external validation. The most sensitive component (Eα) for paraoxon (11–23% of activity, I_{50} (30 min) = 9–11 nM) is also the most sensitive for mipafox (I_{50} (30 min) = 4 nM). This component is spontaneously reactivated after inhibition with paraoxon. The second sensitive component to paraoxon (Eβ, 71–84% of activity; I_{50} (30 min) = 1216 nM) is practically resistant to mipafox. The third component (Eγ, 5–8% of activity) is paraoxon resistant and has I_{50} (30 min) of 3.4 μM with mipafox, similar to NTE (neuropathy target esterase). The role of these esterases remains unknown. Their high sensitivity suggests that they may either play a role in toxicity in low-level long-term exposure of organophosphate compounds or have a protective effect related with the spontaneous reactivation. They will have to be considered in further metabolic and toxicological studies.

Introduction

Organophosphates such as insecticides are a widely used group which is used not only in the agricultural industry, but also in households and public buildings.

The immediate effects of high-level exposure to organophosphorus compounds (OPs) have been well documented and involve inhibition of the enzyme acetylcholinesterase that causes changes in the peripheral, autonomic and central nervous system functions. However, the possible effects of long-term low-level exposure to OPs remain unclear (Sogorb et al., 2010). Many enzyme systems have the potential for interaction with specific OP pesticides. Some published studies suggest the that long-term, low-level exposure to OPs esters may cause neurological and neurobehavioral effects in experimental animals and humans (COT, 1999; Jamal et al., 2002). A number of occupational groups are exposed to OPs pesticides on a regular basis. Incidence of physical and psychological symptoms have been reported by Gulf War veterans exposed to war weapons (RAC report: Research Advisory Committee on Gulf War Veterans' Illnesses, 2008), and by sheep farmers who have used OPs pesticides (Parron et al., 1996). There are studies which report that repeated, low-level exposures to chlorpyrifos may lead to protracted deficits in sustained attention and to increases in impulsivity in the absence of acute (cholinergic) side effects or motivational deficits in rats (Middlemore–Risher et al., 2010). Whether these effects are specific of chlorpyrifos, or are general of OPs, remains unclear.

The urgent need for investigation to determine how specific OPs at low levels affect specific cognition domains and the neurobiological substrates of cognitive effects has been emphasized. Along these lines, elucidating the nature and functional significance of the OP-sensitive pool of esterases in the central nervous system is an important research target (Ray and Richards 2001). The characterization of reactions is needed to identify target proteins, to evaluate the potency of inhibitors and to design prevention and therapy strategies (Sogorb et al., 2004; Worek et al., 2004, 2007).

Highly sensitive soluble esterases to paraoxon have been described in the soluble fraction of chicken peripheral nerve and in chicken serum when they were measured with substrate phenylvalerate. The kinetic behavior was accompanied by a transitory inhibition with spontaneous reactivation. It has been suggested that these esterases play potential roles in toxicity and/or detoxication during low-dose long-term exposure to organophosphorus compounds, which

* Corresponding author.
E-mail address: jorge.estevez@umh.es (J. Estévez).

0041-008X/$ – see front matter © 2011 Elsevier Inc. All rights reserved.
doi:10.1016/j.taap.2011.05.005

warrants further research (Barril et al., 1999; García-Pérez et al., 2003; Estévez et al., 2011). Inhibition of serum esterases has been proposed as a non destructive biomarker for biomonitoring exposure of wild fauna (García-Pérez et al., 2003).

This work analyzes the interaction of soluble chicken brain esterases with two OPs models (paraoxon and mipafox), characterizes its inhibitory sensitivity and deduces the existence of different esterases of varying kinetic behaviors. Susceptible components and the associated inhibition and spontaneous reactivation kinetics are determined by applying the strategy and kinetic models previously described by Estévez and Vilanova (2009).

Chicken tissues were chosen as the model system given the extensive studies into chicken brain and peripheral nerve using paraoxon and mipafox, and because it is a very sensitive specie to OPs for both the cholinergic effect and delayed neuropathy (Barril and Vilanova, 1997; Barril et al., 1999). This animal model was used for testing organophosphorus induced delayed neuropathy and it was the first animal model where NTE (the target protein of organophosphorus induced delayed neuropathy) was found among the esterases of brain membranes (Johnson, 1982; Williams and Johnson, 1981).

The precise analysis of the "spontaneous reactivation-inhibition" kinetics of multi-enzymatic systems has always been hindered by not only systems complex mathematical performance, but also difficulty in interpretation due to their complexity. Additional complexity involves the medium containing a high sensitive component, and some inhibition in the highly sensitive component ("ongoing inhibition") may continue during the substrate reaction (Estévez and Vilanova 2009; Estévez et al., 2010; Estévez et al., 2011).

The aim of this work is to know the kinetic behavior of the soluble esterases of the brain fraction in order to know the irreversible long-term inhibition with paraoxon and mipafox by means of both the model equations described by Estévez and Vilanova (2009) and the 3D fit according to the best kinetic model which can explain the different kinetic phenomena observed and enables a comparison to be made with studies into peripheral nerve. The kinetic characterization of the components will facilitate further studies for isolation and molecular characterization.

Materials and methods

Chemicals compounds

Diethyl p-nitrophenylphosphate (paraoxon, purity >99%) was purchased from Sigma (Madrid, Spain), and both N, N′- di-isopropyl phosphorodiamidefluoridate (mipafox, purity >98%) and phenylvalerate were purchased from Lark Enterprise (Webster, MA, USA). Homogenization buffer was 50 mM Tris–HCl buffer (pH 8.0) containing 1 mM EDTA. A stock solution of 10 mM paraoxon was prepared in dried acetone, and a stock solution of 10 mM mipafox was prepared in 10 mM Tris-citrate buffer (pH 6.0); both were dissolved in homogenization buffer (pH 8.0) containing 1 mM EDTA immediately before the kinetic assays. A stock solution of substrate phenylvalerate (16.8 mM) was prepared in dried N, N-diethylformamide, and diluted in water to 0.54 mM immediately before the enzymatic assays. All other chemicals were of analytical reagent grades.

Tissue preparation

Chicken brains were obtained from a commercial slaughtering house immediately after killing the animals and were kept in cold (0–5 °C) homogenization buffer until use. They were homogenized with a Polytron homogenizer (Kinematica GmbH, Germany) using a PTA 10S head (dispersing aggregates at 70% power (3×30 seconds)) at a concentration of 200 mg fresh tissue/ml in the same buffer.

Subcellular fractionating

The homogenized tissue was centrifuged at 1000*g* for 10 min (4 °C) to precipitate fibers and nuclei. The supernatant was centrifuged at 100,000*g* for 60 min to obtain a precipitate consisting of the mitochondrial and microsomal fractions. Then a final supernatant or cytosol component was used for the soluble activities (soluble fraction). Samples were frozen in liquid nitrogen before use.

Standard assay of phenylvalerate esterase activity (PVase) for kinetic studies

Enzyme assays were carried out as previously described (Estévez et al., 2004) using a procedure based on the colorimetric method for the NTE assay, developed by Johnson (1977). The method was modified and programmed for an automated microassay using the Biomek 2000 (Beckman) workstation as follows:

In a 1-ml microtube, a 200 µl volume of the brain soluble fraction (at an equivalent concentration of 20 mg/ml of the original fresh tissue) was incubated with 20 µl of inhibitor solution, (buffer in controls) at the appropriate concentrations. After the appropriate inhibition time, 200 µl of substrate phenylvalerate (0.54 mM) were added and incubated for 10 min at 37 °C. The reaction was stopped by adding 100 µl of a solution of 2% sodium dodecyl sulfate with 1.23 mM aminoantipyrine (SDS-AAP solution), which was then mixed with 50 µl of 1.21 mM potassium ferricyanide and left for 10 min for color development. A 300 µl volume from each microtube were transferred to a 96-well microplate, and absorbance was read at 510 nm. Standards of phenol, blanks, and spontaneous hydrolysis controls (samples without tissue) were included with the same procedure.

The results were expressed as % activity ($E/E_0 \times 100$) over the control without an inhibitor, and were plotted versus time (t) or versus the inhibitor concentration.

Reactivation kinetics by dilution

High tissue-concentrated samples (200 mg/ml) were preinhibited with either 40 and 1000 nM paraoxon or 10 and 6000 nM mipafox for 30 min at 37 °C. The study of the reactivation process began at that time point by diluting the incubation mixture 10-fold with homogenization buffer. Incubation was continued and 110 µl aliquots were withdrawn at different times between 0 and 180 min and added to tubes containing 200 µl of substrate solution to be incubated for 10 min at 37 °C. The enzymatic reaction was stopped and color was measured as previously indicated.

Paraoxon inhibition kinetics in mipafox-resistant PVase activity

Tissue samples (containing the soluble fraction from 24 mg/ml of brain) were incubated with 100 µM mipafox for 30 min at 37 °C by adding 20 µl of the inhibition solution. Then 20 µl of the paraoxon solution were added to obtain a concentration of 0.6 or 2000 nM of paraoxon. The 110 µl aliquots were withdrawn at different times between 0 and 180 min and added to tubes containing 200 µl of the substrate solution to be incubated for 10 min at 37 °C. The enzymatic reaction was stopped and the color was measured as previously indicated.

Mathematical analysis of the inhibition curves

Model equations were fitted to the experimental inhibition and reactivation kinetics data by a non linear computerized method based on the least squares principle using the Sigma Plot software, version 8, and applying the model equations for a system with several enzymatic components, as described by Estévez and Vilanova

(Estévez and Vilanova, 2009). Additional adaptations of the model equation for our specific situation are indicated in the Results section.

Results

Paraoxon inhibition and reactivation curves in the brain soluble fraction

Fixed time inhibition curve. Chicken brain soluble fractions were incubated with paraoxon, for 30 min at 37 °C (Fig. 1). The fixed time inhibition curve of PVase activity was fitted with exponential decay models for the inhibition without spontaneous reactivation of one, two, or three sensitive enzymatic components with or without resistant fraction according to Estévez and Vilanova (2009). The best fitting model (according to "*F*" test) consisted of two sensitive components (23% and 70%) with estimated I_{50} (30 min) of 9 and 866 nM, respectively, and a resistant component (7%). These estimated I_{50} (30 min) were used to choose the concentrations for the spontaneous reactivation experiment and for the time-progressive inhibition experiment.

Spontaneous reactivation after diluting the inhibitor. Chicken brain soluble fractions were inhibited with paraoxon for 30 min at 37 °C. Two paraoxon concentrations were chosen: 40 nM to inhibit the most sensitive enzymatic component and 1000 nM to inhibit the two enzymatic components detected previously (Fig. 2). The samples were then diluted to around 4 nM and 100 nM of paraoxon residual concentrations respectively, and were incubated at 37 °C to recover activity during the time indicated in Fig. 2.

The sample preinhibited with 40 nM of paraoxon recovered the activity after diluting in a time-progressive manner from 75% to 87% activity in 180 min (around 12% of activity). This suggests that a spontaneous reactivation of the more sensitive component (23% of activity) took place. The spontaneous reactivation should be considered in the kinetic model. Activity increased throughout the time until it reached a ceiling limit. This suggests that a "steady stage" was reached in which the reactivation rate equaled the inhibition rate at a residual concentration of about 4 nM (Fig. 2). This behavior also suggests that the aging reaction may be negligible under these experimental conditions because PVase activity would decrease when aging and inhibition by residual concentration simultaneously occurred. Therefore, aging was not considered in the model equations representing this system's kinetic behavior.

On the contrary, the sample preinhibited with 1000 nM of paraoxon activity remained inhibited over time (180 min), and even a slight inhibition tendency was observed from 65% to 59% (Fig. 2), suggesting that the second component was not reactivated. The first component is able to be spontaneously reactivated but the residual paraoxon concentration (~100 nM) is higher than its I_{50} (30 min) and it remains inhibited. A slight inhibition tendency was observed because not all the second sensitive component was inhibited with 1000 nM of paraoxon and it is slowly progressive inhibited by the residual concentration.

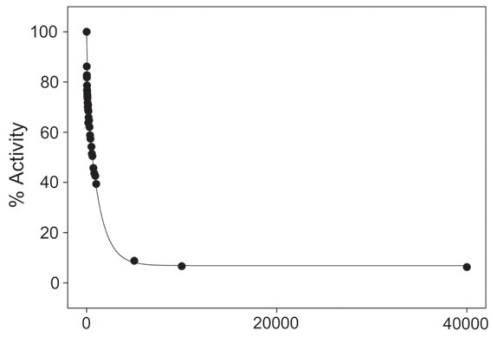

Fig. 1. Paraoxon 30-min fixed-time inhibition curve of soluble brain phenyl valerate esterase activity. A brain soluble fraction from 20 mg tissue/ml was incubated with paraoxon for 30 min at 37 °C, and residual esterase activity was measured. The curve was fitted to a model with a two exponential and a resistant component (*F* test results versus three exponentials components model: $F=0.4477$, $p=0.5164$). Each point represents the mean of three replicates (SD<5%).

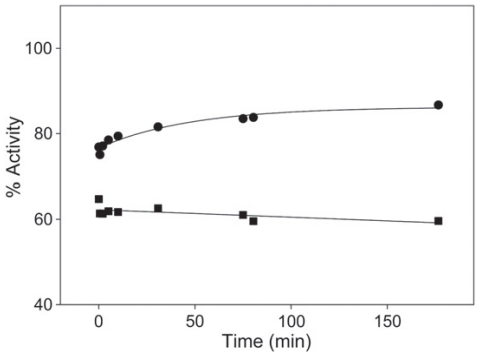

Fig. 2. Spontaneous reactivation after inhibition by paraoxon. Concentrated tissue preparations (200 mg/ml) were inhibited by preincubation with 40 nM (circles) and 1000 nM (squares) of paraoxon at 37 °C for 30 min. Then they were diluted 10-fold with homogenization buffer and maintained for 0, 0.5, 2, 5, 10, 30, 75, 80 or 177 min at 37 °C before measuring activity. Each point represents the mean of two replicates (SD<5%).

The mathematical models for reactivation described by Estévez and Vilanova (2009) corresponding to the one, two or more inhibited enzymes, were applied to the 40 nM inhibition curve. The residual concentration of the inhibitor (4 nM) was considered significant. The best fit according to the *F*-test was a model with only one component, which was spontaneously reactivated and simultaneously inhibited.

$$E = [\mathrm{EI}_0 \cdot k_{1r} / (k_1 \cdot I + k_{1r})] + [\mathrm{EI}_0 \cdot k_{1r} / (k_1 \cdot I + k_{1r})] \cdot e^{-(k_1 \cdot I + k_{1r}) \cdot t} + R$$

Where k_1 is the second order inhibition constant, k_r is the reactivation constant, EI_0 is the proportion (amplitude) of the initial inhibited enzymatic component, and R is the inhibition-resistant enzymatic fraction. The following restriction was applied: $\mathrm{EI}_0 + R = 100\%$. The resulting kinetic parameters and I_{50} (30 min) values are shown in Table 1, line (A).

The I_{50} (30 min) values for the sensitive component (Ei) were obtained by applying the following equation:

$$\%\,\mathrm{Activity\,(Ei)} = 50\,\% = [(k_r \cdot 100) / (k_i \cdot I + k_r)] + [(k_i \cdot I \cdot 100) / (k_i \cdot I + k_r)] \cdot e^{-(k_i \cdot I + k_r)30}$$

The previously estimated kinetic constants were fixed and then successive iterations with different I values were carried out in an electronic spreadsheet to obtain the I value corresponding to 50 ± 0.1% activity.

Time-progressive inhibition curves by paraoxon. Chicken brain soluble fractions were inhibited with paraoxon (11, 100, 600 and 2000 nM) for times of up to 180 min at 37 °C. The kinetic analysis for the inhibition of brain soluble PVase activity with paraoxon resulted in a time-progressive inhibition which is coherent with the covalent irreversible inhibition. The inhibition curves were fitted individually with exponential decay models for the inhibition without spontaneous reactivation of one, two, or three sensitive enzymatic

Table 1
Inhibition by paraoxon. The kinetic constants (k_i) and the proportions of obtained esterase components from the different inhibition and/or reactivation experiments with paraoxon. The I_{50} values were calculated from the kinetic constants for each component. (A) Reactivation after diluting (Fig. 2). (B) Inhibition curve at the pre-inhibition zero time (Fig. 3B). (C) Experiment of time-progressive inhibition with different concentrations in a 3D fitting (Fig. 4). The R^2 coefficients were 0.9437 (A), 0.9887 (B), and 0.9847 (C).

	k_a ($t=0$) (nM^{-1})	$E1$ (%)	k_1 ($nM^{-1}\cdot min^{-1}$)	k_{1r} (min^{-1})	I_{50} (30 min) (nM)	$E2$ (%)	k_2 ($nM^{-1}\cdot min^{-1}$)	I_{50} (30 min) (nM)	R (%)
A		23	0.0031	0.0086	9	77	–		–
B	0.0017	18	–	–	–	82			
C	0.0013	21	0.0023	0.0033	11	71	$1.9\cdot10^{-5}$	1216	8

components with or without resistant fraction according to Estévez and Vilanova (2009). Fig. 3A shows the curves corresponding to the best fit of the individual curve for each paraoxon concentration used according to the *F* test. Although each curve seems to graphically fit the experimental data, no consistent values of the kinetic constants, numbers and the proportion of components were obtained when each curve was analyzed independently using a simple multi-exponential equation.

Evaluation of ongoing inhibition during the substrate reaction. The data extrapolated to the zero inhibition time (Fig. 3 B) indicate that ongoing inhibition during substrate incubation under the assayed conditions is apparently significant. Therefore, ongoing inhibition during substrate incubation needs to be considered in the model (Estévez et al., 2010). This effect is approximately 18% for the highest inhibitor concentration and could hinder the data analysis if is not considered.

Exponential decay models were used to fit the data shown in Fig. 3B. The best model according to the *F*-test was $E_0 \cdot e^{-k_{a'}\cdot x} + R$. Parameter $k_{a'}$ represents the apparent first-order kinetic constant of the inhibition observed during the substrate reaction time.

It was concluded that the proportion of enzyme sensitive to ongoing inhibition is around 18% of total PVase activity, while around 82% is resistant to ongoing inhibition, which justifies that the ongoing inhibition factor should be taken into account, but only for the most sensitive enzymatic component (Table 1, line B).

Kinetic model considering ongoing inhibition and the simultaneous spontaneous reactivation process. The evidence of reactivation (Fig. 2) of one component suggests that a complex kinetic model including reactivation should be used to analyze the kinetic inhibition data. This model should also include several enzymatic components with reactivation and an ongoing inhibition effect for the most sensitive component, but not for the other.

The time-progressive inhibition data were analyzed with the model, which considers inhibition with a simultaneous spontaneous reactivation of the most sensitive component with one, two or three enzymatic components by considering the ongoing inhibition effect in the most sensitive component. The best fitting model (according to the *F* test) consisted in three enzymatic entities: *E*1, the most sensitive, was inhibited and spontaneously reactivated, *E*2, which was only inhibited and *R*, a resistant component. This mathematical model is as follows:

$$E = \left[e^{-k_{a'}\cdot I}\right] \cdot \left\{\left[(k_{r1}\cdot E1_0)/(k_1\cdot I + k_{r1}) + (k_1\cdot I\cdot E1_0)/(k_1\cdot I + k_{r1})\right]\cdot e^{-(k_1\cdot I + k_{r1})\cdot t}\right\} + E2_0\cdot e^{-(k_2\cdot I)\cdot t} + R$$

where k_1 and k_2 are the second order inhibition constants; k_{r1} is the reactivation constant; $E1_0$, $E2_0$ and R are the proportion (amplitude) of the enzymatic components *E*1, *E*2 and *R* respectively. For the most sensitive enzymatic component, the exponential factor $[e^{-k_{a'}\cdot I}]$ was included to correct the "ongoing inhibition" during the substrate reaction (Estévez et al., 2010).

For the purpose of obtaining a coherent solution in the interactive computing estimation, some restrictions were applied: (1) all the parameters (rate constants and amplitudes) should have positive values (>0); (2) component 1 is the most sensitive, therefore $k_1 > k_2$; (3) the following complementary restriction was also applied: $E1_0 + E2_0 + R = 100\%$. A three-dimensional fitting (% of activity versus *t* and

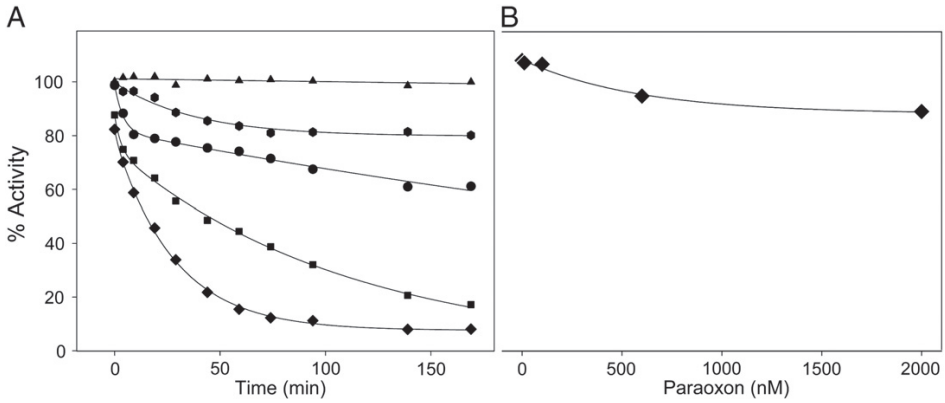

Figs. 3. Kinetics of the time-progressive inhibition by paraoxon concentrations. Preparation containing the soluble fraction of 20 mg fresh tissue/ml was preincubated with 0, 11, 100, 600, 2000 nM paraoxon (superior to the lower plots) for the indicated time. Then, the enzymatic activity was assayed by incubating the substrate phenylvalerate for 10 min. Each point represents the percentage of activity at each time calculated from the linear regression obtained of the 0 nM curve. Panel B shows the inhibition during the time of the reaction with the substrate (0 min inhibition time, "ongoing inhibition"). Each point represents the mean of two replicates (SD<5%).

I) was done with the data described in Fig. 3. The results are provided in Table 1 (line C), and the deduced 3D surface is plotted in Fig. 4.

The I_{50} (30 min) values for the most sensitive component (Ei) were obtained by approximation and by applying the following equation:

$$\%\,\text{Activity (Ei)} = [(k_r \cdot 100) / (k_i \cdot I + k_r)] + [(k_i \cdot I \cdot 100) / (k_i \cdot I + k_r)] \cdot e^{-(k_i \cdot I + k_r) \cdot 30}$$

The previously estimated kinetic constants were fixed, and successive iterations with different *I* values were carried out in an electronic spreadsheet to obtain the *I* value corresponding to 50 ±0.1% activity.

Mipafox inhibition curves in the brain soluble fraction

Fixed-time inhibition curve. Chicken brain soluble fractions were incubated by mipafox for 30 min at 37 °C. The fixed time inhibition curve of PVase activity was fitted with exponential decay models for the inhibition without spontaneous reactivation of one, two, or three sensitive enzymatic components with or without resistant fraction according to Estévez and Vilanova (2009). The best-fitting model (according to "*F*" test) consisted of three sensitive enzymatic components (18%, 6% and 76%) with the estimated I_{50} (30 min) of 6 nM, 1163 nM and around 500 μM, respectively (Fig. 5). The resulting kinetic parameters and I_{50} (30 min) values are shown in Table 2, line (A). These estimated I_{50} (30 min) were used to choose the concentrations for the spontaneous reactivation experiment and for the time-progressive inhibition experiment.

Evaluation of activity after diluting the inhibitor. Chicken brain soluble fractions were inhibited with mipafox for 30 min at 37 °C. Two mipafox concentrations (10 and 6000 nM) were chosen to inhibit the two enzymatic components detected previously (Fig. 6) to be then diluted to around 1 nM and 600 nM of mipafox residual, respectively. Then they were incubated at 37 °C to recover activity for the time indicated in Fig. 6.

After diluting, the activity remained inhibited over time (180 min) from 88% to 83% for the fractions inhibited with 10 nM and ~72% for the fractions inhibited with 6000 nM. This confirms that there is no a spontaneous reactivation after inhibition with mipafox for any of the sensitive components during the experiment time (180 min). Therefore, spontaneous reactivation was not considered in the model equations for the inhibition kinetics with mipafox.

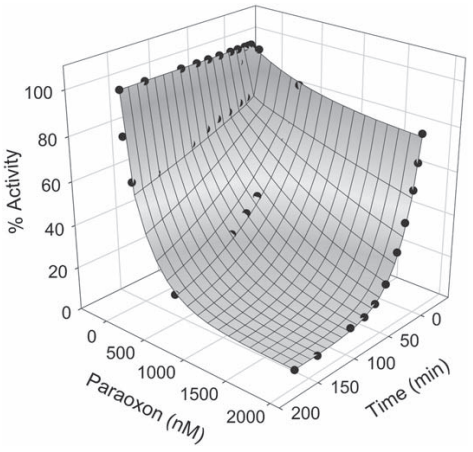

Fig. 4. Representation of the inhibition kinetics of soluble brain PVases by paraoxon. Inhibitory surface obtained by fitting the 3D model equation to the data corresponding to paraoxon inhibition which is done in the soluble fraction of the brain (Fig. 3). The surface reflects the result of the best model according to the *F* test. It corresponds to a model with two sensitive enzymatic components plus other resistant where the most sensitive is inhibited, spontaneously reactivated and affected by ongoing inhibition.

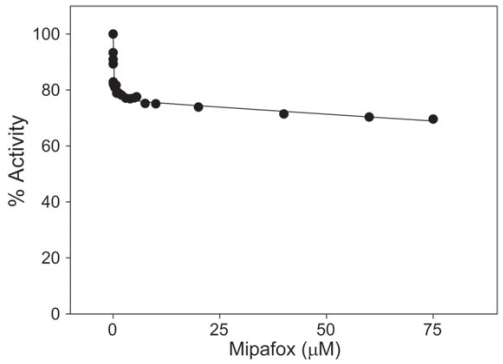

Fig. 5. Mipafox fixed-time inhibition curve. The soluble brain fraction was incubated with the corresponding mipafox concentration (ranging from 0.003 to 75 μM) for 30 min at 37 °C, while residual activity was assayed as described in the methods. The curve was fitted with a tree exponential components model (*F* test results versus two exponential plus a resistant component model: $F = 18.1586$, $p = 0.0004$). Each point represents the mean of three replicates (SD<5%).

Time-progressive inhibition by mipafox. Chicken brain soluble fractions were inhibited with mipafox (10, 100 nM and 80, 100 μM) for times of up to 180 min at 37 °C. This inhibition was time-progressive (~30% of total activity), which is coherent with covalent inhibition. The inhibition curves were fitted individually with exponential decay models for the inhibition without spontaneous reactivation of one, two, or three sensitive enzymatic components with or without resistant fraction according to Estévez and Vilanova (2009). Fig. 7 shows the curves corresponding to the best fit of the individual curve for each mipafox concentration used according to the *F* test. Although each curve seems to graphically fit properly to the experimental data, no consistent values of the kinetic constants, numbers and the proportion of the components have been obtained when fitting each curve individually using a simple multiexponential equation.

Evaluation of ongoing inhibition during the substrate reaction. Extrapolating the data in Fig. 7 to the preincubation zero time inhibition did not converge to 100% (see inserted graph). This indicates that ongoing inhibition during substrate incubation is apparently significant under the assayed conditions. Therefore, ongoing inhibition during substrate incubation needs to be included in the model.

Exponential decay models were used to fit the ongoing inhibition data. The best model according to the *F*-test was $E0 \cdot e^{-ka' \cdot x} + R$ suggesting that it affects only the highest sensitive component and that it could hinder the data analysis if not considered. Parameter $k_{a'}$ represents the apparent first-order kinetic constant. The obtained parameters are shown in the Table 2, line B.

Kinetic model considering ongoing inhibition. The inhibition data presented in Fig. 7 were re-analyzed with a model that considers the "ongoing inhibition" effect $[e^{-k_{a'} \cdot I}]$ in the most sensitive component, which was analyzed by a three-dimensional fitting (% of phenylvalerate esterase activity versus *t* and *I*) to consider all the data simultaneously. According to the *F* test, the best fitting model consisted in three sensitive enzymatic entities, where the most sensitive one was affected by

Table 2
Inhibition by mipafox. The kinetic constants (k_i) and the proportions of components obtained from the different inhibition with mipafox on soluble brain fractions. I_{50} (30 min) values were calculated from the kinetic constants for each component. (A) The fixed-time inhibition experiment (Fig. 5). (B) Inhibition curve at the pre-inhibition zero time (insert in Fig. 7). (**C**) The time-progressive inhibition experiment with different concentrations in a 3D fitting (Fig. 8). The R^2 coefficients were 0.9878 (A), 0.9859 (B), and 0.9352 (C).

	k_a ($t=0$) (nM^{-1})	$E1$ (%)	k_1 ($nM^{-1}\cdot min^{-1}$)	I_{50} (30 min) (nM)	$E2$ (%)	k_2 ($nM^{-1}\cdot min^{-1}$)	I_{50} (30 min) (nM)	$E3$ (%)	k_3 ($nM^{-1}\cdot min^{-1}$)	I_{50} (30 min) (nM)
A	–	18	0.0037	6	6	$2.0\cdot10^{-5}$	1163	76	$4.7\cdot10^{-8}$	497,518
B	0.0049	40	–	–				60		
C	0.0013	11	0.0059	4	5	$6.8\cdot10^{-6}$	3398	84	$3.6\cdot10^{-9}$	645,963

ongoing inhibition, but no by spontaneous reactivation (Estévez and Vilanova, 2009). This mathematic model is as follows:

$$E = \left[e^{-k_a \cdot I}\right] \cdot E1_0 \cdot e^{-(k_1 \cdot I)\cdot t} + E2_0 \cdot e^{-(k_2 \cdot I)\cdot t} + E3_0 \cdot e^{-(k_3 \cdot I)\cdot t}$$

where k_1, k_2, k_3 are the second order inhibition constants, $E1_0$, $E2_0$, $E3_0$ are the proportions (amplitude) of the enzymatic components and $[e^{-k_a \cdot I}]$ is the factor related with ongoing inhibition.

For the purpose of obtaining a coherent solution in the interactive computing estimation, some restrictions were applied: (1) all the parameters (rate constants and amplitudes) should have positive values (>0); (2) component 1 is the most sensitive, therefore $k_1 > k_2$; (3) the following complementary restriction was also applied: $E1_0 + E2_0 + E3_0 = 100\%$. The results are provided in Table 2 (line C), and the deduced 3D surface is plotted in Fig. 8.

Paraoxon inhibition curves of mipafox-resistant PVase activity

In order to distinguish the mipafox-resistant component, which is sensitive to paraoxon, soluble brain fraction samples (24 mg/ml) were inhibited with 100 μM of mipafox for 30 min. Then, samples were inhibited with 0, 600 and 2000 nM of paraoxon up to 180 min (Fig. 9). The mathematical models (exponential decay models for the inhibition without spontaneous reactivation) corresponding to one, two or three sensitive enzymes were applied. The best fit according to the *F*-test was a model with only one sensitive component:

$$E = E1_0 n\, e^{-(k_{1'}\cdot t)}$$

where $k_{1'}$ is the first-order kinetic constant, $E1_0$ is the proportion (amplitude) of the sensitive component. The following restriction was applied: $E1_0 = 100\%$. It may be concluded that only one paraoxon-sensitive component was inside mipafox-resistant activity.

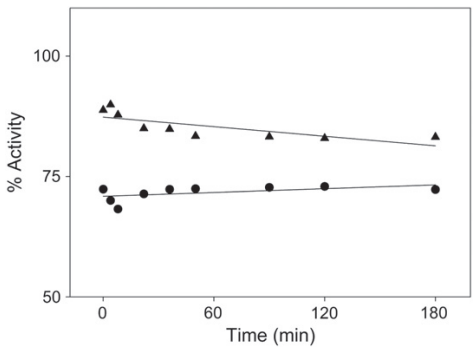

Fig. 6. Spontaneous reactivation after inhibition by mipafox. Two concentrated preparations (200 mg/ml) were inhibited by preincubation with 10 nM (circles) and 6000 nM (triangles) of mipafox, respectively, for 30 min at 37 °C. Then the mixture was diluted 10-fold with homogenization buffer to be then incubated for 0, 4, 8, 22, 36, 50, 65, 90, 120 or 180 min at 37 °C. Each point represents the mean of two replicates (SD<5%).

The insert in Fig. 9 provides the plots of the $k_{1'}$ value from each paraoxon concentrations (0 nM, 600 nM and 2000 nM) versus the corresponding paraoxon concentration. From the slope the second-order constant inhibition rate was calculated ($k_1 = 1.3\cdot10^{-5}\ nM^{-1}\cdot min^{-1}$). The I_{50} (30 min) value calculated was 1800 nM.

Discussion

Kinetic behavior of brain soluble PVases with paraoxon

Paraoxon has been used to discriminate non neuropathic carboxylesterases as it is neither an inducer of OPIDP nor an inhibitor of NTE. Knowing the kinetic behavior of the soluble esterases of the brain with paraoxon is necessary to learn the reversibility of long-term inhibition and to discriminate non neuropathic carboxylesterases in soluble brain fractions. Phenylvalerate is used as a substrate as it seems appropriate to detect esterases that are sensitive to neuropathic OPs such as NTE.

This paper provides evidence that brain soluble esterases activities are extremely sensitive to paraoxon. Nanomolar concentrations of paraoxon are able to inhibit about 92% of total soluble esterases in chicken brains in a time-progressive manner, suggesting covalent irreversible phosphorylation. Céspedes et al. (1997) reported similar results, 91.9% of total soluble esterases were inhibited. The kinetic behavior is coherent with two highly sensitive esterase components.

The spontaneous reactivation experiments not only reveal that a proportion of the inhibited soluble esterase activity is able to reactivate, but that reactivation is also time-progressive (Fig. 4). The results suggest that the esterase fraction which was reactivated is the most sensitive component observed in the inhibition experiments with paraoxon. The spontaneous reactivation phenomenon of preinhibited carboxylesterases taking place with different inhibitors has been described in other works. A reactivation of 40% has been observed in the samples preinhibited with stereoisomer P(−) of soman in NTE studies done with hen brains after 18 hours at 37 °C (Johnson et al., 1985). It has been also observed with paraoxon and with the biotinilated organophosphate S9B in the soluble fraction of the chicken peripheral nerve (Barril et al., 1999; Estévez et al. 2010; Estévez et al., 2011). Moreover, a spontaneous reactivation of complete esterase activity in chicken serum has also been described. It has been suggested that these esterases play potential roles in toxicity and/or detoxication during low-dose long-term exposure to organophosphorus compounds which warrants further research (García-Pérez et al., 2003; Estévez et al., 2011).

The reactivation constant (k_r) as a result of the reactivation experiment after dilution is similar to the k_r obtained from the first sensitive component in the 3D fit of the inhibition experiment (Table 1). This demonstrates the consistency of reactivation and the estimation of constants.

Three enzymatic components were detected in the inhibition experiment with paraoxon. The “ongoing inhibition” effect is considered for the high sensitive enzymatic component, just as Fig. 3 depicts. The proportion of activity affected by ongoing inhibition is similar to the amplitude of the most sensitive component (Table 1),

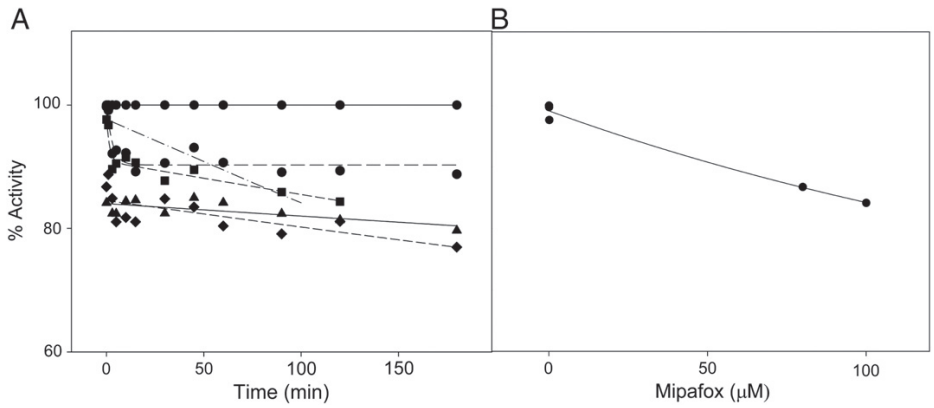

Figs. 7. Kinetics of the time-progressive inhibition by mipafox concentrations. A preparation containing the soluble fraction of 20 mg fresh tissue/ml was preincubated with 0, 0.03, 0.1, 80, 100 μM of mipafox for the indicated time at 37 °C. Each point represents the percentage of activity at each time calculated from the linear regression obtained of the 0 nM curve.Then the enzymatic activity was assayed with phenylvalerate for 10 min. Panel B shows inhibition at the reaction time with the substrate (0 min inhibition time). Each point represents the mean of two replicates (SD<5%).

as estimated in the time-progressive inhibition experiment. Moreover, the $k_{a'}$ constant estimated from the data at the zero time in the time-progressive inhibition is similar to the $k_{a'}$ obtained in the 3D fit (Table 1); $k_{a'}$ has to be considered an operational empiric constant, and not a real kinetic constant. (Estévez and Vilanova 2009; Estévez et al., 2010).

The 3D fit enables all the data in the same fit to be included simultaneously, and it is the best tool to fit the inhibition data in this complex model (Estévez et al., 2004). The model applied assumes three enzymatic components: $E1$, I_{50} (30 min) = 11 nM, displaying both ongoing inhibition and spontaneous reactivation; $E2$, I_{50} (30 min) = 1216 nM, showing progressive inhibition and R that is practically resistant to paraoxon inhibition. The second-order kinetic constant of inhibition and the spontaneous reactivation constant for the reactivated enzymatic component are similar to the constant estimated in the reactivation experiments. The estimated amplitudes (proportion), the inhibition constants and the reactivation constant are similar in both, inhibition and reactivation after diluting, experiments, when spontaneous reactivation is considered. These observations may be considered an internal validation of both the consistency of the results and the applied kinetic model.

Kinetic behavior of brain soluble PVases with mipafox

A portion of brain soluble PVase activity is sensitive to mipafox. Micromolar concentrations of mipafox are able to inhibit about 30% in a time-progressive manner, suggesting covalent irreversible phosphorylation. Kinetic behavior is coherent with two sensitive esterase components, and a third component that is practically resistant to mipafox inhibition at the highest concentrations used, which are the typical concentrations in NTE assay.

The spontaneous reactivation experiments in a soluble chicken brain fraction reveal that inhibited soluble PVase activity is not able to reactivate spontaneously in presence of the residual mipafox concentration. The possible spontaneous reactivation cannot be completely excluded but the data of reactivation experiment suggest that it is not significant for the time of the inhibitory experiment. The "ongoing inhibition" effect is considered for the high sensitive

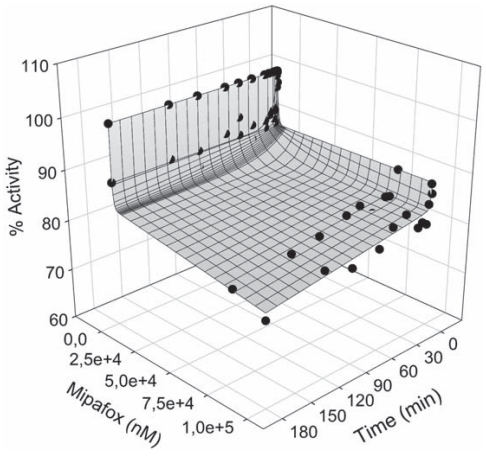

Fig. 8. Representation of the inhibition kinetics of soluble brain PVases by mipafox. Inhibitory surface obtained by fitting the 3D model equation to the data corresponding to mipafox inhibition which is done in the soluble fraction of the brain (Fig. 7). The surface reflects the result of the best model according to the F test. It corresponds to a model with three sensitive enzymatic components where the most sensitive was affected by ongoing inhibition.

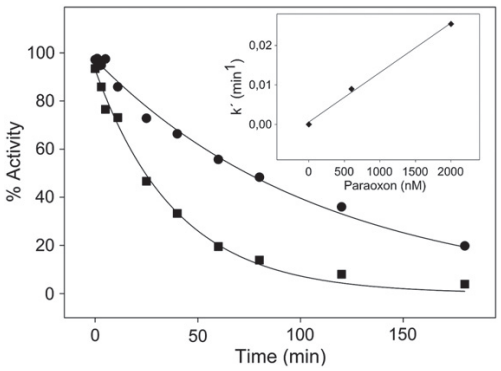

Fig. 9. Kinetics of the time-progressive inhibition of the mipafox-resistant activity by paraoxon. Soluble fraction (from 24 mg/ml brain) was inhibited with 100 μM of mipafox during 30 min at 37 °C. Then, the samples were inhibited with 0, 600 and 2000 nM paraoxon for the indicated time in the graph. The residual enzymatic activity was assayed with phenylvalerate for 10 min. Percentages refer to the activity of the samples preincubated with 0 nM paraoxon at each time. Insert: linear regression of first-order rate constant of the paraoxon sensitive component in the mipafox resistant fraction vs. inhibitor concentration. From the slope is deduced the second order rate constant $k_1 = 1.3\ 10^{-5}\ nM^{-1}\cdot min^{-1}$ and the I_{50} (30 min) = 1800 nM. Each point represents the mean of two replicates (SD<5%).

Table 3
Sensitivity of the different components discriminated by inhibition with mipafox and paraoxon in brain soluble esterases. I_{50} values are indicated (for 30 min) with the proportion of the component in parentheses (%) as (+++) very highly sensitive, (++) highly sensitive, (+) poorly sensitive, and (−) resistant.

	Paraoxon		Mipafox	
Component	Sensitivity	I_{50} nM	Sensitivity	I_{50} nM
E(α) (11–23%)	+++	9–11	+++	4
E(β) (71–84%)	++	1216	–	–
E(γ) (5–8%)	–	–	+	3398

E (α), corresponds to E1 in Table 1 and Table 2 for paraoxon and mipafox.
E (β), corresponds to E2 in Table 1 for paraoxon and E3 in Table 2 for mipafox.
E (γ), corresponds to R in Table 1 for paraoxon and E2 in Table 2 for mipafox.

enzymatic component, just as Fig. 6 shows. The $k_{a'}$ constant estimated from the data at the preinhibition zero time in the time-progressive inhibition is similar to the $k_{a'}$ obtained in the 3D fit (Table 2). The $k_{a'}$ constant has to be considered operational empiric constants, and not real kinetic constants (Estévez and Vilanova 2009; Estévez et al., 2010).

The 3D fit model applied assumes three enzymatic components: *E*1, I_{50} (30 min) = 4 nM, displaying ongoing inhibition, *E*2, I_{50} (30 min) = 3398 nM, showing progressive inhibition and *E*3, which is practically resistant to mipafox inhibition. This model allows estimating the kinetic parameters better than the fitting-model in fixed-time experiment because all the data of the progressive inhibition experiment are analyzed as a whole. The consistency of the estimated parameters was checked by comparing the results of the fixed-time inhibition experiment and the time-progressive inhibition. The comparison is presented in Table 2, while amplitudes (proportion) are similar and inhibition constants are comparable in all the experiments. This consistency may be considered an internal validation of the applied kinetic model and of the results obtained.

Kinetic behavior of brain soluble mipafox-resistant esterases with paraoxon

Only one paraoxon-sensitive component was detected inside mipafox-resistant activity (Fig. 9) with a second-order constant similar to the inhibition constant obtained in inhibition experiments with paraoxon for the second sensitive component (Table 1). Moreover, the proportion (amplitude) obtained with mipafox is also similar with that obtained with paraoxon (Table 3). The results suggest that most of the mipafox-resistant fraction is the second most sensitive paraoxon component. This allows us to establish the components detected with paraoxon versus those detected with mipafox.

Comparison between soluble esterases sensitivities with paraoxon and mipafox

Table 3 presents the suggested interpretation of the relationship among the enzymatic components differentiated with paraoxon and mipafox. The number and amplitudes (proportion) of the components obtained with mipafox are similar to those obtained in the inhibition experiments with paraoxon (Table 3). These observations confirm the consistency of the results and the model applied, and may be considered an external validation. Moreover, the experiment in the mipafox resistant fraction with paraoxon confirms this relationship.

The relative sensitivity of the time-progressive inhibition differs for paraoxon and mipafox (Table 3). The most sensitive component for paraoxon is also the most sensitive component for mipafox, with I_{50} (30 min) = 9–11 nM with paraoxon and 4 nM with mipafox (E(α) in Table 3, corresponding to *E*1 in Table 1 for paraoxon and *E*1 in Table 2 for mipafox). This component represents the 11–23% activity, is spontaneously reactivated with paraoxon, and has similar inhibition and reactivation constants to a component which represents 41–48% of the activity in the soluble peripheral nerve fraction with I_{50} (30 min) = 6–11 nM with paraoxon and 7–12 nM with mipafox (Table 4; Estévez et al., 2004; Estévez et al., 2011).

The second sensitive component to paraoxon with I_{50} (30 min) = 1216 nM is practically resistant to mipafox (E(β) in Table 3, corresponding to *E*2 in Table 1 for paraoxon and *E*3 in Table 2 for mipafox). This component represents the 71–84% of total activity.

The third component is paraoxon-resistant and sensitive to micromolar concentrations of mipafox (*E*(γ) in Table 3, corresponding to *R* in Table 1 for paraoxon and *E*2 in Table 2 for mipafox). This component represents 5–8% activity and fits the operational criteria by being "NTE-like" (40 μM paraoxon-resistant and sensitive to mipafox at μM concentrations), with I_{50} (30 min) with mipafox of 3.4 μM, similarly to NTE, the membrane-bound protein which has I_{50} (30 min) = 4.7 μM with mipafox (Johnson, 1982). Escudero et al. (1997) described an enzymatic fraction, called S-NTE1, in a brain soluble fraction, with I_{50} (30 min) 5.2 μM, which is similar to NTE sensitivity and fits the operational criteria of being NTE. Fraction S-NTE1 was proposed to be a membrane-bound NTE form, solubilized at pH 8.0 and not at pH 6.8. Therefore, the component we have detected as E(γ) might be that described by Escudero et al., 1997 as S-NTE1, which was proposed to be an NTE membrane partly solubilized at pH 8.0 following the homogenization procedure.

Toxicological meaning and applications for measuring NTE activity

In order to discriminate and measure the potential target of delayed neurotoxicity, those esterases sensitive to paraoxon (such as organophosphate that does not induce neuropathy) have been excluded as targets of the neurotoxic process (Johnson, 1969; Johnson, 1982; Johnson, et al., 1985). This work proves that part of the soluble esterase activity of the brain can be progressively inhibited by paraoxon with time, but not permanently so because it is spontaneously reactivated. The results of this work confirm that paraoxon is not the most appropriate tool to discriminate potential targets of neurotoxicity in the soluble fraction of brain due to some fraction being reactivated.

For a routine analysis, we suggest the discrimination of the main esterase components in the soluble brain fraction, which is a simple assay using only one inhibitor. Only two different mipafox concentrations are used: 25 nM for the inhibition of the most sensitive component (~I_{99} (30 min)), and 25 μM for the second most sensitive component (~I_{99} (30 min)) with a 30-min preincubation before

Table 4
Comparison brain/peripheral nerve soluble esterases. The kinetic constants (k_i) and the proportions of components obtained from the different inhibition and/or reactivation experiments with paraoxon and mipafox (Estévez et al., 2004, Estévez et al., 2011). I_{50} values were calculated from the kinetic constants for each component.

		Paraoxon			Mipafox	
	E_0	k_i	k_r	I_{50} (30 min)	k_i	I_{50} (30 min)
	%	($nM^{-1}\cdot\cdot min^{-1}$)	(min^{-1})	nM	($nM^{-1}\cdot\cdot min^{-1}$)	nM
Brain soluble esterases	11–23 (a)	0.0023–0.0031 (a)	0.0033–0.0086 (a)	09–11 (a)	0.0059 (a)	4 (a)
Peripheral nerve soluble esterases	41–43 (b, c)	0.0027–0.0051 (b)	0.0092–0.0190 (b)	06–12 (b)	0.0017–0.0033 (c)	7–12 (c)

(a) From the data in this paper. (b) from the data in the paper: Estévez et al., (2011) (c) from the data in the paper: Estévez et al., (2004).

adding the substrate. These concentrations of mipafox allow the main esterase components to be discriminated and to be separated and purified in future approaches.

It is concluded that three PV-ases components can be discriminated in the soluble brain fraction (Table 3). E(α) (11–23%), highly sensitive to mipafox and paraoxon (nanomolar range); E(β), (71–84%), mipafox-resistant paraoxon-sensitive; and E(γ), (5–8%); sensitive to mipafox (micromolar range), and paraoxon-resistant

The high sensitivity of E(α) esterases with paraoxon and/or mipafox suggests that they might either play a role in toxicity in low-level long-term exposure of organophosphate compounds or have a protective effect in relation to the spontaneous reactivation of some OPs, such as paraoxon, and other di-ethyl/dimethyl phosphates, which may be considered a biodegradation reaction.

Conflict of interest

The authors declare that there are no conflicts of interest.

Funding sources statement

Institutional funds.

References

Barril, J., Vilanova, E., 1997. Reversible inhibition can profoundly mislead studies on progressive inhibition of enzymes: the interaction of paraoxon with soluble neuropathy target esterase. Chem. Biol. Interact. 108, 19–25.

Barril, J., Estévez, J., Escudero, M.A., Céspedes, M.V., Ñiguez, N., Sogorb, M.A., Monroy, A., Vilanova, E., 1999. Peripheral nerve soluble esterases are spontaneously reactivated after inhibition by paraoxon: implications for a new definition of neuropathy esterase. Chem. Biol. Interac. 119–120, 541–550.

Céspedes, M.V., Escudero, M.A., Barril, J., Sogorb, M.A., Vicedo, J.L., Vilanova, E., 1997. Discrimination of carboxylesterases of chicken neural tissue by inhibition with a neuropathic, non-neuropathic organophosphorus compounds and neuropathy promoter. Chem.-Biol. Interac. 106, 191–200.

COT, 1999. Organophosphates. A Report of the Committee on Toxicology of Chemicals in Food. : Consumer Products and the EnvironmentUK Department of Health, London.

Escudero, M.A., Céspedes, M.V., Vilanova, E., 1997. Chromatographic discrimination of soluble neuropathy target esterase isoenzymes and related phenyl valerate esterases from chicken brain, spinal cord, and sciatic nerve. J. Neurochem. 68 (5), 2170–2176.

Estévez, J., Vilanova, E., 2009. Model equations for the kinetics of covalent irreversible enzyme inhibition and spontaneous reactivation: esterases and organophosphorus compounds. Critical Reviews in Toxicol. 39 (5), 427–448.

Estévez, J., García-Perez, A., Barril, J., Pellín, M.C., Vilanova, E., 2004. The inhibition of the high sensitive peripherals nerve soluble esterases by mipafox. A new mathematical processing for the kinetics of inhibition of esterases by organophosphorus compounds. Toxicol. Lett. 151, 243–249.

Estévez, J., Barril, J., Vilanova, E., 2010. Inhibition with spontaneous reactivation and the "ongoing inhibition" effect of esterases by biotinylated organophosphorus compounds: S9B as a model. Chem.-Biol. Interact. 187, 397–402.

Estévez, J., García-Pérez, A., Barril, J., Vilanova, E., 2011. Inhibition with spontaneous reactivation of carboxyl esterases by organophosphorus compounds: paraoxon as a model. Chem. Res. Toxicol. 2011 (24), 135–143.

García-Pérez, A.G., Barril, J., Estévez, J., Vilanova, E., 2003. Properties of phenyl valerate esterase activities from chicken serum are comparable with soluble esterases of peripheral nerves in relation with organophosphorus compounds inhibition. Toxicol. Lett. 142 (1–2), 1–10.

Jamal, G.A., Hansen, S., Julu, P.O.O., 2002. Low level exposures to organophosphorus esters may cause neurotoxicity. Toxicology 181–182, 23–33.

Johnson, M.K., 1969. The delayed neurotoxic effect of some organophosphorus compounds. Identification of the phosphorylation site as an esterase. Biochem. J. 114, 711–717.

Johnson, M.K., 1977. Improved assay of neurotoxic esterase for screening organophosphate for delayed neurotoxicity potential. Arch. Toxicol. 37, 113–115.

Johnson, M.K., 1982. The target for initiation of delayed neurotoxicity by organophosphorus esters: biochemical studies and toxicological applications. ReV. Biochem. Toxicol. 4, 141–212.

Johnson, M.K., Read, D.J., Benschop, H.P., 1985. Interaction of the four stereoisomers of soman (pinacolyl methylphosphonofluoridate) with acetylcholinesterase and neuropathy target esterase of hen brain (11, June 1) Biochem. Pharmacol 34, 1945–1951.

Middlemore–Risher, M.L., Buccafusco, J.J., Terry, A.V., 2010. Repeated exposures to low-level chlorpyrifos results in impairments in sustained attention and increased impulsivity in rats. Neurotoxicology and Teratology 32, 415–424.

Parron, T., Hernandez, A.T., Villanueva, E., 1996. Increased risk of suicide with exposure to pesticides in an intensive agricultural area: a 12 year retrospective study. Forens. Sci. Int 79 (1), 53–63.

RAC report: Research Advisory Committee on Gulf War Veterans' Illnesses, 2008. Gulf war illness and the health of Gulf War veterans. Scientific Findings and RecommendationsUS Government Printing Office, Washington D.C. 2008.

Ray, D.E., Richards, P.G., 2001. The potential for toxic effects of chronic, low-dose exposure to organophosphates. Toxicol Lett 343–351.

Sogorb, M.A., Vilanova, E., Carrera, V., 2004. Future applications of phosphotriesterases in the prophylaxis and treatment of organophosphorus insecticide and nerve agent poisonings. Toxicol Lett. 151 (1), 219–233.

Sogorb, M.A., Vilanova, E., Ramesh, Tetsuo Satoh y, Gupta, G., 2010. Detoxication of anticholinesterase pesticides. Anticholinesterase Pesticides: Metabolism, Neurotoxicity, and Epidemiology. John Willey & Sons. ISBN: 978-0-470-41030-1, pp. 121–133.

Williams, D.G., Johnson, M.K., 1981. Gel electrophoretic identification of hen brain neurotoxic esterase labeled with tritiated diisopropylphosphofluridate. Biochem. J. 209, 817–829.

Worek, F., Thiermann, H., Szinicz, L., Eyer, P., 2004. Kinetic analysis of interactions between human acetylcholinesterase, structurally different organophosphorus compounds and oximes. Biochem. Pharmacol. 68, 2237–2248.

Worek, F., Aurbek, N., Koller, M., Becker, C., Eyer, P., Thiermann, H., 2007. Kinetic analysis of reactivation and aging of human acetylcholinesterase inhibited by different phosphoramidates. Biochem. Pharmacol 73 (11), 1807–1817.

Toxicology 297 (2012) 17–25

Contents lists available at SciVerse ScienceDirect

Toxicology

journal homepage: www.elsevier.com/locate/toxicol

NTE and non-NTE esterases in brain membrane: Kinetic characterization with organophosphates

Iris Mangas*, Eugenio Vilanova, Jorge Estévez

Unidad de Toxicología, Instituto de Bioingeniería, Universidad Miguel Hernández de Elche, Avda. Universidad s.n. ES-03202, Elche, Alicante, Spain

ARTICLE INFO

Article history:
Received 15 February 2012
Received in revised form 27 March 2012
Accepted 29 March 2012
Available online 6 April 2012

Keywords:
Organophophorus
Esterases
Spontaneous reactivation
Brain
Neurotoxicity
Kinetic
NTE

ABSTRACT

Some effects of organophosphorus compounds (OPs) esters cannot be explained by action on currently recognized targets. In this work, we evaluate and characterize the interaction (inhibition, reactivation and "ongoing inhibition") of two model compounds: paraoxon (non-neuropathy-inducer) and mipafox (neuropathy-inducer), with esterases of chicken brain membranes, an animal model, tissue and fractions, where neuropathy target esterase (NTE) was first described and isolated. Four enzymatic components were discriminated. The relative sensitivity of time-progressive inhibition differed for paraoxon and mipafox. The most sensitive component for paraoxon was also the most sensitive component for mipafox (EPα: 4.4–8.3% of activity), with I_{50} (30 min) of 15–43 nM with paraoxon and 29 nM with mipafox, and it spontaneously reactivated after inhibition with paraoxon. The second most sensitive component to paraoxon (EPβ: 38.3% of activity) had I_{50} (30 min) of 1540 nM, and was practically resistant to mipafox. The third component (EPγ: 38.6–47.6% of activity) was paraoxon-resistant and sensitive to micromolar concentrations of mipafox; this component meets the operational criteria of being NTE (target of organophosphorus-induced delayed neuropathy). It had I_{50} (30 min) of 5.3–6.6 μM with mipafox. The fourth component (EPδ: 9.8–10.7% of activity) was practically resistant to both inhibitors. Two paraoxon-resistant and mipafox-sensitive esterases were found using the sequential assay removing paraoxon, but only one was paraoxon-resistant and mipafox-sensitive according to the assay without removing paraoxon. We demonstrate that this apparent discrepancy, interpreted as reversible NTE inhibition with paraoxon, is the result of spontaneous reactivation after paraoxon inhibition of a non-NTE component. Some of these esterases' sensitivity to OPs suggests that they may play a role in toxicity in low-level exposure to organophosphate compounds or have a protective effect related with spontaneous reactivation. The kinetic characterization of these components will facilitate further studies for isolation and molecular characterization.

1. Introduction

Exposure to organophosphorus (OP) esters can cause several toxic effects, including acute cholinergic clinical episodes, the intermediate syndrome, organophosphate-induced delayed polyneuropathy (OPIDP) and chronic neurological effects. Acute toxicity is produced by the irreversible inactivation of the enzyme cholinesterase. Nonetheless, the intermediate syndrome's exact mechanism is not understood, while it is claimed that OPIDP is caused by the inhibition and subsequent aging (dealkylation) of neuropathy target esterase (NTE) (Johnson, 1974). However, the possible effects of long-term low-level exposure to OPs remain unclear (Sogorb and Vilanova, 2010).

Neurological and neurobehavioral effects, which cannot be explained by action on currently recognized targets, have been reported in experimental animals and in humans (COT Report, 1999; Jamal et al., 2002; Middlemore-Risher et al., 2010). The urgent need for investigation to determine how specific OPs at low levels affect specific cognition domains and the neurobiological substrates of cognitive effects has been recently emphasized (Ray and Richards, 2001). Along these lines, elucidating the nature and functional significance of the OP-sensitive pool of esterases in the central nervous system is an important research task. It is necessary to characterize the interactions to identify target proteins, to evaluate the potency of inhibitors, and to design prevention and therapy strategies (Sogorb et al., 2004; Worek et al., 2004, 2007).

Many enzyme systems have the potential for interaction with specific OP pesticides. The target protein of organophosphorus-induced delayed neuropathy (NTE) was first found among the esterases of chicken brain membranes (Johnson, 1969, 1982; Williams and Johnson, 1981). NTE was first described by Johnson

* Corresponding author. Tel.: +34966658516.
E-mail address: imangas@umh.es (I. Mangas).

0300-483X/$ – see front matter © 2012 Elsevier Ireland Ltd. All rights reserved.
http://dx.doi.org/10.1016/j.tox.2012.03.012

(1969) as esteratic activity, which is resistant to paraoxon and sensitive to micromolar concentrations of mipafox, as measured with a differential assay by incubating with 40 μM of paraoxon and 50 μM of mipafox (standard assay; Johnson, 1977). Chemnitius et al. (1983) and Carrington and Abou-Donia (1985) reported how two paraoxon-insensitive, mipafox-sensitive esterases are present in hen brain membranes when the protocol was modified by eliminating the residual paraoxon before adding mipafox (sequential assay; Chemnitius et al., 1983) rather than the standard assay. This mechanism has been explained to be the result of a reversible inhibition of these esterases with paraoxon (Carrington and Abou-Donia, 1986).

Highly sensitive esterases to paraoxon have been described in the soluble fractions of chicken peripheral nerve, chicken brain and chicken serum (Barril et al., 1999; García-Pérez et al., 2003; Estévez et al., 2011; Mangas et al., 2011). Kinetic behavior was accompanied by a transitory inhibition with spontaneous reactivation. It has been suggested that these esterases play potential roles in toxicity and/or detoxification during low-dose long-term exposure to organophosphorus compounds, which warrants further research. The precise analysis of the "spontaneous reactivation-inhibition" kinetics of multi-enzymatic systems has always been hindered by not only systems' complex mathematical performance, but also interpretation difficulties due to their complexity. Complexity heightens as the medium containing a highly sensitive component, and some inhibition in the highly sensitive component ("ongoing inhibition"), may continue during the substrate reaction (Estévez and Vilanova, 2009; Estévez et al., 2010, 2011).

This work analyses the interaction of membrane chicken brain esterases with two models of OPs (paraoxon and mipafox), characterizes its inhibitory sensitivity and deduces the existence of different esterases with varying kinetic behaviors. Susceptible components and the associated inhibition and spontaneous reactivation kinetics are determined by applying the strategy and kinetic models previously described by Estévez and Vilanova (2009). The kinetic characterization of the components is necessary to conduct further isolation and molecular characterization studies.

2. Materials and methods

2.1. Chemical compounds

Diethyl-p-nitrophenylphosphate (paraoxon, purity >99%) was purchased from Sigma (Madrid, Spain), and both N,N′-diisopropyl phosphorodiamidefluoridate (mipafox, purity >98%) and phenylvalerate were acquired from Lark Enterprise (Webster, MA, USA). Homogenization buffer: 50 mM Tris–HCl buffer (pH 8.0) containing 1 mM EDTA. A stock solution of 10 mM paraoxon was prepared in dried acetone, and a stock solution of 10 mM mipafox was prepared in 10 mM Tris–citrate buffer (pH 6.0); both were dissolved in homogenization buffer (pH 8.0) containing 1 mM EDTA immediately before the kinetic assays. A stock solution of substrate phenylvalerate (16.8 mM) was prepared in dried N,N-diethylformamide, and diluted in water to 0.54 mM immediately before the enzymatic assays. All the other chemicals were of analytical reagent grades.

2.2. Tissue preparation

Broiler chicken brains ($n = 8$) were obtained from a commercial slaughtering house immediately after killing the animals and were kept in cold (0–5 °C) homogenization buffer until use. They were homogenized with a Polytron homogenizer (Kinematica Gmbh, Germany) using a PTA 10S head (dispersing aggregates at 70% power (3 × 30 s)) at a concentration of 200 mg fresh tissue/ml in the same buffer.

2.3. Subcellular fractionating

The homogenized tissue was centrifuged at 1000 × *g* for 10 min (4 °C) to precipitate fibers and nuclei. The supernatant was centrifuged at 100 000 × *g* for 60 min to obtain a precipitate consisting of the mitochondrial and microsomal fractions. Samples were frozen in liquid nitrogen before use.

2.4. Standard phenylvalerate esterase activity (PVase) assay for kinetic studies

Enzyme assays were carried out as previously described (Estévez et al., 2011) by following a procedure based on the colorimetric method for the NTE assay developed by Johnson (1977). The method was modified and programmed for an automated microassay using the Biomek 2000 (Beckman) workstation as follows:

In a 1-ml microtube, a 200-μl volume of the brain membrane fraction (at an equivalent concentration of 15 mg/ml of the original fresh tissue) was incubated with 20 μl of inhibitor solution (buffer in controls) at the appropriate concentrations. After the appropriate inhibition time, 200 μl of substrate phenylvalerate (0.54 mM) were added and incubated for 10 min at 37 °C. The reaction was stopped by adding 200 μl of a solution of 2% sodium dodecyl sulfate with 1.23 mM aminoantipyrine (SDS-AAP solution), which was then mixed with 50 μl of 12.1 mM potassium fericyanide and left for 10 min for color development. A 300-μl volume from each microtube was transferred to a 96-well microplate, and absorbance was read at 510 nm. Standards of phenol, blanks, and spontaneous hydrolysis controls (samples without tissue) were included with the same procedure.

The results were expressed as % activity ($E/E_0 \times 100$) over the control without an inhibitor, and were plotted versus time (t) or versus inhibitor concentration. The absorbance of the control without an inhibitor was 1.24 ± 0.04 μA. All the experiments were done by triplicates and each point in the data represents the mean of three replicates (SD < 5%).

2.5. Reactivation kinetics by dilution

High tissue-concentrated samples (200 mg/ml) were preinhibited with either 40 and 1000 nM paraoxon or 40 and 8000 nM mipafox for 30 min at 37 °C. The study of the reactivation process began at that time point by diluting the incubation mixture 10-fold with homogenization buffer. Incubation was continued and 110 μl aliquots were withdrawn at different times between 0 and 180 min and added to tubes containing 100 μl of substrate solution to be incubated for 10 min at 37 °C. The enzymatic reaction was stopped and color was measured as previously indicated.

2.6. Discrimination of potential targets of delayed neurotoxicity sequential NTE assay without removing paraoxon

A 200-μl volume of tissue samples (containing the membrane fraction from 24 mg/ml of brain) were incubated with 40 μM of paraoxon for 30 min at 37 °C by adding 20 μl of the paraoxon solution, and PVase activity was assayed as described previously. Afterward, samples were incubated with variable concentrations of mipafox (0–250 μM), without removing the paraoxon, for 30 min at 37 °C by adding 20 μl of the inhibition solution. Then PVase activity was assayed as described previously. Controls (samples without inhibitors) and spontaneous hydrolysis controls (samples without tissue) were included with the same procedure.

2.7. Sequential NTE assay removing paraoxon before incubation with mipafox

A 2000-μl volume of tissue samples (containing the membrane fraction from 200 mg/ml of brain) were incubated with 40 μM of paraoxon for 30 min at 37 °C by adding 200 μl of inhibition solution or buffer instead of paraoxon in controls. Spontaneous hydrolysis controls (samples without tissue) were included with the same procedure and PVase activity was assayed as described previously. Next, inhibited samples were diluted up to 25 ml with Tris buffer at 4 °C and centrifuged at 100 000 × *g* for 10 min (4 °C). Then the membrane fractions were taken back to 25 ml and samples were centrifuged at 100 000 × *g* for 10 min (4 °C) again. After centrifuging for the second time, sample pellets were taken to 20 ml by diluting the sample to around 0.05 nM of the paraoxon residual concentration. The tissue concentration in the final diluted solution was 20 mg/ml. PVase activity was assayed as described previously in this step. These inhibited and washed diluted membrane fractions were incubated at 37 °C for up to 150 min to reactivation, and PVase activity was assayed. Controls (samples without inhibitors) were included with the same procedure. Recovery of PVase activity after centrifuging was 93% of activity.

After this step, a fixed time mipafox inhibition experiment was done with this paraoxon-inhibited and washed tissue by using variable mipafox concentrations in the range of 0–250 μM for 30 min at 37 °C.

2.8. Mathematical analysis of the inhibition curves

Model equations were fitted to the experimental inhibition and reactivation kinetics data by a non-linear computerized method based on the least squares principle using the Sigma Plot software, version 8 (Systat Software Inc., Chicago, USA), and by applying the model equations for a system with several enzymatic components, as described by Estévez and Vilanova (2009). The additional adaptations of the model equation to our specific situation are indicated in Section 3. *F*-test was used for comparing the kinetic models that have been fit to the data, in order to identify the model that best fits, using Sigma Plot software.

2.9. Kinetic models

2.9.1. Fixed-time inhibition curve

The fixed-time inhibition curves of PVase activity were fitted with exponential decay models for inhibition with spontaneous reactivation, if necessary, of one, two, or more sensitive enzymatic components with or without a resistant fraction, in accordance with (Estévez and Vilanova, 2009). If no spontaneous reactivation was observed, the general model equation for inhibition without spontaneous reactivation was as follows:

$$E = E1_0 \cdot e^{-(k1 \cdot I \cdot t)} + E2_0 \cdot e^{-(k2 \cdot I \cdot t)} + E3_0 \cdot e^{-(k3 \cdot I \cdot t)} + \cdots + En_0 \cdot e^{-(kn \cdot I \cdot t)} + R$$

If spontaneous reactivation was observed for one of the enzymatic components, the general model was as follows:

$$E = \left[\frac{(E1_0 \cdot k1r)}{(k1 \cdot I + k1r)}\right] + \left[\frac{(E1_0 \cdot k1r)}{(k1 \cdot I + k1r)}\right] \cdot e^{-(k1 \cdot I \cdot t + k1r) \cdot t} + E2_0 \cdot e^{-(k2 \cdot t)} + \cdots + En_0 \cdot e^{-(kn \cdot t)} + R$$

where $k1$, $k2$, $k3$ and kn' are the second-order kinetic constants and $k1r$ is the spontaneous reactivation constant.

2.9.2. Evaluation of ongoing inhibition during the substrate reaction

Exponential decay models were used to fit the data of % of activity at the zero inhibition time versus inhibitor concentration in the progressive inhibition experiment. The model applied was $E_0 \cdot e^{-ka' \cdot x} + R$, where parameter ka' represents the apparent first-order kinetic constant of inhibition observed during the substrate reaction time, and E_0 represents the % of activity of the enzymatic component which is affected by the ongoing inhibition effect. The model is shown in Section 3 in each case.

2.9.3. Reactivation experiment data

If spontaneous reactivation was observed, the mathematical models for reactivation corresponding to the one, two or more inhibited enzymes were applied to fit the data. The residual concentration of the inhibitor was considered significant. The best fitting model (according to the F test) is that shown in Section 3. The most complex model applied was:

$$E = \left[\frac{(EI_0 \cdot k1r)}{(k1 \cdot I + k1r)}\right] + \left[\frac{(EI_0 \cdot k1r)}{(k1 \cdot I + k1r)}\right] \cdot e^{-(k1 \cdot I + k1r) \cdot t} + \left[\frac{(EI_0 \cdot k2r)}{(k2 \cdot I + k2r)}\right] + \left[\frac{(EI_0 \cdot k2r)}{(k2 \cdot I + k2r)}\right] \cdot e^{-(k2 \cdot I + k2r) \cdot t} + R$$

which represents a model with three enzymatic components: $E1$ and $E2$, which were inhibited and spontaneously reactivated; R, which was a component resistant to the concentrations assayed.

2.9.4. Time-progressive inhibition data

A three-dimensional fitting (% of activity versus t and I) was done with the data. The time-progressive inhibition data were analyzed with models in accordance with Estévez and Vilanova (2009), which considers inhibition with a simultaneous spontaneous reactivation in those cases where spontaneous reactivation occurs. The best fitting model according to the F test is shown in each case in Section 3.

In the progressive inhibition experiment with paraoxon, the general model equation applied was:

$$E = [e^{-ka' \cdot I}] \cdot \left\{\left[\frac{(kr1 \cdot E1_0)}{(k1 \cdot I + kr1)}\right] + \left[\frac{(k1 \cdot I \cdot E1_0)}{(k1 \cdot I + kr1)}\right] \cdot e^{-(k1 \cdot I + kr1) \cdot t}\right\} + E2_0 \cdot e^{-(k2 \cdot I) \cdot t} + E3_0 \cdot e^{-(k3 \cdot I) \cdot t} + \cdots + En_0 \cdot e^{-(kn \cdot I) \cdot t} + R$$

which represents a model with n enzymatic components; $E1$, which was inhibited and spontaneously reactivated; $E2$, $E3$ and En, which were only inhibited; and R, which was a component resistant to the concentrations assayed. The models with 1, 2 or 3 sensitive-exponential components, with or without resistant components, were tested.

In the progressive inhibition experiment with mipafox, the general model equation applied was:

$$E = [e^{-ka' \cdot I}] \cdot E1_0 \cdot e^{-(k1 \cdot I) \cdot t} + E2_0 \cdot e^{-(k2 \cdot I) \cdot t} + \cdots + En_0 \cdot e^{-(kn \cdot I) \cdot t} + R$$

which represents a model with n enzymatic components; $E1$, $E2$ and En, which were inhibited; and R, a component resistant to the concentrations assayed. The models with 1, 2 or 3 sensitive-exponential components, with or without resistant components, were tested.

In all the mathematical models, $k1$, $k2$, $k3$, …, kn were the second-order inhibition constants; $kr1$ was the reactivation constant; $E1_0$, $E2_0$, $E3_0$, …, En_0 and R were the proportion (amplitude) of enzymatic components $E1$, $E2$, $E3$, En, …, and R, respectively. The exponential factor $[e^{-ka' \cdot I}]$ was included to correct the "ongoing inhibition" during the substrate reaction (Estévez et al., 2010).

For the purpose of obtaining a coherent solution in the interactive computing estimation, some restrictions were applied: (1) all the parameters (rate constants and amplitudes) should have positive values (>0); (2) component 1 was the most sensitive, therefore $k1 > k2$, $k2 > k3$; (3) the following complementary restriction was also applied: $E1_0 + E2_0 + E3_0 + R = 100\%$.

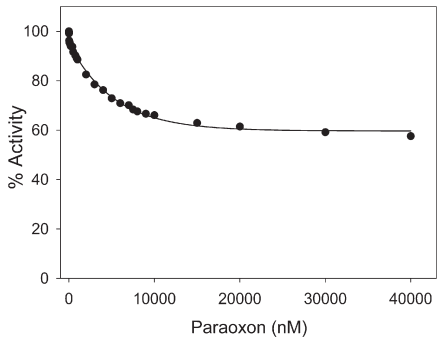

Fig. 1. Paraoxon 30-min fixed-time inhibition curve of particulate brain phenyl valerate esterase activity. A brain particulate fraction from 15 mg tissue/ml was incubated with the corresponding paraoxon concentration for 30 min at 37 °C, and residual esterase activity was measured. The curve line is the best fit according to the F test (two exponential components plus a constant component). Each point represents the mean of three replicates (SD < 5%).

The results were expressed by giving the values of the exponential kinetic constants ($M^{-1}\,min^{-1}$), the proportions/amplitudes of each component (% of activity) and the values of I_{50} (30 min) (concentration for achieving a 50% inhibition of this component deduced from its kinetic parameters (inhibition and reactivation constants)).

The I_{50} (30 min) values for the spontaneously reactivate component (Ei) were obtained by applying the following equation:

$$\%\text{Activity}(Ei) = 50\% = \left[\frac{(kr \cdot 100)}{(ki \cdot I + kr)}\right] + \left[\frac{(ki \cdot I \cdot 100)}{(ki \cdot I + kr)}\right] e^{-(ki \cdot I \cdot kr) \cdot 30}$$

The previously estimated kinetic constants were fixed and then successive iterations with different I values were carried out in an electronic spreadsheet to obtain the I value corresponding to $50 \pm 0.1\%$ activity.

3. Results

3.1. Paraoxon inhibition and reactivation curves in the brain membrane fraction

3.1.1. Fixed-time inhibition curve

Fig. 1 shows the data of chicken brain membrane esterases incubated with paraoxon, for 30 min at 37 °C. The best fitting model, after considering inhibition without spontaneous reactivation, and according to the F test, consisted of two sensitive components (4.8% and 35.5%) with an estimated I_{50} (30 min) of 21 and 3667 nM, respectively, and a resistant component (59.7%). These estimated I_{50} (30 min) were used to choose the concentrations for the spontaneous reactivation experiment and for the time-progressive inhibition experiment.

3.1.2. Spontaneous reactivation after diluting the inhibitor

Chicken brain membrane fractions were inhibited with paraoxon for 30 min at 37 °C. Two paraoxon concentrations were chosen; 40 nM, to inhibit only the most sensitive enzymatic component; 1000 nM, to inhibit the two previously detected sensitive enzymatic components. Samples were then diluted 10-fold to around 4 nM and 100 nM of the paraoxon residual concentrations, respectively, and were incubated at 37 °C to recover activity during 180 min.

The sample preinhibited with 40 nM of paraoxon-recovered activity after dilution in a time-progressive manner from 94.6% to 98.7% activity in 180 min (4.1% of activity). This suggests that a spontaneous reactivation of the most sensitive component (4.8% of activity) took place. Spontaneous reactivation should be considered in the kinetic model. Activity increased over time until

it reached a ceiling limit. This suggests that a "steady stage" was reached in which the reactivation rate equaled the inhibition rate at a residual concentration of about 4 nM. This behavior also suggests that the aging reaction may be negligible under these experimental conditions because PVase activity could decrease if aging and inhibition by residual concentration occurred simultaneously. Therefore, aging was not considered in the model equations representing this system's kinetic behavior.

Conversely, the sample preinhibited with 1000 nM of paraoxon activity remained inhibited over time (180 min), suggesting that the second component was not reactivated. The residual paraoxon concentration (~100 nM) was higher than the I_{50} (30 min) of the most sensitive component and it remained inhibited under this condition.

The mathematical models for reactivation described in Section 2 were applied to the 40 nM inhibition curve. The residual concentration of the inhibitor (4 nM) was considered significant. The best fit according to the *F* test was a model with one component, which was spontaneously reactivated and simultaneously inhibited and a resistant component.

The best fitting model (according to the *F* test) consisted in two enzymatic components: *E*1, which is inhibited and spontaneously reactivated, and *R*, which is a component resistant to the concentration assayed (1000 nM of paraoxon). The kinetic parameters are shown in Table 1, line A. This mathematical model is as follows:

$$E = \left[\frac{EI_0 \cdot k1r}{(k1 \cdot 4 + k1r)}\right] + \left[\frac{EI_0 \cdot k1r}{(k1 \cdot 4 + k1r)}\right] \cdot e^{-(k1 \cdot 4 + k1r) \cdot t} + R$$

3.1.3. Analysis of the fixed-time inhibition curve considering spontaneous reactivation

The paraoxon fixed-time inhibition curve shown in Fig. 1 was fitted to a model by considering the spontaneous reactivation of the most sensitive component. The best fitting model according to the *F* test was:

$$E = \left(\frac{E1_0 \cdot k1r}{k1 \cdot 30 \cdot I + k1r}\right) + \left[\frac{(E1_0 \cdot k1r \cdot t)}{(k1 \cdot 30 \cdot I + k1r)}\right] \cdot e^{-(k1 \cdot I + k1r) \cdot t} + E2_0 \cdot e^{-(k2 \cdot t)} + R$$

The model describes two sensitive components, *E*1 and *E*2 (5.9% and 34.8%), with I_{50} (30 min) of 37 nM and 3916 nM, respectively, and a resistant component (59.3%). The resulting kinetic parameters are shown in Table 1, line (B).

3.1.4. Time-progressive inhibition curves by paraoxon

Chicken brain membrane fractions were inhibited with paraoxon (0, 40, 250, 1000 and 7000 nM) for times of up to 180 min at 37 °C. The kinetic analysis for the inhibition of brain membrane PVase activity with paraoxon resulted in a time-progressive inhibition of around 50% of PVase activity, which is coherent with the covalent irreversible inhibition. Inhibition curves were fitted individually with exponential decay models for inhibition without spontaneous reactivation of one, two, or more sensitive enzymatic components with or without resistant. Fig. 2A shows the curves corresponding to the best fit of the individual curve for each paraoxon concentration used according to the *F* test. Although each curve seemed to graphically fit the experimental data, no consistent values of the kinetic constants, numbers and the proportion of components were obtained when each curve was analyzed independently using a simple multi-exponential equation.

3.1.5. Evaluation of ongoing inhibition during the substrate reaction

Inhibition during the substrate reaction at 0 min of inhibition time is shown in Fig. 2B. The data indicate that ongoing inhibition during substrate incubation under the assayed conditions was apparently significant. Therefore, ongoing inhibition during substrate incubation needs to be considered in the model (Estévez et al., 2010).

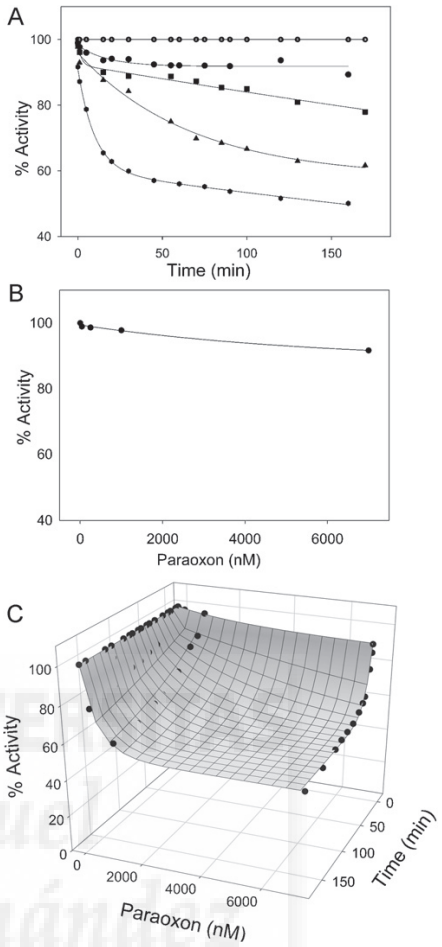

Fig. 2. Kinetics of the time-progressive inhibition by paraoxon. Preparation containing the particulate fraction of 15 mg fresh tissue/ml was preincubated with 0, 40, 250, 1000 and 7000 nM paraoxon (superior to the lower plots of Panel A) for the indicated time. Then enzymatic activity was assayed by incubating the substrate phenylvalerate for 10 min. Panel A shows the best fitting model equation for the individual curve for each concentration. Panel B indicates the inhibition during the time of the reaction with the substrate (0 min inhibition time; "ongoing inhibition"). Panel C offers the inhibitory surface obtained by fitting the 3D model equation to the data. The surface reflects the result of the best model according to the *F* test. Each point represents the mean of two replicates (SD < 5%).

This effect is approximately 8.4% for the highest inhibitor concentration and could hinder the data analysis if not considered, which justifies that the ongoing inhibition factor should be taken into account, but only for the most sensitive enzymatic component.

3.1.6. A kinetic model considering ongoing inhibition and the simultaneous spontaneous reactivation process

The evidence of reactivation (Fig. 2) of one component suggests that a complex kinetic model including reactivation should be used to analyze the kinetic inhibition data. This model should also include several enzymatic components with reactivation and an ongoing inhibition effect for the most sensitive component, but not for the other components.

Table 1
Inhibition by paraoxon. Kinetic constants (*ki*) and proportions of the obtained esterase components from inhibition and/or reactivation experiments with paraoxon. The I_{50} values were calculated from the kinetic constants for each component. (A) Reactivation after diluting; (B) experiment for fixed-time inhibition considering spontaneous reactivation (Fig. 1); (C) experiment of the time-progressive inhibition in a 3D fitting (Fig. 4). The R^2 coefficients were: 0.9991 (A), 0.9437 (B) and 0.9991 (C).

Exp.	$ka\,(t=0)\,(nM^{-1})$	$E1$ (%)	$k1\,(nM^{-1}\,min^{-1})$	$k1r\,(min^{-1})$	I_{50}[a] (nM)	$E2$ (%)	$k2\,(nM^{-1}\,min^{-1})$	I_{50}[a] (nM)	R (%)
A		4.4	0.0012	0.0464	43	95.6[b]	–		–
B	–	5.9	0.0030	0.1100	37	34.8	5.9×10^{-6}	3916	59.3
C	0.00089	8.3	0.0025	0.0272	15	38.3	1.5×10^{-5}	1540	53.4

[a] I_{50} for the 30-min inhibition time.
[b] Esterase activity resistant to 40 nM of paraoxon.

The time-progressive inhibition data were analyzed with a model of one, two or more enzymatic components by considering inhibition with a simultaneous spontaneous reactivation and the ongoing inhibition effect for the most sensitive component. The best fitting model, according to the *F* test, consisted in three enzymatic entities: *E*1, the most sensitive, was inhibited and spontaneously reactivated; *E*2, which was only inhibited; and *R*, a resistant component (Table 1, line C). This mathematical model is as follows:

$$E = [e^{-ka'\cdot I}]\cdot\left\{\left[\frac{(kr1\cdot E1_0)}{(k1\cdot I + kr1)}\right] + \left[\frac{(k1\cdot I\cdot E1_0)}{(k1\cdot I + kr1)}\right]\cdot e^{-(k1\cdot I + kr1)\cdot t}\right\} + E2_0\cdot e^{-(k2\cdot I)\cdot t} + R$$

3.1.7. Mipafox inhibition curves in the brain membrane fraction

3.1.7.1. Fixed-time inhibition curve. Fig. 3 shows the data of the fixed-time experiment where chicken brain membrane fractions were incubated with mipafox for 30 min at 37 °C. The best fitting model consisted of two sensitive enzymatic components (6.9% and 44.1%) with the estimated I_{50} (30 min) of 6 nM and 6903 nM, respectively, and a resistant component (49.0%). The resulting kinetic parameters and I_{50} (30 min) values are shown in Table 2, line (A). The estimated I_{50} (30 min) were used to choose the concentrations for the spontaneous reactivation experiment and for the time-progressive inhibition experiment.

3.1.7.2. Evaluation of activity after diluting the inhibitor. Chicken brain membrane fractions were inhibited with mipafox for 30 min at 37 °C. Two mipafox concentrations were chosen: 40 nM to inhibit only the most sensitive component and 8000 nM to inhibit all the sensitive PVase activity detected previously to be then diluted to around 4 nM and 800 nM of the mipafox residual, respectively. After diluting, the activity remained inhibited over time (180 min) from 94.6% to 89.9% for the fractions inhibited with 40 nM, and from 72.0% to 66.2% for those inhibited with 8000 nM. We consider that there was no significant spontaneous reactivation after inhibition with mipafox for any of the sensitive components during the experiment time (180 min). Therefore, spontaneous reactivation was not considered in the model equations for inhibition kinetics with mipafox.

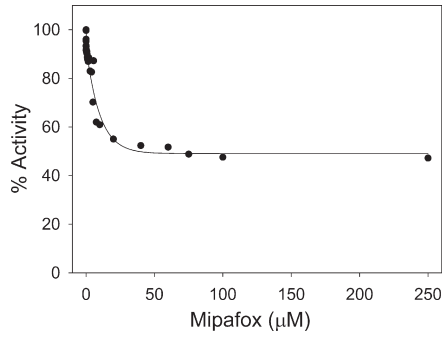

Fig. 3. Mipafox fixed-time inhibition curve. The particulate brain fraction was incubated with the corresponding mipafox concentration (ranging from 0.003 to 250 μM) for 30 min at 37 °C, while residual activity was assayed as described in Section 2. The curve was the best fit according to the *F* test (two exponential components plus a resistant one). Each point represents the mean of three replicates (SD < 5%).

3.1.7.3. Time-progressive inhibition by mipafox. Chicken brain membrane fractions were inhibited with mipafox (0, 200, 800, 3500 and 8000 nM) for times of up to 180 min at 37 °C. This inhibition was time-progressive (~60% of total activity), which is coherent with covalent inhibition. Fig. 4A shows the curves corresponding to the best fit of the individual curve for each mipafox concentration. Although each curve seemed to graphically fit the experimental data properly, no consistent values of the kinetic constants, numbers and the proportion of the components were obtained when fitting each curve individually using a simple multi-exponential equation.

3.1.7.4. Evaluation of ongoing inhibition during the substrate reaction. Inhibition during substrate reaction without preincubation is shown in Fig. 4B. The data indicate that ongoing inhibition during substrate incubation under the assayed conditions was apparently significant. Therefore, ongoing inhibition during substrate incubation needs to be considered in the model (Estévez et al., 2010).

This effect was approximately 10% for the highest inhibitor concentration and could hinder the data analysis if not considered, which justifies that the ongoing inhibition factor should be taken into account, but only for the most sensitive enzymatic component.

3.1.7.5. A kinetic model considering ongoing inhibition. The inhibition data presented in Fig. 4C were re-analyzed with a model that considered the "ongoing inhibition" effect $[e^{-ka'\cdot I}]$ in the most sensitive component, which was analyzed by a three-dimensional fitting (% of activity versus *t* and *I*) to consider all the data simultaneously. The best fitting model consisted in three sensitive enzymatic entities, where the most sensitive one was affected by ongoing inhibition, but not by spontaneous reactivation. This mathematic model is as follows:

$$E = [e^{-ka'\cdot I}]\cdot E1_0\cdot e^{-(k1\cdot I)\cdot t} + E2_0\cdot e^{-(k2\cdot I)\cdot t} + E3_0\cdot e^{-(k3\cdot I)\cdot t}$$

The results are provided in Table 2 (line B), and the deduced 3D surface is plotted in Fig. 2C.

3.2. Discrimination of NTE in the sequential assay removing paraoxon versus the assay without removing paraoxon inhibition protocol

In order to distinguish paraoxon-resistant mipafox-sensitive esterase components, two assays were done: the sequential NTE assay without removing paraoxon and the NTE assay removing paraoxon.

Table 2
Inhibition by mipafox. Kinetic constants (*ki*) and proportions of components obtained by inhibition with mipafox. The I_{50} (30 min) values were calculated from the kinetic constants for each component. (A) Experiment for fixed-time inhibition (Fig. 3); (B) inhibition curve at the preinhibition zero time (insert in Fig. 4B); (C) experiment for time-progressive inhibition with different concentrations in a 3D fitting (Fig. 4C). The R^2 coefficients were: 0.9623 (A); 0.9930 (B) and 0.9671 (C).

Exp.	*ka* (*t* = 0) (nM^{-1})	*E*1 (%)	*k*1 (nM^{-1} min^{-1})	I_{50}[a] (nM)	*E*2 (%)	*k*2 (nM^{-1} min^{-1})	I_{50}[a] (nM)	*R* (%)
A	–	6.9	0.0036	6	44.1	3.3×10^{-6}	7001	49.0
B	2.0×10^{-4}	4.9	0.0008	29	38.6	3.5×10^{-6}	6601	56.5

[a] I_{50} values for the 30-min inhibition time.

3.2.1.1. Sequential NTE assay without removing paraoxon

In this assay, the paraoxon-resistant esterase fraction (resistant to paraoxon 40 μM for 30 min at 37 °C) was incubated with variable concentrations of mipafox from 3 nM to 250 μM at 37 °C in 30 min (Fig. 5A). Paraoxon-resistant activity was 59.6% of total activity.

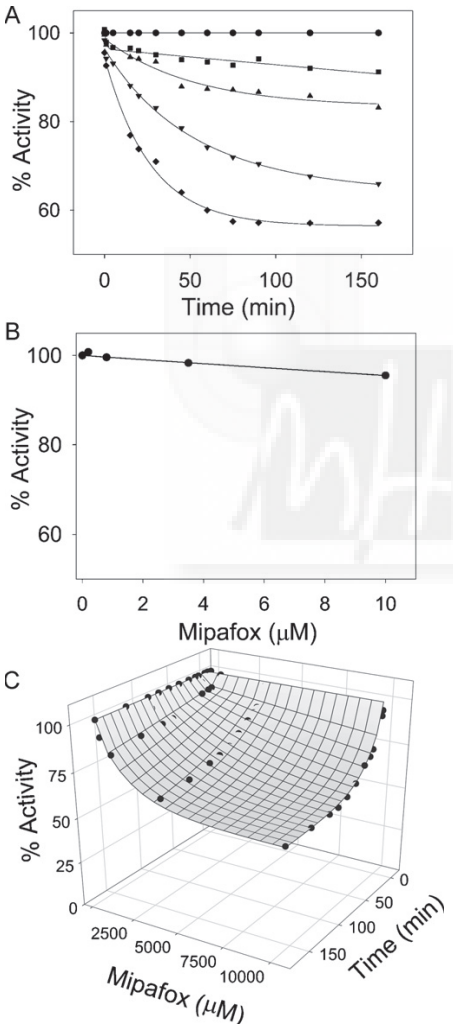

Fig. 4. Kinetics of the time-progressive inhibition by mipafox. A preparation containing the particulate fraction of 15 mg fresh tissue/ml was preincubated with 0, 200, 800, 3500 and 8000 nM of mipafox (superior to the lower plots in Panel A) for the indicated time at 37 °C. Then enzymatic activity was assayed with phenylvalerate for 10 min. Panel A shows the best fitting model equation for the individual curve for each concentration. Panel B reveals inhibition at the reaction time with the substrate (0 min inhibition time). Panel C provides the inhibitory surface obtained by fitting the 3D model equation to the data. The surface reflects the result of the best model according to the *F* test. Each point represents the mean of two replicates (SD < 5%).

The mathematical models (exponential decay models for inhibition without spontaneous reactivation) corresponding to one, two or more sensitive enzymes were applied. The best fit according to the *F* test is shown in Table 3A, and it was a model with one sensitive component and one resistant one; the kinetics parameters are shown in Table 3, line A.

$$E = E1_0 \cdot e^{-(k1' \cdot t)} + R$$

where $k1'$ is the first-order kinetic constant, $E1_0$ is the proportion (amplitude) of the sensitive component and *R* is the resistant component.

3.2.1.2. Sequential NTE assay removing paraoxon

In the sequential protocol, the enzymatic sample was incubated with 40 μM of paraoxon for 30 min at 37 °C and then paraoxon was eliminated by diluting and centrifuging. Paraoxon-resistant activity was 54.9% of total PVase activity. The paraoxon-preinhibited tissue was incubated at 37 °C for 180 min to allow for spontaneous reactivation. Then it was incubated with variable concentrations of mipafox from 3 nM to 250 μM at 37 °C for 30 min (Fig. 5B).

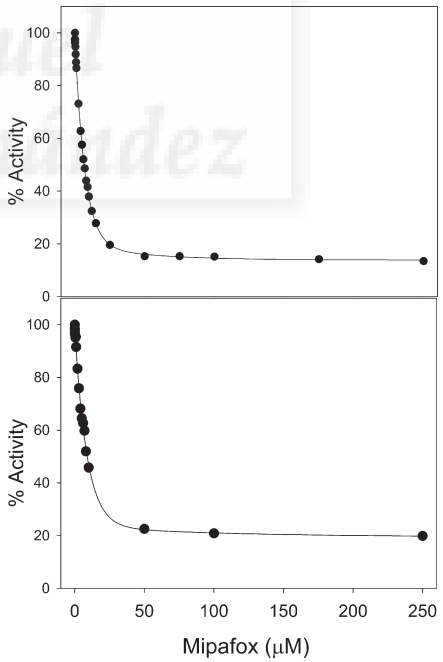

Fig. 5. Inhibition of 40 μM paraoxon-resistant activity with mipafox (the NTE assay). The particulate brain fraction was incubated with 40 μM of paraoxon for 30 min at 37 °C, and then with the corresponding mipafox concentration (ranging from 0.003 to 250 μM) for 30 min at 37 °C. Panel A shows the NTE activity assay, where mipafox was added after the 30-min preincubation with paraoxon without eliminating the residual paraoxon concentration. Panel B offers the assay, where paraoxon was removed and washed off after the 30-min preincubation by two circles of diluting with cold buffer and centrifugation at 4 °C, diluting again, centrifugation and resuspending at the desired concentration. Each point represents the mean of three replicates (SD < 5%).

Table 3
Inhibition by mipafox of paraoxon-resistant activity (NTE assay). Kinetic constants (*ki*) and proportions of the components obtained by inhibition with mipafox of paraoxon 40 μM resistant to soluble brain fractions. The I_{50} (30 min) values were calculated from the kinetic constants for each component. (A) The sequential NTE inhibition assay without removing paraoxon (Fig. 4C); (B) the sequential NTE inhibition assay removing paraoxon (Fig. 5).

Exp.	*E*1 (%)	*k*1 (nM^{-1} min^{-1})	I_{50}[a] (nM)	*E*2 (%)	*k*2 (nM^{-1} min^{-1})	I_{50}[a] (nM)	*R* (%)
A	–	–	–	78.9	3.8×10^{-6}	6080	21.1
B	4.1	0.0005	46	79.9	4.3×10^{-6}	5373	20.0

[a] I_{50} values for the 30-min inhibition time.

The mathematical models (exponential decay models for inhibition without spontaneous reactivation) corresponding to one, two or more sensitive enzymes were applied for mipafox inhibition. The best fit according to the *F* test is shown in Table 3B; it was a model with two sensitive components and a resistant one as follows:

$$E = E1_0 \cdot e^{-(k1 \cdot I \cdot t)} + E2_0 \cdot e - (k2 \cdot I \cdot t) + R$$

The resulting parameters are shown in Table 3B.

4. Discussion

Four enzymatic components have been discriminated in brain membrane-bound esterases and their inhibition has been kinetically characterized by paraoxon and mipafox. These components have been called EPα, EPβ, EPγ and EPδ. This kinetic characterization will facilitate further isolation and molecular characterization studies.

4.1. Kinetic behavior of brain membrane PVases with paraoxon

Paraoxon has been used to discriminate non-neuropathic carboxylesterases as it is neither an inducer of OPIDP nor an inhibitor of NTE. To know the kinetic behavior of brain membrane esterases with paraoxon, it is necessary to learn the reversibility of long-term inhibition and to discriminate non-neuropathic carboxylesterases in membrane brain fractions. Phenylvalerate is an appropriate substrate to detect esterases that are sensitive to neuropathic OPs such as NTE (Johnson, 1969; Estévez et al., 2004; Mangas et al., 2011). This does not mean that it is the best for detecting other esterases. For these reasons, the proportion of components described in this paper is the proportion of activity detected with PV as substrate and it is not the proportion under molecular point of view.

This paper evidences that part of brain membrane esterase activity (around 50% of activity) is extremely sensitive to paraoxon. Concentrations of paraoxon at around micromolar units are able to inhibit about 46.6% of total membrane esterases in chicken brain in a time-progressive manner, suggesting covalent irreversible phosphorylation. Céspedes et al. (1997) reported similar results as these authors found that 52.8% of the total membrane esterases were inhibited using similar concentrations. The kinetic behavior is coherent with two sensitive esterase components.

The spontaneous reactivation experiments reveal that the most sensitive component observed is able to reactivate and that reactivation is time-progressive (Fig. 2). The spontaneous reactivation phenomenon of preinhibited carboxylesterases taking place with different inhibitors has been described in other works. A 40% reactivation has been observed in the samples preinhibited with stereoisomer P(−) of soman in NTE studies done with hen brains after 18 h at 37 °C (Johnson et al., 1985). It has been also observed with not only paraoxon, but also the biotinylated organophosphate S9B in the soluble fraction of the chicken peripheral nerve (Barril et al., 1999; Estévez et al., 2010, 2011). The spontaneous reactivation of complete esterase activity in chicken serum has also been described (García-Pérez et al., 2003). Moreover, the spontaneous reactivation of a highly sensitive component has been recently described in soluble brain esterases (Mangas et al., 2011). It has been suggested that these esterases play potential roles in toxicity and/or detoxification during low-dose long-term exposure to organophosphorus compounds, which warrants further research (García-Pérez et al., 2003; Estévez et al., 2011; Mangas et al., 2011).

Three enzymatic components were detected in the inhibition experiment with paraoxon. The "ongoing inhibition" effect is considered for the high sensitive enzymatic component. The 3D fit enables all the data in the same fit to be included simultaneously, and it is the best tool to fit the inhibition data in this complex model (Estévez et al., 2004). The three enzymatic components detected were as follows: *E*1, I_{50} (30 min) = 15 nM, displaying both ongoing inhibition and spontaneous reactivation; *E*2, I_{50} (30 min) = 1540 nM, showing progressive inhibition; *R*, which is practically resistant to paraoxon inhibition. The estimated amplitudes (proportion), the inhibition constants and the reactivation constant are similar in the inhibition and reactivation, after diluting, experiments. All these observations may be considered an internal validation of the consistency of the results and the applied kinetic model.

4.2. Kinetic behavior of brain soluble PVases with mipafox

A portion of brain membrane PVase activity is sensitive to mipafox. Micromolar concentrations of mipafox are able to inhibit about 43.5% in a time-progressive manner, suggesting covalent irreversible phosphorylation. Kinetic behavior is coherent with two sensitive esterase components, and a portion of 56.5% of activity is practically resistant to mipafox inhibition.

The spontaneous reactivation experiments in a membrane chicken brain fraction reveal that inhibited soluble PVase activity is not able to reactivate spontaneously after mipafox inhibition. The "ongoing inhibition" effect is considered for the highly sensitive enzymatic component. The 3D fit results in three enzymatic components: *E*1, I_{50} (30 min) = 29 nM, displaying ongoing inhibition; *E*2, I_{50} (30 min) = 6601 nM, showing progressive inhibition; *E*3, which is practically resistant to mipafox inhibition. The consistency of the estimated parameters was checked by comparing the results of the fixed-time inhibition and the time-progressive inhibition experiments (Table 2), while amplitudes (proportion) are similar and inhibition constants are comparable in all the experiments.

4.3. Discrimination of NTE in the sequential assay with or without removing paraoxon before incubation with mipafox

Two paraoxon-resistant and mipafox-sensitive esterase components are present using the sequential NTE assay removing paraoxon before incubating with mipafox, but there is only one paraoxon-resistant and mipafox-sensitive component in assay *without removing paraoxon*. Similar results were reported by Carrington and Abou-Donia (1985) and Chemnitius et al. (1983). This mechanism has been explained to be the result of a reversible inhibition of these esterases with paraoxon. It has been considered that inhibition by paraoxon of hen brain particulate NTE shows kinetics compatible with the formation of a reversible intermediate complex between the enzyme and the inhibitor (Carrington and Abou-Donia, 1986). In this work, this discrepancy is explained to be

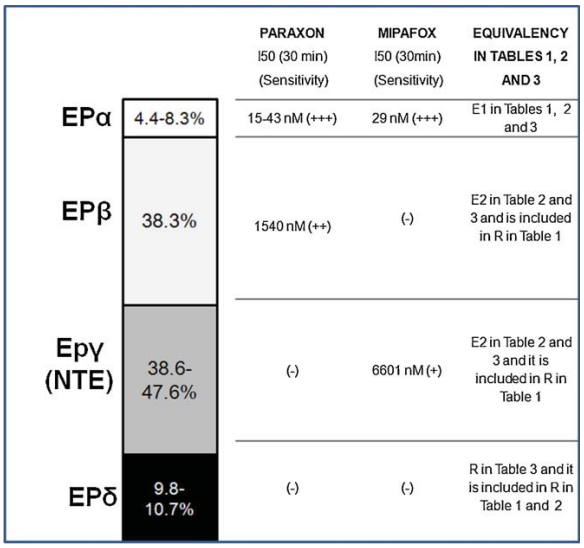

Fig. 6. Discrimination of the esterase components in chicken membrane brain. By globally considering all the data, four enzymatic components were discriminated according to sensitivity to paraoxon and mipafox as follows: EPα, which is very highly sensitive to paraoxon and to mipafox, and spontaneously reactivates after inhibition with paraoxon; EPβ, which is sensitive to paraoxon and resistant to mipafox; EPγ, which is sensitive to mipafox and resistant to paraoxon, and EPδ, which is resistant to both inhibitors. The I_{50} (30 min) values are indicated (for 30 min) with the proportion of the component in parentheses (%) and are "classified" as very sensitive (+++), sensitive (++)/(+) and resistant (−).

the result of spontaneous reactivation after the paraoxon inhibition of the most sensitive component.

In order to discriminate and measure the potential target of delayed neurotoxicity, those esterases sensitive to paraoxon (such as organophosphate that does not induce neuropathy) were excluded as targets of the neurotoxic process (Johnson, 1969, 1982; Johnson et al., 1985). This work proves that part of the membrane esterase activity of the brain can be progressively inhibited by paraoxon with time, but not permanently so because it is spontaneously reactivated. The results of this work confirm that paraoxon is not the most appropriate tool to discriminate potential targets of neurotoxicity in the membrane fraction of brain due to some fraction being reactivated.

The most sensitive component to mipafox in the sequential assay removing paraoxon (*E*1 in Table 3) is detected due to spontaneous reactivation after inhibition with paraoxon, but it is not detected in the assay without removing paraoxon as it remains blocked by paraoxon. This component represents 4.1% of paraoxon-resistant activity (2.5% of total esterase activity).

The consistency of both the estimated parameters and the inhibition constants in the NTE sequential inhibition experiments (Table 3) may be considered an internal validation of the applied kinetic model and of the results obtained.

4.4. Enzymatic components discriminated in the brain membrane fraction.

Fig. 6 shows the suggested interpretation of the enzymatic components differentiated with paraoxon and mipafox. Three enzymatic components have been discriminated in the mipafox and paraoxon inhibition experiments. Moreover, the "NTE experiments" (inhibition of paraoxon-resistant activity with mipafox) allow us to discriminate a fourth enzymatic component because a component resistant to mipafox and paraoxon is observed (Table 3).

EPα (*E*1 in Tables 1–3), is the most sensitive component for both paraoxon and mipafox (I_{50} = 15–43 and 29 nM, respectively), and represents 4.4–8.3% of activity and is spontaneously reactivated with paraoxon. This highly sensitive component has similar inhibition and reactivation constants to a component which represents 41–48% of the activity in the soluble peripheral nerve fraction, I_{50} = 6–11 nM for paraoxon and 7–12 nM for mipafox (Estévez et al., 2004, 2011), and to a component which represents 11–23% of the activity in the soluble brain fraction (I_{50} = 9–11 nM of paraoxon and 4 nM of mipafox; Mangas et al., 2011). The high sensitivity of EPα esterases with paraoxon suggests that they might play a role in toxicity in the low-level long-term exposure of organophosphate compounds, as it is spontaneously reactivated only in chronic exposure may be relevant. This esterase component also may have a protective effect in relation to some OPs' spontaneous reactivation, such as paraoxon, and other di-ethyl/dimethyl phosphates, which may be considered a biodegradation reaction. Moreover, EPα is also highly sensitive to mipafox and it is not permanently inhibited by paraoxon. These esterases, sensitive to paraoxon, are discarded as irrelevant in the standard assay of NTE. However they cannot be ruled out as potential neuropathy targets because are spontaneously reactivated. The organophosphates used to establish the multistep hypothesis of OPIDP have multiple targets and it has been suggested that the association with NTE inhibition may be an epiphenomenon (Winrow et al., 2003).

EPβ is the second most sensitive component to paraoxon (I_{50} = 1540 nM), is resistant to mipafox (*E*2 in Table 1, part of the *R* component for mipafox in Tables 2 and 3) and represents 38.3% of total activity.

EPγ, is paraoxon-resistant and sensitive to micromolar concentrations of mipafox (*E*2 in Tables 2 and 3, included in *R* in Table 1). This component represents 38.6–47.6% of activity and meets the operational criteria of being "NTE" (40 μM paraoxon-resistant and sensitive to mipafox at μM concentrations), with I_{50} (30 min) = 5.3–6.6 μM of mipafox, similarly to NTE (the membrane-bound protein) which has I_{50} (30 min) = 4.7 μM of mipafox under the historical conditions for measuring NTE (Johnson, 1982).

EPδ is the fourth enzymatic component (9.8–10.7% of activity) and is resistant to both inhibitors, and corresponds to *R* in Table 3.

The toxicological consequence of the chemical insults to EPα, EPβ and EPδ remain unknown. The kinetic characterization of these components is necessary for having criteria for monitoring during further isolation and molecular characterization studies into these organophosphorus-sensitive esterases. Further research is needed to establish the toxicological meaning of the data of this paper and the relation to neurotoxicity of organophosphorus compounds.

We suggest that the discrimination of the main esterase components in the membrane brain fraction may be performed with a simple assay using only two different mipafox concentrations: 120 nM (~I_{95} for 30 min) for the inhibition of the most sensitive component; 25 μM (~I_{95} for 30 min) for the second most sensitive component (NTE) and not using paraoxon, thus avoiding possible confusion due to their partial reactivation.

Conflict of interest statement

The authors declare that there are no conflicts of interest.

References

Barril, J., Estévez, J., Escudero, M.A., Céspedes, M.V., Ñiguez, N., Sogorb, M.A., Monroy, A., Vilanova, E., 1999. Peripheral nerve soluble esterases are spontaneously reactivated after inhibition by paraoxon: implications for a new definition of neuropathy esterase. Chem. Biol. Interact. 119–120, 541–550.

Carrington, C.D., Abou-Donia, M.B., 1985. Paraoxon reversible inhibits neurotoxic esterase. Toxicol. Appl. Pharmacol. 79, 175–178.

Carrington, C.D., Abou-Donia, M.B., 1986. Kinetics of substrate hydrolysis and inhibition by mipafox of paraoxon-preinhibited hen brain esterase activity. Biochem. J 236 (June (2)), 503–507.
Céspedes, M.V., Escudero, M.A., Barril, J., Sogorb, M.A., Vicedo, J.L., Vilanova, E., 1997. Discrimination of carboxylesterases of chicken neural tissue by inhibition with a neuropathic, non-neuropathic organophosphorus compounds and neuropathy promoter. Chem. Biol. Interact. 106, 191–200.
Chemnitius, J.M., Haselmeyer, K.H., Zech, R., 1983. Neurotoxic esterase: identification of two isoenzymes in hen brain. Arch. Toxicol. 53, 235–244.
COT Report, 1999. Organophosphates. A report of the Committee on Toxicology of Chemicals in Food, Consumer Products and the Environment. UK Department of Health, London.
Estévez, J., García-Pérez, A., Barril, J., Pellín, M.C., Vilanova, E., 2004. The inhibition of the high sensitive peripherals nerve soluble esterases by Mipafox. A new mathematical processing for the kinetics of inhibition of esterases by organophosphorus compounds. Toxicol. Lett. 151, 243–249.
Estévez, J., Vilanova, E., 2009. Model equations for the kinetics of covalent irreversible enzyme inhibition and spontaneous reactivation: esterases and organophosphorus compounds. Crit. Rev. Toxicol. 39 (5), 427–448.
Estévez, J., Barril, J., Vilanova, E., 2010. Inhibition with spontaneous reactivation and the ongoing inhibition effect of esterases by biotinylated organophosphorus compounds: S9B as a model. Chem. Biol. Interact. 187, 397–402.
Estévez, J., García-Pérez, A., Barril, J., Vilanova, E., 2011. Inhibition with spontaneous reactivation of carboxyl esterases by organophosphorus compounds: paraoxon as a model. Chem. Res. Toxicol. 2011 (24), 135–143.
García-Pérez, A.G., Barril, J., Estévez, J., Vilanova, E., 2003. Properties of phenyl valerate esterase activities from chicken serum are comparable with soluble esterases of peripheral nerves in relation with organophosphorus compounds inhibition? Toxicol. Lett. 142 (1–2), 1–10.
Jamal, G.A., Hansen, S., Julu, P.O.O., 2002. Low level exposures to organophosphorus esters may cause neurotoxicity. Toxicology 181–182, 23–33.
Johnson, M.K., 1969. The delayed neurotoxic effect of some organophosphorus compounds. Identification of the phosphorylation site as an esterase. Biochem. J. 114, 711–717.
Johnson, M.K., 1974. The primary biochemical lesion leading to the delayed neurotoxic effects of some organophosphorus esters. J. Neurochem. 23 (October (4)), 785–789.
Johnson, M.K., 1977. Improved assay of neurotoxic esterase for screening organophosphate for delayed neurotoxicity potential. Arch. Toxicol. 37, 113–115.
Johnson, M.K., 1982. The target for initiation of delayed neurotoxicity by organophosphorus esters: biochemical studies and toxicological applications. Rev. Biochem. Toxicol. 4, 141–212.
Johnson, M.K., Read, D.J., Benschop, H.P., 1985. Interaction of the four stereoisomers of soman (pinacolyl methylphosphonofluoridate) with acetylcholinesterase and neuropathy target esterase of hen brain. Biochem. Pharmacol. 34 (June (11)), 1945–1951.
Mangas, I., Vilanova, E., Estévez, J., 2011. Kinetics of the inhibitory interaction of organophosphorus neuropathy inducers and non-inducers in soluble esterases in the avian nervous system. Toxicol. Appl. Pharmacol. 256 (3), 360–368.
Middlemore-Risher, M.L., Buccafusco, J.J., Terry, A.V., 2010. Repeated exposures to low-level chlorpyrifos results in impairments in sustained attention and increased impulsivity in rats. Neurotoxicol. Teratol. 32, 415–424.
Ray, E., Richards, P.G., 2001. The potential for toxic effects of chronic, low-dose exposure to organophosphates. Toxicol. Lett., 343–351.
Sogorb, M.A., Vilanova, E., Carrera, V., 2004. Future applications of phosphotriesterases in the prophylaxis and treatment of organophosphorus insecticide and nerve agent poisonings. Toxicol. Lett. 151 (1), 219–233.
Sogorb, M.A., Vilanova, E., 2010. Detoxication of anticholinesterase pesticides. In: Satoh, T., Gupta, R.G. (Eds.), Anticholinesterase Pesticides: Metabolism, Neurotoxicity, and Epidemiology. John Willey & Sons, ISBN 978-0-470-41030-1, pp. 121–133.
Williams, D.G., Johnson, M.K., 1981. Gel electrophoretic identification of hen brain neurotoxic esterase labeled with tritiated diisopropylphosphofluridate. Biochem. J. 209, 817–829.
Winrow, C.J., Hemming, M.L., Allen, D.M., Quistad, G.B., Casida, J.E., Barlow, C., 2003. Loss of neuropathy target esterase in mice links organophosphate exposure to hyperactivity. Nat. Genet. 33 (4), 477–485.
Worek, F., Aurbek, N., Koller, M., Becker, C., Eyer, P., Thiermann, H., 2007. Kinetic analysis of reactivation and aging of human acetylcholinesterase inhibited by different phosphoramidates. Biochem. Pharmacol.
Worek, F., Thiermann, H., Szinicz, L., Eyer, P., 2004. Kinetic analysis of interactions between human acetylcholinesterase, structurally different organophosphorus compounds and oximes. Biochem. Pharmacol. 68, 2237–2248.

Chemical Research in Toxicology

Article

pubs.acs.org/crt

Phenylmethylsulfonyl Fluoride, a Potentiator of Neuropathy, Alters the Interaction of Organophosphorus Compounds with Soluble Brain Esterases

Iris Mangas,* Eugenio Vilanova, and Jorge Estévez

Unit of Toxicology and Chemical Safety, Institute of Bioengineering, University "Miguel Hernández" Elche, Alicante, Spain

ABSTRACT: Phenylmethylsulfonyl fluoride (PMSF) is a protease and esterase inhibitor that causes protection or potentiation/promotion of organophosphorus delayed neuropathy (OPIDN) depending on whether it is dosed before or after an inducer of delayed neuropathy. The molecular target of promotion has not yet been identified. Kinetic data of esterase inhibition were first obtained for PMSF with a soluble chicken brain fraction and then analyzed using a kinetic model with a multienzymatic system in which inhibition occurred with the simultaneous chemical hydrolysis of the inhibitor and ongoing inhibition (inhibition during the substrate reaction). The best fitting model was a model with resistant fraction, Eα (28%), and two sensitive enzymatic entities, Eβ (61%) and Eγ (11%), with I_{50} at 20 min of 70 and 447 μM, respectively. The estimated constant of the chemical hydrolysis of PMSF was kh = 0.23 min^{-1}. Eα, which is sensitive to mipafox and resistant to PMSF, became less sensitive to mipafox when the preparation was preincubated with PMSF. Its Eα I_{50} (30 min) of mipafox increased with the PMSF concentration used to preincubate it. Eγ is sensitive to both PMSF and mipafox, and after preincubation with PMSF, Eγ became less sensitive to mipafox and was totally resistant after preincubation with 10 μM PMSF or more. The sensitivity of Eα to paraoxon (I_{50} 30 min from 9 to 11 nM) diminished after PMSF preincubation (I_{50} 30 min 185 nM) and showed no spontaneous reactivation capacity. The nature of these interactions is unknown but might be due to covalent binding at sites other than the substrate catalytic center. Such interactions should be considered to interpret the potentiation/promotion phenomenon of PMSF and to understand the effects of multiple exposures to chemicals.

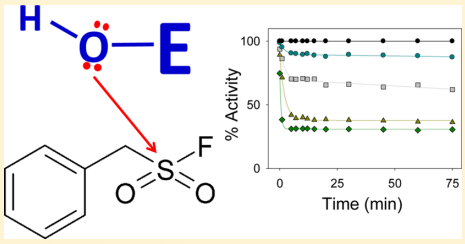

1. INTRODUCTION

Organophosphorus (OP) esters have long since been recognized as irreversible inhibitors of serine proteinases and serine esterases by virtue of their covalent reaction with the serine residue at these enzymes' active site.[1] OPs can cause different human neurotoxicity syndromes by reactions with different serine esterases, including acute cholinergic clinical episodes, the intermediate syndrome, and organophosphate-induced delayed neuropathy (OPIDN). Acute toxicity is produced by the irreversible inactivation of the cholinesterase enzyme. The molecular target for OPIDN is an enzyme in nervous tissues called neuropathy target esterase (NTE). NTE was first described in membrane chicken brain.[2] The multistep hypothesis of OPIDN is as follows: (I) organophosphate toxicants have a specificity for NTE versus AChE; (II) 70−90% of NTE inhibition is required for OPIDN;[2−5] (III) NTE is phosphorylated at the serine residue at the catalytic site; (IV) dialkylphosphoryl-NTE aging is proposed to confer it a "toxic gain of function";[6,7] (V) a toxic gain of function leads to the degeneration of axons.[8,9]

Other NTE inhibitors, such as certain carbamates, phosphinates, and sulfonyl halides like phenylmethylsulfonyl fluoride (PMSF), protect animals against OPIDN when administered before the neuropathic OP compound in vivo.[10,6] The protection relates to the fact that NTE, inhibited by these compounds, does not undergo the aging reaction. When this and other NTE inhibitors, that is, certain esterase inhibitors, including organophosphates, organophosphinates, sulfonyl halides, carbamates, and thiocarbamates,[11−13] are administered to hens, the animal of choice for OPIDN, in conjunction with OPs causing OPIDN, its neurotoxicity is enhanced. Some authors have called this effect classical toxicological potentiation,[11] while other authors have suggested calling it promotion because it is needed, an order of dose, agent induces OPIDN when it is administered to an animal that has been exposed to an initiator.[12] Some of these compounds do not cause axonopathy when administered alone, but others, at exceedingly high doses, cause very mild neuropathy, much higher than those causing the promotion of other axonopathies. Potentiation is nonspecific for the agent causing neuropathy and other toxic axonopathies (i.e., 2,5-hexanedione neuropathy),[14] and traumatic nerve lesions have been promoted by PMSF.[15,16]

The molecular target of promotion has not yet been identified. Several lines of evidence suggest that OPIDN promotion does not involve NTE, although all the promoters identified to date are NTE inhibitors.[17] Only metamidophos

Received: June 7, 2012
Published: September 25, 2012

(*O*,*S*-dimethylphosphorothiomidate) and KBR 2822 (*O*-(2-chloro-2,3,3 trifluorocyclobutyl) *O*-ethyl *S*-propyl phosphorothioate) promote OPIDN at doses causing marginal NTE inhibition.[18,19] It has been reported that given the chemical nature of the promoters, the target has to be an esterase similar to NTE and is, therefore, likely to hydrolyze the same substrate, i.e., phenyl valerate (PV), but is resistant to mipafox.[20,21] Other non-neuropathic NTE inhibitors, such as phenyl-*N*-methyl-*N*-benzyl-carbamate and phenyl-*n*-pentyl-phosphinate, *n*-butyl sulfonyl fluoride, *S*-ethyl hexahydro-1*H*-azepine-1-carbothioate (molinate), *S*-4-chlorobenzyl diethylthiocarbamate (thiobencarb), and KBR-2822, have also been found to promote OPIDN.[12,22,18,23,24] It has been suggested that the target of promotion is embraced in a fraction which has been separated by molecular exclusion chromatography of the soluble fraction from the chick sciatic nerve called peak V_0.[25,26] This fraction was first described by Escudero and co-workers in soluble esterases of the brain, spinal cord, and sciatic nerve.[26,27]

The chicken is the animal model of current use specified by regulatory agencies for the evaluation of the delayed neuropathic potential of organophosphorus esters in humans (OECD 418 and 419 testing guide). The chicken is also the classical animal model employed in OPIDN studies and in studies of the promotion of OPIDN.[12] Chicken brain is the first animal model and tissue in which NTE (the target protein of OPIDP) was found among the esterases of brain membranes.[2,10] Moreover, the in vivo promotion/potentiation effect of PMSF and other promoters has been also assayed in chicken.[11,12]

Recently, three main enzymatic components in the soluble brain fraction of chicken have been discriminated using an inducer (mipafox) and a noninducer (paraoxon) of neuropathy. Three enzymatic components were discriminated, these being Eα, Eβ, and Eγ. Eα (11−23% of activity), with an I_{50} (30 min) of 9−11nM paraoxon and 4 nM mipafox, is spontaneously reactivated after inhibition with paraoxon; Eβ (71−84% of activity), with I_{50} (30 min) of 1216 nM paraoxon, is practically resistant to mipafox; while Eγ (5−8% of activity), with I_{50} (30 min) of 3.4 μM mipafox, is paraoxon-resistant.[28] These esterases have been suggested as possible secondary targets of OPs, whose inhibition may be related to some neurotoxicological effects of OPs with nonidentified targets. Some toxic effects of OPs have been reported in experimental animals and in humans.[29−31] Quite often, these effects cannot be fully correlated with target toxicity, which indicates that they may be toxicologically relevant secondary targets.[32] The high sensitivity of Eα to paraoxon suggests that they might play a role in toxicity in the low-level long-term exposure of organophosphate compounds as they are spontaneously reactivated, only in chronic exposure may prove relevant. These esterase components may also offer a protective effect in relation to spontaneous reactivation after inhibition with some OPs, such as paraoxon and other diethyl/dimethyl phosphates, which may be considered a biodegradation reaction.[28]

In this work, the interaction (kinetic inhibition and modification of sensitivity to organophosphorus compounds) of these esterase components with a promoter of neuropathy (PMSF) is studied to elucidate the possible relationship between these enzymes and the promotion of neuropathy. The question of whether the exposure to one inhibitor to nonsensitive esterases could change the sensitivity to another is raised. A kinetic model was used to analyze the complex situation of the reaction of esterases with PMSF, where the chemical hydrolysis inhibitor and ongoing inhibition have to be considered to analyze the data.[33−35]

2. MATERIALS AND METHODS

Chemicals. Phenylmethylsulfonyl fluoride was purchased from Sigma (Madrid, Spain), diethyl *p*-nitrophenylphosphate (paraoxon, purity >99%) was obtained from Sigma (Madrid, Spain), and both *N*,*N*′-di-isopropyl phosphorodiamidefluoridate (mipafox, purity >98%) and phenyl valerate were acquired from Lark Enterprise (Webster, MA, USA).

Homogenization buffer: 50 mM Tris-HCl buffer (pH 8.0) containing 1 mM EDTA. A stock solution of 50 mM PMSF was prepared in DMSO (dimethylsulfoxide), a stock solution of 10 mM paraoxon was prepared in dried acetone, and a stock solution of 10 mM mipafox was prepared in 10 mM Tris-citrate buffer (pH 6.0). PMSF was dissolved in DMSO, while paraoxon and mipafox were dissolved in the homogenization buffer (pH 8.0) containing 10 mM EDTA immediately before the kinetic assays. A stock solution of substrate phenyl valerate (16.8 mM) was prepared in dried *N*,*N*-diethylformamide and was diluted in water to 0.54 mM immediately before the enzymatic assays. All other chemicals were of analytical reagent grades.

Tissue Preparation. Chicken brains were obtained from a commercial slaughterhouse immediately after killing the animals and were kept in cold (0−5 °C) homogenization buffer until use. They were homogenized with a Polytron homogenizer (Kinematica Gmbh, Germany) using a PTA 10S head (dispersing aggregates at 70% power (3 × 30 s) at a concentration of 200 mg fresh tissue/mL in the same buffer).

Subcellular Fractionation. The homogenized tissue was centrifuged at 1000*g* for 10 min (4 °C) to precipitate debris and nuclei. The supernatant was centrifuged at 100 000*g* for 60 min to obtain a precipitate consisting of the mitochondrial and microsomal fractions (membrane brain fraction) and a final supernatant or cytosol component (soluble brain fraction); soluble brain fractions were used for the kinetic assays. Samples were frozen in liquid nitrogen before use.

Standard Assay of Phenyl Valerate Esterase Activity (PVase) for Kinetic Studies. Enzyme assays were carried out as previously described[28] following a procedure based on the colorimetric method for the NTE assay developed by Johnson.[3] The method was modified and programmed for an automated microassay using the Biomek 2000 (Beckman) workstation as follows: in a 1-mL microtube, a 200-μLvolume of the brain fraction (at an equivalent concentration of 20 mg/mL for the soluble fraction or 15 mg/mL for the membrane fraction of the original fresh tissue) was incubated with 20 μL of inhibitor solution, (buffer in controls) at appropriate concentrations. After an inhibition time, 200 μL of substrate phenyl valerate (0.54 mM) were added and incubated for 10 min at 37 °C. The reaction was stopped by adding 200 μL of a 2% sodium dodecyl sulfate solution with 1.23 mM aminoantipyrine (the SDS-AAP solution), which was then mixed with 50 μL of 1.21 mM potassium ferricyanide and left for 10 min for color development. A 300-μL volume from each microtube was transferred to a 96-well microplate, and absorbance was read at 510 nm. Standards of phenol, blanks, and spontaneous hydrolysis controls (samples without tissue) were included with the same procedure. The results were expressed as % activity ($E/E_0 \times 100$) over the control without an inhibitor and were plotted versus time (t) or versus the inhibitor concentration.

Evaluation of Activity after Diluting the Inhibitor. High tissue-concentrated samples (200 mg/mL) were preinhibited with either 500 or 1000 μM PMSF for 30 min at 37 °C. The study of the reactivation process began at that time point by diluting the incubation mixture 10-fold with homogenization buffer. Incubation continued and 110-μL aliquots were withdrawn at different times between 0 and 180 min and were added to the tubes containing 100 μL of substrate solution to be incubated for 10 min at 37 °C. The enzymatic reaction was stopped, and color was measured as previously indicated.

Mipafox Inhibition Assays in Samples Preinhibited with PMSF. Tissue samples (containing the soluble fraction from 24 mg/mL of brain tissue) were incubated with different concentrations of PMSF: 0, 5, 10, 50, 150, or 4000 μM of PMSF for 20 min at 37 °C. Samples tissues were incubated with the hydrolyzed product of 2000 μM PMSF. PMSF at a concentration of 2000 μM, prepared in DMSO, was left to hydrolyze 40 min at 37 °C. Then, 20 μL of the mipafox solution was added to obtain a concentration of between 0 and 250 μM of mipafox and was incubated for 30 min at 37 °C. Afterward, a standard assay of phenyl valerate esterase activity (PVase) was performed.

Paraoxon Reactivation Assay of PMSF-Preinhibited Samples. Tissue samples (containing the soluble fraction from 200 mg/mL of brain tissue) were incubated with 2000 μM PMSF for 20 min at 37 °C. Then 20 μL of the paraoxon solution was added to obtain a 100 nM concentration of paraoxon and was incubated for 150 min at 37 °C. The study of the reactivation process began at that time point (170 min) of the experiment by diluting the incubation mixture 10-fold with homogenization buffer. Incubation continued, and 110-μL aliquots were withdrawn at different times up to 150 min of the dilution between 170 and 320 min of the experiment time (170, 200, 230, and 320 min), and they were added to the tubes containing 100 μL of substrate solution to be incubated for 10 min at 37 °C. Then, the enzymatic reaction was stopped, and color was measured as previously indicated.

Paraoxon Inhibition Assay in Samples Preinhibited with PMSF. Tissue samples (containing the soluble fraction from 50 mg/mL of brain tissue) were incubated with 4000 μM PMSF for 20 min at 37 °C. Then 20 μL of the paraoxon solution was added to obtain a concentration from 0 to 40 μM of paraoxon and was incubated for 30 min at 37 °C. Afterward, a standard assay of phenyl valerate esterase activity (PVase) was performed.

Mathematical Models. *Fixed-Time Inhibition Curves.* Exponential decay models were fitted to the fixed-time inhibition data of PVase activity by considering the spontaneous hydrolysis, if necessary, of one, two, or more sensitive enzymatic components, with or without a resistant fraction, in accordance with Estévez and Vilanova[34] and with Estévez et al.[36] If no chemical hydrolysis is considered, then the general model equation for inhibition is as follows:

$$E = E1_0 \cdot e^{-(k1 \cdot t \cdot I)} + E2_0 \cdot e^{-(k2 \cdot t \cdot I)} + E3_0 \cdot e^{-(k3 \cdot t \cdot I)} + \ldots + En_0 \cdot e^{-(kn \cdot t \cdot I)} + R$$

If spontaneous hydrolysis is considered, then the general model is as follows:

$$E = E1_0 \cdot e^{(e^{-kh \cdot t} - 1) \cdot k1/kh \cdot I_0} + E2_0 \cdot e^{(e^{-kh \cdot t} - 1) \cdot k2/kh \cdot I_0} + \ldots + En_0 \cdot e^{(e^{-kh \cdot t} - 1) \cdot kn/kh \cdot I_0} + R$$

Evaluation of Ongoing Inhibition during the Substrate Reaction. Exponential decay models were used to fit the data of the % of activity at the zero inhibition time versus the inhibitor concentration in the progressive inhibition experiment. The best fitting model according to the F-test was $E_0 \cdot e^{-ka' \cdot x} + R$, where parameter $k_{a'}$ represented the apparent first-order kinetic constant of inhibition observed during the substrate reaction time, and E_0 represented the % of activity of the enzymatic component affected by the ongoing inhibition effect. The model is shown in the Results section.

Time-Progressive Inhibition Data. A three-dimensional model was fitted to the data (% of activity versus t and I). The time-progressive inhibition data were analyzed with models in accordance with Estévez et al.,[35] which consider inhibition with a simultaneous hydrolysis of the inhibitor. The best fitting model according to the F-test is shown in the Results section.

The general model equation applied is

$$E = E1_0 \cdot e^{(-ka' \cdot I_0 \cdot e^{-(kh \cdot t)}) \cdot e^{(e^{-kh \cdot t} - 1) \cdot k1/kh \cdot I_0}} + E2_0 \cdot e^{(e^{-kh \cdot t} - 1) \cdot k2/kh \cdot I_0} + \ldots + En_0 \cdot e^{(e^{-kh \cdot t} - 1) \cdot kn/kh \cdot I_0} + R$$

which represents a model with n enzymatic components where the inhibitor was spontaneously hydrolyzed: E1, E2, E3, and En, which were inhibited, and R, which was a component resistant to the concentrations assayed. The models with 1, 2, or 3 sensitive-exponential components, with or without resistant components, were tested.

In all the mathematical models, $k1$, $k2$, $k3$, ..., kn were the second-order inhibition constants, kh was the inhibitor hydrolysis constant, and $E1_0$, $E2_0$, $E3_0$, ..., En_0 and R were the proportions (amplitude) of enzymatic components E1, E2, E3..., En and R, respectively. The exponential factor $e(-ka' \cdot I_0 \cdot e(kh \cdot t) - 1)$ was included to correct ongoing inhibition during the substrate reaction.[34,35]

In order to obtain a coherent solution in the interactive computing estimation, some restrictions were applied: (1) all the parameters (rate constants and amplitudes) should have positive values (>0); (2) component 1 was the most sensitive; therefore, $k1 > k2$, $k2 > k3$, $kn > k3$; (3) the following complementary restriction was also applied: $E1_0 + E2_0 + \ldots + En_0 + R = 100\%$.

The results were expressed by giving the values of the exponential kinetic constants ($M^{-1} \cdot min^{-1}$), the proportions/amplitudes of each component (% of activity), and the values of I_{50} (20 min) (concentration to achieve 50% inhibition of this component deduced from its kinetic parameters) (inhibition and hydrolysis constants).

The PMSF I_{50} (20 min) values were obtained by applying the following equation:

$$I_{50}^{20} = \ln 2 / \{(e^{(-kh \cdot 20)} - 1) \cdot ki/kh\}$$

Determination of Variability. All the experiments were done in triplicate, and each point in the data represents the mean of three replicates (SD < 5%).

The F-test was used to compare the kinetic models fitted to the data in order to identify the best fitting model using the Sigma Plot software (version 8, Systat Software Inc., Chicago, USA).

Mathematical Analysis of the Inhibition Curves. Model equations were fitted to the experimental inhibition and reactivation kinetics data by a nonlinear computerized method based on the least-squares principle using the Sigma Plot software, version 8 (Systat Software Inc., Chicago, USA), and by applying the model equations for a system with several enzymatic components, as described by Estévez and Vilanova.[33,35]

3. RESULTS

PMSF Inhibition Curves. *Fixed-Time Inhibition Curve.* PMSF was incubated with a chicken brain soluble fraction for 30 min at 37 °C (Figure 1). Exponential decay models with the

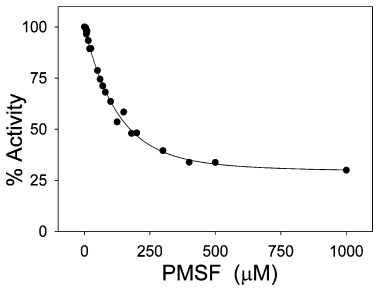

Figure 1. PMSF fixed-time inhibition curve of esterase activity at 30 min of inhibition in a soluble brain fraction. Enzyme preparations were incubated with PMSF concentrations in the range of 0−1000 μM for 30 min at 37 °C, and residual activity was assayed as described in Materials and Methods. Curves showed the best fits according to the F-test (two exponential components, plus a resistant one, including the spontaneous hydrolysis of PMSF). Each point represents the mean of three replicates (SD < 5%).

dx.doi.org/10.1021/tx300257p | Chem. Res. Toxicol. 2012, 25, 2393−2401

Table 1. Inhibition by PMSF of Soluble Esterases of the Brain[a]

	r^2	E1 (%)	$ka(\mu M^{-1})$	kh (min^{-1})	$k1$ ($\mu M^{-1}\cdot min^{-1}$)	I_{50}^{20} (μM)	E2 (%)	$k2$ ($\mu M^{-1}\cdot min^{-1}$)	I_{50}^{20} (μM)	R (%)
(A) fixed-time inhibition	0.9970	61		0.18	0.0015	84	10	0.00040	315	29
(B) 3D fitting of time progressive inhibition	0.9983	61	0.0005	0.23	0.0023	70	11	0.00036	447	28
correspond to the component according to Mangas et al.[28]	Eβ						Eγ			Eα

[a]Kinetic constants ($k1$, $k2$, kh, and ka) and proportions of the esterase components obtained from inhibition experiments with PMSF (E1, E2, and R). The I_{50} (20 min) values were calculated from the kinetic constants for each component.

spontaneous hydrolysis of the inhibitor were fitted to the fixed-time inhibition data of PVase activity with one, two, or more sensitive enzymatic components, with or without a resistant fraction, according to the Materials and Methods section.[35] The best fitting model (according to the F-test) was a model of two sensitive components of 61% and 10% with I_{50} (20 min) of 84 μM and 315 μM, respectively, and a resistant component of 29%. The estimated hydrolysis constant (kh) of PMSF was 0.18 min^{-1} (Table 1, line A).

Evaluation of Activity after Diluting the Inhibitor. PMSF at 500 μM or 1000 μM was incubated with the chicken brain soluble fraction for 30 min at 37 °C. Five hundred micromolar inhibited only the most sensitive component, and 1000 μM inhibited all of the sensitive PVase activity detected previously. Then, samples were diluted to 50 μM and 100 μM of the residual PMSF concentration, respectively. After diluting, activity remained inhibited over time (180 min) from 34.1% to 33.4% for the fractions inhibited with 50 μM and from 28.0% to 28.4% for those inhibited with 1000 μM (see Figure 2). We

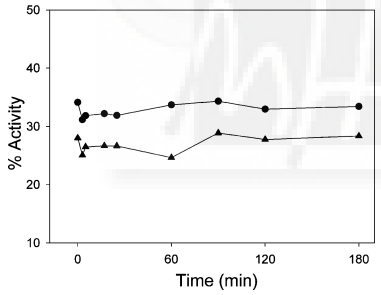

Figure 2. Spontaneous reactivation after inhibition by PMSF. Two concentrated preparations (200 mg/mL) were inhibited by preincubation with 500 μM (●) and 1000 μM (▲) of PMSF, respectively, for 20 min at 37 °C. Then the mixture was diluted 10-fold with homogenization buffer to be then incubated for 0, 4, 8, 22, 36, 50, 65, 90, 120, or 180 min at 37 °C.

consider that there was no significant spontaneous reactivation after inhibition with PMSF for any of the sensitive components during the experiment time (180 min). Therefore, spontaneous reactivation was not considered in the model equations for the inhibition kinetics with PMSF.

Time-Progressive Inhibition Curves by PMSF. Figure 3A shows the inhibition curves of a chicken brain soluble fraction with PMSF (0, 20, 70, 300, and 1000 μM) for times of up to 75 min at 37 °C. The kinetic analysis for the inhibition of brain esterase activity with PMSF resulted in a time-progressive inhibition of around 72% of activity, which is consistent with covalent irreversible inhibition.

Evaluation of Ongoing Inhibition during the Substrate Reaction. The data extrapolated to the zero inhibition time

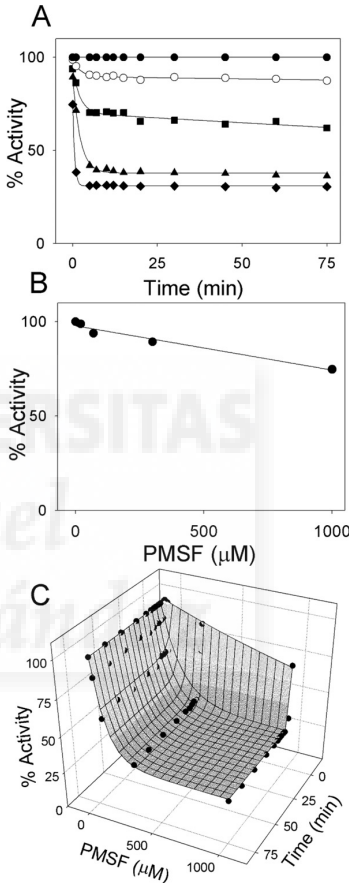

Figure 3. Kinetics of the time-progressive inhibition by PMSF in a soluble brain fraction. A preparation containing the soluble fraction of 20 mg fresh tissue/mL was preincubated with 0, 20, 70, 300, and 1000 μM PMSF (upper to lower plots, plots in panel A) for the indicated time at 37 °C. Then enzymatic activity was assayed with phenyl valerate for 10 min. Panel A shows the best fitting model equation for the individual curve for each concentration. Panel B reveals inhibition at the reaction time with the substrate (0 min inhibition time). Panel C provides the inhibitory surface obtained by fitting the 3D model equation to the data. The surface reflects the result of the best fitting model according to the F-test. Each point represents the mean of two replicates (SD <5%).

(Figure 3B) indicate that ongoing inhibition during substrate incubation was significant under the assayed conditions. Therefore, ongoing inhibition during substrate incubation needs to be considered in the models.[34,35] Approximately 25% of the activity was inhibited during the substrate

dx.doi.org/10.1021/tx300257p | *Chem. Res. Toxicol.* 2012, 25, 2393–2401

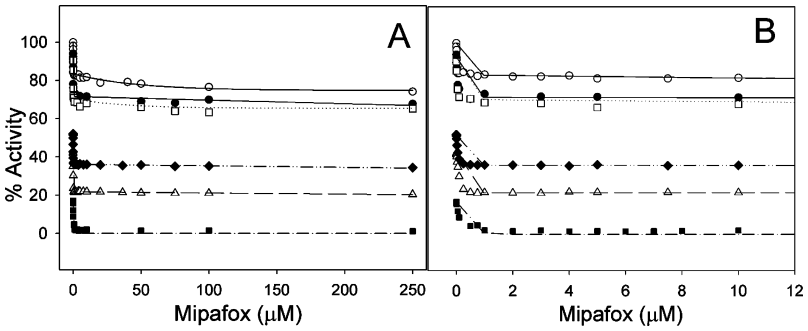

Figure 4. Mipafox fixed-time inhibition curves of PMSF-preinhibited esterase activity at 30 min of inhibition. Enzyme preparations were preincubated with PMSF 0, 5, 10, 50, 150, and 4000 μM (upper to lower plots) for 20 min at 37 °C. Then preinhibited samples were incubated with mipafox at concentrations in the range of 0 to 250 μM for 30 min at 37 °C, and residual activity was assayed (panel A). Panel B is a close-up view of panel A; mipafox ranges from 0 to 12 μM. Curves were fitted with exponential model equations by selecting the best fitting equation according to the F-test. Each point represents the mean of three replicates (SD < 5%).

Table 2. Inhibition by Mipafox of Soluble Esterases of the Brain Pre-Inhibited with PMSF

preincubation (20 min)	total activity after preincubation (%)	Eα (%)	$k\alpha$ ($nM^{-1}\cdot min^{-1}$)	I_{50} (nM)	Eγ (%)	$k\gamma$ ($nM^{-1}\cdot min^{-1}$)	I_{50} (nM)	resistant[a] (%)
buffer	**100**	**21**	**0.00600**	**4**	**8**	**3.0×10^{-6}**	**7,701**	**71**
5 μM PMSF								
expected[a]	*(96)*	*(21)*			*(8)*			*(67)*
observed	93	22	0.00090	26	5	9.0×10^{-7}	25,672	66
10 μM PMSF								
expected[a]	*(93)*	*(21)*			*(8)*			*(64)*
observed	93	21	0.00070	31	0			72
50 μM PMSF								
expected[a]	*(70)*	21			*(7)*			*(42)*
observed	52	16	0,00054	43	0			36
150 μM PMSF								
expected[a]	*(42)*	*(21)*			*(6)*			*(15)*
observed	43	22	0,00031	72	0			21
4000 μM PMSF								
expected[a]	*(21)*	*(21)*			*(0)*			0
observed	17	17	0,00001	222	0			0
hydrolysis product + DMSO								
expected[a]	*(100)*	*(21)*			*(8)*			*(71)*
observed	100	16	0.00200	12	5	3.0×10^{-6}	7,701	79

[a]For Eα or Eγ, as expected, the estimated residual activity of the Eα or Eγ component after preincubation with the indicated PMSF concentration is shown by considering the kinetic parameters of PMSF inhibition in Table 1 and by assuming that preincubation does not affect the behavior with mipafox. In the resistant column, the expected data are the expected estimated value of the Eβ component (resistant to mipafox) after preincubation with the indicated PMSF concentration; however, the observed value may be the residual Eβ, plus the proportion of the Eγ fraction, which might become resistant as a result of preincubation.

incubation time for the highest inhibitor concentration. Data were fitted to the exponential decay models. The best fitting model according to the F-test was $E_0 \cdot e^{-ka \cdot x} + R$. This justifies that the ongoing inhibition factor should be taken into account only for the most sensitive enzymatic component.

Parameter *ka* was 0.0006 μM^{-1}, which represents the apparent first-order kinetic constants of the inhibition observed during the substrate reaction time for the first sensitive component. These constants have to be considered operational empiric constants and not real kinetic constants.[34,35]

Tridimensional Fitting of the Time-Progressive Inhibition Curves by PMSF by Considering Ongoing Inhibition and the Simultaneous Spontaneous Hydrolysis of PMSF. A three-dimensional model (% of activity versus *t* and I), which considered inhibition with the simultaneous hydrolysis of PMSF, and the ongoing inhibition effect were fitted to the data described in Figure 3A with one, two, or more enzymatic components.[35]

The best fitting model (according to the F-test) was a model of two sensitive enzymatic entities and a resistant one according to the Materials and Methods section, where the most sensitive one was affected by the ongoing inhibition effect. The kinetic parameters are shown in Table 1 (line B), and the deduced 3D surface is plotted in Figure 3C.

According to both components and estimated amplitudes, E1 correlated with component Eβ, E2 correlated with component Eγ, and R correlated with component Eα, which were discriminated with paraoxon and mipafox.[28]

Mipafox Inhibition Assays of PMSF-Preinhibited Soluble PVase Activity. Figure 4 shows the mipafox fixed-time

dx.doi.org/10.1021/tx300257p | *Chem. Res. Toxicol.* 2012, 25, 2393–2401

inhibition data of residual activity after preinhibition with 0, 1, 10, 50, 150, or 4000 μM PMSF for 20 min.

A sample was incubated with the chemical hydrolysis product of 2000 μM PMSF for 40 min at 37 °C (the hydrolysis product + DMSO in Table 2). Exponential decay models were fitted to the inhibition data with one, two, or more sensitive components, with or without a resistant component.

Table 2 shows the resistant activity to the PMSF concentrations used and the kinetic parameters of the best fitting model of the mipafox inhibition curves for each experiment (the resistant column). The best fitting models (according to the F-test) in the soluble fraction preinhibited with 0 and 5 μM of PMSF were the models with two sensitive enzymatic entities and a resistant one. The best fitting model (according to the F-test) in the soluble fraction preinhibited with 10, 50, and 150 μM consisted of one sensitive enzymatic entity and a resistant one. The best fitting model (according to the F-test) in the soluble fraction preinhibited with 4000 μM consisted of one sensitive enzymatic entity.

Paraoxon Reactivation Assay of PMSF-Resistant Soluble PVase Activity. The PMSF 2000 μM-resistant fraction (21% of total phenyl valerate esterase activity) was inhibited with 100 nM paraoxon for up to 150 min at 37 °C. Residual activity was 10%. Then, samples were diluted 15-fold to around 6 nM of the paraoxon residual concentration and were incubated at 37 °C for 150 min. The activity remained inhibited over time to around 8−10% of activity, suggesting that there was no spontaneous reactivation of the resistant PMSF esterase activity after inhibition with paraoxon.

Paraoxon Fixed-Time Inhibition Assay of PMSF-Resistant Soluble PVase Activity. Figure 5 shows the paraoxon fixed-time inhibition data of the 4000 μM PMSF-resistant fraction. The resistant activity to PMSF was 18%. Exponential decay models were fitted to the paraoxon inhibition data with one, two, or more sensitive components, with or without a resistant component. The best fitting model (according to the F-test) was a model with one sensitive component, 18% of esterase activity, and with an estimated I_{50} (30 min) of 185 nM ($k1$ = $1.2{\cdot}10^{-4}$ nM^{-1}/min^{-1}).

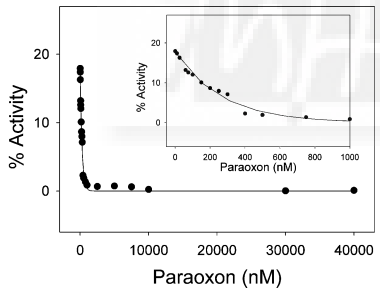

Figure 5. Paraoxon fixed-time inhibition curve of the PMSF-preinhibited esterase activity at 30 min of inhibition. Enzyme preparations were preincubated with PMSF 4000 μM for 20 min at 37 °C. Then, preinhibited samples were incubated with paraoxon at concentrations in the range of 0 to 40 μM for 30 min at 37 °C, and enzymatic activity was assayed. One exponential component model was the best fit according to the F-test. The inset shows the zoomed graph from 0 to 1000 nM paraoxon. Each point represents the mean of three replicates (SD < 5%).

4. DISCUSSION

PMSF is a protease and serine esterase inhibitor that causes both protection and potentiation of organophosphorus-induced delayed neuropathy,[12] for which the molecular target has not yet been identified. There is sufficient evidence to indicate that the molecular target for the aforementioned potentiation/promotion of neuropathy is not membrane-bound protein NTE.[36,37] This promotion/potentiation phenomenon may be significant for our understanding of the potential neurotoxicological consequences of exposure to environmental pollutants that are not considered neurotoxicants. This article provides evidence that micromolar concentrations of PMSF are able to inhibit about 72% of the total soluble phenyl valerate esterases in chicken brain in a time-progressive manner, suggesting covalent irreversible binding by sulfonylation (Figure 3A). The chicken brain was chosen because it is the animal model used for testing and predicting organophosphorus-induced delayed neuropathy in humans (OECD 418 and 419 testing guide), it is the classical animal model employed in OPIDN studies, and the first animal model and tissue in which NTE (the target protein of OPIDN) was found among esterases of the brain membranes.[37,38]

Kinetic Behavior of PMSF with Brain Soluble Esterases. PMSF is spontaneously hydrolyzed in Tris pH 8.0 solutions[39] and in biological preparations.[35] Hence, a kinetic model that considers inhibition and the spontaneous hydrolysis of inhibitors is required to analyze the data of fixed-time and time-progressive experiments.[35] No spontaneous reactivation is observed in the reactivation after the diluting experiment (Figure 2), and spontaneous reactivation is not considered in the mathematical modeling in the fixed-time and time-progressive experiments. The kinetic curves in Figure 3A tend to reach a plateau, and the chemical hydrolysis is the cause of the apparent steady states reached at inhibition times of around 15 min. The 3D fit enables all the data in the same fit to be included simultaneously, and it proves to be the best tool to fit inhibition data in this complex model. The estimated amplitudes (proportion) and inhibition constants are similar in both fixed-time and progressive inhibition experiments (see Table 1). The ongoing inhibition apparent constant (ka') estimated from the data at the zero time of the time-progressive inhibition experiment (Figure 3B) is similar to the ka' obtained in the 3D fit in time-progressive inhibition experiments (Figure 3C). Moreover, the estimated spontaneous hydrolysis constant is similar in all the inhibition experiments, 0.16, 0.23 min^{-1} (see Table 1). This kh is comparable to the kh estimated in kinetic studies in soluble peripheral nerves (0.09−0.13 min^{-1}[35]) and with the deduced chemical hydrolysis constant (0.0198 min^{-1} at 25 °C).[39] The higher temperature (37 °C) in the assay conditions, as well as a possible enzymatic hydrolysis and/or binding to not only other esterases or proteins (such as proteases) but also to other biochemical components in the solution, may increase the global hydrolysis PMSF rate in biological preparations. All these observations may be considered an internal validation of the consistency of the results and the applied kinetic models.

Enzymatic Components Discriminated with PMSF. Three enzymatic entities were detected: E1 (61% of activity) with I_{50} (20 min) = 70 μM, displaying ongoing inhibition; E2 (11%) with I_{50} (20 min) = 447 μM, showing progressive inhibition; and R (28%), which is practically resistant to PMSF inhibition (see Table 1C).

Recently, three enzymatic components in the soluble fraction have been discriminated according to their sensitivity to mipafox and paraoxon: Eα (11−23% of activity) with I_{50} (30 min) of 9−11nM paraoxon and 4 nM mipafox, which is spontaneously reactivated after inhibition with paraoxon; Eβ (71−84% of activity) with I_{50} (30 min) of 1216 nM paraoxon and is practically resistant to mipafox; and Eγ (5−8% of activity), with I_{50} (30 min) of 3.4 μM mipafox, which is paraoxon-resistant.[28] The amplitudes of the components detected with PMSF are similar to those recently discriminated with mipafox and paraoxon, and can be considered an external validation of the quality of fit.[33−35] This observation allows the identification of PMSF-sensitive components with those discriminated with mipafox and paraoxon. According to the estimated amplitudes of the components in the inhibition experiments with PMSF, E1 correlates with Eβ, E2 correlates with Eγ, and R correlates with Eα, as shown in Table 3.

Table 3. Discrimination of Three Esterase Enzymatic Components in a Soluble Brain Fraction by Considering PMSF, Mipafox, and Paraoxon Interactions[a]

component	amplitude (%)	PARAXON I50 (30 min) (sensitivity)	MIPAFOX I50 (30 min) (sensitivity)	PMSF I50 (20 min) (sensitivity)
Eα	11−28%	9−11 nM (+++) (r)	4 nM (+++)	(−)
Eβ	61−84%	1216 nM (++)	(−)	70 μM (++)
Eγ	5−11%	(−)	3398 nM (+)	447 μM (++)

[a]By globally considering all the data, three enzymatic components were discriminated according to sensitivity to PMSF, paraoxon, and mipafox, as follows: Eα, which is very sensitive to paraoxon and to mipafox, spontaneously reactivates after inhibition with paraoxon and is resistant to PMSF inhibition. Eβ, which is sensitive to paraoxon and PMSF and is resistant to mipafox; Eγ, which is sensitive to mipafox and PMSF and is resistant to paraoxon. The I_{50} (30 min) values are indicated with the proportion of the component in parentheses (%) and are classified as very sensitive (+++), sensitive (++)/(+), and resistant (−). The paraoxon and mipafox data from the data in Mangas et al.[28].

These discriminated sensitive enzymatic entities might play a role in the promotion of OPIDN and require further research. With the results presented in this work, we have obtained the appropriate criteria to monitor the isolation of PMSF-sensitive esterases for their further molecular identification and for more robust toxicological studies in order to understand their toxicological involvement by in vivo and in vitro studies.

Effects of Preincubation with PMSF on Mipafox and Paraoxon Sensitivity. The instability of PMSF is an advantage when it is used in sequential assays as all the PMSF disappears from the medium in around 15 min without disturbing further studies. The partial preincubation with PMSF of the soluble fraction affects sensitivity to mipafox of the residual activity of components Eα and Eγ (Table 2). Eα, which is sensitive to mipafox and is resistant to PMSF, becomes less sensitive to mipafox when the preparation is preincubated with PMSF. The I_{50} (30 min) of mipafox increases with the PMSF concentration during preincubation (Table 2). Eγ is sensitive to both PMSF and mipafox, and the residual activity of Eγ after preincubation with PMSF becomes less sensitive after preincubation with 5 μM PMSF and is totally resistant to mipafox after preincubation with 10 μM PMSF or more. Eβ is sensitive to PMSF but is resistant to mipafox, while the residual activity remains resistant to mipafox after preincubation with PMSF. The proportion of the resistant component (R) to mipafox inhibition observed in Table 2 changes when an increased PMSF concentration is used during preincubation. R is Eβ at 0 μM of the preinhibition with PMSF. The observed R value is the proportion of Eβ not inhibited at 5 μM in the preincubation with PMSF. At higher PMSF concentrations, the observed R value is the addition of the non-PMSF-inhibited fraction of Eβ and the non-PMSF-inhibited fraction of Eγ, which becomes resistant to mipafox.

Furthermore, the sensitivity of Eα to paraoxon diminishes after the preincubation with 2000 μM PMSF by changing paraoxon I_{50} (30 min) from 9 to 11 nM to 185 nM, while the spontaneous reactivation capacity previously observed in this component is not shown for PMSF-preincubated Eα.[28] The observed alterations by preincubation with PMSF do not seem to be related with the degradation products of PMSF as the hydrolyzed product of PMSF and DMSO does not affect the activity of and sensitivity to mipafox of any component (Table 2).

Preinhibition with PMSF does not seem to significantly alter the reaction with the substrate because the estimated proportions of the components do not alter. It could be hypothesized that PMSF can interact at other sites other than the substrate center of soluble brain esterases and that it can alter not only the inhibition of Eα and Eγ with mipafox but also the inhibition and spontaneous reactivation of Eα with paraoxon.

Conclusions. This article provides evidence that about 72% of the total soluble phenyl valerate esterases in chicken brain can be inhibited by PMSF in a time-progressive manner, suggesting covalent irreversible binding by sulfonylation. Three enzymatic components have been discriminated for their sensitivity to PMSF, which have been correlated with components Eα, Eβ, and Eγ, which, in turn, have been previously described for inhibition with paraoxon and/or with mipafox (Table 3).

PMSF can interact with Eα and Eγ at a concentration that does not inhibit but which strongly modifies its sensitivity to other esterase inhibitors. For example, Eα becomes 6-fold more resistant after the preincubation with 5 μM PMSF and more than 50-fold more resistant after the preincubation with 4000 μM PMSF. Eγ is around 4-fold more resistant to mipafox after preincubation with 5 μM PMSF and becomes totally resistant after preincubation with 10 μM PMSF or more.

This effect might be due to the interaction of PMSF at sites other than the substrate catalytic center, which is inhibited by mipafox and/or paraoxon, and merits further research. Such interactions should be considered to interpret the potentiation/promotion phenomenon of PMSF and to understand the effects of multiple exposures to chemicals.

AUTHOR INFORMATION

Corresponding Author

*E-mail: imangas@umh.es.

Funding

This work was supported by institutional funds.

Notes

The authors declare no competing financial interest.

ABBREVIATIONS

AChE, acetyl cholinesterase; DMSO, dimethylsulfoxide; EDTA, ethylenediaminetetraacetic acid; NTE, neuropathy target esterase; OECD, Organisation for Economic Cooperation and Development; OP, organophosphorus; PV, phenyl valerate; PMSF, phenylmethylsulfonyl fluoride; OPIDN, promotion of organophosphate-induced delayed neuropathy

REFERENCES

(1) Aldridge, N. W. (1993) The esterases: perspectives and problems. *Chem.-Biol. Interact. 87* (1−3), 463−436.

(2) Johnson, M. K. (1969) The delayed neurotoxic effect of some organophosphorus compounds. Identification of the phosphorylation site as an esterase. *Biochem. J. 114*, 711−717.

(3) Johnson, M. K. (1977) Improved assay of neurotoxic esterase for screening organophosphates for delayed neurotoxicity potential. *Arch. Toxicol. 37*, 113−115.

(4) Johnson, M. K. (1990) Organophosphates and delayed neuropathy-is NTE alive and well? *Toxicol. Appl. Pharmacol. 102* (3), 385−399.

(5) Glynn, P. (2000) Neural development and neurodegeneration: two faces of neuropathy target esterase. *Prog. Neurobiol. 61* (1), 61−74.

(6) Johnson, M. K. (1974) The primary biochemical lesion leading to the delayed neurotoxic effects of some organophosphorus esters. *J. Neurochem. 23*, 785−789.

(7) Johnson, M. K., and Glynn, P. (2001) Neuropathy Target Esterase. In *Handbook of Pesticide Toxicology* (Kriegher, R. I., Ed.) Vol. *2*, pp 953−965, Academic Press, San Diego, CA.

(8) Glynn, P. (1999) Neuropathy target esterase. *Biochem. J. 344* (Pt 3), 625−31.

(9) Winrow, C. J., Hemming, M. L., Allen, D. M., Quistad, G. B., Casida, J. E., and Barlow, C. (2003) Loss of neuropathy target esterase in mice links organophosphate exposure to hyperactivity. *Nat. Genet. 33* (4), 477−485.

(10) Johnson, M. K., and Lauwerys, R. (1969) Protection by some carbamates against the delayed neurotoxic effects of di-isopropyl phosphorofluoridate. *Nature 222* (5198), 1066−1067.

(11) Pope, C. N., and Padilla, S. (1990) Potentiation of organophosphorus-induced delayed neurotoxicity by phenylmethylsulfonyl fluoride. *J. Toxicol. Environ. Health 31*, 261−273.

(12) Lotti, M., Caroldi, S., Capodicasa, E., and Moretto, A. (1991) Promotion of organophosphate-induced delayed polyneuropathy by phenylmethanesulfonyl fluoride. *Toxicol. Appl. Pharmacol. 108*, 234−241.

(13) Lotti, M., Moretto, A., Bertolazzi, M., Peraica, M., and Fioroni, F. (1995) Organophosphate polyneuropathy and neuropathy target esterase: studies with methamidophos and its resolved optical isomers. *Arch. Toxicol. 69* (5), 330−336.

(14) Moretto, A., Bertolazzi, M., Capodicasa, E., Peraica, M., Richardson, R. J., Scapellato, M. L., and Lotti, M. (1992) Phenylmethanesulfonyl fluoride elicits and intensifies the clinical expression of neuropathic insults. *Arch. Toxicol. 66* (1), 67−72.

(15) Moretto, A., Capodicasa, E., Peraica, M., and Lotti, M. (1993) Phenylmethanesulfonyl fluoride delays the recovery from crush of peripheral nerves in hens. *Chem.-Biol. Interact. 87* (1−3), 457−462.

(16) Peraica, M., Capodicasa, E., Moretto, A., and Lotti, M. (1993) Organophosphate polyneuropathy in chicks. *Biochem. Pharmacol. 45* (1), 131−135.

(17) Lotti, M. (2002) Promotion of organophosphate induced delayed polyneuropathy by certain esterase inhibitors. *Toxicology 181−182*, 245−248.

(18) Moretto, A., Bertolazzi, M., and Lotti, M. (1994) The phosphorothioic acid O-(2-chloro-2,3,3-trifluorocyclobutyl) O-ethyl S-propyl ester exacerbates organophosphate polyneuropathy without inhibition of neuropathy target esterase. *Toxicol. Appl. Pharmacol. 129* (1), 133−137.

(19) Lotti, M., Moretto, A., Bertolazzi, M., Peraica, M., and Fioroni, F. (1995) Organophosphate polyneuropathy and neuropathy target esterase: studies with methamidophos and its resolved optical isomers. *Arch. Toxicol. 69* (5), 330−336.

(20) Aldridge, N. (1993) Postscript to the symposium on organophosphorus compound induced delayed neuropathy. V. *Chem.-Biol. Interact. 87* (1−3), 463−466.

(21) Céspedes, M. V., Escudero, M. A., Barril, J., Sogorb, M. A., Vicedo, J. L., and Vilanova, E. (1997) Discrimination of carboxylesterases of chicken neural tissue by inhibition with a neuropathic, non-neuropathic organophosphorus compounds and neuropathy promoter. *Chem.-Biol. Interact. 106*, 191−200.

(22) Johnson, M. K., and Read, D. J. (1993) Prophylaxis against and promotion of organophosphate-induced delayed neuropathy by phenyl di-n-pentylphosphinate. *Chem.-Biol. Interact 87* (1−3), 449−455.

(23) Osman, K. A., Moretto, A., and Lotti, M. (1996) Sulfonyl fluorides and the promotion of diisopropyl fluorophosphate neuropathy. *Fundam. Appl. Toxicol. 33* (2), 294−297.

(24) Moretto, A. (2000) Promoters and promotion of axonopathies. *Toxicol. Lett. 112−113*, 17−21.

(25) Gambalunga, A., Pasqualato, F., and Lotti, M. (2010) Soluble phenyl valerate esterases of hen sciatic nerve and the potentiation of organophosphate induced delayed polyneuropathy. *Chem.-Biol. Interact. 187* (1−3), 340−343.

(26) Escudero, M. A., Barril, J., Tormo, N., and Vilanova, E. (1995) Separation of two forms of neuropathy target esterase in the soluble fraction of the hen sciatic nerve. *Chem.-Biol. Interact. 97* (3), 247−255.

(27) Escudero, M. A., Céspedes, M. V., and Vilanova, E. (1997) Chromatographic discrimination of soluble neuropathy target esterase isoenzimes and related phenyl valerate esterases from chicken brain, spinal cord, and sciatic nerve. *J. Neurochem. 68* (5), 2170−2176.

(28) Mangas, I., Vilanova, E., and Estévez, J. (2011) Kinetics of the inhibitory interaction of organophosphorus neuropathy inducers and non-inducers in soluble esterases in the avian nervous system. *Toxicol. Appl. Pharmacol. 256* (3), 360−368.

(29) Ray, D. E., and Richards, P. G. (2001) The potential for toxic effects of chronic, low-dose exposure to organophosphates. *Toxicol. Lett.*, 343−351.

(30) Jamal., G. A., Hansen, S., and Julu, P. O. O. (2002) Low level exposures to organophosphorus esters may cause neurotoxicity. *Toxicology 181−182*, 23−33.

(31) Middlemore −Risher, M. L., Buccafusco, J. J., and Terry, A. V. (2010) Repeated exposures to low-level chlorpyrifos results in impairments in sustained attention and increased impulsivity in rats. *Neurotoxicol. Teratol. 32*, 415−424.

(32) Nomura, D. K., and Casida, J. E. (2011) Activity-based protein profiling of organophosphorus and thiocarbamate pesticides reveals multiple serine hydrolase targets in mouse brain. *J. Agric. Food Chem. 59* (7), 2808−2815.

(33) Estévez, J., and Vilanova, E. (2009) Model equations for the kinetics of covalent irreversible enzyme inhibition and spontaneous reactivation: Esterases and organophosphorus compounds. *Crit. Rev. Toxicol. 39* (5), 427−448.

(34) Estévez, J., Barril, J., and Vilanova, E. (2010) Inhibition with spontaneous reactivation and the "ongoing inhibition" effect of esterases by biotinylated organophosphorus compounds: S9B as a model. *Chem.-Biol. Interact. 187* (1−3), 397−402.

(35) Estévez, J., Barril, J., and Vilanova, E. (2012) Kinetics of inhibition of soluble peripheral nerve esterases by PMSF: a non-stable compound that potentiates the organophosphorus-induced delayed neurotoxicity. *Arch. Toxicol. 86*, 767−777.

(36) Milatovic, D., Moretto, A., Osman, K. A., and Lotti, M. (1997) Phenyl valerate esterases other than neuropathy target esterase and the promotion of organophosphate polyneuropathy. *Chem. Res. Toxicol. 10*, 1045−1048.

(37) Johnson, M. K. (1982) The target for initiation of delayed neurotoxicity by organophosphorus esters: biochemical studies and toxicological applications. *Rev. Biochem. Toxicol. 4*, 141−212.

(38) Williams, D. G., and Johnson, M. K. (1981) Gel electrophoretic identification of hen brain neurotoxic esterase labeled with tritiated diisopropylphosphofluridate. *Biochem. J. 199* (2), 323−333.

(39) James, G. T. (1978) Inactivation of the protease inhibitor phenylmethylsulfonyl fluoride in buffers. *Anal. Biochem. 86* (2), 574–579.

UNIVERSITAS
Miguel
Hernández

Arch Toxicol
DOI 10.1007/s00204-013-1135-0

MOLECULAR TOXICOLOGY

Kinetic interactions of a neuropathy potentiator (phenylmethylsulfonyl fluoride) with the neuropathy target esterase and other membrane bound esterases

Iris Mangas · Eugenio Vilanova · Jorge Estévez

Received: 4 June 2013 / Accepted: 12 September 2013

Abstract Phenylmethylsulfonyl fluoride (PMSF) is a protease and esterase inhibitor that causes protection, or potentiation/"promotion," of organophosphorus delayed neuropathy (OPIDN), depending on whether it is dosed before or after an inducer of delayed neuropathy, such as mipafox. The molecular target of the potentiation/promotion of OPIDN has not yet been identified. The kinetic data of phenyl valerate esterase inhibition by PMSF were obtained with membrane chicken brain fractions, the animal model and tissue in which neuropathy target esterase (NTE) was first described. Data were analyzed using a kinetic model with a multienzymatic system in which inhibition, simultaneous chemical hydrolysis of the inhibitor and "ongoing inhibition" (inhibition during the substrate reaction) were considered. Three main esterase components were discriminated: two sensitive enzymatic entities representing 44 and 41 %, with I_{50} (20 min) of 35 and 198 μM at 37 °C, respectively, and a resistant fraction of 15 % of activity. The estimated constant of the chemical hydrolysis of PMSF was also calculated (kh = 0.28 min^{-1}). Four esterase components were globally identified considering also previously data with paraoxon and mipafox: EPα (4–8 %), highly sensitive to paraoxon and mipafox, spontaneously reactivates after inhibition with paraoxon, and resistant to PMSF; EPβ (38–41 %), sensitive to paraoxon and PMSF, but practically resistant to mipafox, this esterase component has the kinetic characteristics expected for the PMSF potentiator target, even though paraoxon cannot be a potentiator in vivo due to high AChE inhibition; EPγ (NTE) (39–48 %), paraoxon-resistant and sensitive to the micromolar concentration of mipafox and PMSF; and EPδ (10 %), resistant to all the inhibitors assayed. This kinetic characterization study is needed for further isolation and molecular characterization studies, and these PMSF phenyl valerate esterase components will have to be considered in further studies of OPIDN promotion. A simple test for monitoring the four esterase components is proposed.

Keywords Phenylmethylsulfonyl fluoride (PMSF) · Promotion of OPIDN · Potentiation of OPIDN · Organophosphate-induced delayed neuropathy (OPIDN) · Organophosphate-induced delayed polyneuropathy (OPIDP) · Serine esterases · Brain · Neuropathy target esterase (NTE) · Organophosphorus compounds

Abbreviations

AChE	Acetylcholinesterase
DMSO	Dimethylsulfoxide
EDTA	Ethylenediaminetetraacetic acid
NTE	Neuropathy target esterase
OECD	Organization for economic cooperation and development
OP	Organophosphorus compounds
PV	Phenyl valerate
PMSF	Phenylmethylsulfonyl fluoride
OPIDN	Organophosphate-induced delayed neuropathy

Introduction

Phenylmethylsulfonyl fluoride (PMSF) is a protease and esterase inhibitor that causes protection, or potentiation/"promotion," of organophosphorus-induced

I. Mangas (✉) · E. Vilanova · J. Estévez
Unit of Toxicology and Chemical Safety, Institute of Bioengineering, University "Miguel Hernández", Elche, Alicante, Spain
e-mail: imangas@umh.es

Published online: 27 September 2013

delayed neuropathy (OPIDN) if dosed either before or after an organophosphorus (OP) inducer. OPIDN is a central-peripheral axonopathy caused by certain OP esters in sensitive species, including humans, characterized by the degeneration of some long axons in the central and peripheral nervous system.

The molecular target for OPIDN is considered a protein in nervous tissues showing esterase activity and called neuropathy target esterase (NTE), which is organophosphorylated by some organophosphates. Inhibition (phosphorylation) is not enough to induce neuropathy. Only those OP esters capable of causing the modification induced by the so-called aging reaction (dealkylation of the phosphoryl-enzyme) are neuropathy inducers, except for some phosphoramidates that are able to induce neuropathy without the aging reaction (Vilanova et al. 1987; Johnson et al. 1989, 1991).

NTE is operationally monitored as that esterase activity that hydrolyzes the artificial substrate phenyl valerate (PV), which is resistant to the non-neuropathic OP ester paraoxon (40 μM, 20 min, pH 8.0) and sensitive to the neuropathic OP ester mipafox (50 μM) (Johnson 1977; 1974). NTE is thought to be involved in maintaining the nervous system in adults (Glynn 2000) and is related with lipid homeostasis by catalyzing mainly the deacylation of phosphatidylcholine to glycerophosphocholine (Quistad et al. 2003; Quistad and Casida. 2004). Recently, it has been shown that genomic silencing of the gene encoding NTE or chemical inactivation of NTE activity in mice causes axonal damage and leads to the accumulation of phosphatidylcholine (Read et al. 2009). However, the impairment of the enzymatic activity is not critical for the induction of neuropathy since non-neuropathic compounds inhibit this activity (Zaccheo et al. 2004). Recently, some studies have indicated the essential role of NTE in fetal development (Winrow et al. 2003) and a peak of gene expression has been demonstrated in the early cell differentiation stage (Pamies et al. 2010).

The protection effect to OPIDN is observed if some NTE inhibitors are dosed before neuropathic OP. This effect is detected when carbamates, phosphinates and sulfonyl halides (e.g., PMSF) are administered to hens at doses that block (inhibit) more than 30–40 % of NTE before a high neuropathic dose of a neuropathic OP ester (Johnson and Lauwerys 1969). Protection has been explained to be related to the fact that NTE, which is inhibited by these compounds, does not undergo the aging reaction and consequently protects against further phosphorylation by an inducer.

In contrast, OPIDN is enhanced when some non-neuropathic esterase inhibitors (e.g., PMSF) are dosed after a low non-neuropathic dose of a neuropathy inducer. This effect was first observed in hens when PMSF was administrated after mipafox or DFP, and was called potentiation (Pope and Padilla 1990). Lotti and coworkers reported similar observations in hens treated with chlorpyrifos (Lotti et al. 1991) and called it "promotion" since an order of dosing (first exposure to an "inducer" or initiator, and afterward to the "promoter") is needed.

Several attempts have been made to identify the target of potentiation/promotion of OPIDN, but have proven unsuccessful to date. Several lines of evidence suggest that NTE is not the target of promotion and does not involve direct NTE modification, although all the promoters identified to date are NTE inhibitors (Lotti 2002). Only methamidophos (O,S dimethylphosphorothiomidate) promotes OPIDN at doses and causes marginal NTE inhibition (Lotti et al. 1995). It has been reported that, given the chemical nature of promoters, the target has to be a similar esterase to NTE and is, therefore, likely to hydrolyze the same substrate; i.e., phenyl valerate (PV) (Aldridge 1993). Other non-neuropathic NTE inhibitors, such as some carbamates, phosphinates, sulphonyl fluorides and phosphorothioates, do not promote OPIDN when given at the maximum tolerated doses (Lotti et al. 1991; Moretto et al. 1994; Céspedes et al. 1997; Johnson and Read 1993; Osman et al. 1996; Moretto et al. 2001; Lotti 2002).

The in vivo promotion/potentiation effect of PMSF and other promoters has been widely assayed in chicken (Lotti et al. 1991; Xie et al. 2002; Moretto et al. 1993). Chicken is also the animal model of current use and has been specified by regulatory agencies to evaluate the delayed neuropathic potential of organophosphorus esters in humans (*OECD 418 and 419 testing guide*). The chicken brain membrane esterase model was the first and most studied animal model and is the tissue in which NTE has been found and in which most studies have been done. An alteration in the expression of neurofilament subunit levels not observed in PMSF-protected hens suggested the possible involvement of neurofilament subunits in the development of OIPDN and in the protection of OPIDN (Gupta et al. 2000). However, some other pathway has been suggested in the potentiation delayed neurotoxicity by PMSF and some other axonal cytoskeletal protein/s should be involved in PMSF post-treatment (Xie et al. 2002).

Kinetic model equations and strategies were deduced to evaluate the inhibition of esterases by organophosphorus and related compounds by considering that different molecular phenomena occur simultaneously (ongoing inhibition, spontaneous reactivation). One specific problem with PMSF is its well-known fast degradation by chemical spontaneous hydrolysis in aqueous solutions, which dramatically modifies concentration while the experiment lasts. To that end, kinetic models have been developed and applied to consider the inhibitor's spontaneous chemical hydrolysis (Estévez et al. 2012).

Different serine esterase enzymatic components have been discriminated and their high in vitro sensitivity has been related with the OP neurotoxic effects observed in epidemiological and animal studies (Estévez et al. 2012; Mangas et al. 2011, 2012a, 2012b; Middlemore-Risher et al. 2010; COT report 1999; Jamal et al. 2002; Parron et al. 1996).

In soluble chicken brain fractions, three main serine esterase components, called Eα, Eβ and Eγ, have been discriminated according to their sensitivity to paraoxon, mipafox and PMSF (Mangas et al. 2011, 2012b). Alterations of sensitivity to mipafox have been observed in components Eα and Eγ after preincubation with PMSF at low non-inhibitory concentrations, while alterations of sensitivity to PMSF of component Eγ, also called S-NTE, have been noted after preincubation at low mipafox concentrations. These effects have been interpreted due to the interaction of PMSF and mipafox at sites other than the substrate catalytic center. It has been suggested that such interactions should be considered to not only interpret the potentiation/promotion phenomenon of PMSF, but also to understand the effects of multiple exposures to chemicals (Mangas et al. 2012b; Estevez et al. 2013).

In the membrane fractions of chicken brain, four serine esterase components have been discriminated according to their sensitivity to paraoxon and mipafox, called EPα, EPβ, EPγ and EPδ (Mangas et al. 2012a). It has been suggested that the properties of these esterase components may play potential roles in the toxicity and/or detoxication of OP esters (Mangas et al. 2012a). This work characterizes the kinetic interaction of the chicken brain membrane esterases inhibited by PMSF using kinetic models that have been previously developed in our laboratory by considering that PMSF is unstable in water solutions (Estévez et al. 2012), and it has been applied successfully to analyze the inhibition of soluble esterases by PMSF (Estévez et al. 2012; Mangas et al. 2012b). This work studies also the possible kinetic interactions between the OPs inducer of neuropathy mipafox and PMSF. These results allow establishing comparison of the kinetic behavior with PMSF of different nerve tissues.

Materials and methods

Chemicals

Phenylmethanesulfonyl fluoride was purchased from Sigma (Madrid, Spain, purity >99 % GC). *N*,*N*′-di-isopropyl phosphorodiamidefluoridate (mipafox, purity >98 %) and phenyl valerate were purchased from Lark Enterprise (Webster, MA, USA).

Homogenization buffer: 50 mM Tris–HCl buffer (pH 8.0) containing 1 mM EDTA. A stock solution of 50 mM PMSF was prepared in DMSO (dimethylsulfoxide) and a stock solution of 10 mM mipafox was prepared in 10 mM Tris-citrate buffer (pH 6.0). PMSF was dissolved in DMSO and mipafox was dissolved in homogenization buffer (pH 8.0) immediately before starting the kinetic assays. A stock solution of substrate phenyl valerate (16.8 mM) was prepared in dried *N*,*N*-dimethylformamide and was diluted in water to 0.54 mM immediately before the enzymatic assays (less than 30 min). All the other chemicals were of analytical reagent grades.

Tissue preparation

Chicken brains were obtained from a commercial slaughterhouse immediately after killing the animals and were kept in cold (0–5 °C) homogenization buffer until use. They were homogenized with a Polytron homogenizer (Kinematica Gmbh, Germany) using a PTA 10S head (dispersing aggregates at 70 % power (3 × 30 s) at a concentration of 200 mg fresh tissue/ml in the same buffer.

Subcellular fractionating

The homogenized tissue was centrifuged at 1,000×*g* for 10 min (4 °C) to precipitate debris and nuclei. The supernatant was centrifuged at 100,000×*g* for 60 min to obtain a precipitate consisting of the mitochondrial and microsomal fractions (membrane brain fraction) and a final supernatant or cytosol component (soluble brain fraction). Supernatant soluble fractions were discarded or used for other purposes. Membrane brain fractions were resuspended in buffer at the same concentration of the membranes from 200 mg fresh tissues per mL. Samples were frozen to conserve them in liquid nitrogen and were diluted for the appropriate concentration for use in the kinetic assays.

The assay of inhibition and phenyl valerate esterase activity (PVase) for kinetic studies

Inhibition and enzyme assays were carried out as previously described (Mangas et al. 2011) following a procedure based on the colorimetric method that was developed for the NTE assay (Johnson 1974). The method was modified and programmed for an automated microassay using the Biomek 2000 (Beckman) workstation as follows.

Inhibition

In a 1-mL microtube, a 200 μL volume of the brain fraction (at an equivalent concentration of 15 mg/mL of the original fresh tissue) was incubated with 20 μL of inhibitor solution (buffer in controls) at the appropriate concentrations.

Enzyme activity measurement

After the appropriate inhibition time, 200 µL of substrate phenyl valerate (0.54 mM) was added and incubated for 10 min at 37 °C to measure enzymatic activity. The reaction was stopped by adding 200 µL of a solution of 2 % sodium dodecyl sulfate with 1.23 mM aminoantipyrine (SDS-AAP solution), which was then mixed with 100 µL of 1.21 mM potassium ferricyanide and was left for 10 min for color development. Volumes of 300 µL from each microtube were transferred to a 96-well microplate, and absorbance was read at 510 nm. Standards of phenol, blanks and spontaneous hydrolysis controls (samples without tissue) were included with the same procedure.

The results are expressed as % activity ($E/E_0 \times 100$) over the control without an inhibitor and are plotted versus either time (t) or inhibitor concentration (I).

Mipafox inhibition assay in the samples preinhibited with PMSF

Tissue samples (containing the membrane fraction from 20 mg/ml of brain) were incubated with 20 µM of PMSF for 20 min at 37 °C. Then, 20 µl of the mipafox solution was added to obtain a concentration of mipafox ranging from 0 to 250 µM and was incubated for 30 min at 37 °C. Afterward, esterase enzymatic activity (PVase) was measured as indicated above.

The PMSF inhibition assay in the samples preinhibited with mipafox

Tissue samples (containing the membrane fraction from 15 mg/ml of brain) were incubated with 6 µM mipafox for 30 min at 37 °C. Then, 20 µl of the PMSF solution was added to obtain a concentration of PMSF ranging from 0 to 1,000 µM and was incubated for 20 min at 37 °C. Afterward, enzyme activity (PVase) was measured as described above.

Mathematical models

Inhibition by preincubation

Model equations for the kinetics of inhibition with one, two or more sensitive enzymatic components, with or without a resistant fraction, were applied in accordance with (Estévez and Vilanova 2009) and with (Estévez et al. 2012). For the model with two sensitive enzymatic components (E1 and E2) and a resistant one (R), the general model equation for inhibition is as follows:

$$E = \mathrm{E1}_0 \cdot \mathrm{e}^{-(\mathrm{k1}\cdot t\cdot I)} + \mathrm{E2}_0 \cdot \mathrm{e}^{-(\mathrm{k2}\cdot t\cdot I)} + R, \quad (1)$$

where $\mathrm{E1}_0$ and $\mathrm{E2}_0$ represent the % of activity of the enzymatic component in relation to total activity; k1 and k2 are the first-order kinetic constants of the inhibition; I, inhibitor concentration; and t, the preincubation time with the inhibitor.

If spontaneous hydrolysis was considered, then the general model was as follows:

$$E = \mathrm{E1}_0 \cdot \mathrm{e}^{\left(\mathrm{e}^{-\mathrm{kh}\cdot t}-1\right)\cdot\frac{\mathrm{k1}}{\mathrm{kh}}\cdot I_0} + \mathrm{E2}_0 \cdot \mathrm{e}^{\left(\mathrm{e}^{-\mathrm{kh}\cdot t}-1\right)\cdot\frac{\mathrm{k2}}{\mathrm{kh}}\cdot I_0} + R, \quad (2)$$

where kh is the kinetic constant of the spontaneous chemical hydrolysis of the inhibitor.

If ongoing inhibition (inhibition during the substrate reaction time) was significant, the exponential factor $\mathrm{e}^{\left(-\mathrm{k}a'\cdot I_0\cdot \mathrm{e}^{-(\mathrm{kh}\cdot t)}\right)}$ was included (Estévez and Vilanova 2009).

The general model equation for two sensitive components, both affected by ongoing inhibition, plus a resistant one, was as follows:

$$E = \mathrm{E1}_0 \cdot \mathrm{e}^{\left(-\mathrm{ka}'1\cdot I_0\cdot \mathrm{e}^{-(\mathrm{kh}\cdot t)}\right)\cdot \mathrm{e}^{\left(\mathrm{e}^{-\mathrm{kh}\cdot t}-1\right)\cdot\frac{\mathrm{k1}}{\mathrm{kh}}\cdot I_0}} + \mathrm{E2}_0 \cdot \mathrm{e}^{\left(-\mathrm{ka}'2\cdot I_0\cdot \mathrm{e}^{-(\mathrm{kh}\cdot t)}\right)\cdot \mathrm{e}^{\left(\mathrm{e}^{-\mathrm{kh}\cdot t}-1\right)\cdot\frac{\mathrm{k1}}{\mathrm{kh}}\cdot I_0}} + R \quad (3)$$

Evaluating inhibition during the substrate reaction (ongoing inhibition)

For the situation in which the inhibitor was added at the same time as the substrate (no preincubation with an inhibitor), exponential decay models were used to fit the data of the % of activity versus the inhibitor concentration at zero time during the progressive inhibition experiment. The general model is as follows:

$$E = \mathrm{E1}_0 \cdot \mathrm{e}^{-\mathrm{ka}'1\cdot I} + \mathrm{E2}_0 \cdot \mathrm{e}^{-\mathrm{ka}'2\cdot I} + R, \quad (4)$$

where parameters ka'1 and ka'2 represent the apparent first-order kinetic constants of inhibition observed during the substrate reaction time, and $\mathrm{E1}_0$ and $\mathrm{E2}_0$ represent the % of activity and the enzymatic component affected by the ongoing inhibition effect.

The detection and analysis of inhibition in the presence of a substrate allowed to establish appropriate model equations in the evaluation of the time-progressive inhibition data.

Evaluation of fixed-time inhibition curves

An experiment with different inhibitor concentrations within the range of 0–1,000 µM and a fixed preincubation time with PMSF (20 min) was carried out. Data were plotted as the % of activity versus inhibitor concentration and were analyzed using the model Eq. (2) but fixing $t = 20$ min.

All the experiments were done in three replicates, and each point in the data represents the mean of the replicates (SD < 5 %).

Evaluation of time-progressive inhibition data

Experiments with PMSF concentrations of 0, 10, 25, 75, 150, 250, 400 and 1,000 μM were performed. Tissue samples (membranes from 15 mg/ml) were preincubated with the inhibitor for different times (t) ranging from 0 to 20 min. Substrates were added and a substrate-enzyme reaction lasting 10 min was allowed. The time-progressive inhibition data were plotted as a % of activity versus time (t) and inhibitor concentration (I) and were analyzed with the tridimensional models described in Eq. (3).

All the experiments were done in triplicate, and each point in the data represents the mean of three replicates (SD < 5 %).

Computerized analysis of inhibition curves

Model equations were fitted to the experimental inhibition data by a nonlinear computerized method based on the least squares principle using version 8 of the Sigma Plot software (Systat Software Inc., Chicago, USA). The same software was used to apply an F test to compare the different tested kinetic models in order to identify the best fitting model. The experimental data were fitted to the models by considering one, two or three sensitive component(s), with or without a resistant component. As indicated in the Results, the best fitting model was that with two sensitive and one resistant component, as described in Eqs. (2) and (3) in both experiments, with fixed-time inhibition and time-progressive inhibition.

In order to obtain a coherent solution in the interactive computing estimation, some restrictions were applied: (1) All the parameters (rate constants and amplitudes) should have positive values (>0); (2) component 1 was established to be the most sensitive, therefore, k1 > k2; and (3) the following complementary restriction was also applied: $E1_0 + E2_0 + R = 100$ %.

The results were expressed by giving the values of the exponential kinetic constants ($M^{-1}\cdot min^{-1}$), the proportions/amplitudes of each component (% of activity) and the I_{50} values (20 min) (concentration to achieve 50 % inhibition) of each component, deduced from the kinetic parameter inhibition and hydrolysis constants.

The I_{50} (20 min) values were obtained by applying the following equation:

$$I_{50}^{20} = \text{- Ln } 2/\left\{(e^{(-kh\cdot 20)} - 1)\cdot\frac{ki}{kh}\right\}$$

This value represents the concentration that may cause an inhibition of the enzymatic component of 50 % and a practical indication of sensitivity to the inhibitor under the experimental conditions.

Results

Fixed-time inhibition curve

PMSF was incubated with chicken brain membrane fractions for 20 min at 37 °C (Fig. 1). The exponential decay models for the inhibition with the spontaneous hydrolysis of the inhibitor were fitted to the fixed-time inhibition data according to Estévez et al. (2012). The best fitting model (according to the F test) was a model consisting in two sensitive components of 36 and 51 % with I_{50} (20 min) of 23 and 124 μM, respectively, and a resistant component of 13 %. The hydrolysis constant (kh) estimated from PMSF was 0.23 min^{-1} (Table 1, column A).

Time-progressive inhibition curves by PMSF

Figure 2a shows the inhibition curves of chicken brain membrane fractions with PMSF (0, 10, 25, 75, 150, 250, 400 and 1,000 μM) for times of up to 20 min at 37 °C. Inhibition proved to be time-progressive and was around 85 % of the activity in the membrane fraction, which is coherent with the covalent irreversible inhibition.

Evaluation of ongoing inhibition during the substrate reaction

The non-preincubation data (Fig. 2b) indicate that the inhibition during substrate incubation under the assayed conditions was apparently significant.

Exponential decay models were fitted to the data. The best model (according to the F test) was a model with two

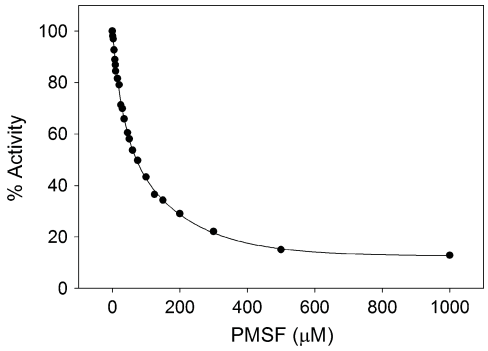

Fig. 1 PMSF fixed-time inhibition curve of esterase activity at 30 min of inhibition in membrane brain fractions. Enzyme preparations were incubated with concentrations within the range of 0–1,000 μM of PMSF for 30 min at 37 °C, and residual activity was assayed as described in the methods. Curves were the best fits according to the F test (two exponential components, plus a resistant one, including the spontaneous hydrolysis of PMSF). *Each point* represents the mean of three replicates (SD < 5 %)

Table 1 Inhibition of membrane brain esterases by PMSF

Parameter (units)	A. Fixed-time	B. Inhibition during substrate	C. 3D time progressive
R^2	0.9993	0.9957	0.9971
kh (min^{-1})	0.23		0.28
Component EP1			
k′a1 (μM^{-1})	–	0.0053	0.0048
EP1 (%)	36	41	44
k1 ($\mu M^{-1} \cdot min^{-1}$)	0.007		0.008
I_{50}^{20} (μM)	23		23
Component EP2			
k′a2 (nM^{-1})	–	0.00051	0.00050
EP2 (%)	51	49	41
k2 ($\mu M^{-1} \cdot min^{-1}$)	0.0013	–	0.0014
I_{50}^{20} ($\mu M^{-1} \cdot min^{-1}$)	124	–	138
Resistant Component			
R (%)	13	10	15

Kinetic constants (ki) and proportions of the esterase components deduced from the inhibition experiments with PMSF. The I_{50} values were calculated from the kinetic constants for each component

components, one sensitive and one resistant, of about 10 % (Table 1, column B). This justifies that the ongoing inhibition factor should be taken into account for both sensitive enzymatic components. Parameters ka′1 and ka′2 represent the apparent first-order kinetic constants of inhibition observed during the substrate reaction time for the first and second sensitive components, respectively.

Fitting time-progressive inhibition by PMSF data

A three-dimensional fitting (% of activity vs *t* and *I*) was done with the data described in Fig. 2a. The time-progressive inhibition data were analyzed with the model by considering inhibition with a simultaneous hydrolysis of PMSF and the ongoing inhibition effect described in Eq. 3. The best fitting model (according to the *F* test) consisted in two sensitive components of 44 and 41 %, and a resistant component of 15 % (Table 1). The deduced 3D surface is plotted in Fig. 2c.

The mipafox inhibition assay in the samples preinhibited with PMSF

This concentration was selected to inhibit half the most sensitive components and some of the least sensitive ones. Two experiments were done. The activity that proved resistant to 20 μM PMSF was 68 % of total activity (Fig. 3, panel A). Figure 3a shows the fixed-time inhibition experiment data with mipafox of the 20 μM PMSF-resistant activity. The exponential decay models with one, two or more

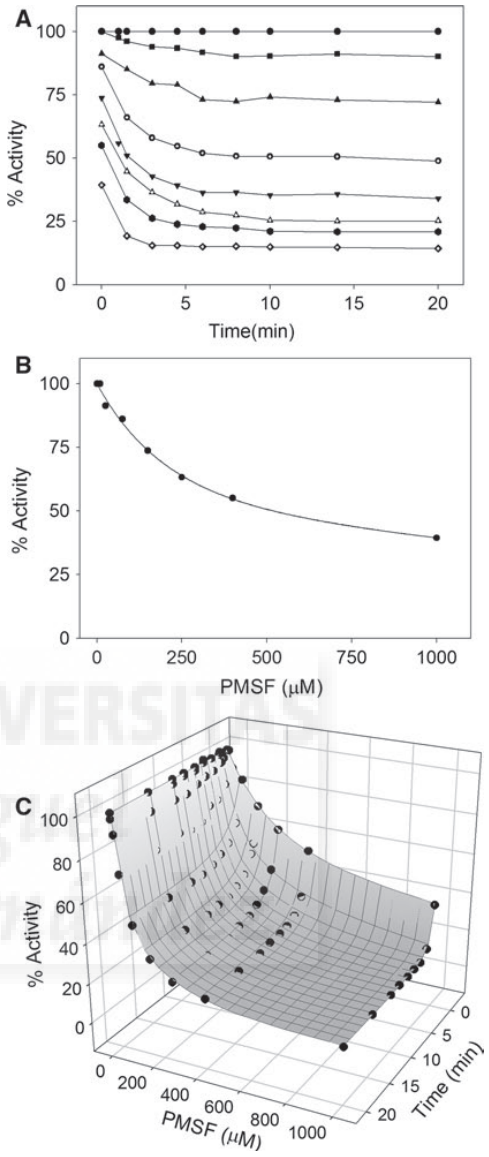

Fig. 2 Kinetics of the time-progressive inhibition by PMSF in membrane brain fractions. A preparation containing the membrane fractions of 15 mg of fresh tissue/ml was preincubated with 0, 10, 25, 75, 150, 250, 400 and 1,000 μM PMSF (*upper* to *lower plots*, plots in **a**) for the indicated time at 37 °C. Then, enzymatic activity was assayed with phenyl valerate for 10 min. **a** The best fitting model equation for the individual curve for each concentration. **b** Reveals inhibition at the reaction time with the substrate (0 min inhibition time). **c** Provides the inhibitory surface obtained by fitting the 3D model equation to the data. The surface reflects the result of the best model according to the *F* test. *Each point* represents the mean of two replicates (SD < 5 %)

sensitive component(s), with or without a resistant component, were fitted to the data. The best fitting model (according to the ′*F*′ test) for two independent experiments was

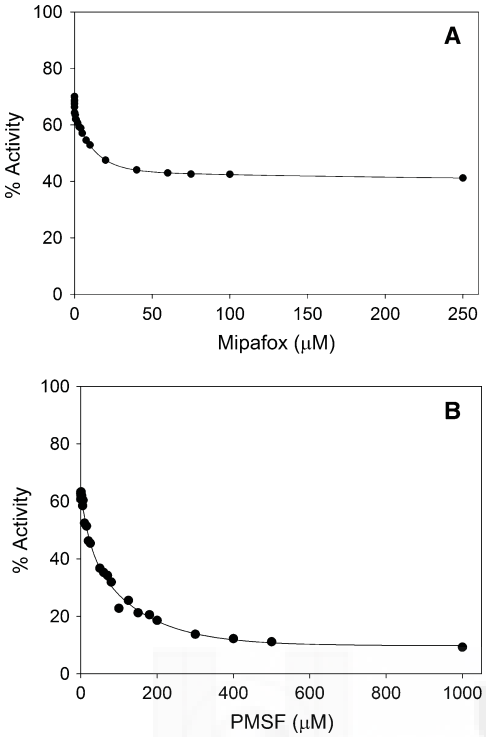

Fig. 3 Sequential inhibition with mipafox and PMSF, and vice versa. **a** The mipafox fixed-time inhibition curve of 20 μM PMSF-preincubated and, **b** the PMSF fixed-time inhibition curve of 6 μM mipafox-preincubated esterase activity. Enzyme preparations were preincubated with 6 μM mipafox for 30 min at 37 °C (**a**) or with 20 μM PMSF for 30 min at 37 °C (**b**). Then, the preinhibited samples were incubated with PMSF at concentrations within the range of 3–250 μM for 20 min (**a**) or with PMSF at concentrations within the range of 15–1,000 μM for 20 min (**b**) at 37 °C, and residual activity was assayed and expressed as the % of activity over a non-inhibited control. Curves were fitted with exponential model equations by selecting the best fitting equation according to the *F* test. *Each point* represents the mean of three replicates (SD < 5 %)

a model consisting in two sensitive components (7–6 and 34–22 %) with I_{50} (30 min) of 20–37 and 3,397–9,667 nM (k1 = $6.1{\cdot}10^{-4}$–$1.1{\cdot}10^{-3}$ $nM^{-1}{\cdot}min^{-1}$ and k2 = $2.4{\cdot}10^{-6}$–$6.7{\cdot}10^{-6}$ $nM^{-1}{\cdot}min^{-1}$), respectively, and a resistant component (37–42 %). These results were compared with previously published data on inhibition with mipafox with no preinhibition (Table 2).

The PMSF inhibition assay in the samples preinhibited with mipafox

The activity resistant to 6 μM mipafox was 63 % of total activity. This concentration was selected in order to inhibit around 25 % of activity. Figure 3b shows the fixed-time inhibition curve with PMSF of 6 μM mipafox-resistant activity. Exponential decay models were fitted to the data. The best fitting model (according to the '*F*' test) was a model consisting in two sensitive enzymatic entities, 17 and 36 % with I_{50} (20 min) of 17 and 103 μM (k1 = $6.0{\cdot}10^{-3}$ $\mu M^{-1}{\cdot}min^{-1}$ and k2 = $1.0{\cdot}10^{-3}$ $nM^{-1}{\cdot}min^{-1}$), and a resistant component, 10 %, by considering the effect of spontaneous hydrolysis, kh = 0.14 min^{-1}. These results in Table 2 were compared to the inhibition data with PMSF obtained in the experiments shown in Figs. 1 and 2 and in Table 1 with no preinhibition.

Table 2 Kinetic data of the interactions of PMSF and mipafox in the inhibition of brain membrane esterases

Preincubation: none		20 μM *PMSF*
Inhibition: mipafox		mipafox
Component		
	(b) I_{50} (% activity)	*(a)* I_{50} (% activity)
EPα (part of *R* in Table 1)	6–29 nM (5–7 %)	20–37 nM (7–6 %)
EPγ (EP1 in Table 1)	6,601–7,001 nM (39–44 %)	3,397–9,667 (34–22 %)
EPβ + EPδ (EP2 + part of *R* in Table 1)	Resistant (49–57 %)	Resistant (37–42 %)
Preincubation: none		6 μM mipafox
Inhibition: PMSF		PMSF
	(a) I_{50} (% activity)	*(a)* I_{50} (% activity)
EPβ (EP2 in Table 1)	138 μM (51 %)	103 μM (36 %)
EPγ (EP1 in Table 1)	23 μM (36 %)	17 μM (17 %)
EPα + EPδ (R in Table 1)	Resistant (13 %)	–
EPδ (part of R in Table 1)	–	Resistant (10 %) (EPα had been preinhibited by the mipafox)

The proportion of the component (%) and inhibitory properties (I_{50}) for inhibition by PMSF or mipafox in membrane fractions is shown. The table provides the data obtained after preincubation with 6 μM mipafox or 20 μM PMSF, but with no preincubation. The I_{50} values are for 20 min in the case of PMSF and 30 min for mipafox. The data shown derive from the experiments done in this work (a) or from the experiments cited in a previously published paper (b) and are indicated in the table footnotes. Those cases for which two numbers are shown represent the range of several experiments under different conditions (fixed-time inhibition, time-progressive inhibition)

(a) From the data in this paper, the two numbers represent the data of two independent experiments under the same conditions (fixed-time inhibition)

(b) From the data of the mipafox inhibition experiments in (Mangas et al. 2012a), the two numbers represent the data from one experiment at the fixed-time inhibition and the other at the time-progressive inhibition

Discussion

The kinetic behavior of PMSF with membrane esterases of brain

The serine/cysteine protease inhibitor (PMSF) has been shown to protect from OPIDN if dosed before a high dose of an OP neuropathic inducer, but it also potentiates the effect if dosed after a low non-neuropathic dose of an inducer. The protection mechanism has been demonstrated to be achieved by blocking the NTE esteratic site, thus protecting against further OP inducer action. However, the molecular target/s of potentiation/promotion has/have not yet been identified with absolute certainty. There is evidence to indicate that it is not NTE, but that it could be found among phenyl valerate esterases (Estévez and Vilanova 2009; Estévez et al. 2010; Milatovic et al. 1997).

This work evidences that micromolar concentrations of PMSF are capable of inhibiting about 85 % of total phenyl valerate esterase activity in membrane chicken brain in a time-progressive manner, suggesting covalent irreversible binding by sulfonation (Fig. 2a). PMSF is spontaneously hydrolyzed in Tris pH 8.0 solutions (James 1978) and in biological preparations (Johnson 1969b; Estévez et al. 2012). Hence, a kinetic model that contemplates the inhibition and the spontaneous hydrolysis of an inhibitor has been applied to the data analyses (Estévez et al. 2012).

Spontaneous reactivation is not considered in the mathematical modeling because it is not seen to be relevant for PMSF. If reactivation simultaneously occurs, then a progressive increase in activity should be observed in the progressive inhibition experiment after 10 min when all the PMSF has been chemically hydrolyzed. However, no recovery of activity is noted, and the kinetic curves in Fig. 2a tend to reach a "plateau" because chemical hydrolysis is the cause of the apparent steady states reached.

The amplitudes (proportion) and the inhibition constants estimated after fitting are similar in both the fixed-time and the progressive inhibition experiments (Table 1). "Ongoing inhibition" apparent constants, ka'1 and ka'2, estimated from the data at the zero time preinhibition, are similar to ka'1 and ka'2 obtained in the 3D fit in the time-progressive inhibition experiments (Table 1). Moreover, the estimated spontaneous hydrolysis constant is similar in all the inhibition experiments 0.23–0.28 min^{-1} (Table 1). These results are comparable to the kh estimated in the kinetic studies in soluble peripheral nerve (0.09–0.13 min^{-1}) in the brain soluble fraction (0.16–0.23 min^{-1}) and are consistent with the deduced chemical hydrolysis constant of 0.0198 min^{-1} at 25 °C (James 1978; Estévez et al. 2012; Mangas et al. 2012b). All these observations may be considered an internal validation of the consistency of the results and the applied kinetic model.

Enzymatic components discriminated with PMSF in brain membranes

Three enzymatic components are detected in chicken brain membranes by their inhibition with PMSF: EP1 (44 %) with I_{50} (30 min) = 23 μM; EP2 (41 %) with I_{50} (20 min) = 138 μM, and *R* (15 %), which is resistant to PMSF inhibition. The "ongoing inhibition" effect is considered for the two sensitive enzymatic components in accordance with the best model fitted to the data at the zero time inhibition. These PMSF-sensitive enzymatic entities are considered to potentially play a role in the potentiation/promotion of OP delayed neuropathy. These parameters are essential to have the appropriate criteria to monitor the isolation and purification of PMSF-sensitive esterases for their further molecular identification and functional characterization and for more robust studies in order to understand their toxicological involvement.

Identification of the components discriminated with PMSF with those discriminated with paraoxon and mipafox

Four enzymatic components have been discriminated in membrane fractions according to their sensitivity to paraoxon and mipafox (Mangas et al. 2012a), namely EPα, EPβ, EPγ (NTE) and EPδ. In this work, only three phenyl valerate esterase components have been discriminated with PMSF. Sequential inhibition experiments with two inhibitors are needed to establish the equivalence of the components detected herein with PMSF with those previously discriminated with paraoxon and mipafox (Fig. 4).

Preincubation with 6 μM mipafox has been performed to preinhibit component EPα and around 50 % of component EPγ (NTE) according to the discriminated enzymatic components and the kinetic parameters published in (Mangas et al. 2012a). The best model to fit to the PMSF fixed-time inhibition data was a model with two sensitive components and one resistant one. These components display similar sensitivities to EP1 and EP2 (Table 1), and the resistant component is resistant to PMSF and mipafox. Moreover, 20 μM PMSF was employed to partially preinhibit components EP1 and EP2 according to the kinetic parameters obtained in this work, and then mipafox was used to estimate the kinetic parameters of the PMSF 20 μM resistant fraction. The best fit to the mipafox inhibition data was a model with two sensitive components and a resistant one. These components have displayed similar sensitivities to EPβ and EPγ (Mangas et al. 2012a). Therefore, the two sensitive components discriminated with PMSF (EP1 and EP2) correspond to components EPβ and EPγ, which are discriminated with paraoxon and mipafox, while the PMSF-resistant component (R) should correspond to components EPα (inhibited

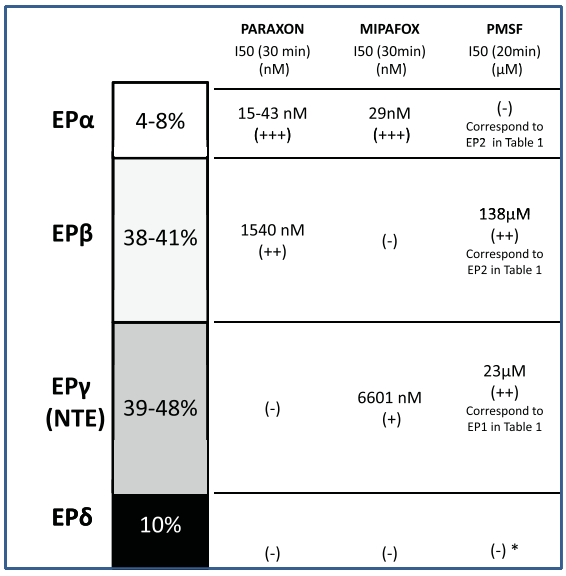

Fig. 4 Discrimination of four esterase enzymatic components in membrane brain fractions by globally considering all the experiments with PMSF, mipafox and paraoxon, and their interactions. By globally considering all the data, four enzymatic components are discriminated according to sensitivity to PMSF, paraoxon and mipafox, as follows: EPα, which is highly sensitive to paraoxon and to mipafox, spontaneously reactivates after inhibition with mipafox and is resistant to PMSF inhibition. EPβ, sensitive to paraoxon and PMSF and resistant to mipafox; EPγ, sensitive to mipafox and PMSF, but resistant to paraoxon; EPδ, resistant to all the inhibitors. The I_{50} values are indicated (for 30 min and 20 min) and are "classified" as: highly sensitive (+++), sensitive (++)/(+) and resistant (−). The paraoxon and mipafox data in (Mangas et al. 2012a)

by 6 μM mipafox), plus EPδ (resistant to mipafox and PMSF).

When globally considering the data, four enzymatic components are discriminated (Fig. 4) according to their sensitivity to paraoxon, mipafox and PMSF in membrane brain fractions: EPα (4–8 % of activity), highly sensitive to paraoxon and mipafox, which is spontaneously reactivated after inhibition with paraoxon and resistant to PMSF; EPβ (38–41 % of activity), sensitive to paraoxon and PMSF, but practically resistant to mipafox; EPγ (NTE) (39–48 % of activity), which is paraoxon-resistant and sensitive to micromolar concentrations of mipafox and PMSF; and EPδ (10 % of activity), which is resistant to all the inhibitors.

Interactions among a potentiator and an inducer of neuropathy: study of the changes in sensitivity in the samples preincubated with another inhibitor

Three enzymatic components (Eα, Eβ and Eγ) have been detected in soluble fractions of brain (Mangas et al. 2011, 2012b). A sharp drop in sensitivity to mipafox has been observed after preincubation to a low non-inhibitory concentration of PMSF (5–2,000 μM of PMSF) in components Eα and Eγ (Mangas et al. 2012a). Similarly, alterations in the sensitivity to PMSF of component Eγ after preincubation at a low mipafox concentration (20 nM) have been reported (Mangas et al. 2012b). It has been proposed that this effect might be due to the interaction of inhibitors at sites other than the substrate catalytic center and that these interactions should be taken into account in potentiation/promotion studies of PMSF (Estevez et al. 2013; Mangas et al. 2012b).

Along these lines, kinetic interaction experiments in NTE and non-NTE membrane esterases are also needed in order to understand these kinds of kinetic interactions. The instability of PMSF has proven an advantage when used in sequential assays as all the PMSF disappears from the medium without disturbing further studies (Mangas et al. 2012b; Estevez et al. 2013).This work reports the sequential assays performed by preincubation with low concentrations of PMSF, followed by inhibition with mipafox and vice versa in order to study if there is any alteration in any of the discriminated membrane esterases. There is no evidence to suggest changes in the sensitivity of any of the components to mipafox after preincubation with PMSF neither in the components' sensitivity to PMSF after mipafox preincubation.

Vicedo et al. (1993) studied the interaction of PMSF and DFP in the inhibition of brain membrane NTE activity (resistant to paraoxon and sensitive to mipafox; EPγ in Table 2). No alteration in the inhibition kinetics of DFP for residual activity takes place after preincubation with PMSF, and vice versa. These results are considered to evidence the possibility of discarding the potential allosteric effects of PMSF and OP inhibitors on NTE. This work confirms and deduces that no alterations occur by sequential interactions with PMSF and mipafox in NTE and in other membrane esterases.

Role of EPα, EPβ, EPγ and EPδ

Besides the efforts and numerous studies (Pope and Padilla 1990; Lotti et al. 1991; Moretto et al. 2007; Estévez et al. 2012; Mangas et al. 2012b), the molecular target of potentiation has not been elucidated yet. Several lines have suggested that the target should be similar to NTE and hydrolyses the same substrate (all the promoters are NTE inhibitors), so this detailed kinetic study of all the membrane phenyl valerate esterases elucidate the possible targets in brain and allow having kinetic parameters to identify them in further purification and molecular studies.

EPγ is NTE, operationally defined as the phenyl valerate esterase activity, which is resistant to the non-neuropathic OP ester paraoxon (40 μM, 20 min, pH 8.0) and sensitive

to the neuropathic OP ester mipafox (50 μM) (Johnson 1977). NTE is a serine hydrolase known for which toxicological and biological roles have been identified, and is molecularly and genomically characterized. It was first identified as the target of inducing delayed neuropathy (Johnson 1969a). A physiological role in maintenance by lysophospholipase activity in adults (Read et al. 2009), in embryonic development (Winrow et al. 2003; Pamies et al. 2010) and in embryonic cell differentiation (Pamies et al. 2010) has been suggested.

The role of the other membrane enzymatic components remains unknown. This work is the first step to elucidate the toxicological meaning of these esterases that in vitro interact with PMSF and OPs compounds. These kinetic data are needed to have the appropriate criteria to discriminate them along further purification and molecular identification studies. The high sensitivity of EPα to paraoxon and mipafox suggests that it might play a role in toxicity in the low-level long-term exposure of organophosphate compounds and it may be relevant only in chronic exposure in relation to spontaneous reactivation after paraoxon inhibition (Parron et al. 1996).

The molecular target of promotion could be found among the esterase components sensitive to PMSF. Components EPβ and EPγ, which are sensitive to PMSF, could potentially contain the target of promotion/potentiation. EPγ (NTE) has been excluded as potential target of the potentiation phenomenon based on in vivo experiments in which animals were predosed with a protector and an inducer blocking 100 % NTE without causing neuropathy. However, after dosing, PMSF neuropathy was developed, suggesting that the site of action for this second PMSF dose is in other site different to NTE (Lotti et al. 1991). Component EPβ is likely to be able to be inhibited in vivo with tolerable doses of PMSF; therefore, it might contain the target of the potentiation phenomenon. EPβ is also sensitive to paraoxon in vitro, but it is unlikely to be inhibited in vivo by tolerable doses of paraoxon, as AChE is much more sensitive (chicken brain AChE I_{50}, 30 min of 0.028 μM, at 37 °C; Kemp and Wallace 1990) than EPβ (I_{50}, 30 min of 1.5 μM). Hence, in in vivo experiments, animals die due to a high AChE inhibition (Lotti et al. 1991), before paraoxon would be able to inhibit EPβ. However, further isolation assays should be done in this membrane esterase component to elucidate their role in toxicity of organophosphorus and their potential role in potentiation of neuropathy.

Special attention has been paid to the serine hydrolases of membrane brain while searching for targets of OPs' neurotoxicity effects. The complete blockade of multitude secondary targets at sublethal doses has been found in membrane fractions of mouse brain when adopting the chemoproteomic "Activity Based Protein Profiling" (ABPP) approach, which uses active site-directed chemical probes to read-out enzymes in complex proteomes (Nomura and Casida 2011). After labeling only active enzymes with the active site serine, the ABPP technology has revealed multiple off-targets of OP and TC pesticides, including several enzymes that play important roles in brain physiology, as well as functionally non-characterized enzymes. Monoacylglycerol lipase (MAGL) and fatty acid amide hydrolase (FAAH) have received special attention as they terminate the signaling of endogenous cannabinoid ligands to the cannabinoid receptor, the blockage of MAGL and FAAH robustly raises the brain endocannabinoid levels, while inhibition of MAGL also disrupts the brain arachidonic acid metabolism (Moser et al. 2004; Nomura et al. 2005). The other targets found have been those involved in regulating endoplasmic reticulum integrity (NTE), palmitoylation states of proteins and dendritic spine formation (APTs), and targets that have poorly or completely uncharacterized physiological functions (ABHD6, APEH and KIAA1363) (Nomura et al. 2008).

We have now the appropriate criteria for a routine protocol of a simple kinetic assay to analyze all the phenyl valerate esterase targets in membrane chicken brain. We suggested the discrimination of the four main esterase components in the membrane brain fraction using four conditions: A: no inhibitor; B: 120 nM of mipafox; C:25 μM of mipafox; D: 25 μM of mipafox + 600 μM of mipafox. The enzymatic components can be estimated as follows: EPα = A–B; EPγ = B–C; EPβ = C–D; EPδ = D. This kinetic assay will be needed in further purification and fractionation assays in order to molecularly identify these esterases.

Conflict of interest The authors declare that there are no conflict of interest.

References

Aldridge N (1993) Postscript to the symposium on organophosphorus compound induced delayed neuropathy. V Chem Biol Interact 87(1–3):463–466

Céspedes MV, Escudero MA, Barril J, Sogorb MA, Vicedo JL, Vilanova E (1997) Discrimination of carboxylesterases of chicken neural tissue by inhibition with a neuropathic, non-neuropathic organophosphorus compounds and neuropathy promoter. Chem-Biol Interact 106:191–200

COT report (1999) Organophosphates. A report of the committee on toxicology of chemicals in food, consumer products and the environment. UK Department of Health, London

Estévez J, Vilanova E (2009) Model equations for the kinetics of covalent irreversible enzyme inhibition and spontaneous reactivation: esterases and organophosphorus compounds. Crit Rev Toxicol 39(5):427–448

Estevez J, Mangas I, Sogorb MA, Vilanova E (2013) Interactions of neuropathy inducers and promoters with soluble esterases. Chem Biol Interact doi:10.1016/j.cbi.2012.11.007

Estévez J, Barril J, Vilanova E (2010) Inhibition with spontaneous reactivation and the "ongoing inhibition" effect of esterases by

biotinylated organophosphorus compounds: S9B as a model. Chem Biol Interact 187:397–402

Estévez J, Barril J, Vilanova E (2012) Kinetics of inhibition of soluble peripheral nerve esterases by PMSF: a non-stable compound that potentiates the organophosphorus-induced delayed neurotoxicity. Arch Toxicol 86(5):767–777

Glynn P (2000) Neural development and neurodegeneration: two faces of neuropathy target esterase. Prog Neurobiol 61(1):61–74 Review

Gupta RP, Abdel-Rahman A, Jensen KF, Abou-Donia MB (2000) Altered expression of neurofilament subunits in diisopropyl phosphorofluoridate-treated hen spinal cord and their presence in axonal aggregations. Brain Res 878(1–2):32–47

Jamal GA, Hansen S, Julu POO (2002) Low level exposures to organophosphorus esters may cause neurotoxicity. Toxicology 181–182:23–33

James GT (1978) Inactivation of the protease inhibitor phenylmethylsulfonyl fluoride in buffers. Anal Biochem 86(2):574–579

Johnson MK (1969a) The delayed neurotoxic effect of some organophosphorus compounds. Identification of the phosphorylation site as an esterase. Biochem J 114:711–717

Johnson MK (1969b) Delayed neurotoxic action of some organophosphorus compounds. Br Med Bull 25(3):231–235

Johnson MK (1974) The primary biochemical lesion leading to the delayed neurotoxic effects of some organophosphorus esters. J Neurochem 23:785–789

Johnson MK (1977) Improved assay of neurotoxic esterase for screening organophosphates for delayed neurotoxicity potential. Arch Toxicol 37:113–115

Johnson MK, Lauwerys R (1969) Protection by some carbamates against the delayed neurotoxic effects of di-isopropyl phosphorofluoridate. Nature 222(5198):1066–1067

Johnson MK, Read DJ (1993) Prophylaxis against and promotion of organophosphate-induced delayed neuropathy by phenyl di-n-pentylphosphinate. Chem Biol Interact 87(1–3):449–455

Johnson MK, Vilanova E, Read DJ (1989) Biochemical clinical tests of the delayed neuropathic potential of some O-alkyl o-dichlorophenyl phosphoramidate analogues of methamidophos (O, S-dimethyl phosphorothioamidate). Toxicology 54:89–100

Johnson MK, Vilanova E, Read DJ (1991) Anomalous biochemical responses in test of the delayed neuropathic potential of methamidophos (O, S-dimethyl phosphoramidates.), its resolved isomers and of some higher O-alkyl homologues. Arch Toxicol 65:618–624

Kemp J, Wallace K (1990) Molecular determinants of the species-selective inhibition of brain acetylcholinesterase. Toxicol Appl Pharmacol 104:246–258

Lotti M (2002) Promotion of organophosphate induced delayed polyneuropathy by certain esterase inhibitors. Toxicology 181–182:245–248 Review

Lotti M, Caroldi S, Capodicasa E, Moretto A (1991) Promotion of organophosphate-induced delayed polyneuropathy by phenylmethanesulfonyl fluoride. Toxicol Appl Pharmacol 108:234–241

Lotti M, Moretto A, Bertolazzi M, Peraica M, Fioroni F (1995) Organophosphate polyneuropathy and neuropathy target esterase: studies with methamidophos and its resolved optical isomers. Arch Toxicol 69(5):330–336

Mangas I, Vilanova E, Estévez J (2011) Kinetics of the inhibitory interaction of organophosphorus neuropathy inducers and non-inducers in soluble esterases in the avian nervous system. Toxicol Appl Pharmacol 256(3):360–368 Epub 2011 May 12

Mangas I, Estevez J, Vilanova E (2012a) NTE and non-NTE esterases in brain membrane: kinetic characterization with organophosphates. Toxicology 297(1–3):17–25

Mangas I, Vilanova E, Estévez J (2012b) Phenylmethylsulfonyl fluoride, a potentiator of neuropathy, alters the interaction of organophosphorus compounds with soluble brain esterases. Chem Res Toxicol 25(11):2393–2401

Middlemore-Risher ML, Buccafusco JJ, Terry AV (2010) Repeated exposures to low-level chlorpyrifos results in impairments in sustained attention and increased impulsivity in rats. Neurotoxicol Teratol 32:415–424

Milatovic D, Moretto A, Osman KA, Lotti M (1997) Phenyl valerate esterases other than neuropathy target esterase and the promotion of organophosphate polyneuropathy. Chem Res Toxicol 10:1045–1048

Moretto A, Capodicasa E, Peraica M, Lotti M (1993) Phenylmethanesulfonyl fluoride delays the recovery from crush of peripheral nerves in hens. Chem Biol Interact 87(1–3):457–462

Moretto A, Bertolazzi M, Lotti M (1994) The phosphorothioic acid O-(2-chloro-2,3,3-trifluorocyclobutyl) O-ethyl S-propyl ester exacerbates organophosphate polyneuropathy without inhibition of neuropathy target esterase. Toxicol Appl Pharmacol 129(1):133–137

Moretto A, Gardiman G, Panfilo S, Colle MA, Lock EA, Lotti M (2001) Effects of S-ethyl hexahydro-1H-azepine-1-carbothioate (molinate) on di-n-butyl dichlorovinyl phosphate (DBDCVP) neuropathy. Toxicol Sci 62(2):274–279

Moretto A, Nicolli A, Lotti M (2007) The search of the target of promotion: phenylbenzoate esterase activities in hen peripheral nerve. Toxicol Appl Pharmacol 219(2–3):196–201

Moser M, Li Y, Vaupel K, Kretzschmar D, Kluge R, Glynn P, Buettner R (2004) Placental failure and impaired vasculogenesis result in embryonic lethality for neuropathy target esterase-deficient mice. Mol Cell Biol 24(4):1667–1679

Nomura DK, Casida JE (2011) Activity-based protein profiling of organophosphorus and thiocarbamate pesticides reveals multiple serine hydrolase targets in mouse brain. J Agric Food Chem 59(7):2808–2815

Nomura DK, Leung D, Chiang KP, Quistad GB, Cravatt BF, Casida JE (2005) A brain detoxifying enzyme for organophosphorus nerve poisons. Proc Natl Acad Sci USA 102(17):6195–6200

Nomura DK, Blankman JL, Simon GM, Fujioka K, Issa RS, Ward AM, Cravatt BF, Casida JE (2008) Activation of the endocannabinoid system by organophosphorus nerve agents. Nat Chem Biol 4:373–378

Osman KA, Moretto A, Lotti M (1996) Sulfonyl fluorides and the promotion of diisopropyl fluorophosphate neuropathy. Fundam Appl Toxicol 33(2):294–297

Pamies D, Reig JA, Vilanova E, Sogorb MA (2010) Expression of neuropathy target esterase in mouse embryonic stem cells during differentiation. Arch Toxicol 84(6):481–491

Parron T, Hernandez AT, Villanueva E (1996) Increased risk of suicide with exposure to pesticides in an intensive agricultural area: a 12 year retrospective study. Forensic Sci Int 79(1):53–63

Pope CN, Padilla S (1990) Potentiation of organophosphorus-induced delayed neurotoxicity by phenylmethylsulfonyl fluoride. J Toxicol

Quistad GB, Casida JE (2004) Lysophospholipase inhibition by organophosphorus toxicants. Toxicol Appl Pharmacol 196(3):319–326

Quistad GB, Barlow C, Winrow CJ, Sparks SE, Casida JE (2003) Evidence that mouse brain neuropathy target esterase is a lysophospholipase. Proc Natl Acad Sci USA 100(13):7983–7987

Read DJ, Li Y, Chao MV, Cavanagh JB, Glynn P (2009) Neuropathy target esterase is required for adult vertebrate axon maintenance. J Neurosci 29(37):11594–11600

Vicedo JL, Carrera V, Barril J, Vilanova E (1993) Properties of partly preinhibited hen brain neuropathy target esterase. Chem Biol Interact 87(1–3):417–423

Vilanova E, Johnson MK, Vicedo JL (1987) The interaction of some unsubstituted phosphoramidates analogues of methamidophos (O, S-dimethyl phosphorothioamidate) with acetylcholinesterase and neuropathy target esterase of hen brain. Pesticide Biochem Physiol 28:224–238

Winrow CJ, Hemming ML, Allen DM, Quistad GB, Casida JE, Barlow C (2003) Loss of neuropathy target esterase in mice links organophosphate exposure to hyperactivity. Nat Genet 33(4):477–485

Xie K, Gupta RP, Abou-Donia MB (2002) Protein levels of neurofilament subunits in the hen central nervous system following prevention and potentiation of diisopropyl phosphorofluoridate (DFP)-induced delayed neurotoxicity. Biochem Pharmacol 63(1):11–19

Zaccheo O, Dinsdale D, Meacock PA, Glynn P (2004) Neuropathy target esterase and its yeast homologue degrade phosphatidylcholine to glycerophosphocholine in living cells. J Biol Chem 279(23):24024–24033

Chemico-Biological Interactions 203 (2013) 245–250

Contents lists available at SciVerse ScienceDirect

Chemico-Biological Interactions

journal homepage: www.elsevier.com/locate/chembioint

Interactions of neuropathy inducers and potentiators/promoters with soluble esterases

Jorge Estévez, Iris Mangas, Miguel Ángel Sogorb, Eugenio Vilanova *

University "Miguel Hernandez" of Elche, Institute of Bioengineering, Unit of Toxicology and Chemical Safety, Alicante, Spain

ARTICLE INFO

Article history:
Available online 28 November 2012

Keywords:
Organophosphorus
Esterases
Phenylmethylsulfonylfluoride
NTE
Neuropathy
Promotion
Potentiation

ABSTRACT

Organophosphorus compounds (OPs) cause neurotoxic disorders through interactions with well-known target esterases, such as acetylcholinesterase and neuropathy target esterase (NTE). However, the OPs can potentially interact with other esterases of unknown significance. Therefore, identifying, characterizing and elucidating the nature and functional significance of the OP-sensitive pool of esterases in the central and peripheral nervous systems need to be investigated. Kinetic models have been developed and applied by considering multi-enzymatic systems, inhibition, spontaneous reactivation, the chemical hydrolysis of the inhibitor and "ongoing inhibition" (inhibition during the substrate reaction time). These models have been applied to discriminate enzymatic components among the esterases in nerve tissues of adult chicken, this being the experimental model for delayed neuropathy and to identify different modes of interactions between OPs and soluble brain esterases. The covalent interaction with the substrate catalytic site has been demonstrated by time-progressive inhibition during ongoing inhibition. The interaction of sequential exposure to an esterase inhibitor has been tested in brain soluble fraction where exposure to one inhibitor at a non inhibitory concentration has been seen to modify sensitivity to further exposure to others. The effect has been suggested to be caused by interaction with sites other than the inhibition site at the substrate catalytic site. This kind of interaction among esterase inhibitors should be considered to study the potentiation/promotion phenomenon, which is observed when some esterase inhibitors enhance the severity of the OP induced neuropathy if they are dosed after a non neuropathic low dose of a neuropathy inducer.

1. Introduction

1.1. Esterases as targets of organophosphorus toxicity

Organophosphorus compounds (OPs) cause several neurotoxic disorders in humans [1]. Acute cholinergic toxicity is caused by covalent organophosphorylation on serine at the acetylcholinesterase catalytic center. Organophosphate-induced delayed neuropathy (OPIDN) is a neurodegeneration observed in humans, for which adult chicken is the most sensitive experimental species, and it is caused by the inhibition and subsequent aging (e.g., net dealkylation) of the membrane protein called neuropathy target esterase (NTE) [2]. Esterase inhibitors such as phenylmethylsulfonyl fluoride (PMSF) have proven capable of enhancing the severity of the OPIDN when animals are dosed after a low non neuropathic dose of a neuropathy inducer. This phenomenon is known as potentiation or promotion of neuropathy [3,4]. The term "promotion" has been suggested for this special class of potentiators because in this case the potentiation effect needs a sequential interaction, first with the substance causing the first chemical insult (the "inducer") and then with the second one ("the promoter"), using a similar nomenclature to that used in carcinogenesis. Changing the order of dosing does not cause potentiation; on the contrary, PMSF protects, thus avoiding a severe degeneration when PMSF if it is used before a high neuropathic dose of an inducer. The target of the potentiation/promotion effect remains unknown, although a soluble fraction of esterases described in our laboratory [5] has been suggested to be implicated [6].

Actions on currently recognized targets cannot explain the neurological and neurobehavioral effects reported in animals and humans caused by low-level long-term OP exposure [7–9]. Many proteins showing esterase activity other than cholinesterases and NTE have the potential for interaction with OPs. Therefore, identifying, characterizing and elucidating the nature and functional significance of the OP-sensitive pool of esterases in the central and peripheral nervous systems is an important research task to not only understand how low levels might affect cognitive effects, but to also design prevention and therapy strategies, which need investigating [10,11,12–14].

* Corresponding author. Tel.: +34 96 6658711.
E-mail address: evilanova@umh.es (E. Vilanova).

0009-2797/$ - see front matter © 2012 Elsevier Ireland Ltd. All rights reserved.
http://dx.doi.org/10.1016/j.cbi.2012.11.007

Kinetic models have been developed and applied to study complex biological preparations by considering multi-enzymatic systems, inhibition, spontaneous reactivation, the chemical hydrolysis of the inhibitor and ongoing inhibition (inhibition during the substrate reaction time) [15,16,17–20]. A summary of the mathematical models is provided in Supplementary material.

1.2. Antecedents of discrimination of enzymatic components in several tissues

The developed kinetic models have been applied in our lab to discriminate enzymatic components among esterases in nerve tissues of adult chicken (Tables 1 and 2). The interest in esterases of the adult chicken nervous system using phenyl valerate as a substrate stems from studies of OPIDN and promotion [4]. The main findings are as follows: In peripheral nerve soluble fraction, three enzymatic components (EI, EII and EIII) have been discriminated by interaction with mipafox [21], paraoxon [17], 1-(saligenin cyclic phospho)-9-biotinyldiaminononane (S9B) [16] and PMSF [19]: EII and EIIII are sensitive to all the tested inhibitors but both are spontaneously reactivated when pre-inhibited with paraoxon, EIIII is also spontaneously reactivated when it is pre-inhibited with S9B while EIII is sensitive only to S9B (Table 1).

In serum, three enzymatic components have been discriminated with mipafox [22] and paraoxon [17,22]; E1 and E2, which are sensitive to paraoxon and mipafox and are spontaneously reactivated when pre-inhibited with paraoxon; and E3, which is resistant.

In the brain, membrane enzymatic components have been discriminated according to their interaction with mipafox and paraoxon [20]: EPα is sensitive to mipafox and paraoxon, and is spontaneously reactivated when pre-inhibited with paraoxon; EPβ is sensitive to paraoxon; EPγ, identified as NTE, is sensitive to mipafox, but is resistant to paraoxon. Finally component EPδ, is resistant to mipafox and paraoxon.

In brain soluble fractions, three enzymatic components have been discriminated with mipafox, paraoxon [18] and PMSF [23] (Table 2): Eα, which is highly sensitive to mipafox and paraoxon, but resistant to PMSF, is spontaneously reactivated when pre-inhibited with paraoxon; Eβ, which is sensitive to paraoxon and PMSF, but is resistant to mipafox; Eγ, which is resistant to paraoxon, and is sensitive to mipafox and PMSF, and is the fraction named "soluble NTE" or S-NTE [24].

In this work, we present additional *in vitro* data showing examples of interactions of esterase inhibitors with the substrate (PV) and how pre-exposure of a non inhibitory concentration of one inhibitor may modify sensitivity to time-progressive inhibition by further exposure to other inhibitors. The data have been compared with previous data of the esterase components obtained in our laboratory according to kinetic criteria. The biological material used as example is the soluble fraction of chicken nerve tissue as this is the animal experimental model employed for assaying OP-delayed neuropathy and the model in which the neuropathy promotion phenomenon is usually studied.

Table 1
Enzymatic components in chicken nerve tissues. Components were discriminated using kinetic analysis of the time-progressive inhibition at several inhibitor concentrations. The kinetic models applied are described in the specific publications and are based on the approaches described by [15,19]. The proportions of the components and their corresponding I50 at 30 min are indicated. In some cases, a range is indicated in which several experiments are considered. R is the component resistant to the highest tested concentration. (r) The component is spontaneously reactivated.

Tissue Component	Proportion	Paraoxon I50 (30 min)	Mipafox I50 (30 min)	PMSF I50 (30 min)	S9B I50 (30 min)
Peripheral nerve soluble fraction[a]					
EI	41–52%	6–12 nM (r)	11–12 nM	0.58–0.77 μM	5 nM
EII	33–41%	0.24–0.26 nM (r)	69–71 nM	6.8–17 μM	0.20 nM(r)
EIII	15–22%	R	R	R	83 nM
Serum[b]					
E1	21–22%	0.43 nM (r)	>100 nM		
E2	72–75%	13.7 nM (r)	3.6–4 nM		
E3	5.0–5.6%	R	R		
Membrane fraction of brain[c]					
EPα	4–8%	15–43 nM (r)	29 nM		
EPβ	38%	1540 nM	R		
EPγ (NTE)	39–48%	R	6601 nM		
EPδ	10–11%	R	R		

[a] Extracted from [19].
[b] Extracted from [17] and [22].
[c] Extracted from [20].

Table 2
Enzymatic components in the soluble brain fraction discriminated with different inhibitors. The corresponding I50 values (30 min) are shown. For mipafox, the I50 values in the sample pre-incubated with PMSF at the indicated concentration are also provided. R is the component that is resistant to the highest tested concentration.

	Proportion (%)[a]	PMSF I50 (20 min)[a]	Paraoxon I50 (30 min)[a]	Mipafox I50 (30 min)[a]	MIPAFOX[a] I50 (30 min) pre-incubated with PMSF 20 min			
					5 μM	50 μM	150 μM	4000 μM
Eα	11–28%	R	9–11 nM (r)	4 nM	26 nM	43 nM	72 nM	222 nM
Eβ	61–84%	70 μM	1216 nM	R	R	R	*	*
Eγ	5–11%	447 μM	R	3398 nM	25.7 nM	R	R	*

(r) The component is spontaneously reactivated.
[a] Extracted from the data in [23].
* Preinhibited by PMSF.

2. Material and methods

2.1. Chemicals and biological preparations

Buffer for homogenization and enzymatic reactions: Buffer; 50 mM Tris–HCl buffer (pH 8.0) containing 1 mM EDTA. *O,O′*-Diethyl p-nitrophenyl phosphate (paraoxon, total impurities ⩽10%) and phenylmethylsulfonyl fluoride (PMSF); were obtained from Sigma–Aldrich S.A. (Madrid, Spain), *N,N′*-di-isopropyl phosphorodiamidefluoridate (mipafox, purity >98%) and phenylvalerate (PV, purity >98%)) were acquired from Lark Enterprise (Webster, MA, USA). Stock solutions of inhibitors (paraoxon, PMSF, mipafox) and substrate (PV) were prepared according to [17,18,23] and were diluted 1:30 in water (0.54 mM) immediately before use.

Tissue preparation: The soluble fraction of chicken sciatic nerve and chicken brain was prepared as previously described in [17,18].

2.2. Progressive inhibition by paraoxon and spontaneous reactivation in the presence of substrate

Inhibition assay: Samples were incubated with paraoxon in the presence of the substrate under the following conditions: 0.026 nM of paraoxon, the soluble fraction from 0.48 mg fresh tissue/ml and 267 μM of phenyl valerate (final concentrations in buffer) Aliquots (1 ml) were extracted from the reaction pool at different inhibition times and added to 1 ml of a 2% w/v SDS solution with 1.23 mM aminoantipyrine and 0.5 ml of 12.1 mM potassium hexacyanoferrate III to stop the reaction. After 10 min, absorbance was read at 510 nm. Blanks and spontaneous hydrolysis controls (samples without tissue) were assayed.

Reactivation assay: A highly concentrated preparation (0.1 ml containing the soluble fraction of sciatic nerves from 200 mg fresh tissue/ml) was inhibited with 10 nM paraoxon for 45 min in buffer a final volume of 0.11 ml. After the inhibition time the sample was diluted 1/42 with 20.89 ml of buffer and 21 ml of substrate to dilute paraoxon to 0.026 nM. Reactivation was allowed to take place for 164 min in the presence of substrate. Aliquots (1 ml) extracted from the reaction pool at different inhibition times, were treated and measured as above.

2.3. PMSF inhibition kinetics in samples pre-incubated with mipafox

Tissue samples of 182 μl (containing the soluble fraction from 24 mg/ml of brain) were incubated with 20 nM mipafox for 30 min at 37 °C in a final volume of 200 μl. Then 20 μl of PMSF solution in dimethylsulfoxide (DMSO) was added to obtain the following PMSF concentrations: 0, 20, 70, 300 or 1000 μM. Mixtures were incubated for different times (0, 1, 1.5, 3, 4.5, 6, 8, 10, 14 and 20 min) and phenylvalerate esterase activity (PVase) was measured as described by [23]. A three-dimensional model was fitted to the data (% of activity versus *t* and [I]). The time-progressive inhibition data were analyzed with the models described before in [19], which consider inhibition with a simultaneous hydrolysis of the inhibitor (see Supplementary material).

2.4. Mipafox inhibition assay in samples pre-incubated with paraoxon or paraoxon plus PMSF

Tissue samples of 160 μl (containing the soluble fraction from 50 mg/ml of brain) were incubated with 10 μM paraoxon or Tris pH 8 for 30 min at 37 °C in a final volume of 180 μl. Then 20 μl of PMSF 10 μM or DMSO was added. Afterward, mipafox solutions were added to concentrations of 0, 10, 100 and 250 μM in a final volume of 220 μl. Following incubation for 30 min at 37 °C, phenylvalerate esterase activity was measured as described by [23].

3. Results

3.1. Ongoing inhibition

Fig. 1 shows the results of inhibition and spontaneous reactivation in the presence of the substrate. Panel A in Fig. 1 shows the time progression of absorbance, while Panel B in Fig. 1 presents the percent of activity relative to control. Inhibition of phenyl valerate esterase (PVases) activity by 0.026 nM paraoxon in the presence of substrate is time-progressive (see the square points in Fig. 1B), suggesting that the ongoing inhibition is covalent inhibition. The figure also depicts an experiment in which the sample was pre-inhibited with 10 nM paraoxon for 30 min. Afterward it was diluted with buffer and substrate to the 0.026 nM of paraoxon. Therefore the spontaneous reactivation took place in the presence

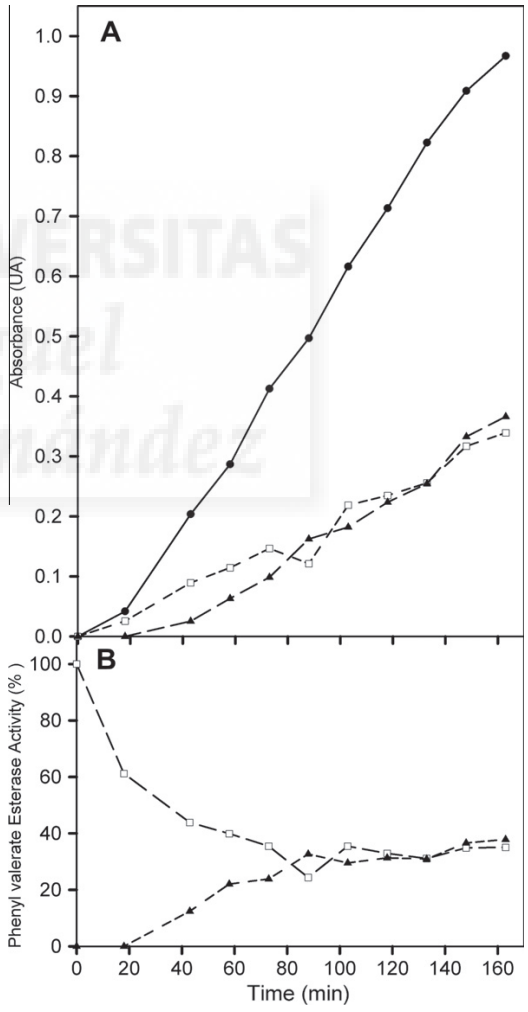

Fig. 1. Time-progressive inhibition and spontaneous reactivation in the presence of substrate. Panel A: Absorbance of (●) control samples without paraoxon (□), samples in the presence of 0.026 nM paraoxon and (▲) samples pre-inhibited with 10 nM of paraoxon and after diluted to 0.026 nM paraoxon before addition of phenyl valerate. Panel B: Percentage of absorbance of samples in Panel A relative to controls (□) in the presence of 0.026 nM paraoxon and (▲) when the pre-inhibited sample was diluted (residual concentration of 0.026 nM paraoxon). The controls used were the samples without paraoxon, as shown in Panel A (●). Each point represents the mean of three replicates (SD < 5%).

Table 3
Kinetic parameters of the inhibition by PMSF of resistant brain soluble esterases after pre-incubation with 20 nM mipafox. Samples were pre-incubated for 30 min with 20 nM mipafox and then time-progressive inhibition by PMSF was assayed. The kinetic parameters were deduced by analyzing the data with a kinetic model equation of two sensitive components, and by considering the spontaneous hydrolysis of PMSF (kh) and a significant ongoing inhibition (ka′) of the most sensitive component (Eα). (A) No pre-incubation with mipafox (data taken from [23]); (B) Pre-incubation with 20 nM mipafox (the original data in this work).

		Component Eα	Component Eβ				Component Eγ		
kh (min^{-1})		Eα (%)	ka′ (μM^{-1})	Eβ (%)	kβ (μM^{-1} min^{-1})	$I50^{20}$ (μM)	Eγ (%)	kγ (μM^{-1} min^{-1})	$I50^{20}$ (μM)
(A)	0.23	28*	0.0005	61	0.0023	70	11	0.00036	447
(B)	0.28	–**	0.0007	71	0.0026	76	9	0.000026	7560

* Sensitive to mipafox but resistant to PMSF.
** Inhibited by preincubation with mipafox.

of substrate and was also time-progressive, a process we call "ongoing reactivation".

3.2. Change of sensitivity of the different enzymatic components in the brain soluble fraction to an inhibitor once pre-incubated with another inhibitor

The brain soluble fraction was pre-incubated for 30 min with 20 nM mipafox. In accordance with [18] the component Eα was expected to be completely inhibited and Eβ and Eγ were expected to remain unaltered (see I50 in Table 3). The fraction resistant to 20 nM mipafox was 80% of the total esterase activity. This residual activity was tested for a time-progressive inhibition with different concentrations of PMSF (Fig. 2A). The data extrapolated to zero inhibition time with PMSF (Fig. 2B) indicate that ongoing inhibition during the substrate incubation under the assay conditions was significant (36% for the highest PMSF concentration). Therefore, ongoing inhibition during substrate incubation was considered in the model and also the chemical hydrolysis of PMSF; the tridimensional fittings are shown in Fig. 2C. Two sensitive components of 88.4% and 11.6% were estimated according to the best fitting model (according to the *F*-test); they represent 71% and 9% of total PVase, respectively. The resulting alterations of the kinetic parameters are provided in Table 3, and they have been compared with the parameters of PMSF inhibition with no pre-incubation with mipafox. Eβ showed a similar inhibition constant and I50 value to the non pre-incubated sample, but the Eγ inhibition constant with mipafox was one order of magnitude lower and the I50 value was more than 10-fold higher, but a similar proportion was observed.

In another experiment (Table 4), the brain soluble fraction was pre-incubated with 10 μM paraoxon, which might inhibit Eα and Eβ according to [18]. Residual activity is component Eγ, which is resistant to paraoxon and sensitive to mipafox. It was then incubated with 10, 100 and 250 μM mipafox. The observed inhibition was much lower than expected for the properties deduced for Eγ in the non pre-incubated samples. Similar experiments were done by including pre-incubation with 10 μM paraoxon for 30 min followed by 20 min with 10 μM PMSF, which was not expected to cause significant inhibition of component Eγ. Once again, the inhibition observed after further incubation with mipafox showed less inhibition than expected (Table 4).

4. Discussion

4.1. "Ongoing inhibition" during the substrate reaction.

Several enzymatic components had been discriminated among esterases in nerve tissues of adult chicken (Table 1) by applying the different kinetic models described in the Supplementary material. These kinetic models are based on reactions where the inhibitor interacts with the catalytic center of an enzyme.

Inhibition by I OP compounds and other serine-esterase inhibitors, such as PMSF, is time-progressive, thus evidencing that this inhibition is due to a covalent reaction. It is usually interpreted to be due to the phosphorylation of the serine group at the active center. However, inhibition is normally tested in the absence of the substrate; subsequently, the substrate is added to measure residual activity. In this paper, we describe specific experiments showing the interaction of paraoxon in the hydrolysis of phenylvalerate (substrate) by soluble esterases of the peripheral nerve. This tissue was chosen because around 85% of total activity is able to be spontaneously reactivated once it is preinhibited by paraoxon [17]. Paraoxon is able to block the enzymatic reaction in the presence of the substrate ("ongoing inhibition") in a time-progressive manner, indicating that a covalent reaction takes place. In addition, the soluble esterases pre-inhibited with paraoxon are able to be spontaneously reactivate in the presence of the substrate ("ongoing reactivation"); this reaction is also time-progressive, thus evidencing that this spontaneous reactivation is mediated by a covalent reaction. Ongoing inhibition was also observed to a greater or lesser extent in the soluble esterases of the peripheral nerve with S9B, paraoxon and PMSF [16,17,19], soluble esterases and membrane esterases of brain with mipafox, paraoxon and PMSF [18,20,23], and serum with paraoxon [17]. Therefore, it may be necessary to introduce "ongoing inhibition" and "ongoing reactivation", when significant, into the kinetic model if a precise analysis is the objective.

4.2. Interaction among inhibitors: changes in the sensitivity in samples pre-incubated with other inhibitors

Recently Mangas and coworkers [23] reported experiments done by pre-incubating the brain soluble fraction with PMSF and by subsequently performing the kinetic analysis of progressive inhibition by mipafox on residual PMSF resistant activity. A summary of the observations is provided in Table 2. Enzymatic component Eα was resistant to PMSF and highly sensitive to mipafox, but sensitivity to mipafox inhibition lowered when the soluble fraction was pre-incubated with increasing PMSF concentrations. Component Eγ (sensitive to PMSF and mipafox) becomes resistant to mipafox after pre-incubation at a low PMSF concentration, which causes only partial inhibition. These results were interpreted as the covalent irreversible interaction of PMSF at sites other than the substrate catalytic center because the PMSF was quickly removed through chemical hydrolysis. It was suggested that this kind of interaction should be considered to interpret the potentiation/promotion phenomenon of PMSF.

The promotion effect appears when some non neuropathic esterase inhibitors (non neuropathic inhibitors) are dosed after a low non neuropathic dose of a neuropathy inducer [4]. According to this temporal sequence the inhibition experiment with PMSF was performed with the soluble fraction of brain previously preincubated with mipafox. The data provided in Results suggest that component Eγ is not inhibited by 20 nM mipafox in the brain sol-

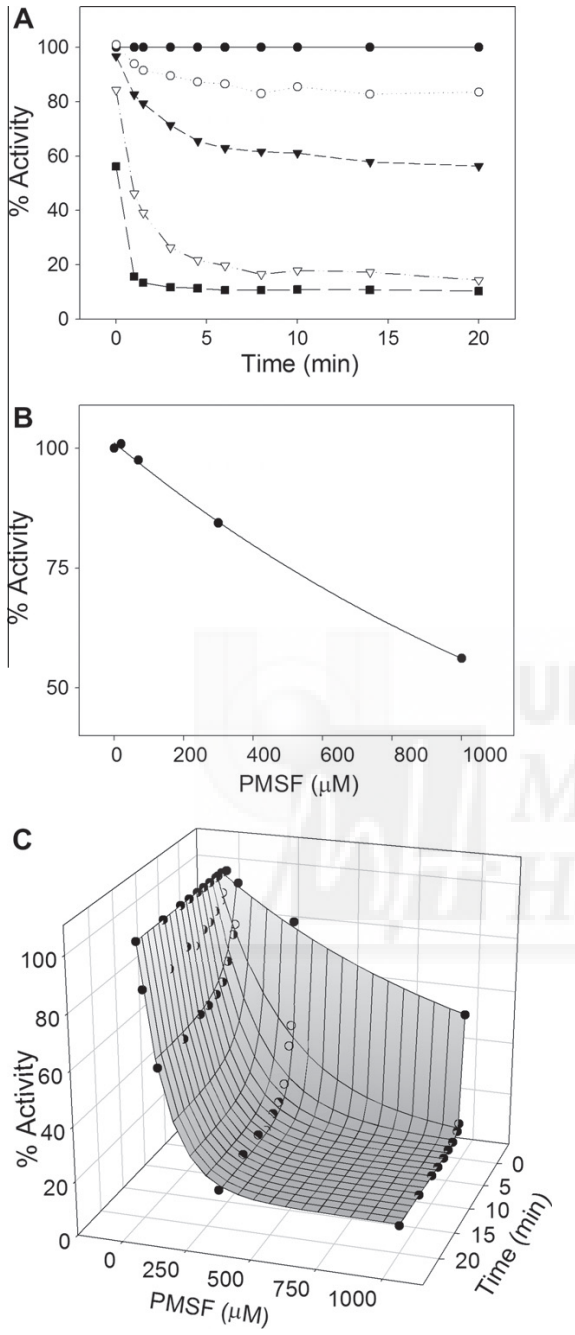

Fig. 2. Kinetics of the time-progressive inhibition by PMSF of the mipafox pre-inhibited soluble esterases. Preparations containing the soluble fraction of 24 mg fresh tissue/ml were pre-incubated with 20 nM mipafox for 30 min at 37 °C (100% of activity is the 20 nM mipafox resistant fraction). Afterward, samples were incubated with 0, 20, 70, 300 or 1000 μM PMSF (upper to lower plots) for the indicated time. The panels represent a single experiment and each point represents the mean of three replicates (SD < 5%). Panel A shows the time-progressive inhibition for each concentration. Panel B shows inhibition at the reaction time with the substrate (zero time inhibition, "ongoing inhibition"). Panel C provides the inhibitory surface obtained by fitting the 3D model equation to the data. The surface reflects the result of the best fitting model according to the *F*-test.

Table 4
Inhibition by mipafox in component Eγ after pre-incubation with paraoxon. The percentage inhibition expected of component Eγ after inhibition with mipafox in non pre-incubated samples was calculated from the kinetic parameters obtained for the inhibition with mipafox in [18].

Pre-incubation	% Inhibition of the Eγ component with mipafox			
	(0 μM)	(10 μM)	(100 μM)	(250 μM)
10 μM paraoxon–DMSO	0	15.2	34.8	36.6
10 μM paraoxon–10 μM PMSF	0	26.4	39.5	43.6
% Inhibition expected without preincubation:	0	59.4	100	100

uble fraction. However, when the sample is pre-incubated at this mipafox concentration, it displays much less sensitivity to PMSF with a I50 value one order of magnitude higher to that deduced when analyzing the non pretreated sample (Table 3) but Eβ shows the same sensitivity to the non pre-incubated sample. Interaction between mipafox and PMSF in the active center was not expected because the mipafox concentration was much lower than the PMSF concentration (nM versus μM).

In addition the enzymatic component Eγ (resistant to paraoxon, but sensitive to mipafox and PMSF) becomes more resistant to mipafox and shows less inhibition than expected (Table 4) once the soluble brain fraction is pre-incubated with paraoxon (10 μM) or paraoxon (10 μM) plus PMSF (10 μM), The interaction between paraoxon or PMSF and mipafox in the active center is not expected because the concentration of paraoxon or PMSF is lower (25-fold lower) than the higher concentration of mipafox used.

The percentages of the activity of the enzymatic components are similar in the preincubated and the non-preincubated samples. This suggests that the catalysis of the substrate (phenylvalerate) is not modified and that the changes in sensitivity to these inhibitors noted after pre-incubating the brain soluble fraction with PMSF, mipafox or paraoxon may be mediated by other centers.

Vicedo and coworkers [25] studied the interaction of PMSF and DFP in the inhibition of brain membrane NTE activity (resistant to paraoxon and sensitive to mipafox; EPγ in Table 1). No alteration in the inhibition kinetics of DFP was observed for the residual activity after pre-incubation with PMSF, and vice versa.

4.3. Final remarks

The target site of time-progressive inhibition most probably occurs at the active catalytic site, as demonstrated in well-known serine esterases, such as cholinesterases and NTE. In this paper, our data on inhibition in the presence of the substrate are also compatible with the usually accepted hypothesis that inhibition is due to covalent organophosphorylation by OPs (sulfonylation by PMSF) at the substrate catalytic center. However, the interaction by which pre-incubation at a non inhibitory concentration changes the sensitivity of some enzymatic components to other inhibitors is most probably due to interaction at sites other than the substrate catalytic center because it is caused at concentrations that do not provoke *per se* significant inhibition. Such interactions should be considered in order to interpret the potentiation/promotion phenomenon of PMSF, and to understand the effects of multiple exposures to chemicals. The fact that some esterases are not inhibited by PMSF or mipafox does not mean they should be rejected as potential targets of the "promotion" phenomenon caused by PMSF because the interactions with other non esterase sites

seem to modify the protein properties and probably affect their actual biological function.

Acknowledgments

Thanks to Helen Warburton and to Oksana Lockridge for their help in English language editing. This work was supported by the institutional funds from the University Miguel Hernández, Elche.

Appendix A. Supplementary data

Supplementary data associated with this article can be found, in the online version, at http://dx.doi.org/10.1016/j.cbi.2012.11.007.

References

[1] M. Jokanović, M. Kosanović, Neurotoxic effects in patients poisoned with organophosphorus pesticides, Environ. Toxicol. Pharmacol. 29 (3) (2010) 195–201.
[2] M.K. Johnson, The primary biochemical lesion leading to the delayed neurotoxic effects of some organophosphorus esters, J. Neurochem. 23 (October 4 1974) 785–789.
[3] C.N. Pope, S. Padilla, Potentiation of organophosphorus-induced delayed neurotoxicity by phenylmethylsulfonyl fluoride, J. Toxicol. Environ. Health 31 (1990) 261–273.
[4] M. Lotti, S. Caroldi, E. Capodicasa, A. Moretto, Promotion of organophosphate-induced delayed polyneuropathy by phenylmethanesulfonyl fluoride, Toxicol. Appl. Pharmacol. 108 (1991) 234–241.
[5] M.A. Escudero, M.V. Céspedes, E. Vilanova, Chromatographic discrimination of soluble neuropathy target esterase isoenzymes and related phenyl valerate esterases from chicken brain, spinal cord, and sciatic nerve, J. Neurochem. 68 (5) (1997) 2170–2176.
[6] A. Gambalunga, F. Pasqualato, M. Lotti, Soluble phenyl valerate esterases of hen sciatic nerve and the potentiation of organophosphate induced delayed polyneuropathy, Chem. Biol. Interact. 187 (1–3) (September 6 2010) 340–343.
[7] COT Report, Organophosphates, A report of the Committee on Toxicology of Chemicals in Food, Consumer Products and the Environment, UK Department of Health, London, 1999.
[8] G.A. Jamal, S. Hansen, P.O. Julu, Low level exposures to organophosphorus esters may cause neurotoxicity, Toxicology 181–182 (2002) 23–33.
[9] M.L. Middlemore-Risher, J.J. Buccafusco, A.V. Terry, Repeated exposures to low-level chlorpyrifos results in impairments in sustained attention and increased impulsivity in rats, Neurotoxicol. Teratol. 32 (2010) 415–424.
[10] M.A. Sogorb, E. Vilanova, V. Carrera, Future applications of phosphotriesterases in the prophylaxis and treatment of organophosphorus insecticide and nerve agent poisonings, Toxicol. Lett. 151 (1) (2004) 219–233.
[11] F. Worek, H. Thiermann, L. Szinicz, P. Eyer, Kinetic analysis of interactions between human acetylcholinesterase, structurally different organophosphorus compounds and oximes, Biochem. Pharmacol. 68 (2004) 2237–2248.
[12] F. Worek, N. Aurbek, M. Koller, C. Becker, P. Eyer, H. Thiermann, Kinetic analysis of reactivation and aging of human acetylcholinesterase inhibited by different phosphoramidates, Biochem. Pharmacol. 73 (11) (2007) 1807–1817.
[13] E. Ray, P.G. Richards, The potential for toxic effects of chronic, low-dose exposure to organophosphates, Toxicol. Lett. (2001) 343–351.
[14] M.A. Sogorb, E. Vilanova, Detoxication of anticholinesterase pesticides, in: T. Satoh, R.G. Gupta (Eds.), Anticholinesterase Pesticides: Metabolism, Neurotoxicity, and Epidemiology, John Willey & Sons, 2010, pp. 121–133. ISBN 978-0-470-41030-1.
[15] J. Estévez, E. Vilanova, Model equations for the kinetics of covalent irreversible enzyme inhibition and spontaneous reactivation: esterases and organophosphorus compounds, Crit. Rev. Toxicol. 39 (5) (2009) 427–448.
[16] J. Estévez, J. Barril, E. Vilanova, Inhibition with spontaneous reactivation and the ongoing inhibition effect of esterases by biotinylated organophosphorus compounds: S9B as a model, Chem. Biol. Interact. 187 (2010) 397–402.
[17] J. Estévez, A. García-Pérez, J. Barril, E. Vilanova, Inhibition with spontaneous reactivation of carboxyl esterases by organophosphorus compounds: paraoxon as a model, Chem. Res. Toxicol. 24 (2011) 135–143.
[18] I. Mangas, E. Vilanova, J. Estévez, Kinetics of the inhibitory interaction of organophosphorus neuropathy inducers and non-inducers in soluble esterases in the avian nervous system, Toxicol. Appl. Pharmacol. 256 (2011) 360–368.
[19] J. Estévez, J. Barril, E. Vilanova, Kinetics of inhibition of soluble peripheral nerve esterases by PMSF: a non-stable compound that potentiates the organophosphorus-induced delayed neurotoxicity, Arch. Toxicol. 86 (5) (2012) 767–777.
[20] I. Mangas, E. Vilanova, J. Estévez, NTE and non-NTE esterases in brain membrane: kinetic characterization with organophosphates, Toxicology 297 (1–3) (2012) 17–25.
[21] J. Estévez, A. García-Pérez, J. Barril, M.C. Pellín, E. Vilanova, The inhibition of the high sensitive peripherals nerve soluble esterases by mipafox. A new mathematical processing for the kinetics of inhibition of esterases by organophosphorus compounds, Toxicol. Lett. 151 (2004) 243–249.
[22] A.G. García-Pérez, J. Barril, J. Estévez, E. Vilanova, Properties of phenyl valerate esterase activities from chicken serum are comparable with soluble esterases of peripheral nerves in relation with organophosphorus compounds inhibition?, Toxicol Lett. 142 (1–2) (2003) 1–10.
[23] I. Mangas, E. Vilanova, J. Estévez, Phenylmethylsulfonyl fluoride -a promoter of neuropathy- alters the interaction of organophosphorus compounds with soluble brain esterases, Chem. Res. Toxicol. (2012), http://dx.doi.org/10.1021/tx300257ptx300257p.
[24] E. Vilanova, M.A. Escudero, J. Barril, NTE soluble isoforms: new perspectives for targets of neuropathy inducers and promoters, Chem. Biol. Interact. 119–120 (1999) 525–540.
[25] J.L. Vicedo, V. Carrera, J. Barril, E. Vilanova, Properties of partly preinhibited hen brain neuropathy target esterase, Chem. Biol. Interact. 87 (1–3) (1993) 417–423.

5.2. Submitted paper

UNIVERSITAS
Miguel
Hernández

SEPARATING ESTERASE TARGETS OF ORGANOPHOSPHORUS COMPOUNDS IN THE BRAIN BY PREPARATIVE CHROMATOGRAPHY

Mangas I., Vilanova E., Benabent M., Estévez J.

University "Miguel Hernandez" of Elche (Alicante, Spain). Institute of Bioengineering. Unit of Toxicology and Chemical Safety

(*) Corresponding author imangas@umh.es

Abstract

Low level exposure to organophosphorus esters (OPs) may cause long-term neurological effects and affect specific cognition domains in experimental animals and humans. Most of these effects cannot be explained by action on known targets. Soluble carboxylesterases (EC 3.1.1.1) of chicken brain have been kinetically discriminated using paraoxon, mipafox and phenylmethyl sulfonilfluoride as inhibitors and phenyl valerate as a substrate. Three different enzymatic components were discriminated and called Eα, Eβ and Eγ. In this work, a fractionation procedure with various steps was developed using protein native separation methods by preparative HPLC. Gel permeation chromatography followed by ion exchange chromatography allowed enriched fractions with different kinetic behaviours. The soluble fraction of chicken brain was fractionated and total esterase activity, proteins and enzymatic components Eα, Eβ and Eγ were monitored in each subfraction. After the analysis, 13 fractions were pooled and conserved. The preincubation of the soluble fraction of chicken brain with the organophosphorus mipafox gave rise to a major change in the ion exchange chromatography profile, but not in the molecular exchanged chromatography profile, suggesting that mipafox permanently modifies the ionic properties of numerous proteins.

Keywords

Organophosphorus compounds, neurotoxicity targets, carboxylesterases, serine hydrolases, OPIDN, protein separation, chromatography

INTRODUCTION

Organophosphorus compounds (OPs) and unknown neurotoxicological targets

Organophosphorus compounds (OPs) have been used for several purposes, but mainly pesticides and warfare agents. However, the amount of OPs pesticides being used is declining, especially in developed countries. Notwithstanding, OPs continue to be one of the most important classes of insecticides today (Casida and Durkin., 2013), and it has been reported that 96% of individuals in the US have measurable levels of OPs chlorpyrifos metabolites in their urine (Barr et al., 2004). These compounds can cause several neurotoxic disorders, some of them with molecular identified targets (the cholinergic crisis, the intermediate syndrome and OPIDN), and others with no molecular targets identified to date and their mechanisms are misunderstood (neurobehavioral and cognition long-term toxicity, chronic neuropsychological effects, potentiation of OPIDN, etc; Roldán-Tapia et al., 2005; Jamal et al., 2002; COT report, 1999; Ray and Richards., 2001).

Acute cholinergic toxicity is caused by covalent organophosphorylation at the acetylcholinesterase catalytic center. Organophosphate-induced delayed neuropathy (OPIDN) is caused by the inhibition and subsequent aging (dealkylation) of the membrane protein called neuropathy target esterase (NTE; Glynn 1999; Glynn 2000). . The intermediate syndrome it is likely a delayed effect of acetylcholinesterase inhibition and acetylcholine accumulation.

However, an increasing number of epidemiological and animal studies have associated subtle, long term central nervous system neurotoxicity -neurobehavioral, cognitive and neuropsychological consequences- with past overt OP, which cannot be explained with known targets (Brown and Brix., 1998; Parrón et al., 2011; Roldán-Tapia et al., 2005; Yokoyama et al., 1998; Hoffman et al., 2007; Liu et al., 1999). Despite the number of epidemiological studies and several reviews on this topic having been published, the authors have reached conflicting conclusions probably due to the different studies design. Ross and colleagues (2013) used the meta-analysis to quantify and evaluate data published in 14 studies with more than 1600 participants occupationally exposed to long-term low-levels of OPs, defined as repeated or prolonged exposure to doses that do not produce recognized clinical symptoms of acute toxicity. They concluded that there is sufficient evidence to accept a significant association between low-level exposure to OPs and impaired neurobehavioral function. However, what do not come over clearly are the exact exposure conditions, if these effects exist at doses lower than the cholinesterase inhibition. The need to investigate how specific low-level OPs affect

certain cognition domains and the neurobiological substrates of these effects has been emphasized (Casida and Quistad., 2004). Ray and Richards., (2001) reviewed data until 2001 and they proposed that any chronic effects of low-level exposures would likely occur via a mechanism that is independent of AChE inhibition.

Potentiation of neuropathy is a neurotoxic effect caused by some esterase inhibitors, not only by some OPs, but also by some carbamates and sulfonylfluorides (e.g., PMSF), when potentiators are administered to hens in conjunction with OPs causing OPIDN, and neurotoxicity is enhanced (Pope and Padilla., 1990; Lotti et al., 1991). Despite the efforts made either the mechanism or the target for potentiation remains unknown. It has been reported that, given the chemical nature of promoters, the target has to be a similar esterase to NTE and it is likely to hydrolyze the same substrate (Moretto et al., 1994; Céspedes et al., 1997).

Potential unknown molecular targets of OPs toxicity

Many enzyme systems have the potential for interaction with specific OPs and the possibility of the existence of noncholinergic, non-neuropathic targets have been elucidated by various approaches: (1) The AChE knockout mouse display no AChE activity in any tissue and is supersensitive to OP toxicity (Lockdridge and Schopfer, 2006); (2) Secondary target effects that are not specific of AChE inhibitors were observed in zebra fish (Behra et al., 2004); (3) Different OP pesticides cause different degrees of toxicity despite similar levels of AChE inhibition (Pope., 1999); (4) There is no correlation between AChE inhibition and the disposition of [3H]-soman, [3H]-DFP and [3H]-sarin in the brain (Little et al., 1988); (5) Low doses of OP inhibitors produce distinct effects that depend on the identity of the OP (Moser., 1995); (6) Low levels of chlorpyrifos impaired cognitive function without significantly inhibiting AChE activity and without down regulating cholinergic receptors in rats (Jett et al., 2001) and (7) Biotinylated OP FP-biotin labels at least 12 proteins in mouse plasma at doses without cholinergic effects (Peeples et al., 2005).In addition to the known cholinesterases and NTE, others proteins have been observed to covalently bind to OP in experimental assays and *in vitro* experiments: other serine esterases (KIAA1363 protein, monoacylglycerol lipase, fatty acid amide hydrolase, kynurenine formamidase..), muscarinic receptors and other unknown targets (Casida and Quistad., 2004; Nomura et al., 2008; Nomura and Casida., 2011; Richards et al., 1999, Richards et al., 2000; Murray et al., 2003; Murray et al., 2005). A long these lines, most of the OPs molecular targets so far identified are esterases and lucidating the nature and functional significance of all the OP-sensitive pool of esterases in the central nervous system to find novel toxicologically relevant target proteins is an important research task.

Unknown OPs sensitive esterases in nerve tissues

Kinetic models have been developed and applied to identify OP-binding enzymes in complex biological preparations. These models consider multi-enzymatic systems with inhibition, spontaneous reactivation, chemical hydrolysis of inhibitor and ongoing inhibition or inhibition during the substrate reaction time. The enzymatic components among esterases in nerve tissues of adult chicken have been discriminated using these models and esterases that are highly sensitive to OPs have been described in the soluble fractions of chicken peripheral nerve, chicken brain and chicken serum (Barril et al., 1999; Garcia et al., 2003; Estévez et al., 2004; Estévez and Vilanova, 2009; Estévez et al., 2010; Estévez et al., 2011; Estévez et al., 2012; Mangas et al., 2011; 2012b), and in the membrane fraction of chicken brain (Mangas et al., 2012a; Mangas et al., 2013). It has been suggested that these esterases play potential roles in toxicity and/or detoxication during low-dose long-term exposure to organophosphorus compounds, which warrants further research.

Special attention has been paid to the phenyl valerate esterases of soluble fractions of chicken brain interacting with OPs (Mangas et al., 2011; 2012b; Estévez et al., 2013). Three enzymatic components have been discriminated with mipafox (an inducer of OPIDN), paraoxon (a non-inducer of OPIDN, and PMSF (an inhibitor model of OPIDN potentiation). These esterase components have been called: Eα, which is highly sensitive to mipafox and paraoxon, but resistant to PMSF, and is spontaneously reactivated when pre-inhibited with paraoxon; Eβ, which is sensitive to paraoxon and PMSF, but resistant to mipafox; Eγ, which is resistant to paraoxon, sensitive to mipafox and PMSF, which is the fraction that has been named "soluble NTE" or S-NTE (Vilanova et al., 1990). The high sensitivity of Eα to paraoxon and mipafox suggests that it might play a role in toxicity in low-level long-term exposure of organophosphate compounds, and that it may be relevant only in chronic exposure given it is spontaneously reactivated after paraoxon inhibition. In components Eα and Eγ, the exposure to an esterase inhibitor has been seen to modify sensitivity to further exposure to others without any interaction with the hydrolysis of the substrate. Eα becomes less sensitive to PMSF when the preparation is pretreated with mipafox (Mangas et al., 2012b), and is less sensitive to mipafox or to paraoxon after pre-exposure to PMSF (Estévez et al., 2013). Moreover, component Eα loses its spontaneous reactivation capability after pre-exposure to PMSF. The I50 (30 min) of component Eγ to mipafox increases with the PMSF concentration used in pre-incubation and Eγ becomes less sensitive to mipafox or paraoxon after pre-incubation with PMSF (Mangas et al., 2012a; Estévez et al., 2013). It has been suggested that such interactions could be related to the potentiation of the OPIDN effect (Mangas et al., 2012b; Estévez et al., 2013). A simple

method using two mipafox concentrations to discriminate these three components has been proposed (Figure 1; Mangas et al., 2011).

Aims

In this work, esterase components that are sensitive to OPs in a soluble fraction of chicken brain have been fractionated using various preparative high performance chromatography steps. The distribution of the different enzymatic components has been studied in the several fractions obtained. This procedure has concentrated on the proteins in the soluble fraction of chicken brain that interact with OPs. Enriched samples were obtained with enzymatic activities of toxicological interest. The protein profile after inhibition with mipafox was studied, while the ion exchanged chromatography profile of proteins after treatment with mipafox revealed that numerous proteins peaks changed.

MATERIAL AND METHODS

Chemicals and biological preparations

Homogenization buffer: 50 mM Tris-HCl buffer (pH 8.0) containing 1 mM EDTA, N, N´- diisopropyl phosphorodiamidefluoridate (mipafox, purity >98%) and phenyl valerate were acquired from Lark Enterprise (Webster, MA, USA).

A stock solution of 10 mM mipafox was prepared in 10 mM Tris-citrate buffer (pH 6.0) and was diluted in homogenization buffer (pH 8.0) immediately before the kinetic assays. A stock solution of substrate phenyl valerate (16.8 mM) was prepared in dried N, N- diethylformamide, and diluted in water to 0.54 mM immediately before the enzymatic assays. All the other chemicals were of analytical reagent grade.

Tissue preparation

Broiler chicken brains (n=15) were obtained from a commercial slaughtering house immediately after animals were killed and were kept in cold (0-5ºC) homogenization buffer until use. They were homogenized with a Polytron homogenizer (Kinematica Gmbh, Germany) using a PTA 10S head (dispersing aggregates at 70% power (3x30 seconds) at a concentration of 200 mg fresh tissue/ml in the same buffer.

Subcellular fractionating

The homogenized tissue was centrifuged at 1,000xg for 10 min (4ºC) to precipitate fibers and nuclei. The supernatant was centrifuged at 100,000xg for 60 min to obtain the soluble fraction of chicken brain. Samples were frozen in liquid nitrogen before use.

Mipafox inhibition microassay

Based on the phenyl valerate esterase components discrimination method published in (Mangas et al., 2011), a microassay was developed using the Biomek 2000 Automatized Workstation (Beckman Instruments, Spain). Tissue samples of 100 µl (containing the soluble fraction from 20 mg/ml of brain or equivalent phenyl valerate esterase activity) were incubated with 25 µM mipafox, 25 nM mipafox or homogenization buffer in controls for 30 min at 37ºC at a final volume of 110 µl. Then phenyl valerate esterase activity was measured as described by (Figure 1; Mangas et al., 2011). The following activities were assayed: A activity (total PVase activity), B activity (25 nM mipafox-resistant PVase), C activity (25µM mipafox resistant PVase), Eα (sensitive to 25 nM mipafox) calculated as the difference (A-B) activities, Eβ (resistant to 25 µM mipafox) calculated as the activity of C and Eγ (sensitive to micromolar concentration of mipafox) calculated as the difference of (B-C) activities.

Protein determination

Protein was measured according to Bradford (1976), adapted to a robotic microassay in a Biomek 2000 (Beckman) workstation, using from 10-70 µl of sample. Protein was estimated with a calibration curve of BSA standards.

Ultrafiltration for protein concentration

A volume of up to 15 ml was introduced into Ultracel-Amicon Ultra-15 (Millipore Corporation, Spain) filters, with a pore size of 3 KDa or 10 KDa. This was centrifuged at 4,000×g at 4ºC for the time required to concentrate the samples to the volume required. PVase activity recovered in the concentrated solution after ultrafiltration of the soluble fraction from sciatic nerves at pH 8 was >98% and the recovered protein measured by Bradford were around 70-80%.

Fractionation procedure

A volume of 80 ml of soluble brain fraction (at a concentration of 200 mg fresh tissue/ml) was defrost at 37ºC and concentrate by Ultrafiltration with 10 KDa Millipore filters at 4ºC up to 3.5 ml (corresponding to ~ 1700 mg of original fresh tissue per milliliter). High performed liquid chromatography was performed in a UFLC Shimadzu equipped with a fraction collector at 4ºC as follows:

Molecular exclusion chromatography was performed at 4°C in a 300 x 7.8 mm BioSep-SEC-s3000 (part no: 00H-2146-KO), balanced with 50 mM Tris buffer at pH 7.5. Fifty consecutive injections of 200 µl were performed in the molecular exclusion chromatography procedure, which was eluted in the column with 50 mM Tris /1 mM EDTA pH 7.5 buffer at a flow rate of 1 ml/min, and 30 x 0.5 ml fractions were obtained for each injection. The subfractions corresponding to the 50 consecutive chromatograms were collected and accumulated in the same tubes. Absorbance at 280 nm was recorded continuously, while protein and enzymatic activities were measured in each subfraction. The dead volume was determined by the elution volume of dextrane blue (VD', = 5, 489 ml). The elution volume of potassium ferricyanide (Ver = 11, 304 ml) was used to calculate the inclusion volume (Vi = Ver - V, = 5, 815 ml). The column was calibrated using standard proteins, as shown in Figure 1 (Gel Filtration Markers Kit-Sigma Aldrich for proteins to 29 KDa to 700 KDa), Albumin, bovine serum, 66,000 MW; Alcohol Dehydrogenase, yeast, 150,000 MW ; β-Amylase, sweet potato, 200,000 MW; Apoferritin, horse spleen; Blue dextran, 2,000,000 MW; Carbonic Anhydrase, bovine erythrocytes, 29,000; Thyroglobulin, bovine, 669,000 MW. Molecular weights were calculated by making comparisons with a calibration curve using standard proteins (MW-GF-1000 Kit, Sigma Chem. Co.) and plotting log (MW) versus (kD). The behavior within the molecular weight range used was linear, with a correlation coefficient of 0.994 (Figure 2).

Ion exchange chromatography of the samples obtained in the molecular exclusion chromatography was performed at 4°C in a 75 x 7.8 mm BioSep-DEAE-PEI (part no: CHO-1680), balanced with 50 mM Tris buffer pH 7.5. A 2-ml volume from the previous fractionation step was eluted in the column with 50 mM Tris /1 mM EDTA pH 7.5 buffer at a flow rate of 1 ml/min. Samples were eluted at the 1 ml/min[1] flow rate. A stepwise gradient with 0.5 M NaCl was optimized per sample applied, 50 subfractions of 1.2 ml were collected at 4ºC and the subfractions corresponding to two consecutive chromatograms accumulated in the same tubes. Absorbance at 280 nm was recorded continuously, while protein and enzymatic activities were measured in each subfraction.

Chromatography of the samples inhibited by mipafox

A 15-ml volume of the soluble fraction of chicken brain was thawed and divided into two samples: one was incubated with 25 µM mipafox and the other (control) with homogenization buffer for 30 min at 37ºC. Afterwards, samples were diluted up to 15 ml with an ultrafiltrate of a 10 KDa pore size, the procedure was repeated twice and each sample was concentrated up to 1.2 ml. Then six consecutive injections of 0.2 ml were done by the molecular exclusion chromatography procedure per sample (inhibited

and control), and 30 subfractions of 0.5 ml were obtained per injection at 4ºC. The collected subfractions were pooled and centrifuged at 4,000×g at 4ºC for the time needed to reach a volume of 2 ml.. This 2-ml volume was eluted in the ion-exchanged column at 4°C (BioSep-DEAE-PEI, part No: CHO-1680) with 50 mM Tris /1 mM EDTA pH 7.5 buffer at a flow rate of 1 ml/min. The same stepwise gradient with 0.5 M NaCl was used.

RESULTS

Fractionation by molecular exclusion chromatography

Figure 3 shows the profile of activity, protein and absorbance of the 30 subfractions obtained by molecular exclusion chromatography. Total PVase activity (A activity) showed three peaks (Fig. 3, upper plot). However, the activity profile of Eα (activity sensitive to 25 nM mipafox) showed just one peak. The activity profile of Eβ was distributed along the three peaks and Eγ activity showed just one peak. The lowest plot of Figure 3 shows the absorbance at the 280 nm profile of the chromatography of the 50 injections done.

Subfractions were pooled after considering the total activity profile, the distribution of the components and the protein profile as follows: Fraction S1: (Ve from 4.50 ml to 6.00 ml; total volume of 75 ml), maximum at Ve 5.25 ml, *K*d = 0.66 and an approximately MW of 1075 KDa; Fraction S2: (Ve from 6.01 to 8.50 ml; total volume of 125 ml), maximum at Ve 6.75 ml, *K*d = 1.23 and an approximately MW of 294 KDa; Fraction S3: (Ve from 8.51 ml to 9.00 ml; total volume of 25 ml), maximum at Ve of 8.75 ml, *K*d = 1.59 and an approximately MW of 52 KDa; Fraction S4: (Ve=from 9.01 to 15 ml), without enzymatic activity. **Table 1** shows the purification characteristics of fractions S1, S2, S3 and S4.

Fractionation by ion exchange chromatography

Fraction S1

Fraction S1 was underwent to the anionic exchange chromatography method (Fig. 4). More than 70% of PVase activity and around 100% of the protein were recovered (Table 2). The profile of A activity is shown along the whole chromatogram, but five different major peaks of activity were observed (Fig. 4, upper plot): However, the profile of activity of component Eα (sensitive to 25 nM mipafox) showed just three major peaks (see Fig. 4, Eα). The activity profile of component Eγ, sensitive to mipafox, displayed very poor activity (Fig. 4, Eγ). The profile of component Eβ, resistant to 25 μM mipafox, showed just two major peaks (Fig. 4, Eβ). The proteins profile at 280 nm

showed at least five different major peaks (dotted line, Fig. 4). The subfractions with PVase activity were grouped into four fractions: the S1D1 fraction (Ve=2.73-3.93 ml), containing most PVase activity with more than 98% of Eα (Table 2). The purification factor of component Eα in relation to the soluble fraction was 260 and represents more than 50% of total Eα activity in soluble chicken brain. The S1D2 fraction (Ve=14.-20.73 ml), containing the activity of components Eα and Eβ; the S1D3 fraction (Ve=20.74-26.73 ml), containing a mixture of the three components); the S1D4 fraction (Ve=26.74-35.14 ml, containing a mixture of the three components).

Fraction S2

Fraction S2 underwent anionic exchange chromatography (Fig. 5). More than 80% of PVase activity and 80% of the protein were recovered (Table 2). A major portion of protein was eluted after retention and was separated into eight major peaks. The profile of activity A showed five different peaks of activity (Fig. 5, upper plot), although the profile of activity Eα displayed just four (Fig. 5, Eα). The profile of activity Eγ (Fig. 5, Eγ) exhibited just two small peaks, while that of component Eβ showed two major peaks containing most PVase activity, which were resistant to 25 μM mipafox (Fig. 5, Eβ). The protein profile at 280 nm showed at least four different peaks (dotted line, Fig. 5). The subfractions with PVase activity were grouped into four fractions: the S2D1 fraction (Ve=2.73-5.13 ml), containing mainly activity Eα; the S2D2 fraction (Ve=17.73-18.33 ml, containing mainly Eα and a little Eβ); the S2D3 fraction (Ve from 21.93 ml to 31.53 ml, containing mainly Eβ). The S2D4 fraction (Ve= 31.53-47.13 ml, containing mainly Eβ). The majority of PVase activity was recovered in fractions S2D3 and S2D4, but mainly Eβ.

Fraction S3

Fraction S3 underwent anionic exchange chromatography (Fig. 6). More than 50% of PVase activity and 100% of the protein were recovered (Table 2). The profile of proteins showed at least six major different peaks. The profile of activity A displayed mainly four different peaks (Fig. 6, upper plot): However, the profile of Eα showed just one (Fig. 6, Eα). The profile of Eγ (Fig.6, Eγ) exhibited three peaks and that of Eβ evidenced very poor activity (Fig. 6, Eβ). Proteins were separated into at least four different peaks (dotted line, Fig. 6). The subfractions with PVase activity were grouped into four fractions: S3D1 (Ve= 1.53 -3.93 ml, containing a mixture of Eα and Eβ); S3D2 (Ve=15.93-19.53 ml, containing a mixture of the three components); S3D3 (Ve=19.53-21.93 ml, containing mainly Eγ) and S3D4 fraction (Ve from 21.93 ml to 26.73 ml, containing mainly Eγ). The majority of PVase activity was recovered in fractions S3D1, mainly component Eα, and S3D4, mainly Eγ.

Chromatography of the samples inhibited and not inhibited by mipafox

Molecular exclusion chromatography

Figure 7 shows the chromatogram of the 12 samples injected in the molecular exclusion chromatography column, six of which were inhibited first by 25 μM mipafox (black lines) and six were not (dotted lines). No difference in separation by size was observed between the chromatogram of the samples inhibited and the control ones. When considering the protein profile, the subfractions were pooled as follows: Fraction S1: (Ve=4.50-6.00 ml); Fraction S2: (Ve= 6.01-8.50 ml); Fraction S3: (Ve=8.51 - 9.00 ml). S1, S2 and S3 were pooled and ultrafiltered up to 1.2 ml.

Ion exchange chromatography

Figures 8 depicts the profiles of absorbance at 280 nM of the S1, S2 and S3 fractions (pretreated and not) during the ion exchange chromatography procedure. The chromatograms of fraction S1 (pretreated and not) are comparable and no important changes were observed after inhibition with 25 μM mipafox. However, the chromatograms of fractions S2 and S3 (pretreated and not) gave a different chromatography profile of absorbance at 280 nm, and showed numerous peak changes in the area and during the elution time after inhibition with mipafox.

DISCUSSION

Highly OPs-sensitive esterases have been kinetically discriminated in chicken brain and their inhibition has been related with the non identified-target neurotoxic effects of OPs (long term central nervous system neurotoxicity, neurobehavioral and neuropsychological effects, potentiation of OPIDN…). In order to link these sets of proteins which *in vitro* are very sensitive to OPs with their toxicological and biological relevance, a separation and isolation procedure of these proteins is necessary for further molecular identification of these enzymatic entities (Mangas et al., 2011; 2012a; 2012b; Estévez et al., 2011; 2012; 2013). In this work, the HPLC separation method was done and esterase activity and mipafox inhibition were following along a separation method. The three esterase components previously discriminated in kinetic studies were discriminated in all the obtained fractions.

The soluble fraction of chicken brain displayed phenyl valerate esterase activity of 574 nmol/min g of fresh tissue. The activity and the chromatography profile of the soluble brain fraction in BioSep s-3000 of phenyl valerate esterase activity were similar to a previous molecular exchange separation of this tissue (Escudero et al., 1997). The soluble chicken brain fraction was separated into three different fractions of PVase

activity. In this work, these fractions were pooled at 4ºC, conserved and called S1, S2 and S3. The recovery yield of protein and enzymatic activity was around 100% and the chromatography procedure was high reproducible in the more than 50 chromatograms (Fig. 3). The majority of activity was recovered in S2 (around 60% of activity), with 30% recovered in S1 and 15% in S3. The recovered protein yields were similar (19% in S1, 58% in S2 and 10 in S3), and 13% of proteins were removed in fraction S4 with no enzymatic activity. Fraction S1 contained a mixture of Eα and Eβ, fraction S2 contained mainly Eβ, while fraction S3 contained a mixture of Eγ and Eβ. The purification factor in relation to the activities noted in the soluble fraction injected from the obtained fractions was around 1 for total phenyl valerate esterase activity. However, Eα was enriched with a purification factor of 3 in S1 and of 3.3 in S3; Eγ, with a purification factor of 3.3 in S3 and Eβ, was not actually enriched in any of the fractions, and this activity was found along the whole chromatogram.

The ion exchange separation method of all these fractions allowed the separating each of these fractions in more than five different fractions with a different kinetic behavior with OPs. The protein recovery yield was around 100% in all the fractions and the recovery of enzymatic activity was around 50% in S1, 100% in S2 and 70% in S3. This loss of enzymatic activity, but not in the quantity of proteins, may be related to some modifications in the structure of proteins that inactivate them.

Several attempts and long efforts have been made to isolate the novel target proteins that interact with OPs by protein separation methods, whose results have room for improvement (Escudero et al., 1997; Richards et al., 1999; Murray et al., 2005; Richards et al., 1999; Murray et al., 2003). In this work, a simple method separates the whole group of esterases of the soluble fraction of chicken brain in a procedure lasting a few hours. Thirteen different samples with a wide range of purification factors (shown in Table 2) for the three discriminated enzymatic components were obtained. Activity Eα is completely isolate from activities Eβ and Eγ in the fraction called S1D1, moreover it has a purification factor of more than 260 as compared to the soluble fraction. Component Eβ was found in different fractions, with the highest purification factor of 9.3 in S1D1. Component Eγ was also found in different fractions, which were more enriched in S1D1 (a purification factor of 8.6), S1D2 (a purification factor of 8.6) and S3D2 (a purification factor of 8.6). The poor enriched factors of components Eβ and Eγ in the obtained fractions were related to the complexity of the problem: a wide range of proteins interacting with OPs in brain, different isoforms with the same kinetic behavior, a different oligomer complex of varying sizes (with several retention times in the gel filtration chromatography), but with the same kinetic behavior. We conclude that

the different kinetic components in the soluble fraction are actually due to several molecular entities that can be separated by preparative chromatography, and that the kinetic properties of these fractions can explain the behavior of the whole pool of esterases in the soluble fraction.

Different results were obtained when the same separation procedure was carried out with samples pretreated with mipafox. The molecular exclusion chromatography protein profile was the same when proteins were pretreated and when they were not. However distinct profiles were observed in the ion exchange chromatography of S2 and S3. No significant changes were seen in the S1-treated and the S1-untreated samples during the ion exchange chromatography process. This fact indicates that perhaps just one or a few proteins interact with mipafox in this fraction where most of the activity is component Eα. Many peaks changed in the profiles of fractions S2 and S3. These results may suggest that treatment with mipafox modifies the ionic properties of a wide range of proteins in fractions S2 and S3, where Eβ and Eγ are present, this hypothesis requires further research.

This work is needed for the further molecular characterization of these enzymatic entities to help elucidate their toxicological and biological significance. Moreover this separation methos could be useful to discriminate known esterases targets of OPs (cholinesterases and NTE). The advantage is that we have a simple procedure lasting a few hours to obtain samples of native proteins enriched with enzymatic activities. These samples seem to be simple enough to be studied in future molecular identification studies by proteomics analyses. This separation method would be used in further protein purification and molecular identification by proteomics analyses of these esterases targets of OPs.

Tables

Table 1. Purification values for the fractionation of phenyl valerate esterase activity by gel filtration chromatography from the soluble fraction of chicken brain of 160 mg of tissue prepared as the supernatant and concentrated by ultrafiltration. The indicated activity (nmol/min), specific activity (nmol/min/mg protein) and purification factor in relation to the original soluble extract

	Volume (ml)	Activity (nmol/min)/specific activity (U/mg)				protein (mg)
		Purification factor				
Fraction		**A**	**Eα**	**Eβ**	**Eγ**	
1. Soluble extract	10	9176/136	989/15	7219/107	967/14	67,2
2. S1	75	2658/183	639/44	1925/133	94/6	14,5
		1,3	**3,0**	**1,2**	**0,4**	
3. S2	125	5660/126	156/3	5227/116	277/6	44,9
		0,9	**0,2**	**1,1**	**0,4**	
4. S3	25	1385/173	383/48	662/ 83	341/43	8,0
		1,3	**3,3**	**0,8**	**3,0**	
4. S4	200	3161/298	717/68	2000/189	445/42	10,6
5. Total		9704	1179	7814	711	78
Yield (%)		106	119	108	74	116

Table 2. Purification values for the fractionation of fractions S1, S2 and S3 by ion exchange chromatography from the soluble fraction of chicken brain of 160 mg of tissue prepared as the supernatant and concentrated by ultrafiltration. The indicated activity (nmol/min), specific activity (nmol/min/mg protein) and purification factor in relation to the original soluble extract.

	Volume (ml)	Activity (nmol/min) /specific activity (U/mg)				Protein (mg)
		Purification factor				
Fraction		A	Eα	Eβ	Eγ	
1. S1 injected	2,0	1297/183	312/44	939/133	46/6	7,1
2. S1D1	1,2	165/3904	162/3834	5/114	4/86	0,0
		28,6	**260,4**	**1,1**	**6,0**	
3. S1D2	6,0	170/138	138/112	0 /0	165/135	1,2
		1,0	**7,6**	**0,0**	**9,3**	
4. S1D3	6,0	150/64	89/38	29/12	147/63	2,3
		0,5	**2,6**	**0,1**	**4,4**	
5. S1D4	8,4	147/50	54/18	19/7	269/92	2,9
		0,4	**1,2**	**0,1**	**6,4**	
6. S1D5	14,4	297/100	88/30	36/12	456/154	3,0
		0,7	**2,0**	**0,1**	**10,7**	
Yield S1 (%)		**72**	**170**	**111**	**148**	**134**
1. S2 injected	2,0	2695/123	76/4	2550 /116	135/6	21,9
2. S2D1	2,4	75/58	69/53	6/5	16 / 12	1,3
		0,4	**3,6**	**0,0**	**0,9**	
3. S2D2	3,6	87/97	66/73	0/0	48/53	0,9
		0,7	**5,0**	**0,0**	**3,7**	
4. S2D3	6,0	843/89	166/17	33 / 4	644/68	9,5
		0,6	**1,2**	**0,0**	**4,7**	
5. S2D4	14,4	1200/164	129/18	170/23	901/123	7,3
		1,2	**1,2**	**0,2**	**8,6**	
Yield S2 (%)		**82**	**564**	**63**	**155**	**87**
1. S3 injected	2,0	676/173	187/48	323/83	166/43	3,9
2. S3D1	2,4	21/20	14/13	7/6	27/25	1,1
		0,1	**0,9**	**0,1**	**1,7**	
3. S3D2	3,6	145/362	66/166	76/189	28/70	0,4
		2,7	**11,2**	**1,8**	**4,8**	
4. S3D3	2,4	70/70	29/29	39/39	18/18	1,0
		0,5	**2,0**	**0,4**	**1,2**	
5. S3D4	4,8	119/79	44/29	65/65	43/29	1,5
		0,6	**2,0**	**0,4**	**2,0**	
Yield S3 (%)		**53**	**82**	**36**	**112**	**103**

Figures

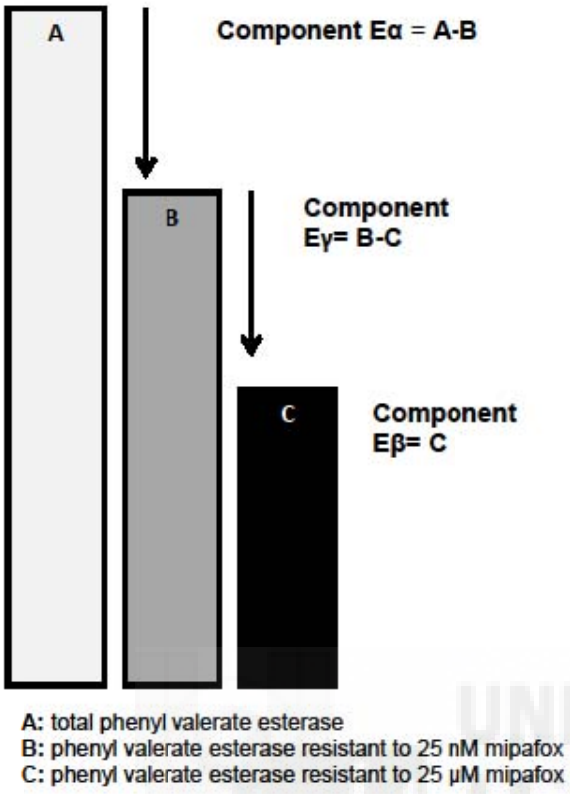

Figure 1. Discriminating assay of the three phenyl valerate esterase components in a soluble fraction of chicken brain. A simple test with discriminate inhibitor concentrations: Activity A was measured as total phenyl valerate esterase, activity B as phenyl valerate esterase activity resistant to 25 nM mipafox for 30 min at 37ºC, and activity C as activity resistant to 25 µM mipafox for 30 min at 37ºC. The percentage of the each esterase component is: Eα (sensitive to 25 nM mipafox) calculated as the difference of (A-B) activities, Eβ (resistant to 25 µM mipafox) calculated as activity C and Eγ (PVase resistant to paraoxon, but sensitive to 25 µM mipafox) calculated as the difference of (B-C) activities.

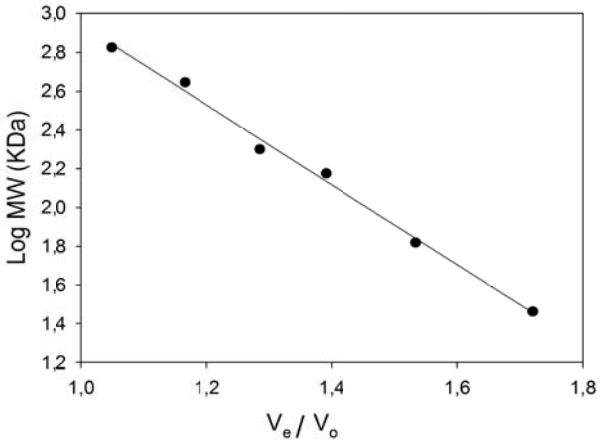

Figure 2. Calibration curve of the gel filtration chromatography column. Molecular exclusion chromatography was performed at 4°C in a 300 x 7.8 mm BioSep-SEC-s3000 (part no: 00H-2146-KO) balanced with 50 mM Tris buffer pH 7.5. The column was calibrated using standard proteins (Gel Filtration Markers Kit-Sigma Aldrich for proteins of 29 KDa to 700 KDa) and plotting log (MW) versus (kD). Albumin, bovine serum, 66,000 MW; Alcohol Dehydrogenase, yeast, 150,000 MW ; β-Amylase, sweet potato, 200,000 MW; Apoferritin, horse spleen; Blue dextran, 2,000,000 MW; Carbonic Anhydrase, bovine erythrocytes, 29,000; Thyroglobulin, bovine, 669,000 MW. The correlation coefficient was 0.994.

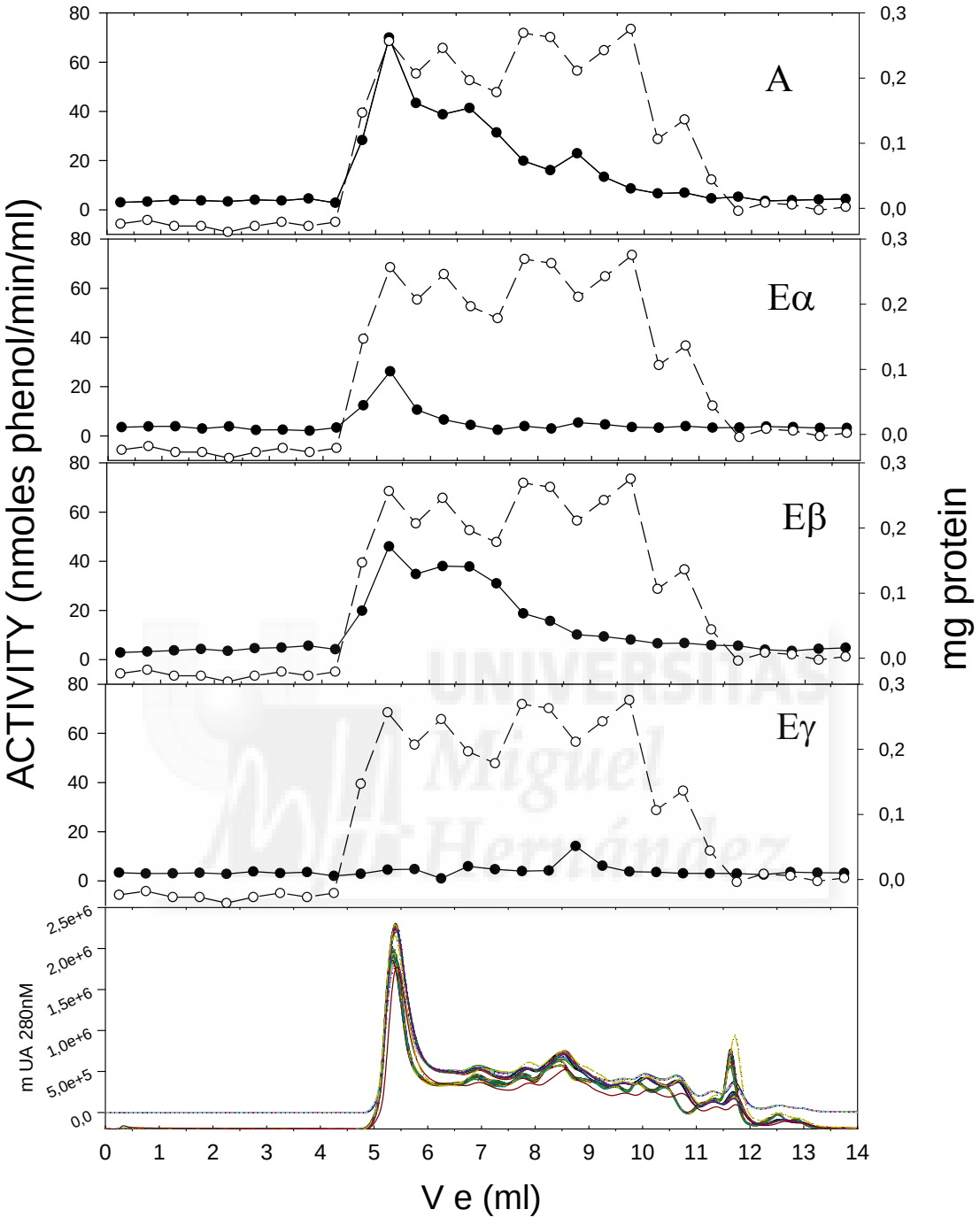

Figure 3. Molecular exclusion chromatography in BioSep-s3000 of the soluble fraction of chicken brain. It is showed the profile of activities, in nmol·min^{-1}·ml^{-1}, protein in mg, and absorbance at 280 nm of the 30 subfractions obtained by molecular exclusion chromatography. Activity A: total phenyl valerate esterase (PVase) activity. Activity Eα: activity PVase sensitive to 25 nM mipafox; Activity Eβ: Activity PVase resistant to mipafox; Activity Eγ: Activity PVase sensitive to 25 µM mipafox and resistant to paraoxon. Protein is expressed in total mg for the collected fraction. Black filled circles represent phenyl valerate esterase activity, white empty circles with dash lines depict the protein measured by the Bradford method; continuous lines in the lowest panel refer to the absorbance (280 nM) measured in the independent 50 repeated chromatograms.

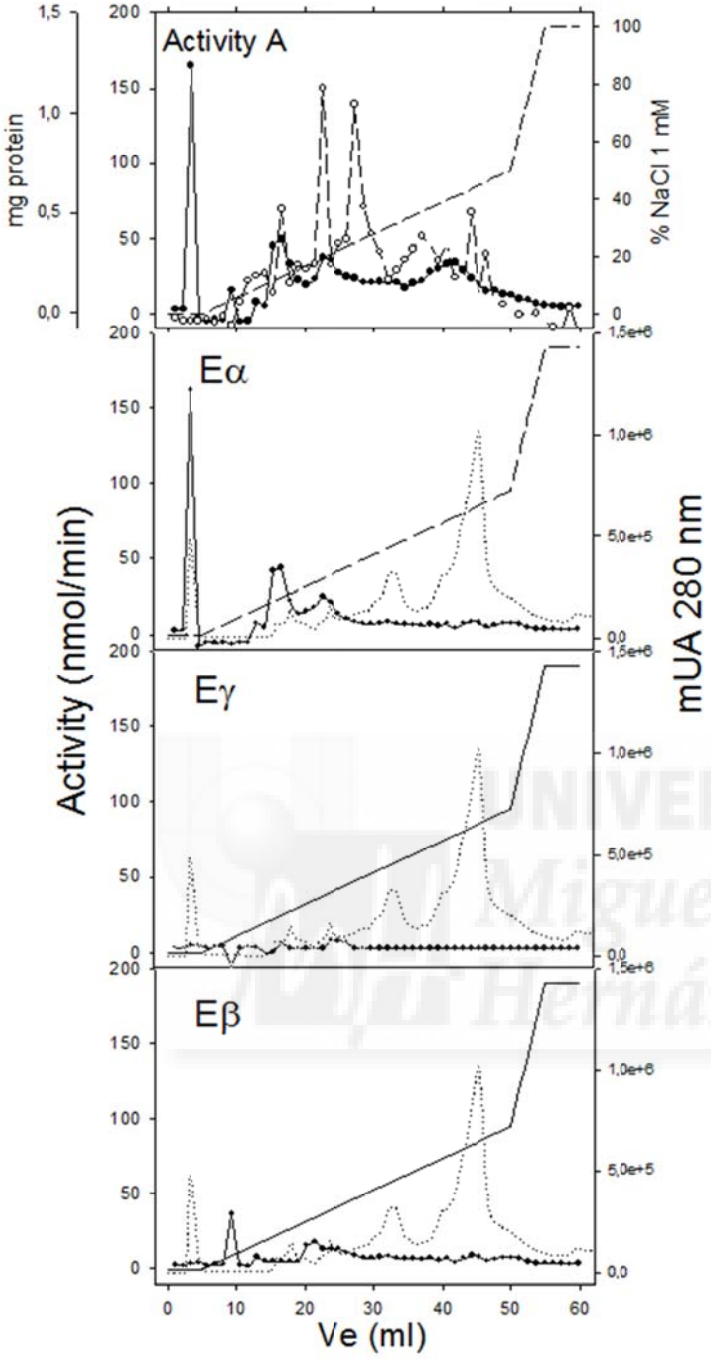

Figures 4. Ion exchange chromatography in BioSep-DEAE-PEI of fraction S1 obtained in the molecular exclusion chromatography. It is showed the profile of activities, in nmol·min^{-1}·ml^{-1}, protein in mg, and absorbance at 280 nm of the 50 subfractions obtained by ion exchange chromatography of S1. Activity A: total phenyl valerate esterase (PVase) activity. Activity Eα: activity PVase sensitive to 25 nM mipafox; Activity Eβ: Activity PVase resistant to mipafox; Activity Eγ: Activity PVase sensitive to 25 µM mipafox and resistant to paraoxon. Protein is expressed in mg/ml of the collected fraction.

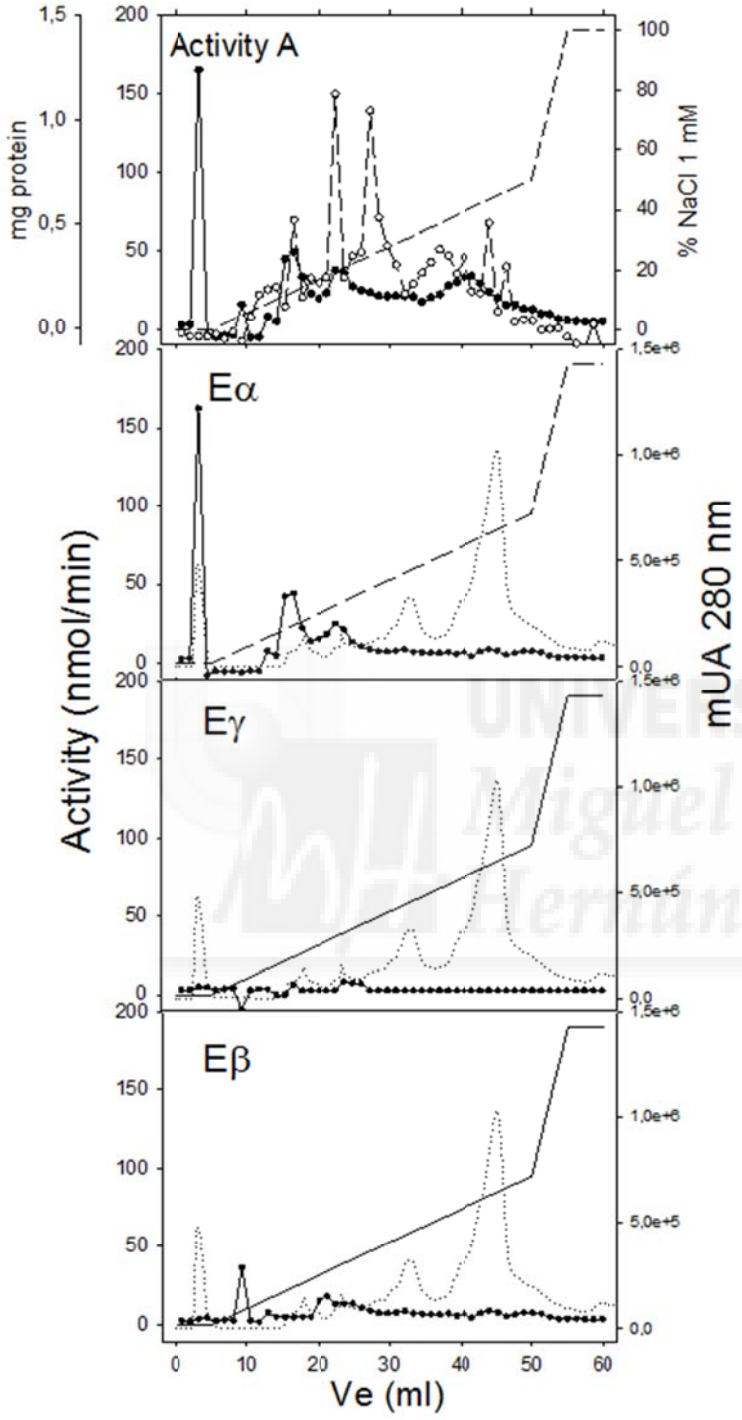

Figures 5. Ion exchange chromatography in BioSep-DEAE-PEI of fraction S2 obtained in the molecular exclusion chromatography. It is showed the profile of activities, in nmol·min^{-1}·ml^{-1}, protein in mg, and absorbance at 280 nm of the 50 subfractions obtained by ion exchange chromatography of S2. Activity A: total phenyl valerate esterase (PVase) activity. Activity Eα: activity PVase sensitive to 25 nM mipafox; Activity Eβ: Activity PVase resistant to mipafox; Activity Eγ: Activity PVase sensitive to 25 µM mipafox and resistant to paraoxon. Protein is expressed in mg/ml of the collected fraction.

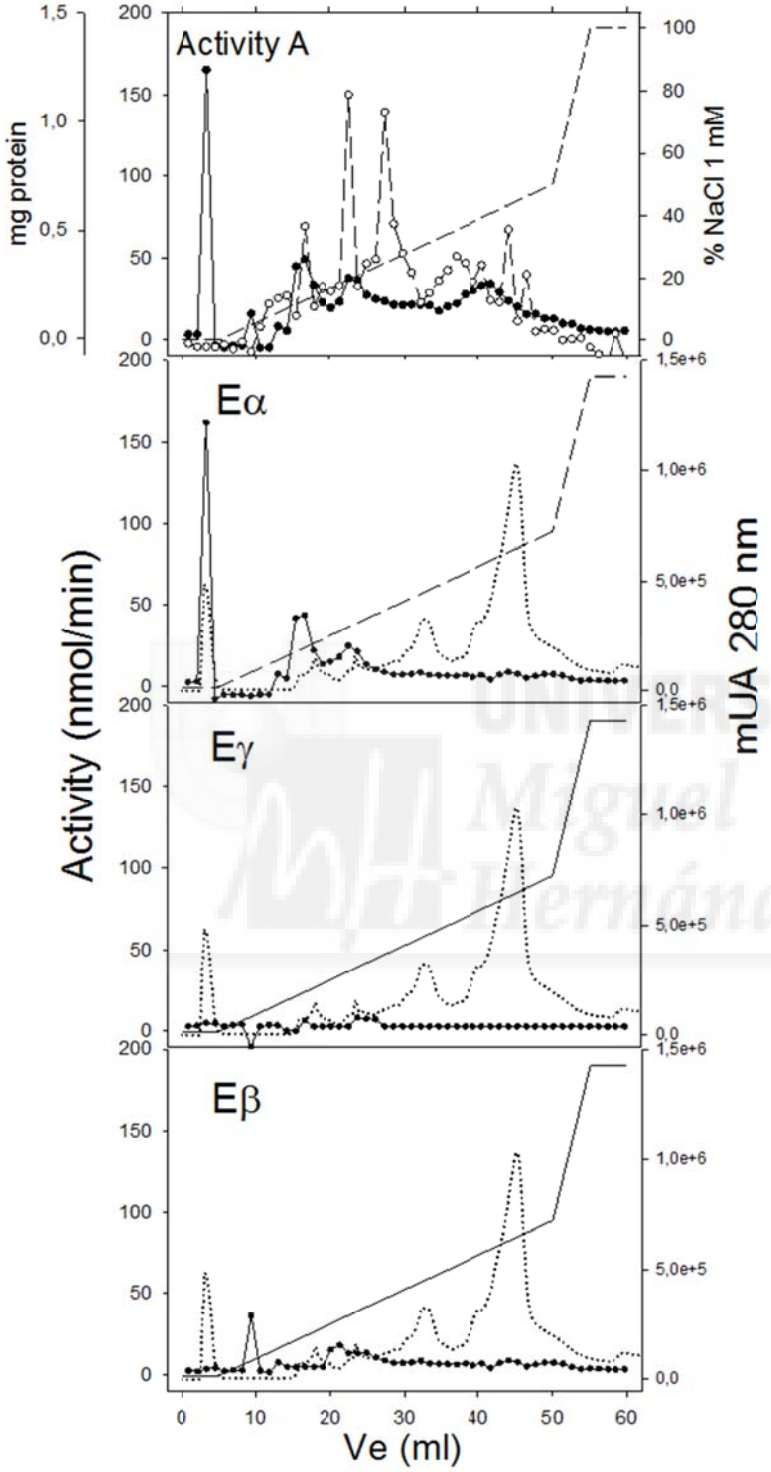

Figures 6. Ion exchange chromatography in BioSep-DEAE-PEI of fraction S3 obtained in the molecular exclusion chromatography. It is showed the profile of activities, in nmol·min^{-1}·ml^{-1}, protein in mg, and absorbance at 280 nm of the 50 subfractions obtained by ion exchange chromatography of S3. Activity A: total phenyl valerate esterase (PVase) activity. Activity Eα: activity PVase sensitive to 25 nM mipafox; Activity Eβ: Activity PVase resistant to mipafox; Activity Eγ: Activity PVase sensitive to 25 μM mipafox and resistant to paraoxon. Protein is expressed in mg/ml of the collected fraction.

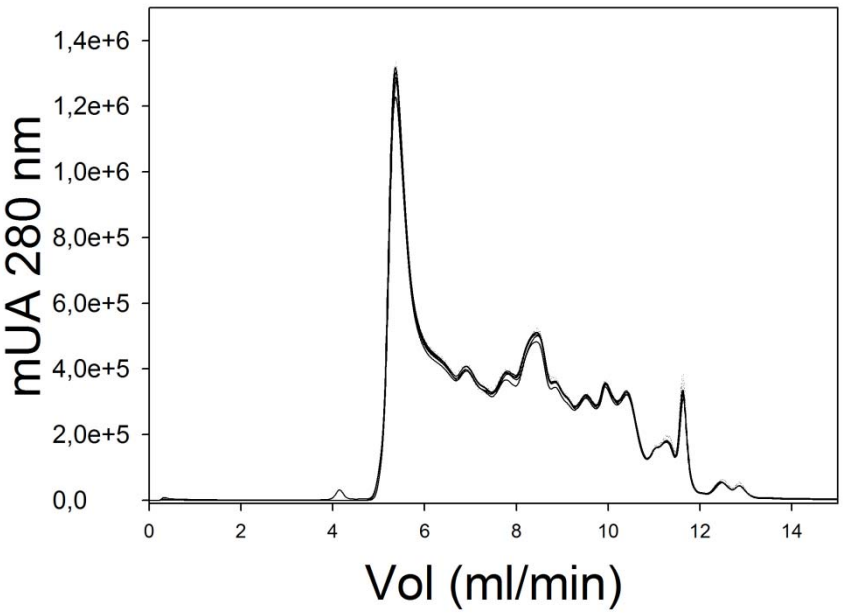

Figure 7. Molecular exclusion chromatography in BioSep-s3000 of the soluble fraction of chicken brain inhibited and not inhibited by mipafox. It is showed the profile absorbance at 280 nM of the twelve injections done. Six injections were done of the sample inhibited by 25 μM mipafox for 30 min at 37ºC (six black lines) and six injections of the not inhibited sample (six dotted lines).

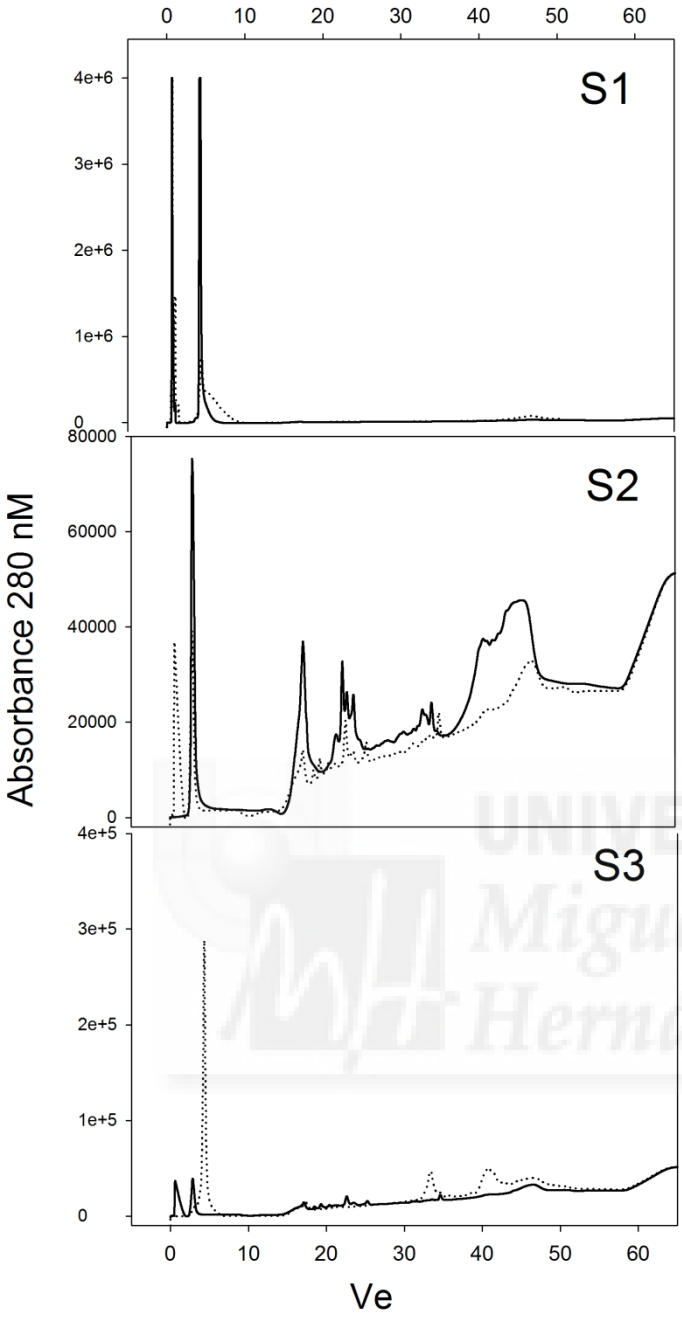

Figures 8. Ion exchange chromatography in BioSep-DEAE-PEI of fractions S1, S2 and S3. It is showed the profile absorbance at 280 nM of the injections done. Inhibited by 25 µM mipafox for 30 min at 37ºC (black line) and not inhibited by mipafox (dotted line) from the fractions obtained in the molecular exclusion chromatography.

References

Barr, D.B., Wong, L.Y., Bravo, R., Weerasekera, G., Odetokun, M., Restrepo, P., Kim, DG., Fernandez, C., Whitehead, R.D. Jr., Perez, J., Gallegos, M., Williams, B.L., Needham, L.L., 2004. Urinary concentrations of dialkylphosphate metabolites of organophosphorus pesticides: National Health and Nutrition Examination Survey 1999-2004. Int J Environ Res Public Health. 2011 Aug; 8(8):3063-98

Barril, J., Estévez, J., Escudero, M.A., Céspedes, M.V., Níguez, N., Sogorb, M.A., Monroy, A., Vilanova, E., 1999. Peripheral nerve soluble esterases are spontaneously reactivated after inhibition by paraoxon: implications for a new definition of neuropathy target esterase. Chem Biol Interact. May 14; 119-120:541-50.

Behra M, Etard C, Cousin X, Strähle U. The use of zebrafish mutants to identify secondary target effects of acetylcholine esterase inhibitors. Toxicol Sci. 2004 Feb;77(2):325-33.

Bradford, M.M., 1976. A rapid and sensitive method for the quantitation of microgram quantities of protein utilizing the principle of protein-dye binding. Anal Biochem. 1976 May 7; 72:248-54.

Brown, M.A., Brix, K.A., 1998. Review of health consequences from high-, intermediate- and low-level exposure to organophosphorus nerve agents. J Appl Toxicol. Nov-Dec;18(6):393-408.

Casida, J.E., Durkin, K.A., 2013. Anticholinesterase insecticide retrospective. Chem Biol Interact. 2013 Mar 25; 203(1):221-5.

Casida, J.E., Quistad, G.B., 2004. Organophosphate toxicology: safety aspects of non-acetylcholinesterase secondary targets. Chem. Res. Toxicol. 17:983–98

Céspedes, M.V., Escudero, M.A., Barril, J., Sogorb, M.A., Vicedo, J.L., Vilanova, E., 1997. Discrimination of carboxylesterases of chicken neural tissue by inhibition with a neuropathic, non-neuropathic organophosphorus compounds and neuropathy promoter Chem Biol Interact. Oct 24; 106(3):191-200.

COT report., 1999. Organophosphates. A report of the commitee on Toxicology of Chemicals in Food, Consumer Products and the Environment. UK Department of Health, London.Directorate, 2002.

Escudero, M.A., Céspedes, M.V., Vilanova, E., 1997. Chromatographic discrimination of soluble neuropathy target esterase isoenzymes and related phenyl valerate esterases from chicken brain, spinal cord, and sciatic nerve. J Neurochem. May;68(5):2170-6.

Estévez J, Mangas I, Sogorb MÁ, Vilanova E. 2013. Interactions of neuropathy inducers and potentiators/promoters with soluble esterases. Chem Biol Interact. 203(1), 245-50.

Estévez J., and Vilanova, E., 2009. Model equations for the kinetics of covalent irreversible enzyme inhibition and spontaneous reactivation: Esterases and organophosphorus compounds. Crit. Rev. Toxicol. 39(5), 427–448

Estévez, J., Barril, J., Vilanova, E., 2010. Inhibition with spontaneous reactivation and the "ongoing inhibition" effect of esterases by biotinylated organophosphorus compounds: S9B as a model. Chem. Biol. Interac. 187, 397–402.

Estévez, J., Barril, J., Vilanova, E., 2012. Kinetics of inhibition of soluble peripheral nerve esterases by PMSF: a non-stable compound that potentiates the organophosphorus-induced delayed neurotoxicity. Arch. Toxicol. 86, 767–777.

Estévez, J., García-Perez, A., Barril, J., Pellín, MC., Vilanova, E., 2004. The inhibition of the high sensitive Peripherals nerve soluble esterases by Mipafox. A new mathematical processing for the kinetics of inhibition of esterases by organophosphorus compounds. Toxicol. Lett. 151, 243-249.

Estévez, J., García-Pérez, A., Barril, J., Vilanova, E., 2011. Inhibition with Spontaneous Reactivation of Carboxyl Esterases by Organophosphorus Compounds: Paraoxon as a Model. Chem. Res. Toxicol. 24, 135–143

Garcia-Pérez, A.G., Barril, J., Estévez, J., Vilanova, E., 2003. Properties of phenyl valerate esterase activities from chicken serum are comparable with soluble esterases of peripheral nerves in relation with organophosphorus compounds inhibition. Toxicol Lett. Apr 30;142(1-2):1-10

Glynn, P., 1999. Neuropathy target esterase. Biochem J. 344 Pt 3:625-31.

Glynn, P., 2000. Neural development and neurodegeneration: two faces of neuropathy target esterase. Prog Neurobiol. May;61(1):61-74.

Hoffman, A., Eisenkraft, A., Finkelstein, A., Schein, O., Rotman, E., Dushnitsky, T., 2007. A decade after the Tokyo sarin attack: a review of neurological follow-up of the victims. Mil Med. Jun; 172(6):607-10.

Jamal, G.A., Hansen, S., Julu, P.O.O., 2002. Low level exposures to organophosphorus esters may cause neurotoxicity. Toxicology 181-182, 23-33.

Jett DA, Navoa RV, Beckles RA, McLemore GL. Cognitive function and cholinergic neurochemistry in weanling rats exposed to chlorpyrifos. Toxicol Appl Pharmacol. 2001 Jul 15;174(2):89-98.

Little PJ, Scimeca JA, Martin BR. Distribution of 3H]diisopropylfluorophosphate, [3H]soman, [3H]sarin, and their metabolites in mouse brain. Drug Metab Dispos. 1988 Jul-Aug;16(4):515-20.

Liu, J., Olivier, K., Pope, C.N., 1999. Comparative neurochemical effects of repeated methyl parathion or chlorpyrifos exposures in neonatal and adult rats. Toxicol Appl Pharmacol. Jul 15;158(2):186-96.

Lockdridge, O., and Schopfer, 2006. Biomarkers of Organophosphate Exposure, cap 48 in Toxicology of Organophosphate and Carbamate Compounds.

Lotti, M., Caroldi, S., Capodicasa, E., Moretto, A., 1991. Promotion of organophosphate-induced delayed polyneuropathy by phenylmethanesulfonyl fluoride. Toxicol Appl Pharmacol. Apr; 108(2):234-41.

Mangas I, Vilanova E, Estévez J. NTE and non-NTE esterases in brain membrane: kinetic characterization with organophosphates. Toxicology. Jul 16; 297(1-3):17-25.

Mangas I, Vilanova E, Estévez J., 2011. Kinetics of the inhibitory interaction of organophosphorus neuropathy inducers and non-inducers in soluble esterases in the avian nervous system. Toxicol Appl Pharmacol. Nov 1; 256(3):360-8.

Mangas I, Vilanova E, Estévez J., 2012. Phenylmethylsulfonyl fluoride, a potentiator of neuropathy, alters the interaction of organophosphorus compounds with soluble brain esterases. Chem Res Toxicol. Nov 19; 25(11):2393-401.

Moretto, A., Bertolazzi, M., Lotti, M., 1994. The phosphorothioic acid O-(2-chloro-2,3,3-trifluorocyclobutyl) O-ethyl S-propyl ester exacerbates organophosphate polyneuropathy without inhibition of neuropathy target esterase. Toxicol Appl Pharmacol. Nov;129(1):133-7.

Moser VC. Comparisons of the acute effects of cholinesterase inhibitors using a neurobehavioral screening battery in rats. Neurotoxicol Teratol. 1995.Nov-Dec;17(6):617-25. PubMed PMID: 8747743.

Murray, A., Rathbone, A.J., Ray, D.E., 2003. Characterisation of non-acetlycholinesterase actions of organophosphates by identification of novel protein targets of action. Br. Neurosci. Assoc. Abstr., 17, p. 136

Murray, A., Rathbone, A.J., Ray, D.E., 2005. Novel protein targets for organophosphorus pesticides in rat brain. Environ Toxicol Pharmacol. May; 19(3):451-4.

Nomura, D.K., Blankman, J.L., Simon, G.M., Fujioka, K., Issa, R.S., 2008. Activation of endocannabinoid system by organophosphorus nerve agents. Nat. Chem. Biol. 4:373–78

Nomura, D.K., Casida, J.E., 2011. Activity-based protein profiling of organophosphorus and thiocarbamate pesticides reveals multiple serine hydrolase targets in mouse brain. J. Agric. Food Chem. 59:2808–15

Parrón, T., Requena, M., Hernández, A.F., Alarcón, R., 2011. Association between environmental exposure to pesticides and neurodegenerative diseases. Toxicol Appl Pharmacol. Nov 1;256(3):379-85.

Peeples ES, Schopfer LM, Duysen EG, Spaulding R, Voelker T, Thompson CM, Lockridge O. Albumin, a new biomarker of organophosphorus toxicant exposure,identified by mass spectrometry. Toxicol Sci. 2005 Feb;83(2):303-12.

Pope CN. Organophosphorus pesticides: do they all have the same mechanism of toxicity? J Toxicol Environ Health B Crit Rev. 1999 Apr-Jun;2(2):161-81.

Pope, C.N., Padilla, S., 1990. Potentiation of organophosphorus-induced delayed neurotoxicity by phenylmethylsulfonyl fluoride. J Toxicol Environ Health 31:261–273

Ray, .E., Richards, P.G., 2001. The potential for toxic effects of chronic, low-dose exposure to organophosphates. Toxicol Lett ,343-351.

Richards, P.G., Johnson, M.K., Ray, D.E., 2000. Identification of acylpeptide hydrolase as a sensitive site for reaction with organophosphorus compounds and a potential target for cognitive enhancing drugs. Mol. Pharmacol., 58, pp. 577–583.

Richards, P.G., Johnson, M.K., Ray, D.E., Walker, C., 1999. Novel protein targets for organophosphorus compounds. Chem. Biol. Interact., 119–120 (1999), pp. 503–511.

Roldan-Tapia, L., Parron, T. Sanchez Santed. F., 2005. Neuropsychological effects of long term exposure to organophosphate pesticides, Neurotoxicology & Teratology 27 (2)

Ross SM, McManus IC, Harrison V, Mason O. Neurobehavioral problems following low-level exposure to organophosphate pesticides: a systematic and meta-analytic review. Crit Rev Toxicol. 2013 Jan;43(1):21-44.

Vilanova E, Barril J, Carrera V, Pellin MC., 1990. Soluble and particulate forms of the organophosphorus neuropathy target esterase in hen sciatic nerve. J Neurochem. Oct;55 (4):1258-65.

Yokoyama, K., Araki, S., Murata, K., Nishikitani, M., Okumura, T., Ishimatsu, S., 1998. Chronic neurobehavioral effects of Tokio subway Sarin poisoning in relation to posttraumatic stress disorder. Arch Environ Health; 53(4):249–56.

UNIVERSITAS
Miguel
Hernández

5.3. Conference publications

UNIVERSITAS
Miguel
Hernández

Title: INHIBITION AND SPONTANEOUS REACTIVATION OF ESTERASES BY ORGANOPHOSPHORUS COMPOUNDS IN PRESENCE OF THE SUBSTRATE: PARAOXON AS A MODEL.

Authors: J. Estévez, **I. Mangas,** E. Vilanova.

Type of participation: Poster
CONGRESS: XII INTERNATIONAL CONGRESS OF TOXICOLOGY (ICT XII)
Place of celebration: Barcelona (Spain). Date: 19-23 July 2010

Ref. journal: Toxicology Letters. Volume: 196 Pages S320-S321 Date: 17 July 2010

ABSTRACT:

The kinetic analysis of the inhibition of esterases by organophosphorus compounds is sometimes unable to yield consistent results by fitting simple inhibition kinetic models to experimental data of complex systems. In vitro experiments involve pre-incubating the enzyme preparation with an inhibitor concentration (I) during the inhibition times (t), and then incubating with a substrate during the enzyme–substrate reaction time (ts) to measure the residual enzyme activity (E). During the substrate reaction, inhibition is not usually significant due to the dilution of the inhibitor and the protective effect of the substrate. However some inhibition may occur for the high potent inhibitors. In this work, this is known as “ongoing inhibition”. The kinetic data were obtained for 0.026nM concentration of paraoxon incubated for up to two hours forty-three minutes with soluble fraction of chicken peripheral nerve in presence of phenylvalerate as substrate. At 18 min of inhibition at 37 ◦C the percentage of activity was around 61% and the percentage of residual activity at long time was around 35%. This inhibition is clearly time-progressive. The spontaneous reactivation of paraoxon-inhibited phenylvalerate esterases has also been observed in the chicken peripheral nerve soluble fraction in the presence of phenylvalerate. The kinetic data were obtained for preincubated samples with 10nM of paraoxon and then they were diluted with buffer and phenylvalerate up to the residual concentration of paraoxon was 0.026 nM. After that the samples were incubated for up to two hours forty-three minutes. At 43 min ofreactivation at 37 ◦C the percentage of activity was around 9% and at long time was around 32%. This spontaneous reactivation is clearly time-progressive. The results show the “ongoing inhibition” and“ongoing reactivation” may be taken into account in the kinetic models to analyze the interaction by paraoxon of soluble chicken peripheral nerve phenylvalerate esterases.

UNIVERSITAS
Miguel
Hernández

INHIBITION AND SPONTANEOUS REACTIVATION OF ESTERASES BY ORGANOPHOSPHORUS COMPOUNDS IN PRESENCE OF THE SUBSTRATE: PARAOXON AS A MODEL.

Jorge Estévez*, Iris Mangas and Eugenio Vilanova
Unidad de Toxicología y Seguridad Química, Instituto de Bioingeniería,
Universidad Miguel Hernández de Elche, Elche (Spain). * jorge.estevez@umh.es

INTRODUCTION

The kinetic analysis of the inhibition of esterases by organophosphorus compounds is sometimes unable to yield consistent results by fitting simple inhibition kinetic models to experimental data of complex systems. In vitro experiments involve pre-incubating the enzyme preparation with an inhibitor concentration (I) during the inhibition times **(t),** and then incubating with a substrate during the enzyme-substrate reaction time (ts) to measure the residual enzyme activity (E). During the substrate reaction, inhibition is not usually significant due to the dilution of the inhibitor and the protective effect of the substrate. However some inhibition may occur for the high potent inhibitors. In this work, this is known as "ongoing inhibition" [2].

MATERIALS AND METHODS

Enzyme preparation: soluble fractions of chicken sciatic nerves (from 200 mg fresh tissue/ml) according to [1]
Inhibitor: Paraoxon **(**O,O'-diethyl **p**-nitrophenyl **p**hosphate**)**
Inhibition assay: The inhibitor was incubated (final concentration 0.026 nM) with enzyme preparation (final concentration 0.48 mg fresh tissue/ml) and in presence of 20 ml of the substrate (phenylvalerate) in a final volume of 42 ml, for the time indicated in **Figures 2A** and **2B**. In these times aliquots were extracted of the reaction pool for measuring residual activity by colorimetric method [1, 3].
Reactivation assay: A high concentrated preparation (0.1 ml soluble fraction from 200 mg fresh tissue/ml) was inhibited with 10 nM paraoxon at final volume of 0.11 ml for 45 min and then diluted 1/42 with 20 ml of buffer and 21 ml of substrate dilution, decreasing paraoxon to around 0.026 nM and then allowed for reactivation for 164 min in presence of the substrate. PVase activity were monitored in aliquots withdrawn at different times during and reactivation periods by colorimetric method [1, 3].

RESULTS

1. Inhibition of peripheral nerve soluble PVase activity with paraoxon in presence of phenylvalerate as the substrate, represented in **Fig. 2A** and **Fig. 2B**, shows a time progressive inhibition.
2. Spontaneous reactivation of pre-inhibited peripheral nerve soluble PVase activity with paraoxon in presence of phenylvalerate as the substrate, represented in **Fig. 2A** and **Fig. 2B**, shows a time progressive spontaneous reactivation.

DISCUSION AND CONCLUSIONS

During the substrate reaction, inhibition is not usually significant given the dilution of the inhibitor and the protective effect of the substrate. However some inhibition may occur for the highly potent inhibitors. This is known as "ongoing inhibition". The **Fig. 1** shows the ongoing inhibition effect (10 minutes of reaction time) for the inhibition of paraoxon [4], S9B [5] and mipafox [6]. The ongoing inhibition effect usually affects the more sensitive enzymatic component in multy-enzymatic assays [2]. The **Table 1** shows different kinetic parameters obtained from [4], [5] and [6]. On the one hand the ongoing inhibition apparent constant seems to be higher when the second order inhibition constant is higher just as S9B and mipafox show in **Table 1**. This might be right according to the sensitivity of the enzyme by the different inhibitors. However the ongoing inhibition in the inhibition by paraoxon does not seem to behave with that tendency.
On the other hand the ongoing inhibition and progressive spontaneous reactivation in presence of the substrate (ongoing reactivation in this work) are simultaneously occurring in the standard assay (**Fig. 2A** and **2B)**. At 43 min of reactivation the percentage of activity was around 9 % and at long time it was around 32%. Then the ongoing reactivation has also to take into account in the experimental assays because according to the standard assay [1,3] the sample is diluted when the substrate is added after the pre-inhibition time. This may be the cause of the low ongoing inhibition apparent constant for the paraoxon because the spontaneous reactivation constant is the highest and the ongoing reactivation may counteract the ongoing inhibition.

REFERENCES

[1] Estévez et al. (2004). Toxicol. Letters. 151:243-249
[2] Estévez and Vilanova (2009). Crit Rev Toxicol; 39(5): 427–448
[3] Johnson, M.K. (1977). Arch. Toxicol. 37, 113–115.
[4] Estévez et al. (2008). Toxicol. Letters 180(s) S32-S246
[5] Estévez et al. (2010). Chem Biol Interact. doi:10.1016/j.cbi.2010.05.008
[6] Estévez et al. (2004). Toxicol. Letters . 151, 171–181

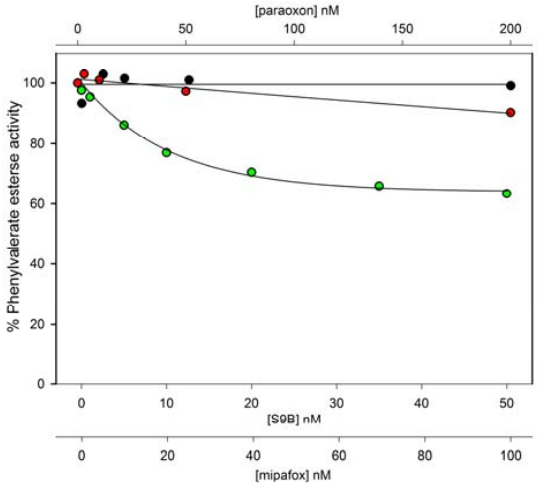

Fig. 1. Fixed-time inhibition curve of phenyl valerate esterase activity at zero time of preinhibition with different inhibitors. This figure shows the "ongoing" inhibition effect. The data corresponds to [4], [5], and [6]. The black circles show the ongoing inhibition by mipafox, the red circles show the ongoing inhibition by paraoxon and the green circles show the ongoing inhibition by S9B.

Table 1. Kinetic parameters deduced for the most sensitive component in soluble peripheral nerve in presence of different inhibitors. The table shows different kinetic parameters for the most sensitive component in soluble peripheral nerve with paraoxon, S9B and mipafox. The inhibition with mipafox showed negligible ongoing inhibition effect. ka' is the apparent first order constant for the ongoing inhibition, k is the inhibition second order constant, kr is the spontaneous reactivation constant and E_0 is the activity proportion for the most sensitive component.

	E_0 (%)	ka' (nM^{-1})	k ($nM^{-1}\cdot min^{-1}$)	kr (min^{-1})	I_{50} nM
Paraoxon [4]	37	0.0015	1.798	0.428	0.24
S9B [5]	33	0.1213	0.116	0.005	0.22
Mipafox [6]	48	-	$2.12\cdot10^{-3}$	-	11

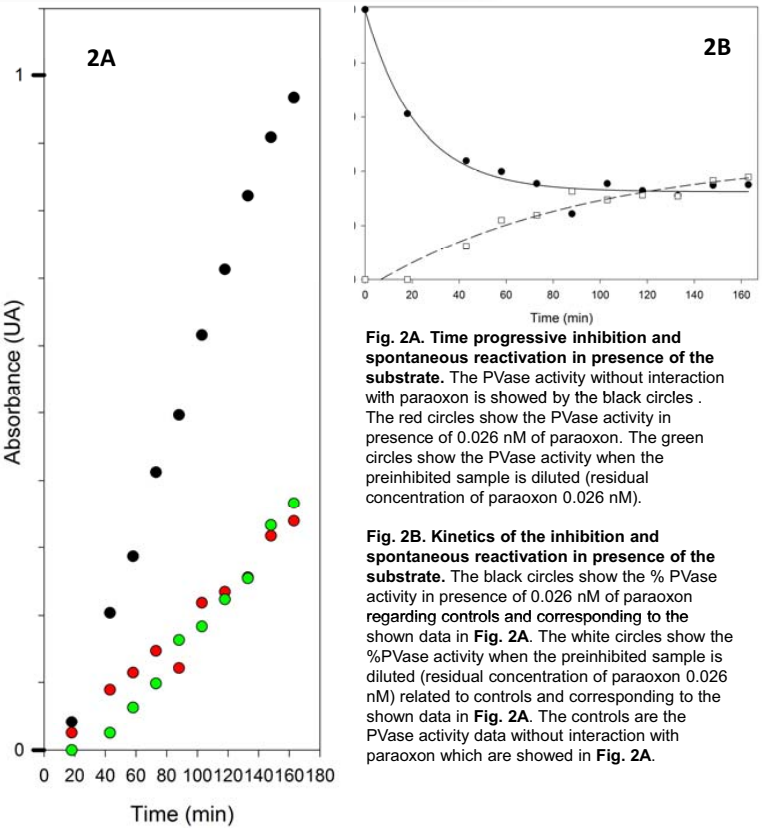

Fig. 2A. Time progressive inhibition and spontaneous reactivation in presence of the substrate. The PVase activity without interaction with paraoxon is showed by the black circles . The red circles show the PVase activity in presence of 0.026 nM of paraoxon. The green circles show the PVase activity when the preinhibited sample is diluted (residual concentration of paraoxon 0.026 nM).

Fig. 2B. Kinetics of the inhibition and spontaneous reactivation in presence of the substrate. The black circles show the % PVase activity in presence of 0.026 nM of paraoxon regarding controls and corresponding to the shown data in **Fig. 2A**. The white circles show the %PVase activity when the preinhibited sample is diluted (residual concentration of paraoxon 0.026 nM) related to controls and corresponding to the shown data in **Fig. 2A**. The controls are the PVase activity data without interaction with paraoxon which are showed in **Fig. 2A**.

UNIVERSITAS
Miguel
Hernández

Title: KINETIC INTERACTION OF SOLUBLE ESTERASES OF BRAIN AND PHENYLMETHYLSULPHONYL FLUORIDE (PMSF), AN INHIBITOR PROTECTING AND POTENTIATING THE ORGANOPHOSPHORUS DELAYED NEUROTOXICITY.

Authors: E. Vilanova, **I. Mangas,** J. Estévez,

Type of participation: Poster
CONGRESS: Congress: 50TH ANNUAL MEETING OF THE SOCIETY OF TOXICOLOGY
Place of celebration: Washington DC (USA) **Date:** 6-10 March 2011

Ref. journal: The Toxicologist. . Volume: 120 Pages 450-451

ABSTRACT:

The kinetic analysis of esterase inhibition by acylating compounds (organophosphorus carbamates and sulfonylfluorides) is sometimes unable to yield consistent results by fitting simple inhibition kinetic models to experimental data of complex systems. Kinetic data were obtained for phenylmethylsulfonylfluoride (PMSF) tested at different concentrations incubated for around three hours with soluble fraction of chicken brain. PMSF is a protease and esterase inhibitor causing protection or potentiation ("promotion") of organophosphorus delayed neurotoxicity depending of if it is dosed previously or after an inducer of delayed neurotocity and it is unstable in water solution.

A kinetic model equation was deduced assuming a multienzymatic system with three different molecular phenomena occurring simultaneously:(1) Inhibition; (2) spontaneous chemical hydrolysis of the inhibitor; (3) ongoing inhibition (inhibition during the substrate reaction). A three-dimensional fit of the model was applied for analysing the experimental data. The best fitting model is compatible with a resistant component (28%) and two sensitive enzymatic entities (61%and 11%). The corresponding second order rate constants of inhibition (ki=2.3×103 and 3.6×102 M-1×min-1, respectively) and the chemical hydrolysis constant of PMSF (kh=0.2285 min-1) were simultaneously estimated. These parameters were similar to those deduced in fixed time inhibition experiments. The consistency of results in both experiments was considered an internal validation of the methodology. The results were also consistent with a significant ongoing inhibition.

This kinetic data are useful for the identification, characterization and understanding the role of soluble esterases in the molecular mechanisms of protection and potentiation.

UNIVERSITAS
Miguel
Hernández

Kinetic interaction of soluble esterases of brain and PMSF, an inhibitor protecting and potentiating the organophosphorus delayed neurotoxicity

Eugenio Vilanova , Iris Mangas and Jorge Estévez

Unidad de Toxicología y Seguridad Química, Instituto de Bioingeniería, Universidad Miguel Hernández, Elche (Spain)

INTRODUCTION

PMSF (phenylmethanesulfonylfluoride) is a protease and esterase inhibitor causing protection or potentiation ("promotion") of the organophosphorus delayed polyneuropathy (~~OPIDN~~). The molecular target of promotion has not yet been identified . Some other possible situations (e.g. spontaneous reactivation, spontaneous inhibitor hydrolysis, ongoing inhibition) have to be considered to analyze the data [1,2]. The interaction of soluble brain esterases with PMSF, which is instable in water solution [3] is characterized using a kinetic model with three different molecular phenomena occurring simultaneously: (1) Inhibition; (2) spontaneous chemical hydrolysis of the inhibitor and (3) ongoing inhibition (inhibition during the substrate reaction) using kinetic models previously developed in our laboratory [1, 2]

MATERIALS AND METHODS

Enzyme preparation: soluble fractions of chicken brain (from 20 mg fresh tissue/ml) according to [4]. **Enzyme assays**: Enzyme preparation was preincubated with PMSF for the time indicated in each experiment and then substrate (phenylvalerate) was added for measuring residual activity by colorimetric method [1, 5, 6]. For **reactivation assay**, a high concentrated preparation was inhibited with 400 and 1000 µM of PMSF for 30 min and then diluted and allowed for reactivation before measuring activity. **Mathematical analysis** of the inhibition curves: Model equations for a system with several enzymatic components were applied as described by Estévez and Vilanova (2009) [2] but including the spontaneous hydrolysis of PMSF according to [6].

RESULTS

Chemical hydrolysis of the PMSF is included in the kinetic model according to the next reactions:

$$E + I \xrightarrow{k} EI \quad \text{and} \quad I + OH^- \xrightarrow{kh} P$$

If the decrease of the inhibitor concentration by inhibition reaction is supposed negligible versus chemical hydrolysis then the equation for the associated differential equations to previous reactions is [6]

$$E = E_0 \cdot e^{(e^{-kh \cdot t} - 1) \cdot \frac{k}{kh} \cdot I_0}$$

1 Evaluation of activity after diluting the inhibitor. The activity remained inhibited over reactivation time at 26-28 % (1000 µM) and 31-34 % (400 µM; Fig 1). This confirms that there is no a spontaneous reactivation after 180 min.

2 Fixed-time inhibition curve was properly fitted with a model with two enzymatic sensitive and a resistant component (Fig2, Table 1A) and considering spontaneous PMSF hydrolysis.The best fit model according to ´F´ test was:

$$E = E1_0 \cdot e^{(e^{-kh \cdot t} - 1) \cdot \frac{k1}{kh} \cdot I_0} + E2_0 \cdot e^{(e^{-kh \cdot t} - 1) \cdot \frac{k2}{kh} \cdot I_0} + Er$$

Where k1,k2 are the inhibition constants, kh is the hydrolysis constant, $E1_0$, $E2_0$ are the proportion of the initial enzymatic components, and R is the enzymatic fraction resistant to inhibition.

3 Time-progressive inhibition . The inhibition was time-progressive (~70 % of total activity), which is coherent with covalent inhibition (Fig. 3A).

4 Evaluation of ongoing inhibition during the substrate reaction. Extrapolating the data in Fig. 3A to the preincubation zero time inhibition did not converge to 100% (see 3B). This indicates ongoing inhibition during substrate incubation.

5 A three-dimensional fit including ongoing inhibition and spontaneous hydrolysis and no spontaneous reactivation. The best fit according to F test was:

$$E = E1_0 \cdot e^{(ka \cdot I_0)} \cdot e^{(e^{-kh \cdot t} - 1) \cdot \frac{k1}{kh} \cdot I_0} + E2_0 \cdot e^{(e^{-kh \cdot t} - 1) \cdot \frac{k2}{kh} \cdot I_0} + Er$$

Where ka' is the the exponential constant of the ongoing inhibition. Results in **Table 1** and the 3D surface in **Fig4**.

•CONCLUSIONS

•The inhibition by PMSF of esterase activity of soluble fraction brain is coherent with a kinetic model considering a multi-enzymatic system, a significant spontaneous hydrolysis of the inhibitor and "ongoing inhibition" of the most sensitive component with no spontaneous reactivation.

•The best fitting model is compatible two sensitive enzymatic entities, 61% and 11%, with I_{50} (30 min) 67 µM and 435 µM respectively, considering the effect of spontaneous hydrolysis. They are higher than those deduced from the kinetic constants (10,0 and 64,2 µM, respectively). A 28% of the activity was resistant.

•These sensitive enzymatic entities might play a role in promotion of OP delayed polyneuropathy and the spontaneous hydrolisis should be considered in *in vitro* and *in vivo* studies.

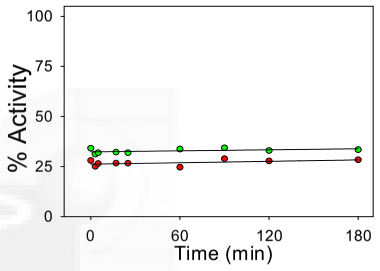

Fig. 1. Spontaneous reactivation after inhibition by PMSF. Two concentrated preparations (200 mg/ml) were inhibited by preincubation with 1000 µM (red circles) and 400 µM (green circles) of PMSF respectively, for 30 min at 37ºC. Then the mixture was diluted 10- fold with homogenization buffer to be then incubated for 0, 4, 8, 22, 36, 50, 65, 90, 120 or 180 min at 37ºC.

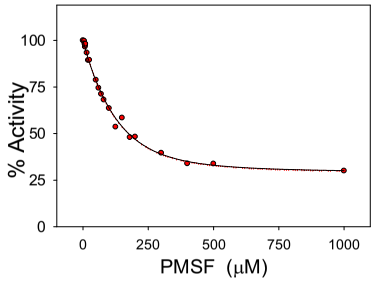

Fig. 2. PMSF fixed-time inhibition curve of phenyl valerate esterase activity at 30 min of inhibition. Enzyme preparation was incubated at concentrations in the range of 0-1000 µM of PMSF for 30 min at 37 ºC and then essayed the enzymatic activity with phenylvalerate for 10 min. The curve was fitted with exponential model equations including spontaneous hydrolysis of PMSF selecting the best fitting equation according to the F-test: (See Table 1).

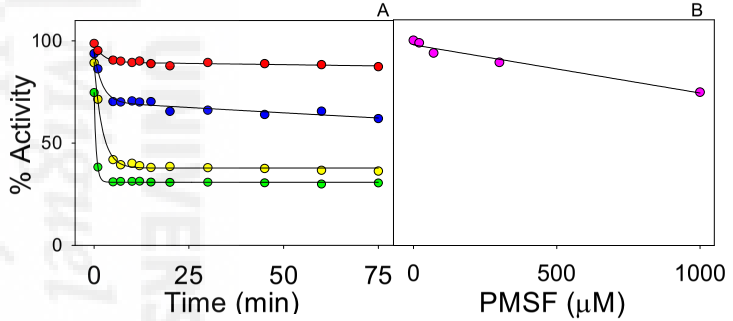

Figures 3. Kinetics of the time-progressive inhibition by PMSF concentrations. Panel B shows the inhibition at the reaction time with the substrate (cero time inhibition). Preparations containing the soluble fraction of 20 mg fresh tissue/ml t were preincubated with 0, 20, 70, 300, 1000 µM pmsf (upper to lower plots) for the indicated time. Then, the enzymatic activity was assayed by incubating the substrate phenylvalerate for 10 min. Panel B shows the inhibition during the substrate (0 min inhibition time, "ongoing inhibition").

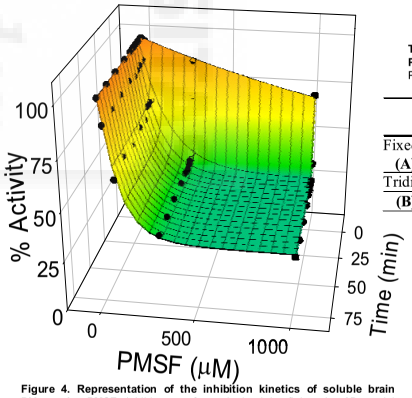

Figure 4. Representation of the inhibition kinetics of soluble brain PVases by PMSF. Inhibitory surface obtained by fitting the 3D model equation to the data corresponding to PMSF inhibition which is done in the soluble fraction of the brain (Figure 3). The surface reflects the result of the best model according to the F test. It corresponds to a model with two sensitive enzymatic components plus other resistant where the most sensitive is affected by ongoing inhibition.

Table 1. Kinetic parameters and I_{50} (30 min) obtained from the different experiments of inhibition with PMSF on soluble fraction of brain. (**A**) Fixed-time inhibition with different inhibitor concentrations (Fig 2). (**B**) Progressive inhibition (Fig 4).

	R^2	ka nM^{-1}	kh min^{-1}	E1 (%)	k1 $\mu M^{-1} \cdot min^{-1}$	I_{50}^{30} µM	E2 (%)	k2 $\mu M^{-1} \cdot min^{-1}$	I_{50}^{30} µM	R (%)
Fixed-time inhibition										
(A)	0.9970		0.162	63	0.0013	87	8	0.00036	310	29
Tridimensional fitting of progression-time experiment										
(B)	0.9983	0.0005	0.229	61	0.0023	67	11	0.00036	435	28

REFERENCES

[1] Estévez et al., (2004). Toxicol. Letters. 151:243-249
[2] Estévez and Vilanova., (2009). Crit Rev Toxicol . 39(5): 427–448
[3] James GT. (1978), Anal Biochem 86: 574-579
[4] Vilanova et al., (1990). Neurochemistry 55:1258-1265
[5] Estévez et al., (2009). Toxicology letters 189:S-S213
[6] Johnson, M.K., (1977). Arch. Toxicol. 37, 113-115.

UNIVERSITAS
Miguel
Hernández

Title: KINETIC CARACTERIZATION OF ORGANOPHOSPHORUS COMPOUNDS IN ESTERASES OF BRAIN MEMBRANE

Authors: I. Mangas, E. Vilanova, J. Estévez,

Type of participation: Poster
CONGRESS: XIII INTERNATIONAL CONGRESS OF TOXICOLOGY (ICT XIII),
Place of celebration: Paris (France). Date: 28 August 2011
Ref. journal: Toxicology Letters. Volume: 205 Page S231

ABSTRACT:

Some neurotoxic effects in experimental animals and in humans of organophosphorus (OPs) esters cannot be explained by action on presently recognised targets.

In this work were evaluate and characterize the interaction (inhibition, reactivation and "ongoing inhibition") of two OPs models, paraoxon (non neuropathy-inducer) and mipafox (neuropathy-inducer), with brain particulate esterases of chicken.

The results of this work discriminates four enzymatic components. The relative sensitivity of the time-progressive inhibition differs for paraoxon and mipafox. The most sensitive component for paraoxon is also the most sensitive component for mipafox (4-8 % of activity) with I50 (30 min) of 9-19 nM with paraoxon and 6-29 nM with mipafox, and it is spontaneous reactivated with paraoxon. The second sensitive component to paraoxon (38% of activity) has I50 (30 min) of 1540 nM and is practically resistant to mipafox. The third component (38-40% of activity) is paraoxon resistant and is sensitive to micromolar concentrations of mipafox, this component fit the operational criteria of being NTE (target of organophophorus induced delayed neuropathy) and it has I50 (30 min) with mipafox of 5.3-6.7 µM. The fourth component (9-12% of activity) is practically resistant to both inhibitors. The high sensitivity of these esterases suggests that they may either play a role in toxicity in low-level exposure to organophosphate compounds or have a protective effect related with the spontaneous reactivation.

UNIVERSITAS
Miguel
Hernández

KINETIC CARACTERIZATION OF ORGANOPHOSPHORUS COMPOUNDS IN ESTERASES OF BRAIN MEMBRANE

Iris Mangas , Eugenio Vilanova, and Jorge Estévez*
Unidad de Toxicología y Seguridad Química, Instituto de Bioingeniería,
Universidad Miguel Hernández de Elche, Elche (Spain). * jorge.estevez@umh.es

INTRODUCTION. In this work the interaction (inhibition, spontaneous reactivation and "ongoing inhibition") of two model OPs, paraoxon (non neuropathy-inducer) and mipafox (neuropathy-inducer), with esterases of chicken brain particulate fraction (membranes) were characterized.

MATERIALS AND METHODS. Enzyme preparation: particulate fractions (membranes) of chicken brain (from 200 mg fresh tissue/ml). Inhibitors: Paraoxon (O,O'-diethyl p-nitrophenyl phosphate) and N, N´- di-isopropyl phosphorodiamidefluoridate (mipafox). Enzyme assay: Inhibitor was preincubated with enzyme preparation for the time indicated in each experiment and then substrate (phenylvalerate) was added for measuring residual activity by colorimetric method [1,2].

RESULTS. The observations at fixed-time inhibition at different concentrations are shown in **Fig 1.** The **Fig. 2** show the result of reactivation after diluting experiments of samples preinhibited, results are coherent with a reactivation of component E1 inhibited by paraoxon but not reactivation with any component inhibited by mipafox (Parameters in Table 1). The time progressive inhibition experiment for several inhibitor concentrations is shown in **Fig 3.** The inhibition curves were analyzed with kinetic models according to [3] where the most sensitive component which is simultaneously spontaneously reactivated for the case of paraoxon, and a resistant component, and considering that a possible ongoing inhibition (significant inhibition during substrate incubation) is occurring for the most sensitive component.

For time progressive inhibition by paraoxon:

$$E = [e^{-ka' \cdot I}] \cdot \{[(kr1 \cdot E1_0)/(k1 \cdot I + kr1)] + [(k1 \cdot I \cdot E1_0)/(k1 \cdot I + kr1)] \cdot e^{-(k1 \cdot I + kr1) \cdot t}\} + E2_0 \cdot e^{-(k2 \cdot I) \cdot t} + R$$

And for mipafox:

$$E = [e^{-ka' \cdot I}] \cdot E1_0 \cdot e^{-(k1 \cdot I) \cdot t} + E2_0 \cdot e^{-(k2 \cdot I) \cdot t} + R$$

(ka' exponential constant of the ongoing inhibition [4], k1, k2 inhibition constants, kr1 the reactivation constant; $E1_0$, $E2_0$ and R th proportion (amplitude) of the enzymatic components E1, E2 and R the resistant one, respectively.

An experiment were done of concurrent inhibition with 40 µM paraoxon and variable mipafox concentration for evaluating NTE (neuropathy target esterase) activity as the activity resistant to 40 µM paraoxon and sensitive to mipafox (range 0,1 to 250 µM) and the best fitting model was:

$$E = E1_0 \cdot e^{-(k1 \cdot I) \cdot 30} + R$$

The estimated kinetic parameters are shown in the **Table 1**

CONCLUSIONS. The results of this work discriminates four enzymatic components according to the sensitivity to paraoxon and mipafox as follows:

Name	Sensitivity	Equivalency in Table
E(α)	Very sensitive to paraoxon and to mipafox and spontaneously reactivated after paraoxon inhibition	**E1** for paraoxon and for mipafox
E(β)	Sensitive to paraoxon and resistant to mipafox	**E2** for paraoxon and included in **R** for mipafox
E(γ)	Resistant to paraoxon and sensitive to mipafox, with a I_{50} for 30 min similar to NTE (NTE I_{50} = 4.7 µM at 30 min; [5])	Included in **R** for paraoxon and is **E2** for mipafox
E(δ)	Resistant to both inhibitors	Included in **R** for paraoxon and for mipafox

The high sensitivity to paraoxon of the non-NTE esterases, suggests that they may either play a role in toxicity at low-level exposure to OPs or have a protective effect related with the spontaneous reactivation. They will have to be considered in further metabolic and toxicological studies.

REFERENCES

[1] Mangas et al. (2011). Toxicol Appl Pharmacol. doi:10.1016/j.taap.2011.05.005
[2] Johnson, M.K. (1977). Arch. Toxicol. 37, 113–115.
[3] Estévez and Vilanova (2009). Crit Rev Toxicol; 39(5): 427–448
[4] Estévez et al. (2010). Chem Biol Interact. 187, 397-40
[5] Johnson, M. K., 1982. ReV. Biochem. Toxicol. 4, 141–212.

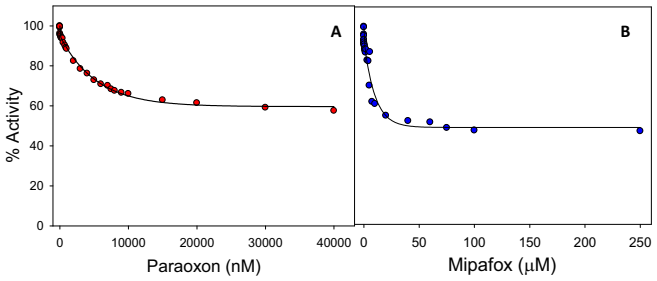

Figures 1. Paraoxon (A) and mipafox (B) 30-min fixed-time inhibition curve. A brain particulate fraction from 15 mg tissue/ml was incubated with the inhibitor for 30 min at 37ºC. The best fit model to both curves were the same model as in the time progressive inhibition experiment.

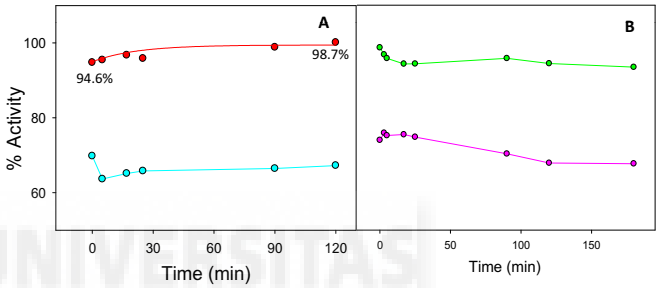

Figures 2 . Spontaneous reactivation after inhibition by paraoxon (A) or mipafox (B). Concentrated tissue preparations (200 mg/ml) were inhibited by preincubation with 40 nM (red) and 1000 nM (blue) of paraoxon or 40 nM (green) and 8000 nM (pink) of mipafox at 37º C for 30 min. Then they were diluted 10-fold with buffer and maintained up to 180 min at 37ºC before measuring activity. The sample preinhibited with 40 nM of paraoxon (red) recovered activity from 94.6 % to 98.7 % of activity

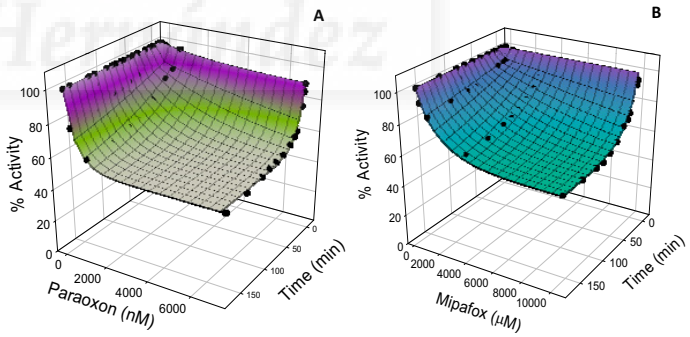

Figures 3. 3-D plotting of the inhibition kinetics of particulate brain PVases by paraoxon (A) mipafox (B). A preparation containing the particulate fraction of 15 mg fresh tissue/ml was preincubated with 0, 40, 250, 1000 and 7000 nM paraoxon (**A**) or 0, 200, 800, 3500 and 8000 nM of mipafox (**B**) for the indicated time at 37ºC before measured PV ase activity. The surface reflects the result of the best model according to the F test.

Table 1. Kinetic parameters from fitting model equations to inhibition. The I_{50} values were calculated from the kinetic constants for each component. PARAOXON: (**A**) Reactivation after diluting (Fig. 2A);(**B**) Experiment for fixed time inhibition considering spontaneous reactivation (Fig. 1A); (**C**) Experiment of time-progressive inhibition (Fig 3A). **MIPAFOX:** (**A**) Experiment for fixed time inhibition (Fig. 1B); (**B**) Experiment for time-progressive inhibition (Fig. 2B). **(C)** NTE concurrent assay (mipafox inhibition in the presence of 40 µM paraoxon)

	ka (t=0) (nM^{-1})	E1 %	k1 ($nM^{-1}.min^{-1}$)	k1r (min^{-1})	I_{50} (30 min) nM	E2 %	k2 ($nM^{-1}.min^{-1}$)	I_{50} (30 min) nM	R %
	PARAOXON								
A		4.4	0.0012	0.0464	43	95.6*	-		-
B	-	5.9	0.0030	0.1100	37	34.8	$5.9 \cdot 10^{-6}$	3916	59.3
C	0.00089	8.3	0.0025	0.0272	15	38.3	$1.5 \cdot 10^{-5}$	1540	53.4
	MIPAFOX								
A	-	6.2	0.0042	-	6	40.1	$4.3 \cdot 10^{-6}$	5373	53.7
B	$2.0 \cdot 10^{-4}$	4.9	0.0008	-	29	38.6	$3.5 \cdot 10^{-6}$	6601	56.5
C	-	-	-	-	-	36.2	$3.6 \cdot 10^{-6}$	6618	8.6

* Correspond to the fraction resistant to 40 nM of paraoxon (E2 and R)

UNIVERSITAS
Miguel
Hernández

Title: **DIFFERENTIAL INTERACTIONS OF NEUROPATHY INDUCERS, NON-INDUCERS AND PROMOTERS WITH SOLUBLE AND MEMBRANE ESTERASES: KINETIC APPROACHES.**

Authors: J. Estévez, **I. Mangas,** MA. Sogorb, E. Vilanova

Type of participation: Oral
CONGRESS: The 11th Meeting on Cholinesterases
Place of celebration: Kazan (Russia) **Date:** 4-9 June 2012

Cholinesterases, serine-peptidases and neuropathy target esterase (NTE) are known proteins which carboxylesterase or peptidase enzymatic activity which are covalently inhibited by organophosphorus compounds (OPs) and other acylating chemicals as sulphonyl fluorides (i.e: PMSF). The acute or delayed neurotoxicological effects of aceylcholinestesase or NTE inhibition are well known. The biological function of acetylcholinestese and peptidase are known and related directly with their catalytic esterase properties but for NTE, a membrane bound protein, it is no clear: a phosphatidyl deacylase activity has been suggested for a function on lipid homeostasis in adults for axon maintenance. More recently a critical role of NTE in cell differentiation and embryonic development is under study. In mammals, avian and other species, other carboxylesterases with unknown toxicological and biological function are interacting with OPs. Using inhibition kinetic approaches to complex systems, several components of sensitive carboxylesterases have been discriminated considering the sensitivity (inhibition rate constant) and spontaneous reactivation (dephosphorylation) soluble and membrane fractions of chicken nerves (model animal for OP delayed neuropathy). Peripheral nerve soluble fraction contain 3 components, two of them highly sensitive (nmolar levels) to paraoxon, mipafox, S9B and PMSF (micromolar level), two of them spontaneously reactivated after paraoxon inhibition and one with S9B. In brain soluble fraction 4 components were discriminated, with different sensitivities to the inhibitors and their sensitivity change when preincubated with low no inhibitory concentration of PMSF, demonstrating some kind of interaction in no catalytic site. In brain membrane, also 4 components are discriminated (one of them is NTE) and their sensitivity is significantly changed by pre-exposure to PMSF. How this PMSF interaction may have a role in the so called potentiation/promotion effect is under study. The role in detoxication as scavengers or by their spontaneous reactivating properties also needs to be clarified. Other tyrosine carboxylesterase (as the esterase activity of albumin) also show spontaneous reactivation and has been suggested a role in detoxication of OP and carbamates. The kinetic discrimination of esterase allows us to have now better criteria to design which fraction of esterases should be isolated and molecularly characterize.

UNIVERSITAS
Miguel
Hernández

Title: KINETIC INTERACTION OF PMSF (A NEUROPATHY PROMOTER) WITH MEMBRANE BOUND ESTERASES WHICH ARE SENSITIVE OR RESISTANT TO ORGANOPHOSPHORUS INDUCERS OF DELAYED NEUROPATHY

Authors: E. Vilanova, **I. Mangas,** J. Estévez,

Type of participation: Poster
CONGRESS: 52TH ANNUAL MEETING OF THE SOCIETY OF TOXICOLOGY
Place of celebration: San Francisco (USA) Date: 13 March 2012

ABSTRACT:

Purpose: Some neurotoxic effects of organophosphorus (OPs) esters cannot be explained by action on presently recognized targets. In this work kinetic experiments with paraoxon and mipafox in chicken brain membrane were done to establish the relationship among the enzymatic components with this models OPs and to discriminate the potential targets of delayed neurotoxicity from other esterases using kinetic approaches. The chicken brain membranes were chosen because it was the first tissue where NTE (the target protein of organophosphorus induced delayed neuropathy) was found.

Methods: Typical time-progressive inhibition assays with paraoxon and mipafox, concurrent assay (incubating paraoxon and mipafox together) and a sequential assay (where paraoxon was removed before adding mipafox) were done.

Results and conclusions: Two paraoxon-resistant and mipafox-sensitive esterases were found using the sequential assay but only one paraoxon-resistant and mipafox-sensitive using the concurrent assay. Four esterase components can be establish: EPα: 4.1-4.9% of activity which is sensitive to paraoxon (I50 30 min=15nM) and mipafox (I50 30 min=29nM) and it is spontaneously reactivated after paraoxon inhibition; EPβ: 38.3% of activity wich is paraoxon sensitive (I50 30 min=1540nM) and practically resistant to mipafox; EPγ: 38.6-47.6% of activity which is resistant to paraoxon and it is sensitive to mipafox (this may be identify as NTE, the target of OP delayed neurotoxicity) and EPδ: 9.80-10.7% of activity which is practically resistant to both inhibitors. The data showed in this work will facilitate further studies for isolation and molecular characterization of esterases which might either play a role in toxicity of organophosphates .

UNIVERSITAS
Miguel
Hernández

Kinetic interaction of PMSF (neuropathy promoter) with membrane bound esterases which are sensitive or resistant to organophosphorus inducers of delayed neuropathy

Eugenio Vilanova, Iris Mangas and Jorge Estévez

Unidad de Toxicología y Seguridad Química, Instituto de Bioingeniería, Universidad Miguel Hernández, Elche (Spain)

Abstract #1397

Introduction

PMSF (phenylmethanesulfonylfluoride) is a protease and esterase inhibitor causing protection or promotion of the organophosphorus delayed polyneuropathy and of other axonopathies such as. 2,5-hexanedione neuropathy as well as traumatic neuropathy [1,2]. The molecular target of promotion has not yet been identified. In this work, the interaction of chicken brain membrane esterases with PMSF, which is instable in water solution [3], is characterized using kinetic models previously developed in our laboratory [3,4].

Objectives

To identify the relevant carboxylesterases in the potentiation of delayed neuropathy by study the interaction of membrane brain esterases with PMSF using a kinetic model with three different molecular phenomena occurring simultaneously (1) Inhibition; (2) spontaneous chemical hydrolysis of the inhibitor; (3) ongoing inhibition (inhibition during the substrate reaction) and to discriminate the esterase fractions sensitive or resistant to PMSF among those sensitive or resistant to mipafox or paraoxon.

Methods

Enzyme preparation: Membrane fractions of chicken brain (from 15 mg fresh tissue/ml) according to [5].

Inhibitor: Phenylmethanesulfonylfluoride (PMSF)

Inhibition assays: Enzyme assays were carried out as previously described in [6].

Mathematical analysis of the inhibition curves: Model equations for a system with several enzymatic components were applied as described by Estévez and Vilanova (2009) [2] including the spontaneous hydrolysis of PMSF according to Estevez et al (2012) [3].

References

- [1] Moretto et al., 1993; Chem-Biol. Interact. 87, 457-462
- [2] Peraica et al., 1993. Biochem. Pharmacol. 45, 131-135
- [3] Estévez et al., 2012. Arch Toxicol. DOI 10.1007/s00204-012-0817-3
- [4] Estévez and Vilanova., 2009. Crit Rev Toxicol . 39(5): 427–448
- [5] Vilanova et al., 1990. Neurochemistry 55:1258-1265
- [6] Mangas et al., 2011. Toxicology letters 205 S. S231

Results

1. Evaluation of spontaneous reactivation. The activity remained inhibited over time in the time-progresive inhibition experiment (**Fig. 1**) in spite of PMSF is removed because it is unstable and chemically hydrolyses. No spontaneous reactivation is observed in Figure 1 .

2. Fixed-time inhibition curve. It was properly fitted with a model with two enzymatic sensitive components and a resistant one as follow **(Fig 2; Table 1A)**:

$$E = E1_0 \cdot e^{(e^{-kh \cdot t_{-1}}) \cdot \frac{k1}{kh} \cdot I_0} + E2_0 \cdot e^{(e^{-kh \cdot t_{-1}}) \cdot \frac{k2}{kh} \cdot I_0} + R$$

2. Time-progressive inhibition by PMSF. The inhibition was time-progressive (~85 % of total activity), which is coherent with covalent inhibition **(Fig. 1).** The data were properly fitted with a three-dimensional fit including ongoing inhibition and spontaneous hydrolysis **(Fig. 3; Table 1B).** The best fit according to F test was:

$$E = E1_0 \cdot e^{(ka \cdot I_0)} \cdot e^{(e^{-kh \cdot t_{-1}}) \cdot \frac{k1}{kh} \cdot I_0} + E2_0 \cdot e^{(kb \cdot I_0)} \cdot e^{(e^{-kh \cdot t_{-1}}) \cdot \frac{k2}{kh} \cdot I_0} + R$$

k1,k2 are the inhibition constants, kh is the hydrolysis constant, ka´ and kb´ are the the exponential constant of the ongoing inhibition . E10, E20 are the proportion of the initial enzymatic components, and R is the enzymatic fraction resistant to inhibition.

4. Time-progressive inhibition by PMSF of Mipafox resistant membrane fraction. Tissue fraction was incubated with mipafox 20 µM, the resistant fraction was incubated with PMSF at concentrations in the range of 0-1000 µM of PMSF for 20 min at 37 ºC and then the enzymatic activity was assayed. The best fitting model is compatible with a resistant component and one sensitive component **(Table 1C).**

Table 1. Kinetic parameters and I_{50} (30 min) obtained from the different experiments of inhibition with PMSF on membrane fraction of brain.

R^2	ka	kb	kh	E1	k1	I_{50}^{30}	E2	k2	I_{50}^{30}	R
	nM^{-1}	nM^{-1}	min^{-1}	(%)	$\mu M^{-1} \cdot min^{-1}$	µM	(%)	$\mu M^{-1} \cdot min^{-1}$	µM	(%)
A. Fixed-time inhibition										
0.9993			0.23	36	0.007	21	51	0.0013	119	13
B. Tridimensional fitting of progression-time experiment										
0.9971	0.0056	0.0007	0.28	44	0.008	25	41	0.0014	138	15
C. PMSF fixed-time inhibition of 20 µM resistant fraction										
0.9734			0.30	-	-	-	47	0.0014	144	12

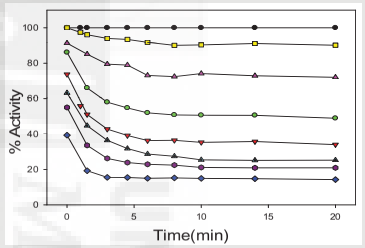

Figure 1. Kinetics of the time-progressive inhibition by PMSF concentrations. Preparations containing the membrane fraction of 15 mg fresh tissue/ml t were preincubated with 0, 10, 25, 75, 150, 250, 400 and 1000 µM PMSF (upper to lower plots) for the indicated time. Then, the enzymatic activity was assayed by incubating the substrate phenylvalerate for 10 min.

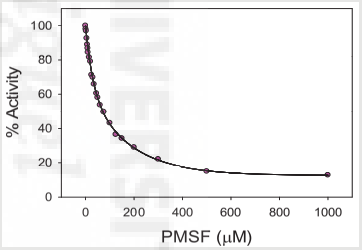

Figure 2. PMSF fixed-time inhibition curve of esterase activity. Enzyme preparation was incubated at concentrations in the range of 0-1000 µM of PMSF for 20 min at 37 °C and then the enzymatic activity was assayed . The curve was fitted with exponential model equations including spontaneous hydrolysis of PMSF selecting the best fitting equation according to the F-test. **Table 1A**.

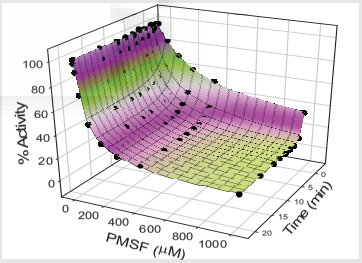

Figure 3. Representation of the inhibition kinetics of membrane brain esterases by PMSF. Inhibitory surface obtained by fitting the 3D model equation to the data corresponding to PMSF inhibition which is done in the membrane fraction of the brain (Fig. 2). The surface reflects the result of the best model according to the F test. It corresponds to a model with two sensitive enzymatic components plus other resistant where the most sensitive is affected by ongoing inhibition (**Table 1B**).

Conclusions

- Most of the membrane fraction of brain (85%) can be time-progresively inhibited by PMSF in an irreversible and permanent manner.
- Considering PMSF inhibition data and those with mipafox and paraoxon [6] four enzymatic components were discriminated according to their sensitivity to paraoxon, mipafox and PMSF **(Fig. 4)** as follows:

EPα, which is very highly sensitive to paraoxon and to mipafox and resistant to PMSF, and spontaneously reactivates after inhibition with paraoxon.

EPβ, which is sensitive to paraoxon and PMSF and it is resistant to mipafox.

EPγ, which is sensitive to mipafox and PMSF and it is resistant to paraoxon. This component fit the operational criteria of being **NTE** and has I50 (30 min) with mipafox and PMSF similar to NTE.

EPδ, which is resistant to all inhibitors. Very sensitive (+++), sensitive (++)/(+) and resistant (-). (r) Spontaneously reactivated.

- We have the appropriate criteria to monitor the isolation of PMSF, Mipafox and paraoxon sensitive esterases in brain membrane for their further molecular identification in order to understand their role in the mechanism of induction, protection or potentiation of delayed neurotoxicity .

		PARAXON I50 (30 min) (nM)	MIPAFOX I50 (30min) (nM)	PMSF I50 (30 min) (µM)
EPα	4-8%	9 nM (+++) r	29nM (+++)	(-)
EPβ	35-51%	1540 nM (++)	(-)	138µM (++)
Epγ (NTE)	36-45%	(-)	6710 nM (+)	25µM (++)
EPδ	7-14%	(-)	(-)	(-)

Figure 4. Conclussions: Discrimination of four esterase components in chicken membrane brain.

UNIVERSITAS
Miguel
Hernández

Title: **PMSF ALTERS THE INTERACTION OF CHICKEN BRAIN ESTERASES WITH ORGANOPHOSPHOROUS COMPOUNDS.**

Authors: I. Mangas, J. Estévez, E. Vilanova,

Type of participation: Poster
CONGRESS: The 11th Meeting on Cholinesterases
Place of celebration: Kazan (Russia) **Date:** 4-9 June 2012

ABSTRACT:

Phenylmethylsulfonylfluoride (PMSF) is a protease and esterase inhibitor causing protection or potentiation ("promotion") of organophosphorus delayed neurotoxicity, depending if dosed in vivo before or after the OP inducer. The protection effect is well-known to be caused by the covalent inhibition and so blocking of NTE (neuropathy target esterase) avoiding the further interaction of the neuropathic OP inducer. However the target of the promotion effect is not well identified although the possible role of other soluble esterases has been proposed. PMSF is unstable in water solution but it can cause permanent covalent inhibition of esterases and proteases. In this work, evidences that the exposure to PMSF can modify esterases which enzymatic activity is not inhibited by PMSF but strongly modify its sensitivity against OP inhibitors. Kinetic data of the esterase inhibition were obtained for (PMSF) tested at different concentrations incubated with particulate and soluble fractions of chicken brain. The best fitting model for the soluble fraction is a model with two sensitive enzymatic entities (61% and 11%) and a resistant component (28%). The corresponding second order rate constants of inhibition (ki=0.0023 µM-1x min-1 and 0.00036 µM-1×min-1, respectively) and the chemical hydrolysis constant of PMSF (kh=0.23 min-1) were simultaneously estimated. The best fitting model for the membrane fraction is a model with two sensitive enzymatic entities (44% and 41%) a resistant component (14%). The corresponding second order rate constants of inhibition (ki=0.0076 nM-1x min-1 and 0.0014 nM-1×min-1, respectively) and the chemical hydrolysis constant of PMSF (kh=0.28 min-1) were simultaneously estimated. Kinetic interaction of incubated both esterase fractions with PMSF before adding mipafox (an inducer of delayed neurotoxicity) at different concentrations for 30 min was study. The best fitting model with mipafox for the soluble fraction preincubated with PMSF and the best fitting model with mipafox for the membrane fraction preincubated with PMSF showed than preincubation to PMSF altered the sensitivity to mipafox of enzymatic components in soluble fraction but not significantly in the membrane bound esterases.

UNIVERSITAS
Miguel
Hernández

PMSF ALTERS THE INTERACTION OF CHICKEN BRAIN ESTERASES WITH ORGANOPHOSPHOROUS COMPOUNDS

Iris Mangas, Jorge Estevez; Eugenio Vilanova

Unit of Toxicology and Chemical Safety. Institute of Bioengineering.
University "Miguel Hernández" Elche-Alicante. Spain

Introduction

PMSF is a protease and esterase inhibitor causing protection or promotion of the organophosphorus delayed polyneuropathy and of other toxic axonopathies such as e.g. 2,5-hexanedione neuropathy as well as traumatic neuropathy [1,2]. The molecular target of promotion has not yet been identified. PMSF is spontaneously hydrolyzed in biological preparation and a kinetic model which considers the inhibition and the spontaneous hydrolysis of inhibitor is required to analyses the inhibition data [3, 4] . Time-progresive inhibition data were obtained at different concentrations of PMSF incubated with soluble and membrane fractions of chicken brain. Also the residual activity after preinhibition with different concentrations of PMSF were incubated with mipafox to discriminate the sensitive or resistant esterase components to PMSF among those sensitive or resistant to mipafox recently described [5] in order to understand their role in the mechanism of induction, protection or potentiation of OPIDN.

Results

Time-progressive inhibition by PMSF. Soluble fractions of 20 mg fresh tissue/ml were preincubated with 0, 20, 70, 300 and 1000 µM PMSF (1A) and membrane fractions of 15 mg fresh tissue/ml were preincubated with 0, 10, 25, 75, 150, 250, 400 and 1000 µM PMSF (2B). The inhibition was time-progressive (~72% of total activity in soluble (Fig. 1) and ~85 % of total activity in membranes (Fig. 1) , which is coherent with covalent inhibition. Then, the enzymatic activity was assayed by incubating the substrate phenylvalerate for 10 min. Panels B reveals inhibition at the substrate reaction time. Panels C provides the inhibitory surface of the best model according to the F test obtained by fitting the 3D model equation to the data . For the soluble fraction (Table 1A):

$$E = E1_0 \cdot e^{(ka \cdot I_0)} \cdot e^{\left(e^{-kh \cdot t}-1\right) \cdot \frac{k1}{kh} \cdot I_0} + E2_0 \cdot e^{\left(e^{-kh \cdot t}-1\right) \cdot \frac{k2}{kh} \cdot I_0} + R$$

For the membrane fraction (Table 1B):

$$E = E1_0 \cdot e^{(ka1' \cdot I_0)} \cdot e^{\left(e^{-kh \cdot t}-1\right) \cdot \frac{k1}{kh} \cdot I_0} + E2_0 \cdot e^{(ka2' \cdot I_0)} \cdot e^{\left(e^{-kh \cdot t}-1\right) \cdot \frac{k2}{kh} \cdot I_0} + R$$

k1 and k2 are the inhibition constants, kh is the hydrolysis constant, ka1' and ka2´ are the the exponential constant of the ongoing inhibition . $E1_0$, $E2_0$ are the proportion of the initial enzymatic components, R is the fraction resistant to inhibition and I_0 is the initial concentration of PMSF.

Fixed-time mipafox inhibition assays in PMSF-incubated soluble PVase activity. Exponential decay models were fitted to the mipafox inhibition data with one, two or more enzymatic components, with or without resistant component. The Table 2 shows the resistant activity to the PMSF concentrations used and the kinetic parameters of the best fitted model acording to F-test for each experiment. (*) For Eα or Eγ, as "Expected", it is indicated the estimated residual activity of the Eα or Eγ component after the preincubation with the indicated PMSF concentration, considering the kinetic parameters of the PMSF inhibition and assuming that the preincubation would not affect the behavior with mipafox. In the "Resistant" column, the "expected" data are the estimated value of the Eβ component (resistant to mipafox) that is expected after preincubation with the indicated PMFS concentration; however the observed value may be the residual Eβ plus the proportion of the Eγ fraction converted to resistant.

References

[1] Moretto et al., 1993; Chem-Biol. Interact. 87, 457-462
[2] Peraica et al., 1993. Biochem. Pharmacol. 45, 131-135
[3] Estévez et al., 2012. Arch Toxicol. DOI 10.1007/s00204-012-0817-3
[4] Estévez and Vilanova., 2009. Crit Rev Toxicol . 39(5): 427–448
[5] Mangas et al., 2011. Toxicology and Applied Pharmacology 260 (3): 360-368

Figures and tables

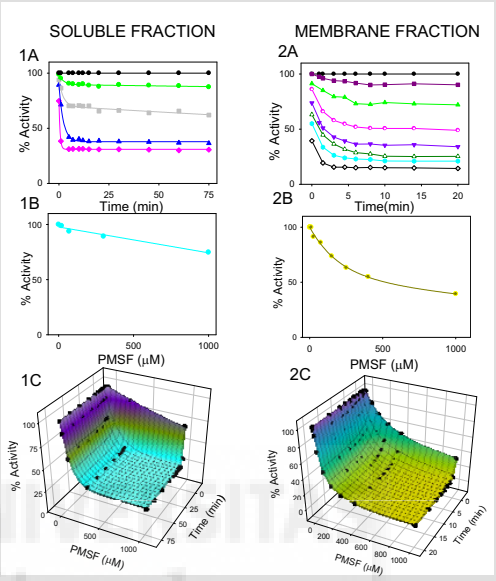

Fig 1. Kinetics of the time-progressive inhibition by PMSF in soluble fraction and membrane fraction of chicken brain at 37ºC

Table 1. PMSF kinetic parameters and I_{50} (20 min)

	E1 (%)	Ka1´/ka2´ (μM^{-1})	kh (min^{-1})	k1 ($\mu M^{-1} \cdot min^{-1}$)	I_{50}^{20} (μM)	E2 (%)	k2 ($\mu M^{-1} \cdot min^{-1}$)	I_{50}^{20} (μM)	R (%)
A.	61	0.0005/ -	0.23	0.0023	72	8	0.00036	435	29
B.	44	0.0048/ 0.0005	0.28	0.0080	25	41	0.0014	138	15

Preincubation (20 min)	Total activity after pre-incubation (%)	Eα (%)	I_{50} (20 min) (nM)	Eγ (%)	I_{50} (20 min) (nM)	(*)Resistant (%)
Buffer	100	21	4	8	7,701	71
5 µM PMSF	*(96)*	*(21)*	26	*(8)*	25,672	(67)
(*)Expected	93	22		5		66
Observed						
10 µM PMSF	(93)	*(21)*	31	(8)	-	(64)
(*)Expected	93	21		0		72
Observed						
150 µM PMSF	(42)	(21)	72	(6)	-	(15)
(*)Expected	43	22		0		21
Observed						
4000 µM PMSF	(21)	(21)	222	(0)	-	0
(*)Expected	17	17		0		0
Observed						

Table 2. Inhibition by mipafox of soluble esterases of brain preinhibited with PMSF

Conclusions

In soluble fraction can be discriminated three different entities according to their sensitivity to mipafox and PMSF: Eα (11-28% of activity) with I_{50} (30 min) 4 nM mipafox and resistant to PMSF; Eβ (61-84% of activity) with I_{50} (30 min) of 72 µM PMSF and resistant to mipafox and Eγ (5-8% of activity)with I_{50} (30 min) of 3.4 µM mipafox and of 435 µM PMSF.
Preincubation to PMSF without inhibit the esterase activity alters the sensitivity to mipafox of components Eα and Eγ: Eγ become resistant to mipafox and Eα become less sensitive to mipafox . This effect might be due to the interaction on sites different to the substrate catalytic center of soluble brain phenylvalerate esterases, which should be considered for interpreting the potentiation/promotion phenomenon of PMSF and in the understanding of effects of multiple exposures to chemicals.

UNIVERSITAS
Miguel
Hernández

Title: KINETIC IDENTIFICATION OF ORGANOPHOSPHATE-SENSITIVE ESTERASES IN BRAIN MEMBRANE

Authors: E. Vilanova, **I. Mangas,** J. Estévez,

Type of participation: Poster
CONGRESS: XIV INTERNATIONAL CONGRESS OF TOXICOLOGY (ICT XIV)
Place of celebration: Stockholm (Sweden) Date: 19-23 June 2012

ABSTRACT:

Some neurotoxic effects of organophosphorus (OPs) esters cannot be explained by action on presently recognized targets. In this work kinetic experiments with paraoxon and mipafox in chicken brain membrane, where NTE (neuropathy target esterase) was first found, were done to establish the relationship among the enzymatic components with this models OPs and to discriminate the potential targets of delayed neurotoxicity.

Two assays were done, a concurrent assay, incubating with 40 µM of paraoxon and 250 µM of mipafox and a sequential assay where paraoxon was removed before adding mipafox.

Two paraoxon-resistant and mipafox-sensitive esterases were found using the sequential assay but only one paraoxon-resistant and mipafox-sensitive using the concurrent assay. This apparent discrepancy is a result of spontaneous reactivation after paraoxon inhibition of a non- NTE component. Four esterase components with different properties can be establish: EPα: 4.1-4.9 % of activity with I50 (30 min) of 15-43 nM with paraoxon and 29 nM with mipafox and which is spontaneously reactivate after paraoxon inhibition; EPβ: 38.3 % of activity has I50 (30 min) of 1540 nM with paraoxon and is practically resistant to mipafox; EPγ: 38.6-47.6 % of activity which is NTE and EPδ: 9.80-10.7 % of activity which is practically resistant to both inhibitors. The kinetic characterization of these components is necessary for further studies for isolation and molecular characterization of these esterases which might either play a role in toxicity of organophosphate compounds or have a protective effect in relation to the spontaneous reactivation.

UNIVERSITAS
Miguel
Hernández

KINETIC IDENTIFICATION OF ORGANOPHOSPHATE-SENSITIVE ESTERASES IN BRAIN MEMBRANE

Eugenio Vilanova, Iris Mangas, Jorge Estevez
imangas@umh.es

Unit of Toxicology and Chemical Safety. Institute of Bioengineering.
University "Miguel Hernández" Elche-Alicante. Spain

Introduction: Some effects of organophosphorus compounds (OPs) esters cannot be explained by action on currently recognized targets. In this work the interaction (inhibition, reactivation and "ongoing inhibition") of two model OPs, paraoxon (non neuropathy-inducer) and mipafox (neuropathy-inducer), were evaluate and characterize with esterases of chicken brain membranes. This animal model was chosen because the neuropathy target esterase (NTE) was first described and isolated. Sequential experiments with paraoxon and mipafox were done to establish the relationship among the enzymatic components with these models OPs.

Experimental design and Results:

1. Reactivation kinetics by dilution. High tissue-concentrated samples were inhibited with either 40 and 1000 nM paraoxon or 40 and 8000 nM mipafox for 30 min at 37ºC according to [1, 2] . Then preincubated samples were diluted 10-fold with buffer and activity was measured. Spontaneous reactivation was observed after inhibition only in the samples preinhinited with 40 nM of paraoxon.

2. Kinetics of the time-progressive inhibition by paraoxon and mipafox. Membrane fraction of 15 mg fresh tissue/ml was preincubated with , 40, 250, 1000 and 7000 nM paraoxon **(Fig. 1A)** or 0, 200, 800, 3500 and 10000 nM of mipafox **(Fig. 2A)** at 37ºC, then enzymatic activity was assayed. Panels B provides the inhibitory surface obtained of the best fit according to the F test [3] . For **paraoxon** the best 3D model equation was (estimated kinetic parameters in **Table 1A**):

$$E = [e^{-ka' \cdot t}] \cdot \{[(kr1 \cdot E1_0)/(k1 \cdot I + kr1)] + [(k1 \cdot I \cdot E1_0)/(k1 \cdot I + kr1)] \cdot e^{-(k1 \cdot I + kr1) \cdot t}\} + E2_0 \cdot e^{-(k2 \cdot I) \cdot t} + R$$

For **mipafox** was (estimated kinetic parameters in **Table 1B**):

$$E = [e^{-ka' \cdot t}] \cdot E1_0 \cdot e^{-(k1 \cdot I) \cdot t} + E2_0 \cdot e^{-(k2 \cdot I) \cdot t} + R$$

ka' exponential constant of the ongoing inhibition, k1, k2 inhibition constants, kr1 the reactivation constant; $E1_0$, $E2_0$ and R the proportion (amplitude) of the enzymatic components E1, E2 and R the resistant one, respectively.

3. Inhibition of 40 µM paraoxon-resistant activity with mipafox (NTE assay). Two assays were performed. In both the tissue samples were preincubated with 40 µM of paraoxon for 30 min. Then paraoxon was removed in one of them by two circles of diluting with cold buffer and centrifugation at 4ºC. After that a fixed time inhibition with mipafox was done (range from 0.03 to 250 µM) for 30 min at 37ºC in both assays. **Table 1C** shows the estimated kinetic parameters of the mipafox fixed inhibition assay in the samples without eliminating the paraoxon, and **Table 1D** the kinetic parameters removing paraoxon.

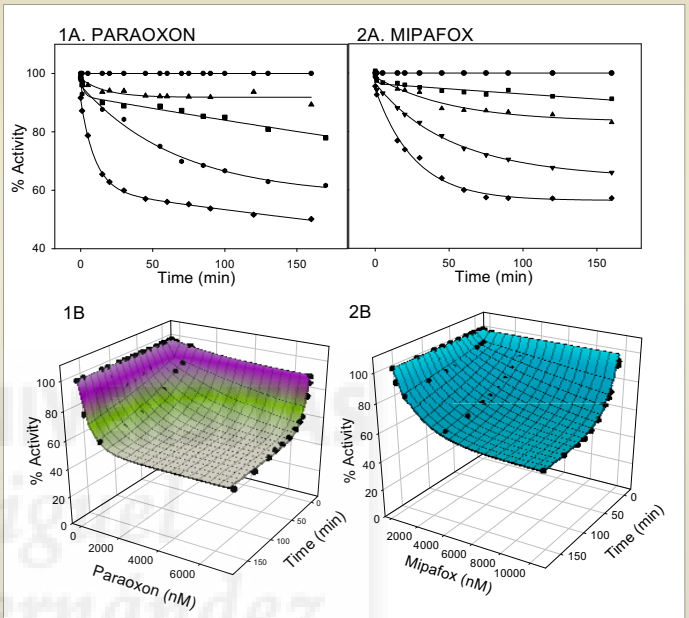

Table 1. Estimated kinetic parameters

	E1 (%)	Ka (nM^{-1})	K1r ($nM^{-1} \cdot min^{-1}$)	k1 ($nM^{-1} \cdot min^{-1}$)	I_{50}^{30} (nM)	E2 (%)	k2 ($nM^{-1} \cdot min^{-1}$)	I_{50}^{30} (nM)	R (%)
A.	8.3	0.0009	0.0025	0.0272	15	38.3	$1.5 \cdot 10^{-5}$	1540	53.4
B.	4.9	0.0003	-	0.0008	29	38.6	$3.5 \cdot 10^{-6}$	6601	56.1
C.	-	-	-	-	-	78.9	$3.8 \cdot 10^{-6}$	6080	21.1
D.	4.1	-	-	0.0005	46	79.9	$4.3 \cdot 10^{-6}$	5373	20.0

Conclusions:

Discrimination of the esterase components in chicken membrane brain. Four enzymatic components were discriminated according to sensitivity to paraoxon and mipafox: EPα., Epβ, Epγ and Epδ (**Table 2**). The kinetic characterization of these components will facilitate further studies for isolation and molecular characterization.

NTE assay. Two paraoxon-resistant and mipafox-sensitive esterases were found using the sequential assay removing paraoxon, but only one was found in the assay without removing the paraoxon. This apparent discrepancy, previously interpreted as reversible NTE inhibition with paraoxon [4, 5] is the result of spontaneous reactivation after paraoxon preinhibition of a non NTE component (**EPα**).

The high sensitivity of **EPα** with paraoxon suggests that might play a role in toxicity in the low-level long-term exposure of organophosphate compounds, as it is spontaneously reactivated only in chronic exposure may be relevant. EPα is also highly sensitive to mipafox and it is resistant to permanent inhibition with paraoxon. These esterases apparently sensitive to paraoxon, discarded as irrelevant in the standard assay of NTE, can be ruled out as potential neuropathy targets if they are going to be quickly and spontaneously reactivated.

Table 2. Enzymatic components discriminated.

Component	Amplitude (%)	PARAXON I50 (30 min) (Sensitivity)	MIPAFOX I50 (30min) (Sensitivity)
EPα	4.9-8.3%	15 nM (+++) (r)	29 nM (+++)
EPβ	38.3%	1540 nM (++)	(-)
EPγ NTE	38.6-47.6%	(-)	6710 nM (+)
EPδ	9.8-10.7%	(-)	(-)

Very sensitive (+++), sensitive (++)/(+) and resistant (-). (r) Spontaneously reactivated.

References: [1] Mangas et al. (2011). Toxicol Appl Pharmacol, 256, Issue 3, 360-368. [2] Mangas et al., (2012), Toxicology., 97(1-3):17-25.
[3] Estévez and Vilanova., (2009). Crit Rev Toxicol . 39(5): 427–448 . [4] Carrington and Abou- Donia ., (1985). Toxicol- Appl- Pharmacol- 79, 175-178.

UNIVERSITAS
Miguel
Hernández

Title: INTERACTIONS OF A PROMOTER OF NEUROPATHY AND ESTERASES OF MEMBRANE AND SOLUBLE FRACTIONS OF BRAIN

Authors: **I. Mangas,** J. Estévez, E. Vilanova

Type of participation: Poster
Congress: 53TH ANNUAL MEETING OF THE SOCIETY OF TOXICOLOGY
Place of celebration: San Antonio (USA) **Date:** 10-14 March 2013

Ref. journal: The Toxicologist. . Volume: 120 Pages 256-257

ABSTRACT:

PMSF is a protease and esterase inhibitor causing protection or potentiation ("promotion") of organophosphorus delayed neurotoxicity depending of if it is dosed previously or after an inducer of delayed neurotoxicity and it is unstable in water solution. Kinetic data of the esterase inhibition were obtained for phenylmethylsulfonylfluoride (PMSF) tested at different concentrations incubated for twenty minutes with particulate fraction (membranes) of chicken brain. A kinetic model equation was deduced assuming a multienzymatic system with three different molecular phenomena occurring simultaneously: (1) Inhibition; (2) spontaneous chemical hydrolysis of the inhibitor; (3) ongoing (inhibition during the substrate reaction). A three-dimensional fit of the model was applied for analysing the experimental data. The best fitting model is compatible with a resistant component (14%) and two sensitive enzymatic entities (44% and 41%). The corresponding second order rate constants of inhibition (ki=0.0076 nM-1x min-1 and 0.0014 nM-1×min-1, respectively) and the chemical hydrolysis constant of PMSF (kh=0.28 min-1) were simultaneously estimated. The consistency of results in fixed time and progressive inhibition experiments was considered an internal validation of the methodology. Mipafox resistant fraction was assayed with different concentrations of PMSF. The best fitting model is compatible with a resistant component and one sensitive component with ki=0.0014 nM-1xmin-1 (12% and 47% of total esterase activity) and with chemical hydrolysis constant of kh=0.30 min-1. The results allowed to discriminate the esterase fractions sensitive or resistant to PMSF among those sensitive or resistant to mipafox or paraoxon, in order to understand their role in the mechanism of induction, protection or potentiation of delayed neurotoxicity

UNIVERSITAS
Miguel
Hernández

INTERACTIONS OF A PROMOTER/POTENTIATOR OF NEUROPATHY AND ESTERASES OF MEMBRANE AND SOLUBLE FRACTIONS OF BRAIN

Iris Mangas , Jorge Estévez and Eugenio Vilanova (imangas@umh.es)
Unidad de Toxicología y Seguridad Química, Instituto de Bioingeniería, Universidad Miguel Hernández, Elche (Spain)

Introduction

PMSF (phenylmethyl sulfonylfluoride) is a protease and esterase inhibitor causing protection or promotion/potentiation of the organophosphorus delayed polyneuropathy, caused by inhibition of Neuropathy Target Esterase by certain inducers as mipafox. PMSF is also exacerbating the clinical and pathological signs of other toxic axonopathies such as e.g. 2,5-hexanedione neuropathy as well as traumatic neuropathy [1,2].
The molecular target/s of this effect has not yet been identified.

Objectives

1. To obtain kinetic data of phenylvalerate esterase inhibition for PMSF with chicken brain soluble and a membrane fractions.
2. To analyze these data using kinetic models with a multi-enzymatic system in which inhibition occurred with the simultaneous chemical hydrolysis of the inhibitor and inhibition during the substrate reaction [3,4]
3. (3.1) To study the effect of preincubation with PMSF in the sensitivity to mipafox and (3.2) the effect of preincubation with mipafox in the sensitivity to PMSF in both brain fractions.
4. To discriminate the esterase fractions sensitive or resistant to PMSF among those sensitive or resistant to mipafox or paraoxon [5,6] .

Methods

Enzyme preparation: Soluble and membrane fractions of chicken brain (from 20 and 15 mg fresh tissue/ml respectively) [5,6]. **Inhibitor:** Phenylmethanesulfonylfluoride (PMSF). **Inhibition assays:** Enzyme assays were carried out as previously described in [5,6]. **Mathematical analysis of the inhibition curves:** Model equations for a system with several enzymatic components were applied [4] including the spontaneous hydrolysis of PMSF [3].

References

[1] Moretto et al., 1993; Chem-Biol. Interact. 87, 457-462. **[2]** Peraica et al., 1993. Biochem. Pharmacol. 45, 131-135. **[3]** Estévez et al., 2012. Arch Toxicol. DOI 10.1007/s00204-012-0817-3. **[4]** Estévez and Vilanova., 2009. Crit Rev Toxicol . 39(5): 427–448 **[5]** Mangas et al., 2011.Toxicology and Applied Pharmacology 260(3): 360-368. **[6]** Mangas et al., 2012. Toxicology. 2012 Jul 16;297(1-3):17-25.

PMSF kinetic data

1. Soluble fractions were preincubated with 0, 20, 70, 300 and 1000 µM **(A)** and membrane fractions with 0, 10, 25, 75, 150, 250, 400 and 1000 µM PMSF **(D)**, the inhibition was time-progressive (~72% in soluble and ~85 % in membrane fraction, of total activity). Panels **B** and **E** reveal the inhibition during the substrate reaction time.

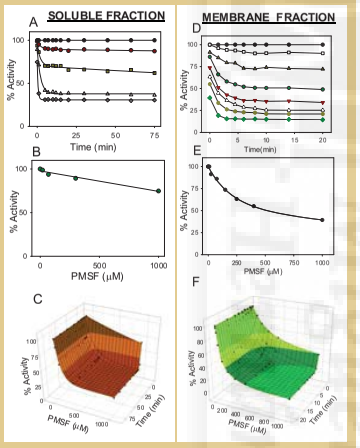

2. Panels **C** and **F** provides the inhibitory surface of the best model according to the F test obtained by fitting the 3D model equation to the data. For the soluble fraction (Table 1A):

$$E = E1_0 \cdot e^{\left(-ka \cdot I_0 \cdot e^{-(kh \cdot t)} - 1\right)} \cdot e^{\left(e^{-kh \cdot t} \cdot 1\right)} \cdot \frac{k1}{kh} \cdot I_0 + E2_0 \cdot e^{\left(-kb \cdot I_0 \cdot e^{-(kh \cdot t)} - 1\right)} \cdot \frac{k2}{kh} \cdot I_0 + R$$

For the membrane fraction (Table 1B):

$$E = E1_0 \cdot e^{\left(-ka \cdot I_0 \cdot e^{-(kh \cdot t)} - 1\right)} \cdot e^{\left(e^{-kh \cdot t} \cdot 1\right)} \cdot \frac{k1}{kh} \cdot I_0 + E2_0 \cdot e^{\left(e^{-kh \cdot t} \cdot 1\right)} \cdot \frac{k2}{kh} \cdot I_0 + R$$

Where k1 and k2 are the inhibition constants, kh is the hydrolysis constant, ka and kb are the exponential constant of the ongoing inhibition . $E1_0$, $E2_0$ are the proportion of the initial enzymatic components, R is the fraction resistant to inhibition and I_0 is the initial concentration of PMSF.

Table 1. Kinetic parameters and I_{50} (20 min) obtained from the PMSF kinetic experiments.

	E1 (%)	Ka/ko (μM^{-1})	kh (min^{-1})	k1 ($\mu M^{-1} \cdot min^{-1}$)	I_{50}^{20} (µM)	E2 (%)	k2 ($\mu M^{-1} \cdot min^{-1}$)	I_{50}^{20} (µM)	R (%)
A.Soluble fraction	61	0.0005	0.23	0.0023	72	8	0.00036	435	29
B.Membrane fraction	44	0.0048/0.0005	0.28	0.0080	25	41	0.00140	138	15

Alterations of sensitivity

3.1. Mipafox kinetic parameters after PMSF incubation

Soluble fraction: **Table 2** shows the inhibition by mipafox of soluble esterases of brain preinhibited with 0, 5, 10, 150 and 2000 µM PMSF. Exponential decay models were fitted to the mipafox inhibition data with one, two or more enzymatic components, with or without resistant component. Similar experiment was done incubating soluble brain fraction with the PMSF hydrolysis product.

Preincubation (20 min)	Total activity after PMSF-incubation (%)	Eα (%)	I_{50} (20 min) (nM)	Eγ (%)	I_{50} (20 min) (nM)	(*) R (%)
Buffer	100	21	**4**	8	**7,701**	**71**
5 µM PMSF						
(*)(Expected)	*(96)*	*(21)*		*(8)*	**25,67**	**(67)**
Observed	93	22	**26**	5	**2**	**66**
10 µM PMSF						
(*)(Expected)	(93)	*(21)*		(8)		**(64)**
Observed	93	21	**31**	0	-	**72**
150 µM PMSF						
(*) (Expected)	(42)	(21)		(6)		**(15)**
Observed	43	22	**72**	0	-	**21**
4000 µM PMSF						
(*) (Expected)	(21)	(21)		(0)		**0**
Observed	17	17	**222**	0	-	**0**
Hydrolysis product	(100)	(21)	**12**	(8)		**(71)**
(*)Expected	100	16		5	7,701	**79**
Observed						

(*)For *Eα* or Eγ, as "Expected", it is indicated the estimated residual activity of the *Eα* or Eγ component after the preincubation with the indicated PMSF concentration, considering the kinetic parameters of the PMSF inhibition in Table 1, assuming that the preincubation would not affect the behavior with mipafox. In the "Resistant" column, the "expected" data are the estimated value of the Eβ component (resistant to mipafox) that is expected after preincubation with the indicated PMFS []; however the observed value may be the residual Eβ plus the proportion of the Eγ fraction that might be converted to resistant as a consequence of the preincubation.

3.2. PMSF kinetic parameters after mipafox incubation

Soluble brain fraction was incubated with 20 nM mipafox for 30 min to inhibit the component Eα, afterwards a progressive inhibition experiment with 0, 20, 70, 300 and 1000 µM PMSF was done. Two sensitive components of 71% and 9% were estimated, with I_{50} (20 min) of 76 µM and 7560 µM respectively. Which correspond to components Eβ and Eγ. The sensitivity of Eγ is more than 15-fold higher.

Membrane fraction: Similar experiments were done in membrane fraction. None alteration of sensitivity with mipafox was observed after PMSF preincubation, either none alteration in PMSF sensitivity after mipafox preincubation.

Enzymatic components

4. Figs. 2. Discrimination of esterase enzymatic components in chicken brain considering PMSF, mipafox and paraoxon interactions.

Three enzymatic components were discriminated in soluble fraction called Eα, Eβ and Eγ.
Four enzymatic components were discriminated in membrane fraction called EPα, EPβ and EPγ and Epδ.
Paraoxon and mipafox data from the data in [] for soluble fraction and [] for membrane fraction.

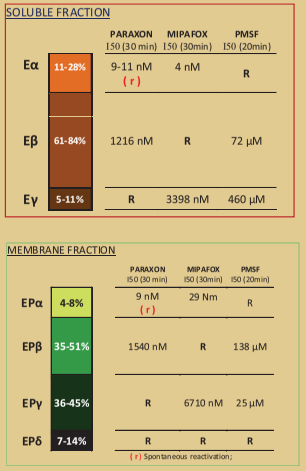

Conclusion

Preincubation of soluble fraction with PMSF or mipafox altered the sensitivity to the inhibition by the other inhibitor on enzymatic components which have not been inhibited in the preincubation. However not significantly changes were observed in in the membrane bound esterases. It is concluded that PMSF and mipafox can interact with some soluble esterases not inhibiting but strongly modifying their sensitivity against OP inhibitors.
These results can be interpreted by an interaction of PMSF and mipafox at sites other than the substrate catalytic center. This kind of interactions should be considered to interpret the potentiation/promotion phenomenon of PMSF and to understand the effects of multiple exposures to chemicals.

UNIVERSITAS
Miguel
Hernández

Title: ESTERASES INTERACTING WITH ORGANOPHOSPHORUS COMPOUNDS DIFFERENT TO CHOLINESTERASES AND NEUROPATHY TARGET ESTERASE IN NERVE TISSUES

Authors: Estévez J, **Mangas I,** Sogorb MA, Benabent M, Vilanova E

Type of participation: Poster
Congress: 14TH INTERNATIONAL NEUROTOXICOLOGY ASSOCIATION MEETING

Place of celebration: (Egmond aan Zeen, The Netherlands), **Date:** 9-13 June 2013

ABSTRACT:

Serin esterases and peptidase enzymatic activity are covalently inhibited by organophosphorus compounds (OPs) and other acylating chemicals as sulphonyl fluorides (i.e: PMSF) or carbamates. Cholinesterases, and neuropathy target esterase (NTE) are well known examples as well as the neurotoxicological consequence their covalent inhibition by organophosphorylation, solphonylation or carbamoylation. The biological function of acetylcholinestese are well known and related directly with their catalytic esterase properties but not well established for NTE. A role of NTE protein in cell differentiation and embryonic development is under study. In mammals, avian and other species, other carboxylesterases with unknown toxicological and biological function are interacting with OPs. Kinetic models have been developed and applied for analyzing the time progressive inhibition in complex systems, containing several esterase sensitive components and considering the sensitivity (inhibition rate constant) and spontaneous reactivation (dephosphorylation). In some cases (i.e: PMSF) the inhibitor is unstable changing the concentration along the time of testing and this should be considered in the mathematical kinetic model. Other factor to be considered in the kinetic model is: "ongoing" inhibition during the time of measuring residual activity, interactions between inhibitor in studies with two inhibitors, aging reaction of inhibited enzyme. Example are shown analyzing the esterase component on membrane and/or soluble esterases in peripheral nerve, brain and serum of chicken, the animal model for testing the OP delayed neuropathy and other neurotoxicological studies. In each tissue, several main esterase components with different properties for inhibition, reactivation have been discriminated and evaluated with the model inhibitor, paraoxon, mipafox, and PMSF, and S9B. These kinetic studies allow identifying which are the esterases that need to be molecularly identified to understand the toxicity and for developing methodologist for clinical diagnostic in humans and in experimental animal studies.

UNIVERSITAS
Miguel
Hernández

ESTERASES INTERACTING WITH ORGANOPHOSPHORUS COMPOUNDS DIFFERENT TO CHOLINESTERASES AND NEUROPATHY TARGET ESTERASE IN NERVE TISSUES

Jorge Estevez, Iris Mangas, Miguel Angel Sogorb, Monica Benavent, Eugenio Vilanova

Unit of Toxicology and Chemical Safety. Institute of Bioengineering.

University "Miguel Hernández" Elche-Alicante. Spain

Introduction

Organophosphorus compounds (OPs) can induce several distinct neurotoxic effects depending on the dose, frequency of exposure, type of OP, and host factors (1):These effects include acute cholinergic toxicity which target and mechanism is well-known (inhibition of AChE), the organophosphorus induced delayed polyneuropathy (OPIPN), which target is neuropathy target esterase (NTE) and mechanism is not completely understood. Other toxic effects as chronic neurotoxicity and developmental neurotoxicity have been described but molecular targets are unknown. Many enzyme systems have the potential for interaction with specific OP. Cholinesterases and serine-peptidases are known proteins with carboxylesterase or peptidase enzymatic activity which are covalently inhibited by organophosphorus compounds (OPs) and other acylating chemicals as sulphonyl fluorides (i. e: PMSF). Protective and potentiation-promotion effects have been described for PMSF and the targets of these interaction remain unknown. The aim of this work is to show that based in inhibitory-kinetic properties different esterase enzymatic components can be discriminated in nerve tissues.

Methods and results

Phenylvalerate (PV) is used as substrate and esterase activity measured by the release of phenol (7,8). Mathematical models equations were developed in our group to analyses kinetic data of complex systems where different kinetic components are inhibited and different kinetic reactions are present as spontaneous reactivation, chemical hydrolysis of the inhibitor and/or ongoing inhibition (2,3,4,5,6,7,8). This mathematical models were used to analyses the interaction (fixed time inhibition, spontaneous reactivation, ongoing inhibition and progressive inhibition), between different inhibitors (paraoxon, mipafox, phenylmethylsulfonylfluoride (PMSF) and S9B) with chicken nerve tissues (soluble fraction of peripheral nerve, soluble fraction of brain and membrane fraction of brain). **Figure 1** shows the example of the kinetic curves of PMSF inhibition on brain soluble and membrane fractions. **Figure 2** shows the discrimination of the esterase components in several tissues.

Fig 1. Kinetics of the time-progressive inhibition of soluble and membrane fractions of chicken brain by PMSF.

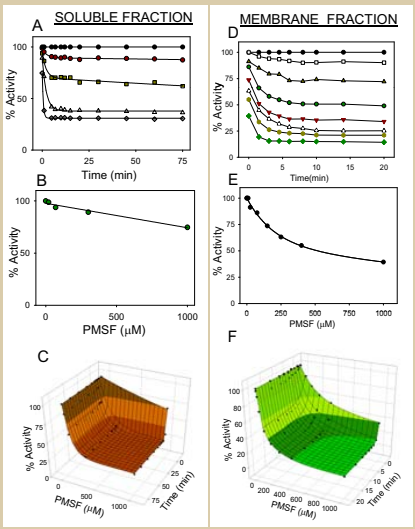

The soluble fractions (A) from 20 mg brain /ml) and the membrane fractions (B) from 15 mg/ brain/ ml were preincubated with PMSF in the range 10 to 1000 µM The residual enzymatic activity was assayed with phenylvalerate for 10 min (6) Percentages refer to the activity of the samples preincubated without inhivitor at each time. The inhibition was time-progressive (~72% in soluble and ~85 % in membrane fraction). Panels B and E reveal the inhibition during the substrate reaction time (ongoing inhibition). Panels C and F show the deduced 3D surface.

Conclusions

Fig.2. Using inhibition kinetic approaches the following esterase component were discriminated:

A PERIPHERAL NERVE SOLUBLE FRACTION

		PARAXON I50 (30 min)	MIPAFOX I50 (30min)	PMSF I50 (30min)	S9B I50 (30 min)
EI	41-52%	6-12 nM (r)	11-12 nM	R	5 nM
EII	33-41%	0.24-0.26 nM	69-71 nM	6.8-17 µM	0.20 nM (r)
EIII	15-22%	R	R	R	83 nM

B. BRAIN SOLUBLE FRACTION

		PARAXON I50 (30 min)	MIPAFOX I50 (30min)	PMSF I50 (20min)
Eα	11-28%	9-11 nM (r)	4 nM	R
Eβ	61-84%	1216 nM	R	72 µM
Eγ	5-11%	R	3398 nM	460 µM

C. BRAIN MEMBRANE FRACTION

		PARAXON I50 (30 min)	MIPAFOX I50 (30min)	PMSF I50 (20min)
EPα	4-8%	9 nM (r)	29 Nm	R
EPβ	35-51%	1540 nM	R	138 µM
EPγ or NTE	36-45%	R	6710 nM	25 µM
EPδ	7-14%	R	R	R

(r) Spontaneous reactivation;
R= Resistant to the highest tested concentration

INTERACTIONS AMONG INHIBITORS

- Preincubation with low non-inhibitory concentration of PMSF or mipafox decrease the sensitivity to the other inhibitors on Eα and Eγ enzymatic components in brain soluble fraction but not significant alteration is observed in the membrane bound esterases.The effect is irreversible.
- Therefore PMSF and mipafox can interact with some soluble esterases in a site different to the catalytic center not strongly modifying its sensitivity against other OP inhibitors.
- The role of these esterase enzymatic components in OPs neurotoxicity and/or detoxication needs to be clarified.
- The kinetic discrimination allows us to have now better criteria to design which fraction of esterases should be isolated and molecularly characterized to understand the neurotoxicological and biological role of esterases.

References. (1) Ray and Richards .,2001. Toxicol Lett ,343-351. (2) Estévez and Vilanova., 2009. Crit Rev Toxicol . 39(5): 427–44 (3) Estévez J., Barril J., Vilanova E., 2010. Inel. Chem.Biol. Interac. 187 397–402. (4) Estevez J., Mangas I., Sogorb M.A., Vilanova E., 2013b Chem. Biol. Interac. DOI: 10.1016.. (5) Estévez J, García-Pérez A, Barril J, Vilanova E., 2011 Chem Res Toxicol. 24(1):135-43. (6) Mangas I., Vilanova E., Estévez J., 2011. Toxicol Appl Pharmacol. Nov 1;256(3):360-8 (7) Mangas I, Vilanova E, Estévez J.Chem Res Toxicol. 2012 Nov 19;25(11):2393-401. (8) Mangas I., Estevez J., Vilanova E., 2012a. Toxicology. 2012 Jul 16;297(1-3):17-25

UNIVERSITAS
Miguel
Hernández

Title: THEORETICAL KINETIC ASPECTS OF ENZYMES REACTING WITH OPS

Authors: Vilanova E, **Mangas I,** Sogorb MA, Estévez J

Type of participation: Oral
Congress: 14TH INTERNATIONAL NEUROTOXICOLOGY ASSOCIATION MEETING

Place of celebration: (Egmond aan Zeen, The Netherlands), **Date:** 9-13 June 2013

ABSTRACT

Serin esterases and peptidase enzymatic activity are covalently inhibited by organophosphorus compounds (OPs) and other acylating chemicals as sulphonyl fluorides (i.e: PMSF) or carbamates. Cholinesterases, and neuropathy target esterase (NTE) are well known examples as well as the neurotoxicological consequence their covalent inhibition by organophosphorylation, solphonylation or carbamoylation. The biological function of acetylcholinestese are well known and related directly with their catalytic esterase properties but not well established for NTE. A role of NTE protein in cell differentiation and embryonic development is under study. In mammals, avian and other species, other carboxylesterases with unknown toxicological and biological function are interacting with OPs. Kinetic models have been developed and applied for analyzing the time progressive inhibition in complex systems, containing several esterase sensitive components and considering the sensitivity (inhibition rate constant) and spontaneous reactivation (dephosphorylation). In some cases (i.e: PMSF) the inhibitor is unstable changing the concentration along the time of testing and this should be considered in the mathematical kinetic model. Other factor to be considered in the kinetic model are: “ongoing” inhibition during the time of measuring residual activity, interactions between inhibitor in studies with two inhibitors, aging reaction of inhibited enzyme. Example are shown analyzing the esterase component on membrane and/or soluble esterases in peripheral nerve, brain and serum of chicken, the animal model for testing the OP delayed neuropathy and other neurotoxicological studies. In each tissue, several main esterase components with different properties for inhibition, reactivation have been discriminated and evaluated with the model inhibitor, paraoxon, mipafox, and PMSF, and S9B. These kinetic studies allow identifying which are the esterases that need to be molecularly identified to understand the toxicity and for developing methodologist for clinical diagnostic in humans and in experimental animal studies.

UNIVERSITAS
Miguel
Hernández

6. UNPUBLISHED RESULTS

UNIVERSITAS
Miguel
Hernández

6.1. OPTIMIZATION OF THE AUTOMATABLE MICROASSAY OF PHENYL VALERATE ESTERASES

In the present study, the first step was to develop an automatable microassay for phenyl valerate esterase (PVase) activity using the Biomek 2000 workstation. Optimization of the microassay for phenyl valerate esterases is based on the necessity to study this activity in tissues with limited activity or availability, and because a large number of samples must be processed. Standards of phenol, blanks and controls of spontaneous hydrolysis (samples without an enzyme) and of the color produced by the tissue itself (samples without a substrate), were included in the same automated process. Activity in nmol/min was calculated using the phenol standard calibration curve (**Figure 6.1**) and corrections were made for possible spontaneous hydrolysis and tissue-generated color. The colorimetric method employed was based on the phenol measurement method, adapted to the NTE assay, devised by Johnson et al. (1977). In some experiments, different tissue concentrations and enzyme-substrate reaction times were tested, as detailed in each case. Both assay linearity with tissue concentration and linearity with reaction time were studied (**Figure 6.2**).

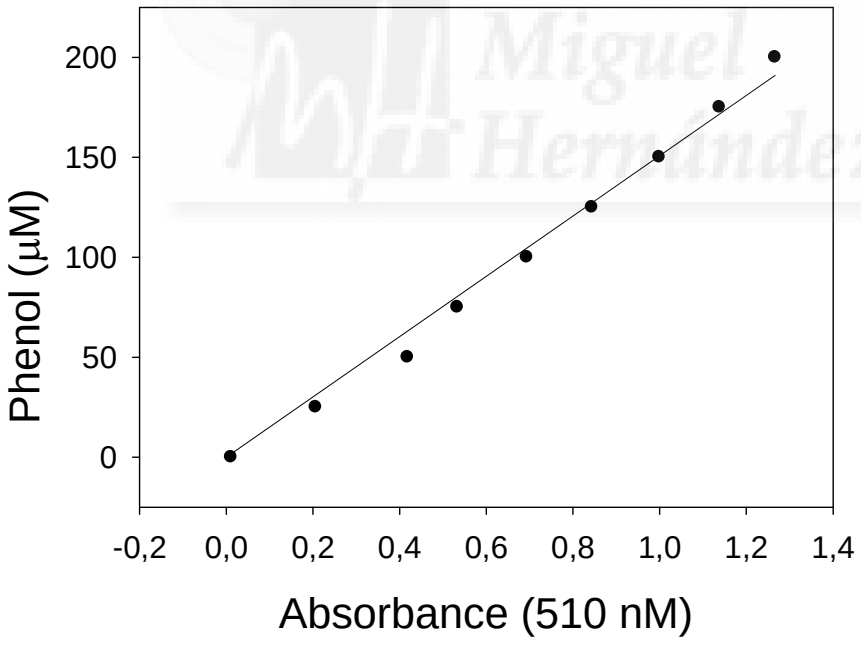

Figure.6.1. Phenol calibration curve. A 220-µl volume of phenol was incubated at 37ºC for 10 min. Then 200 µl of 2% SDS/1.23 aminoantipyrine solution were added. Absorbances were measured at 510 nm. The panel shows that absorbances (n=3) were corrected with blanks (a solution without phenol containing the same 2% SDS/1.23 aminoantipyrine solution). The linear regression parameters were y0 =-9.196, m= 160.80 and R2 = 0.9978.

Automation reduced the manual assay time and increased reproducibility, allowing to take routine measurements. This test may be extrapolated to measure other esterases that yield phenols and chlorophenols as reaction products.

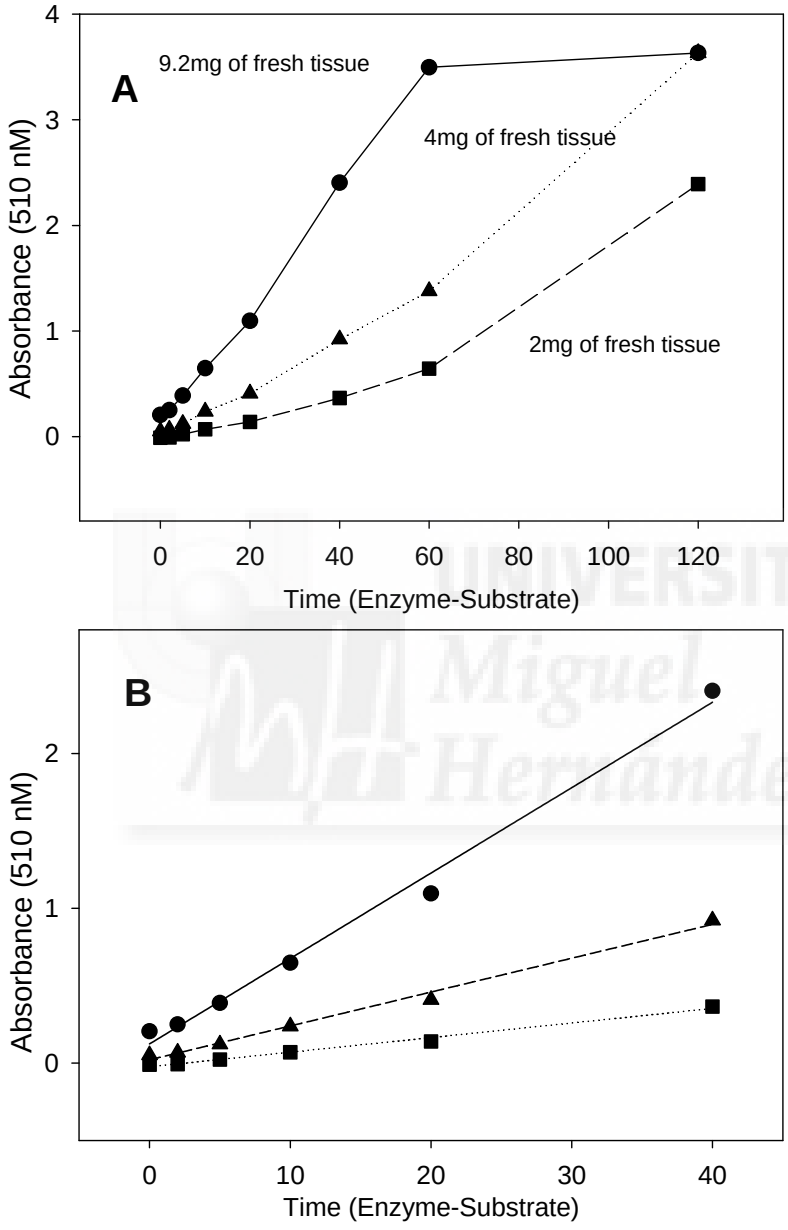

Figure 6.2. Phenyl valerate esterase activities with variation in the amount of tissue (brain soluble fraction) and the enzyme-substrate reaction time present in the microassay using a Biomek 2000 workstation. Absorbance at 510 nm after 10 min of stopping reaction is shown. Absorbance was corrected for the spontaneous hydrolysis of a control without tissue. (A) Plotting all the data; (B) Plotting within the 0 to 40 min range, considered linear.

Linearity with reaction time for different tissue concentrations

Figure 6.2 shows phenyl valerate esterase activity versus the substrate incubation time for 2, 4 and 9.2 mg of tissue in the assay. Assays without tissue were used as a control of the non enzymatic hydrolysis of the substrate. A response was considered linear to an incubation time of 40 min. A concentration of 9.2 mg of tissue and an incubation time of 10 min were chosen for the conditions of the general enzymatic assay in order to minimize the assay time and to obtain a good signal.

Study of enzymatic activity stability

Figure 6.3 shows the stability of enzymatic activity in the tissue preparation of soluble and membrane samples at 20 mg/ml of fresh tissue incubated for up to 90 min at 37ºC. Enzymatic activity was stable at 37ºC of both fractions.

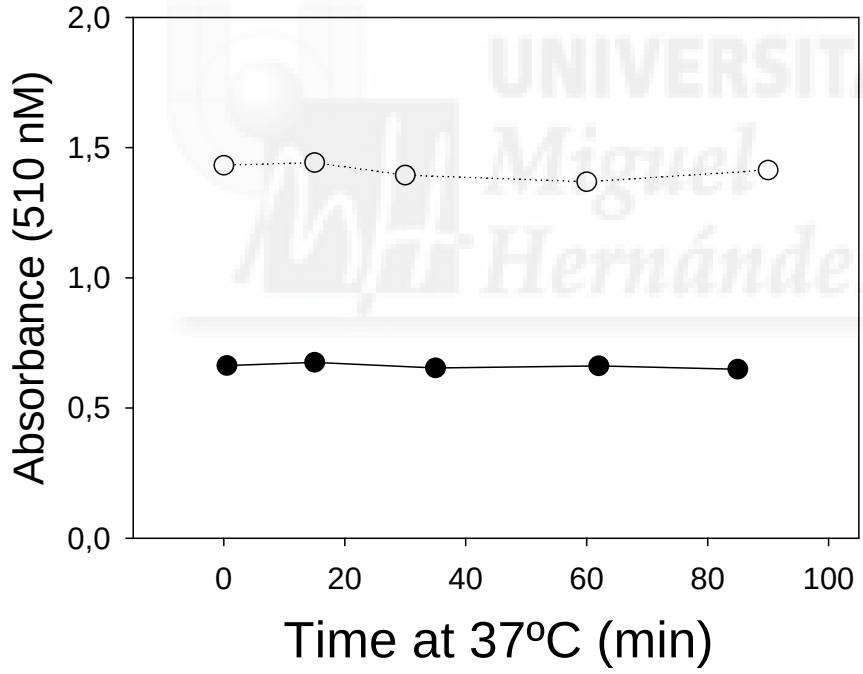

Figure 6.3. Stability of enzyme activity at 37ºC in the membrane (white circles) and soluble (black circles) fractions of chicken brain obtained at 20 mg/ml of fresh tissue. Absorbance of the enzyme-substrate reaction was measured. It represents the absorbance of samples (300 µl preparation) according to the procedure described in the Materials and Methods. Points represent the main value of three replicates and standard deviation was always < 5% of the value.

6.2. TANDEM MASS SPECTROMETRY APPROACH TO STUDY A FRACTIONATED SAMPLE

6.2.1. Brief introduction to proteomics studies of OP target esterases

Mass spectrometry of OP-adducted proteins

Protein mass spectrometry (MS) has been used as a valuable tool to identify OP-adducted proteins employing peptide mass fingerprinting to match the isolated proteins to protein sequences by analyzing the organophosphate insecticide proteins adducts of AChE and BuChE (Grigoryan et al., 2009; Doorn et al., 2001; Jennings et al., 2001). Advances in protein MS have been most useful to identify not only the adduction of different OPs compounds to isolated proteins, but also the post inhibition processes as spontaneous reactivation or aging reactions. However, mass fingerprinting is not normally useful when the sample is too complex, and liquid chromatography tandem mass spectrometry (LC-MSMS) should be used to identify large-scale proteins in complex samples based on genomic information (Lin et al., 2003).

Esterases and protein databases

Many enzyme systems have the potential to interact with specific OPs and various proteins have been observed to covalently bind to OP in previous experimental assays in *in vitro* and *in vivo* experiments.

Proteins are classified in databases according to their evolution, their function or their structure, and a wide variety of protein databases exist. In this work, esterases of chicken (Gallus Gallus) brain have been selected as the potential proteins with phenyl valerate esterase activity, based on their capability to catalyze phenyl valerate hydrolysis and because most of the currently known targets of OPs are esterases, mainly serine esterases.

Esterases are enzymes that split esters into an acid and an alcohol by hydrolysis, and they are classified by the enzyme commission as EC 3.1 based on the reaction that they catalyzed (Webb., 1992). However through convergent evolution, completely different protein folds can catalyze an identical reaction and would, therefore, be assigned an identical EC number. Indeed many enzymes have not already been classified because information on enzyme functions is lacking and their catalytic activity is not known.

PROSITE and NCBI are database that identifies and uniquely specifies a protein by its amino

acid sequence, where entries are derived from genome sequencing projects (Sigris et al., 2013). PROSITE is a functional motif database in which enzymes are classified by families and domains. It is based on the observation that most proteins can be grouped based on similarities in their sequences into a limited number of families. The proteins or protein domains belonging to a particular family generally share functional attributes and are derived from a common ancestor. By analyzing the constant and variable properties of such groups of similar sequences, it is possible to derive a signature for a protein family or domain, which distinguishes its members from all other unrelated proteins. Esterases are classified in PROSITE with accession number PS50187 and common domain GXSXG, where X can be any residue and S is the nucleophilic serine. However, this could well be a very common domain in the sequence of a protein and this domain does not confer any characteristic enzymatic activity to the protein.

ESTHER (Esterases and alpha/beta-Hydrolase Enzymes and Relatives) is a database, created in 1994, which collects and annotates all the published information relating to the gene and protein sequences of α/β-hydrolase fold superfamily of proteins (Hotelier et al., 2004). Ollis and coworkers (1992) described this superfamily of proteins as a group of proteins in which the secondary structure is an α/β-hydrolase fold, a β-sheet core of five to eight strands connected by α-helices to form an α/β/α sandwich. The superfamily members diverged from a common ancestor into a number of hydrolytic enzymes with a wide range of substrate specificities (cholinesterases or lipases), together with other proteins with no recognized catalytic activity (neuroligins, homologous to cholinesterases, but devoid of enzymatic activity). In enzyme hydrolases, catalytic triad residues are presented on loops, of which one (the nucleophile elbow) is the most conserved feature of the fold (Lenfant et al., 2012).

Any catalytic α/β-hydrolase can be sensitive to OPs due to the nucleophilic nature of the catalytic triad, normally in a serine residue and known as serine esterases (AChE, BuChE, NTE), otherwise with different residues acting as the nucleophilic residue, such as hystidine (e.g., hormone-sensitive lipase-like). ESTHER also contains a number of unknown and unrelated proteins. A three-dimensional model was used as a template, with the coordinates of T. californica AChE was generated to explore the geometry of the catalytic triad (Lenfant et al., 2012).

6.2.2. Materials and methods of the LCMSMS study

The protein samples obtained in the separation study were diluted in TNE (50 mM Tris pH 8.0, 100 mM NaCl, 1 mM EDTA) buffer and were transported in cold to the Biomolecular / Proteomics Mass Spectrometry Facility at the University of California-San Diego where mass spectrometry study was done. **Figure 6.4** shows a scheme of the tandem liquid chromatography mass spectrometry (LC-MSMS) procedure, which was as follows:

In solution tryptic digestion

Tryptic digestion was done in solution according to Guttman et al., (2009) ,as shown in **Figure 6.4.** RapiGest SF reagent (Waters Corp.) was added to 100 µl of S1D1 (containing 0.25 mg/ml of protein) at a final concentration of 0.1%. Samples were boiled for 5 min. TCEP (Tris (2-carboxyethyl) phosphine) was added to 1 mM (final concentration) and samples were incubated at 37ºC for 30 min. Subsequently, samples were carboxymethylated with 0.5 mg/ml of iodoacetamide at 37ºC for 30 min, followed by neutralization with 2 mM TCEP (final concentration). Protein samples were prepared as indicated above, and were digested with trypsin (trypsin:protein ratio = 1:50) overnight at 37ºC.

RapiGest was degraded and removed by treating samples with 250 mM HCl at 37ºC for 1 h followed by centrifugation at 14000 rpm at 4ºC for 30 min. The supernatant was then transferred to a new tube, and peptides were extracted and desalted using Aspire RP30 desalting columns (Thermo Scientific).

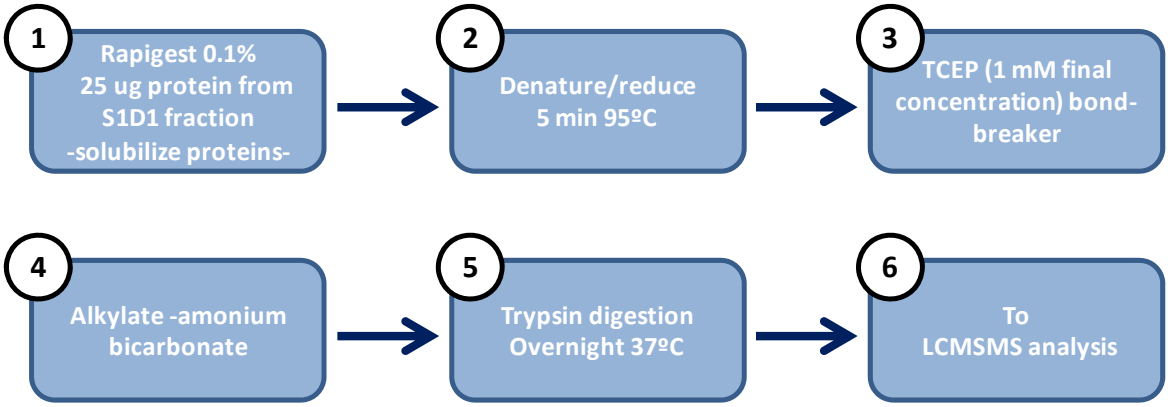

Figure 6.4. The in solution tryptic digestion procedure of S1D1.

Liquid chromatography-Tandem Mass Spectrometry (LC-MS-MS)

The trypsin-digested peptides from a previous step were analyzed by high pressure liquid chromatography (HPLC) coupled with tandem mass spectroscopy (LC-MS/MS) using nano-spray ionization (McCormack et al 1997). The nanospray ionization experiments were performed and the MS data were acquired, as shown in **Figure 6.5**. A mass spectrometer TripleTof 5600 hybrid mass spectrometer (ABSCIEX), interfaced with nano-scale reversed-phase HPLC (Tempo), was used with a 10 cm-100 micron ID glass capillary packed with 5-µm C18 ZorbaxTM beads (Agilent Technologies, Santa Clara, CA, USA). Peptides were eluted from the C18 column into the mass spectrometer using a linear gradient (5–60%) of acetonitrile at a flow rate of 250 µl/min for 1 h. The buffers used to create the acetonitrile gradient were: buffer A (98% H2O, 2% acetonitrile, 0.2% formic acid, and 0.005% trifluoroacetic acid) and buffer B (100% acetonitrile, 0.2% formic acid, and 0.005% trifluoroacetic acid).

MS/MS data acquisition

MS/MS data were acquired in a data-dependent manner in which the MS1 data was acquired for 250 ms at m/z of 400-1250 Da, while the MS/MS data were acquired from m/z of 50-2000 Da. For the independent data acquisition (IDA), parameters were adquired at MS1-TOF 250 milliseconds, followed by 50 MS2 events of 25 milliseconds each and an IDA criterion of over a 200-count threshold and charge state of +2-4 with a 4-second exclusion.

MS/MS data processing, peptide and protein identification

The collected LCMSMS data were analyzed using MASCOT® (Matrix Sciences) and Protein Pilot 4.0 (ABSCIEX) for peptide identification by comparing to genomic data. The genomic data of Gallus gallus was provided by the Ensemble database. The Gallus gallus genome was sequenced in the Sequencing Center at the Washington University School of Medicine in St. Louis in 2004 as the first avian genome to be sequenced (ICGSC., 2004). Proteins were predicted using the predictprotein online resource.

Bioinformatic search of potential targets

In order to search the potential targets of the binding of OPs, sequences of proteins were provided by NCBI and ESTHER free access databases.
Three searches were done in NCBI with the following search terms:

- ✓ Gallus gallus AND serine hydrolases
- ✓ Gallus gallus AND esterases

- ✓ Gallus gallus AND serine esterases

A search was made in the ESTHER database with the search term: Gallus gallus
Our own protein databases were created with the sequences of the proteins found.

In order to identify common sequences in datasets, we made stand-alone BLAST+ searches (Camacho et al., 2009) using each protein sequence in the previous databases.

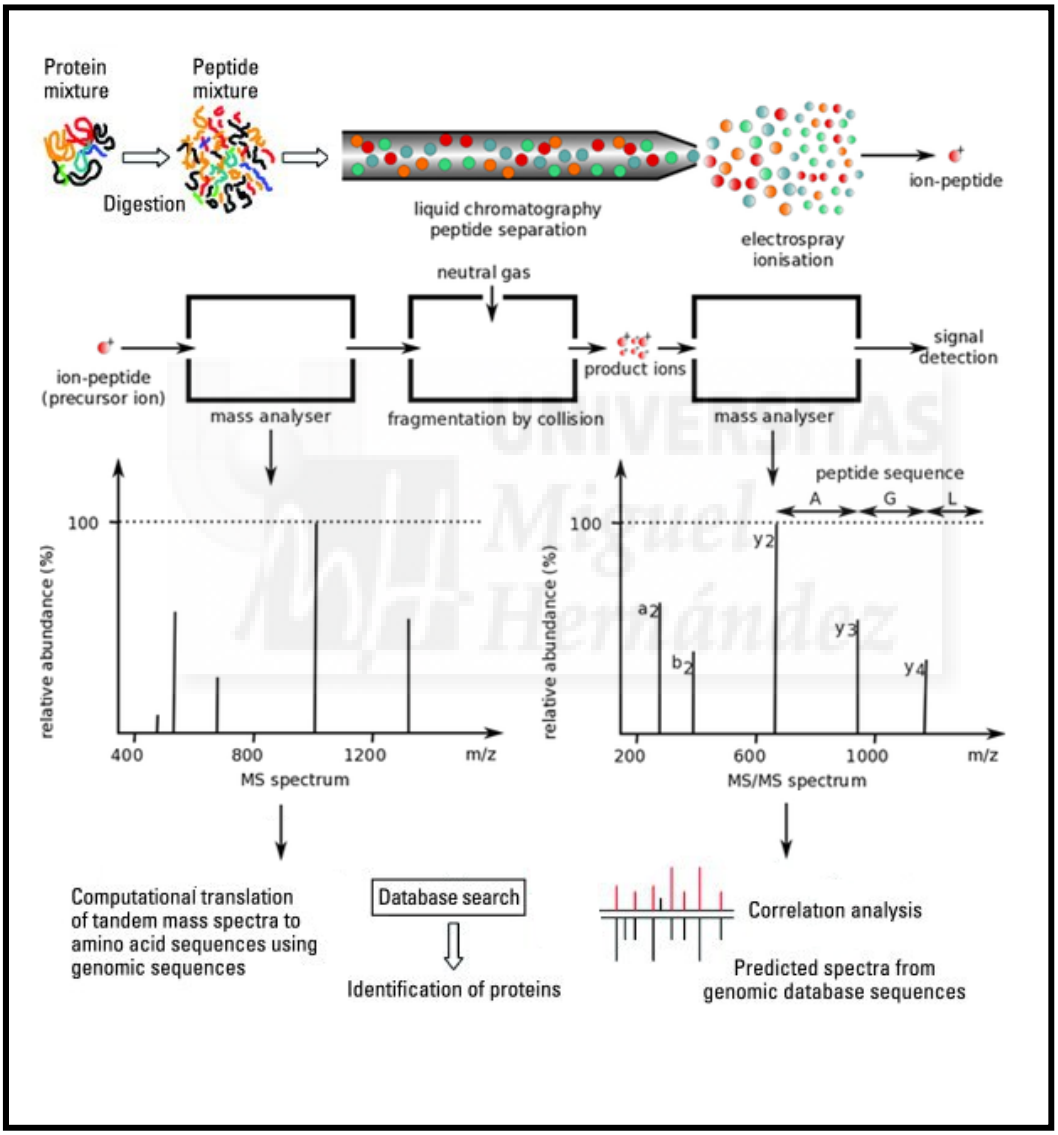

Figure 6.5. Scheme of workflow of the LC-MSMS procedure of the S1D1 fraction. 1. Protein mixtures were digested by trypsin into peptides and were separated by a reverse phase C18 column. 2 Peptides were ionized using nanospray ionization in a TripleTof 5600 mass spectrometer. 3. The collected LCMSMS data were analyzed for peptide and protein identification by comparing to genomic data.

6.2.3. Results and discussion

Proteome profile of fraction S1D1

Fraction S1D1 was selected to analyze and test the proteomic analysis because: (1) it is the fraction obtained with the highest purification factor (more than 26-fold higher than the second purification factor); (2) this fraction only contained one type of phenyl valerate esterase enzymatic component, **Eα;** (3) **Eα** is a toxicologically interesting component according to the kinetic experiments because it is highly sensitive and may have more than one catalytic center that interacts with OPs and PMSF.

From the S1D1 fraction obtained by chromatography, 259 proteins with multiple peptide details were identified from the 2818 peptides of the 7692 spectra with a 5% FDR (False Discovery Rate) based on the LCMSMS bioinformatics analyses using Protein Pilot.

Table 6.1 at the end of this **Section** shows the protein identification table with the protein identification parameters, where parameters are defined as follows:

- **Unused (ProtScore):** A measure of the protein confidence for a detected protein calculated from the peptide confidence for the peptides from the spectra that have not already been completely "used" by higher-scoring winning proteins.
- **% Cov (Coverage):** The percentage of matching amino acids from the identified peptides with confidence greater than 0 divided by the total number of amino acids in the sequence.
- **Accession #:** The accession number for the protein.
- **Peptides (95%):** The confidence of the number of distinct peptides was at least 95%. Multiple modified and cleaved states of the same underlying peptide sequence are considered distinct peptides because they have different molecular formulas. Multiple spectra of the same peptide, due to replicate acquisition or different charge states, only count once.

Bioinformatics search for potential esterases targets of organophosphorus

The amino acid sequences of the 259 proteins identified in our LCMSMS experiment (**Table 6.1**) were downloaded from GenBank using a custom Perl script and a dataset was created with the sequences (**p1**).

In addition:
We downloaded the 58 chicken sequences corresponding to the α/β-hydrolase fold proteins present in the ESTHER database (Lenfant et al., 2013) (**p2**).
We downloaded the 105 protein sequences present as chicken serine hydrolases in NCBI (**p3**).
We downloaded the 77 protein sequences present as chicken esterases in NCBI (**p4**).
We downloaded the 68 sequences present as chicken esterases in NCBI (**p5**).

In order to identify common sequences in the datasets, we carried out stand-alone BLAST+ searches (Camacho et al., 2009) using each protein sequence in datasets (**p2, p3, p4, p5**) as the query against a local database containing the 259 sequences from the LCMSMS experiment **(p1)**.

The alignments produced by these searches allowed us to identify a single sequence, which one, which was identical in datasets **p2, p3 and p4** and in **p1.** Only one of the 259 proteins was found in the other four databases (serine hydrolases, esterases, serine esterases and the alpha-beta hydrolases fold). This protein is that called "cholinesterase precursor" or butyrylcholinesterase. **Figure 6.6** shows the sequence protein coverage with matching the amino acids identified of the cholinesterase precursor in S1D1 by the LCMSMS experiment.

MVWANGMSICARFLMWLLLLFMFIRKVVPEDNVITTEKGR**VRGTNLQ**
VLGGTVTAFLGIPYGKPPIGRLRFQKPEPFEKWSGIWKATKHANSCY
QLIDTTYPGFPGTEMWNPKTNLSEDCLYLNVWIPSPKPKNATVMVWI
YGGSFETGSTSLPVYDGKFLARVERVIVVSMNYR**TGALGFLALPGNK**
EVPGNAGLFDQRLALQWVQENIASFGGNPKSVTIFGESAGSASVSYH
ILSPKSHPLFTR**AIMQSGSANAPWAAITASEAR**RRTVALAKQLKCPT
SDETELILCLQDKDPKDILENEVYVVKYFSLLHIYFCPTVDGDFLAD
MPEALIKNGIFKQTQVLVGVNKDEGTSFLVYGVPGFSKDSDSLINKT
QFEVALTLSFPQVSKLAIESIIFQYTDWENEQKPEHYR**DAMDDVIGD**
YHIICPAVEFAKTIAEVGNNVFFYFFEHRSSKLPWPEWMGVMHGYEI
EFVFGLPLERRVNYTKAEEILSRSMLRYWASFAKTGNPNGTLINGTR
WPVFTSTEQKYLTLNTDASEILTKLRAQQCRFWNMFFPKVLEMTGNI
DEAEREWKAGFHRWNNYMMDWKNQFNDYTSKKERCAGSN

Figure 6.6. Sequence protein coverage of cholinesterase precursor or butyrylcholinesterase in the LCMSMS experiment. Sequence of cholinesterase precursor of Gallus gallus with matching the amino acids identified in green color in the LCMSMS experiment.

Final remarks and key outstanding questions

According to the protein classification in databases it seems plausible that the phenyl valerate esterase activity in fraction S1D1 is due to the butyrylcholinesterase enzyme. However, this bioinformatics analysis is not conclusive and there is evidence to suggest that proteins other than serine hydrolases or alpha-beta hydrolases could interact with OPs and the phenyl valerate esterases can be members of other families of proteins that have not been analyzed in this work. Further work is needed to achieve the complete physical isolation and biochemical characterization of the phenyl valerate esterase enzyme in this fraction and in others. This study done with fraction S1D1 demonstrated that the samples obtained in the fractionation procedure are appropriate for further proteomic analyses. Ongoing studies are underway in our laboratory to confirm this hypothesis and to identify if the phenyl valerate esterase activity of S1D1 is due to this protein. Further studies are planned to identify all the proteins responsible for the esterase components discriminated in this work, which is a long-term objective of our laboratory.

UNIVERSITAS
Miguel
Hernández

Table 6.1 Protein identification parameters of the LCMSMS analysis of S1D1

N	Unusedd	%Cov(50)	%Cov(95)	Accession	Name	Peptides(95%
1	393,0	99,700	99,700	gi|46048961	glyceraldehyde-3-phosphate dehydrogenase [Gallus gallus]	797
2	77,8	73,140	73,140	gi|363736327	PREDICTED: d-3-phosphoglycerate dehydrogenase [Gallus gallus]	94
3	71,8	78,870	73,400	gi|45382651	pyruvate kinase muscle isozyme [Gallus gallus]	52
4	59,2	44,750	39,410	gi|292494926	contactin-1 preproprotein [Gallus gallus]	32
5	56,05	51,850	50,000	gi|312836787	microtubule-associated protein tau [Gallus gallus]	56
6	53,4	67,460	67,460	gi|118085057	PREDICTED: acetyl-CoA acetyltransferase A, mitochondrial [Gallus gallus]	38
7	53,11	73,510	73,510	gi|118405176	actin-related protein 2/3 complex subunit 1A [Gallus gallus]	38
8	50,19	31,520	30,790	gi|71896389	ATP-citrate synthase [Gallus gallus]	27
9	49,85	39,600	35,840	gi|237858639	neurofascin isoform 3 precursor [Gallus gallus]	31
9	0	42,580	38,530	gi|237858652	neurofascin isoform 8 precursor [Gallus gallus]	31
9	0	36,680	33,200	gi|237858646	neurofascin isoform 6 precursor [Gallus gallus]	31
9	0	42,380	38,350	gi|237858643	neurofascin isoform 5 precursor [Gallus gallus]	31
10	42,8	62,640	62,640	gi|330417943	fructose-bisphosphate aldolase C [Gallus gallus]	28
11	42,51	65,240	61,710	gi|57529492	3-ketoacyl-CoA thiolase, mitochondrial [Gallus gallus]	24
12	41,2	78,100	78,100	gi|118405198	cytochrome c [Gallus gallus]	25
13	40,75	62,550	57,450	gi|50733505	PREDICTED: tubulin polymerization-promoting protein isoform 2 [Gallus gallus]	27
13	0	67,120	61,640	gi|118086293	PREDICTED: tubulin polymerization-promoting protein isoform 1 [Gallus gallus]	27
14	40,11	41,790	39,870	gi|57529674	far upstream element-binding protein 1 [Gallus gallus]	24
15	38,61	59,520	56,390	gi|118093509	PREDICTED: isocitrate dehydrogenase [NADP] cytoplasmic [Gallus gallus]	28
16	36,84	64,110	53,590	gi|45383528	actin-related protein 3 [Gallus gallus]	27
17	35,86	50,470	50,470	gi|45382959	multifunctional protein ADE2 [Gallus gallus]	25
18	35,19	15,460	13,690	gi|118093278	PREDICTED: microtubule-associated protein 2 [Gallus gallus]	22
19	35,11	42,710	41,170	gi|45382077	radixin [Gallus gallus]	19
20	35	46,760	45,800	gi|45383752	creatine kinase U-type, mitochondrial precursor [Gallus gallus]	23
21	34,24	47,640	47,440	gi|45383884	UTP--glucose-1-phosphate uridylyltransferase [Gallus gallus]	25
22	33,88	54,330	54,330	gi|118093746	PREDICTED: actin-related protein 2/3 complex subunit 2 [Gallus gallus]	21

23	33,44	7,399	6,301	gi|363733912	PREDICTED: ankyrin-2 [Gallus gallus]	17
24	32,17	52,270	48,380	gi|74048411	eukaryotic translation elongation factor 1 alpha 2 [Gallus gallus]	39
25	30,51	72,120	64,850	gi|45382979	destrin [Gallus gallus]	24
26	30,48	57,070	51,730	gi|118097740	PREDICTED: arf-GAP with dual PH domain-containing protein 1 [Gallus gallus]	23
27	29,44	28,350	28,350	gi|61098444	clathrin coat assembly protein AP180 [Gallus gallus]	23
28	27,28	38,920	38,920	gi|57529439	6-phosphogluconate dehydrogenase, decarboxylating [Gallus gallus]	16
29	26,93	50,310	45,770	gi|363739376	PREDICTED: serine hydroxymethyltransferase, cytosolic [Gallus gallus]	19
30	25,33	47,730	37,480	gi|314122254	RNA-binding protein Nova-1 isoform 1 [Gallus gallus]	14
30	0	47,830	37,060	gi|314122361	RNA-binding protein Nova-1 isoform 2 [Gallus gallus]	13
31	25,23	39,090	37,560	gi|45382569	actin-related protein 2 [Gallus gallus]	29
32	25	68,340	68,340	gi|118094464	PREDICTED: peroxiredoxin-1 isoform 1 [Gallus gallus]	21
33	24,08	36,490	32,210	gi|45384338	tubulin beta-7 chain [Gallus gallus]	19
34	23,99	23,300	22,770	gi|363747386	PREDICTED: citrate synthase, mitochondrial-like [Gallus gallus]	26
35	22,04	68,540	68,540	gi|50756357	PREDICTED: actin-related protein 2/3 complex subunit 3 [Gallus gallus]	18
36	20,08	89,900	65,660	gi|269784810	acylphosphatase-1 [Gallus gallus]	15
37	19,88	74,550	74,550	gi|261490820	peptidylprolyl isomerase A (cyclophilin A) [Gallus gallus]	24
38	19,32	53,070	46,930	gi|118101125	PREDICTED: aflatoxin B1 aldehyde reductase member 4 [Gallus gallus]	18
39	16,93	69,880	69,280	gi|52138701	cofilin-2 [Gallus gallus]	13
40	16,4	25,910	23,060	gi|363735855	PREDICTED: heterogeneous nuclear ribonucleoprotein A3 homolog 1-like [Gallus gallus]	8
41	16,11	24,110	24,110	gi|45384004	bifunctional purine biosynthesis protein PURH [Gallus gallus]	10
42	15,68	26,940	25,530	gi|363728430	PREDICTED: glycogen synthase kinase-3 beta [Gallus gallus]	10
43	15,27	20,870	19,470	gi|363742292	PREDICTED: splicing factor, proline- and glutamine-rich [Gallus gallus]	9
44	15,25	28,570	24,690	gi|296011017	fascin [Gallus gallus]	8
45	14,71	59,260	54,500	gi|45383015	protein DJ-1 [Gallus gallus]	9
46	14,69	53,130	49,110	gi|122692295	ubiquitin carboxyl-terminal hydrolase isozyme L1 [Gallus gallus]	8
47	14,25	46,700	33,480	gi|46048916	peptidyl-prolyl cis-trans isomerase FKBP3 [Gallus gallus]	8
48	14	79,550	79,550	gi|118085711	PREDICTED: acyl-CoA-binding protein [Gallus gallus]	9
49	14	25,110	25,110	gi|136429	RecName: Full=Trypsin; Flags: Precursor	31
50	13,38	30,950	26,360	gi|71896753	heterogeneous nuclear ribonucleoproteins A2/B1 [Gallus gallus]	8
51	13,08	88,780	88,780	gi|310772235	cystatin B (stefin B) [Gallus gallus]	8

52	12,97	34,040	31,310	gi|57529813	mitotic checkpoint protein BUB3 [Gallus gallus]	9
53	12,88	43,220	38,690	gi|363741723	PREDICTED: uncharacterized protein LOC419143 [Gallus gallus]	11
54	12,01	4,869	3,937	gi|313661476	spectrin beta chain, brain 1 [Gallus gallus]	6
55	11,92	40,580	37,200	gi|45382027	peptidyl-prolyl cis-trans isomerase B precursor [Gallus gallus]	6
56	11,62	24,670	18,360	gi|71895115	paraspeckle component 1 [Gallus gallus]	6
57	11,53	20,000	20,000	gi|45382927	actin, cytoplasmic 1 [Gallus gallus]	10
57	0	15,430	15,430	gi|56119084	actin, cytoplasmic type 5 [Gallus gallus]	8
58	11,45	13,130	13,130	gi|363729859	PREDICTED: uncharacterized protein LOC396097 [Gallus gallus]	6
59	11,03	30,460	27,810	gi|45384514	heterogeneous nuclear ribonucleoprotein A/B [Gallus gallus]	8
60	10,11	43,540	34,690	gi|50732241	PREDICTED: actin-related protein 3B [Gallus gallus]	14
61	10,05	28,160	24,680	gi|50729038	PREDICTED: aldo-keto reductase family 1 member B10 [Gallus gallus]	6
62	10,01	34,380	34,380	gi|86129578	peroxiredoxin-6 [Gallus gallus]	7
63	10	26,550	20,100	gi|45383446	nucleolysin TIAR [Gallus gallus]	5
64	10	28,650	28,650	gi|363747263	PREDICTED: poly(rC)-binding protein 2-like isoform 2 [Gallus gallus]	5
64	0	28,740	28,740	gi|363747261	PREDICTED: poly(rC)-binding protein 2-like isoform 1 [Gallus gallus]	5
64	0	18,240	18,240	gi|363747267	PREDICTED: poly(rC)-binding protein 2-like isoform 4 [Gallus gallus]	4
64	0	17,500	17,500	gi|363747265	PREDICTED: poly(rC)-binding protein 2-like isoform 3 [Gallus gallus]	4
65	10	54,550	54,550	gi|45384218	superoxide dismutase [Cu-Zn] [Gallus gallus]	6
66	9,99	18,520	18,520	gi|50755288	PREDICTED: betaine--homocysteine S-methyltransferase 1 [Gallus gallus]	5
67	9,92	36,360	36,360	gi|50742739	PREDICTED: 40S ribosomal protein S12 [Gallus gallus]	7
68	9,81	45,830	41,670	gi|118101780	PREDICTED: adenylate kinase 2, mitochondrial [Gallus gallus]	7
69	9,57	18,740	16,580	gi|45382845	cholinesterase precursor [Gallus gallus]	6
70	9,35	45,450	45,450	gi|310772215	phosphatidylethanolamine-binding protein 1 [Gallus gallus]	5
71	9,05	35,430	28,350	gi|363741113	PREDICTED: eukaryotic translation initiation factor 4H-like isoform 1 [Gallus gallus]	5
71	0	38,790	31,030	gi|363741115	PREDICTED: eukaryotic translation initiation factor 4H-like isoform 2 [Gallus gallus]	5
72	8,91	69,160	69,160	gi|47777293	putative ISG12-2 protein [Gallus gallus]	5
73	8,89	41,830	41,830	gi|45384260	nucleoside diphosphate kinase [Gallus gallus]	5
74	8,81	14,790	14,790	gi|118094764	PREDICTED: cystathionine gamma-lyase [Gallus gallus]	5
75	8,54	6,488	6,488	gi|71896353	heterogeneous nuclear ribonucleoprotein M [Gallus gallus]	5
76	8,29	7,631	7,631	gi|363728659	PREDICTED: synaptojanin-1 [Gallus gallus]	6

77	8,12	23,210	21,200	gi|71895451	twinfilin-2 [Gallus gallus]	4
78	8,09	15,430	9,043	gi|1346344	Keratin, type II cytoskeletal 6A (Cytokeratin-6A) (CK 6A) (K6a keratin) (Cytokeratin-6D) (CK n s 5)	6
78	0	13,300	9,043	gi|166900097	Keratin, type II cytoskeletal 6B (Cytokeratin-6B) (CK 6B) (K6b keratin)	6
79	8,09	43,080	38,460	gi|46048696	carbonic anhydrase 2 [Gallus gallus]	8
80	8	51,690	51,690	gi|363740052	PREDICTED: dynein light chain 1, cytoplasmic [Gallus gallus]	5
81	8	22,000	22,000	gi|296090736	APEX nuclease (multifunctional DNA repair enzyme) 1 [Gallus gallus]	4
82	7,95	18,370	18,370	gi|363738596	PREDICTED: synapsin-2 [Gallus gallus]	6
83	7,72	22,860	22,860	gi|363733567	PREDICTED: extracellular superoxide dismutase [Cu-Zn] [Gallus gallus]	4
84	7,51	11,150	9,443	gi|45384370	heat shock cognate 71 kDa protein [Gallus gallus]	4
84	0	8,991	7,256	gi|55742654	heat shock 70 kDa protein [Gallus gallus]	3
85	7,49	38,920	35,140	gi|45383612	prostaglandin D2 synthase, brain precursor [Gallus gallus]	6
86	7,31	18,410	18,410	gi|118090053	PREDICTED: hydroxyacyl-coenzyme A dehydrogenase, mitochondrial [Gallus gallus]	4
87	7,28	28,890	24,890	gi|46048866	elongation factor 1-beta [Gallus gallus]	4
88	7,07	5,610	5,610	gi|363740208	PREDICTED: neurofilament heavy polypeptide [Gallus gallus]	4
89	6,66	32,110	27,980	gi|45382333	hypoxanthine-guanine phosphoribosyltransferase [Gallus gallus]	5
90	6,55	3,609	3,609	gi|363736905	PREDICTED: uncharacterized protein KIAA1107 [Gallus gallus]	4
91	6,45	2,924	2,924	gi|363727445	PREDICTED: protein piccolo, partial [Gallus gallus]	4
92	6,4	15,450	13,090	gi|50731811	PREDICTED: V-type proton ATPase subunit C 1 [Gallus gallus]	3
93	6,37	13,270	9,242	gi|118102801	PREDICTED: glial fibrillary acidic protein [Gallus gallus]	3
94	6,23	3,575	3,575	gi|363738723	PREDICTED: tubulin monoglycylase TTLL3-like [Gallus gallus]	8
95	6,2	44,370	44,370	gi|71896007	actin-related protein 2/3 complex subunit 5 [Gallus gallus]	7
96	6,16	9,262	7,719	gi|57530377	YTH domain family protein 3 [Gallus gallus]	3
97	6,13	5,781	5,781	gi|363731246	PREDICTED: reticulon-4 [Gallus gallus]	4
98	6,1	41,670	41,670	gi|45383498	peptidyl-prolyl cis-trans isomerase FKBP1A [Gallus gallus]	3
99	6	8,969	8,969	gi|363739956	PREDICTED: rabphilin-3A [Gallus gallus]	3
100	6	22,700	22,700	gi|363745254	PREDICTED: hemoglobin subunit alpha-D-like [Gallus gallus]	3
101	6	10,070	10,070	gi|71896957	eukaryotic translation initiation factor 2A [Gallus gallus]	3
102	6	24,360	24,360	gi|47604951	ubiquitin-40S ribosomal protein S27a [Gallus gallus]	3
102	0	49,780	49,780	gi|118098428	PREDICTED: polyubiquitin-B isoform 1 [Gallus gallus]	3

102	0	49,780	49,780	gi|118098426	PREDICTED: polyubiquitin-B isoform 2 [Gallus gallus]	3
102	0	17,190	17,190	gi|47604954	ubiquitin-60S ribosomal protein L40 [Gallus gallus]	2
103	6	7,389	7,389	gi|45383738	aconitate hydratase, mitochondrial [Gallus gallus]	3
104	6	10,660	10,660	gi|363732214	PREDICTED: stromal membrane-associated protein 1 [Gallus gallus]	4
105	5,8	17,430	17,430	gi|363743510	PREDICTED: protein phosphatase 1 regulatory subunit 1B [Gallus gallus]	3
106	5,73	36,230	36,230	gi|363743624	PREDICTED: 40S ribosomal protein S28 [Gallus gallus]	5
107	5,64	23,870	18,110	gi|57529406	VAMP (vesicle-associated membrane protein)-associated protein B and C [Gallus gallus]	4
108	5,57	17,140	17,140	gi|119331154	profilin-2 [Gallus gallus]	3
109	5,24	11,610	7,585	gi|363739982	PREDICTED: beta-adrenergic receptor kinase 2 [Gallus gallus]	4
110	4,71	25,340	17,190	gi|50751150	PREDICTED: calcyclin-binding protein [Gallus gallus]	3
111	4,68	16,550	12,060	gi|45382953	aspartate aminotransferase, mitochondrial precursor [Gallus gallus]	3
112	4,54	14,760	14,760	gi|56118964	sialic acid synthase [Gallus gallus]	3
113	4,5	7,541	4,699	gi|294459928	putative tyrosine-protein phosphatase auxilin [Gallus gallus]	3
114	4,35	4,101	4,101	gi|118100169	PREDICTED: AP-1 complex subunit beta-1 [Gallus gallus]	3
115	4,31	13,040	10,560	gi|61098278	epsin-2 [Gallus gallus]	2
116	4,26	24,760	24,760	gi|45382053	thioredoxin [Gallus gallus]	3
117	4,19	31,080	31,080	gi|57525242	endothelial differentiation-related factor 1 homolog [Gallus gallus]	3
118	4,16	30,400	18,940	gi|363744423	PREDICTED: GTP:AMP phosphotransferase, mitochondrial-like [Gallus gallus]	2
119	4,14	1,644	1,432	gi|363738506	PREDICTED: protein bassoon-like [Gallus gallus]	3
120	4,12	13,820	9,706	gi|167860143	protein quaking [Gallus gallus]	2
121	4,09	9,872	6,216	gi|363741936	PREDICTED: leucine-rich repeat-containing protein 47 [Gallus gallus]	2
122	4,08	27,270	18,880	gi|50736242	PREDICTED: acyl-coenzyme A thioesterase 13 [Gallus gallus]	2
123	4,07	14,020	12,880	gi|129270064	ribosomal protein S3A [Gallus gallus]	2
124	4,03	10,620	10,620	gi|57525423	V-type proton ATPase subunit E 1 [Gallus gallus]	2
125	4,03	8,952	6,550	gi|363736265	PREDICTED: tubulin alpha-5 chain-like [Gallus gallus]	3
126	4,03	6,061	5,859	gi|363740701	PREDICTED: uncharacterized protein LOC417413 [Gallus gallus]	2
127	4,02	15,770	15,770	gi|363733172	PREDICTED: aminoacyl tRNA synthase complex-interacting multifunctional protein 1 [Gallus	2
128	4	33,260	28,990	gi|52138699	tubulin beta-2 chain [Gallus gallus]	16
128	0	30,560	26,290	gi|363730444	PREDICTED: tubulin beta-2 chain-like [Gallus gallus]	15

128	0	19,960	15,700	gi|71896411	tubulin beta-5 chain [Gallus gallus]	9
129	4	37,230	33,330	gi|54020687	elongation factor 1-alpha 1 [Gallus gallus]	13
130	4	51,690	51,690	gi|118100425	PREDICTED: uncharacterized protein LOC417663 [Gallus gallus]	5
131	4	17,890	17,890	gi|71894779	actin-related protein 2/3 complex subunit 1B [Gallus gallus]	4
132	4	10,090	10,090	gi|45382879	aldo-keto reductase family 1 member B10 [Gallus gallus]	4
132	0	9,494	9,494	gi|50764028	PREDICTED: aldo-keto reductase family 1 member B10 [Gallus gallus]	3
132	0	9,494	9,494	gi|363745122	PREDICTED: aldo-keto reductase family 1 member B10-like [Gallus gallus]	3
132	0	9,494	9,494	gi|343790924	aldo-keto reductase family 1, member B1 (aldose reductase) [Gallus gallus]	3
133	4	5,782	5,782	gi|71896465	programmed cell death 6-interacting protein [Gallus gallus]	2
134	4	11,110	11,110	gi|50758110	PREDICTED: malate dehydrogenase, mitochondrial [Gallus gallus]	2
135	4	8,802	8,802	gi|71894833	DAZ-associated protein 1 [Gallus gallus]	2
136	4	20,380	20,380	gi|363746869	PREDICTED: 3-hydroxyacyl-CoA dehydrogenase type-2, partial [Gallus gallus]	3
137	4	6,790	6,790	gi|363731161	PREDICTED: protein FAM49B-like [Gallus gallus]	2
137	0	2,786	2,786	gi|57530257	protein FAM49A [Gallus gallus]	1
137	0	2,432	2,432	gi|363742424	PREDICTED: protein FAM49A-like [Gallus gallus]	1
138	4	12,940	12,940	gi|167860152	ketosamine-3-kinase [Gallus gallus]	2
139	4	3,820	3,820	gi|119331100	alpha-adducin [Gallus gallus]	2
140	4	20,340	20,340	gi|118099214	PREDICTED: V-type proton ATPase subunit G 1 [Gallus gallus]	2
141	4	11,080	11,080	gi|71895145	lanC-like protein 1 [Gallus gallus]	3
142	4	9,868	9,868	gi|57530393	transcription elongation factor A protein 1 [Gallus gallus]	2
142	0	4,333	4,333	gi|118100673	PREDICTED: transcription elongation factor A protein 2 [Gallus gallus]	1
143	4	16,900	16,900	gi|52138655	hemoglobin subunit alpha-A [Gallus gallus]	3
143	0	16,900	16,900	gi|363745252	PREDICTED: hemoglobin subunit alpha-A-like [Gallus gallus]	3
144	4	8,387	8,387	gi|50757671	PREDICTED: fructosamine-3-kinase [Gallus gallus]	2
145	4	7,508	7,508	gi|45383766	L-lactate dehydrogenase B chain [Gallus gallus]	2
146	4	6,190	6,190	gi|363733272	PREDICTED: glutathione reductase, mitochondrial [Gallus gallus]	2
147	3,82	8,396	8,396	gi|46048906	T-complex protein 1 subunit delta [Gallus gallus]	2
148	3,77	3,226	3,226	gi|57529634	phenylalanyl-tRNA synthetase beta chain [Gallus gallus]	2
149	3,74	43,370	25,900	gi|50730609	PREDICTED: gamma-glutamylaminecyclotransferase-like isoform 2 [Gallus gallus]	4
149	0	45,860	27,390	gi|363729086	PREDICTED: gamma-glutamylaminecyclotransferase-like [Gallus gallus]	4

149	0	45,860	27,390	gi|118084648	PREDICTED: gamma-glutamylaminecyclotransferase-like isoform 1 [Gallus gallus]	4
150	3,72	8,333	8,333	gi|363738456	PREDICTED: mannose-1-phosphate guanyltransferase beta-A [Gallus gallus]	2
151	3,71	9,797	7,095	gi|71897147	nmrA-like family domain-containing protein 1 [Gallus gallus]	2
152	3,69	12,880	12,880	gi|71895183	obg-like ATPase 1 [Gallus gallus]	3
153	3,68	23,020	17,740	gi|363743744	PREDICTED: complement factor D-like [Gallus gallus]	3
154	3,61	7,888	4,947	gi|60302812	cysteinyl-tRNA synthetase, cytoplasmic [Gallus gallus]	2
155	3,45	5,653	5,653	gi|118102980	PREDICTED: keratin, type I cytoskeletal 12 [Gallus gallus]	5
156	3,42	12,500	12,500	gi|45382061	triosephosphate isomerase [Gallus gallus]	2
157	3,16	37,880	21,210	gi|45384320	fatty acid-binding protein, brain [Gallus gallus]	2
158	3,09	14,070	14,070	gi|50729726	PREDICTED: transgelin-3 [Gallus gallus]	3
159	2,97	11,940	11,940	gi|61098280	hydroxyacylglutathione hydrolase, mitochondrial precursor [Gallus gallus]	2
160	2,95	20,130	20,130	gi|57525148	ubiquitin-conjugating enzyme E2 L3 [Gallus gallus]	2
161	2,82	6,352	6,352	gi|45383614	CUGBP Elav-like family member 2 [Gallus gallus]	2
161	0	2,680	2,680	gi|60302694	CUGBP Elav-like family member 1 [Gallus gallus]	1
162	2,64	8,171	8,171	gi|71897227	seryl-tRNA synthetase, cytoplasmic [Gallus gallus]	2
163	2,52	8,141	8,141	gi|363729408	PREDICTED: LOW QUALITY PROTEIN: phosphatidylinositol-binding clathrin assembly protein gallus]	3
164	2,49	16,480	5,495	gi|118086105	PREDICTED: lanC-like protein 2 [Gallus gallus]	1
165	2,45	20,390	20,390	gi|61098334	ubiquitin-conjugating enzyme E2 N [Gallus gallus]	2
166	2,44	8,208	3,237	gi|118099274	PREDICTED: dynamin-1 isoform 1 [Gallus gallus]	2
166	0	6,573	1,526	gi|363740333	PREDICTED: dynamin-1 [Gallus gallus]	1
166	0	6,474	1,503	gi|363740329	PREDICTED: dynamin-1 [Gallus gallus]	1
166	0	6,504	1,510	gi|118099276	PREDICTED: dynamin-1 isoform 2 [Gallus gallus]	1
167	2,34	19,140	19,140	gi|50738930	PREDICTED: CB1 cannabinoid receptor-interacting protein 1 [Gallus gallus]	2
168	2,28	6,233	2,981	gi|45382519	microtubule-associated protein 6 homolog [Gallus gallus]	1
169	2,27	2,984	0,728	gi|363735591	PREDICTED: eukaryotic translation initiation factor 3 subunit A [Gallus gallus]	1
170	2,21	5,096	5,096	gi|363742917	PREDICTED: selenium-binding protein 1-A [Gallus gallus]	2
170	0	4,969	4,969	gi|363742887	PREDICTED: selenium-binding protein 1-A-like [Gallus gallus]	2
171	2,19	27,060	18,820	gi|363745968	PREDICTED: splicing factor 1-like, partial [Gallus gallus]	1
172	2,05	4,510	2,706	gi|46195836	RNA-binding protein 12 [Gallus gallus]	2

172	0	4,545	2,727	gi|363741413	PREDICTED: RNA-binding protein 12-like [Gallus gallus]	2
173	2,03	3,696	3,696	gi|114326309	vimentin [Gallus gallus]	2
174	2,01	1,518	1,518	gi|45384450	tyrosine-protein phosphatase non-receptor type 11 [Gallus gallus]	1
175	2,01	3,989	3,989	gi|50752941	PREDICTED: tropomodulin-2 [Gallus gallus]	1
176	2	34,440	30,790	gi|237858648	neurofascin isoform 7 precursor [Gallus gallus]	28
176	0	34,700	31,030	gi|237858641	neurofascin isoform 4 precursor [Gallus gallus]	28
177	2	35,960	31,690	gi|153792017	tubulin beta-3 chain [Gallus gallus]	19
178	2	20,000	20,000	gi|363740848	PREDICTED: actin, cytoplasmic 2-like [Gallus gallus]	9
179	2	7,143	4,464	gi|118129666	PREDICTED: keratin, type II cytoskeletal 73-like [Gallus gallus]	2
179	0	7,143	4,464	gi|363746437	PREDICTED: keratin, type II cytoskeletal 73-like [Gallus gallus]	2
179	0	3,868	3,868	gi|363745016	PREDICTED: keratin, type II cytoskeletal 1-like [Gallus gallus]	2
179	0	5,376	5,376	gi|363745510	PREDICTED: keratin, type II cytoskeletal 75-like, partial [Gallus gallus]	2
179	0	3,448	3,448	gi|363745018	PREDICTED: keratin, type II cytoskeletal 75-like [Gallus gallus]	2
180	2	6,284	6,284	gi|363745008	PREDICTED: keratin, type II cytoskeletal 8-like, partial [Gallus gallus]	3
180	0	7,179	5,175	gi|47575885	keratin, type II cytoskeletal 5 [Gallus gallus]	3
181	2	1,688	1,688	gi|71895375	threonyl-tRNA synthetase, cytoplasmic [Gallus gallus]	1
182	2	1,658	1,658	gi|45383540	protein enabled homolog [Gallus gallus]	1
183	2	1,632	1,632	gi|45382453	elongation factor 2 [Gallus gallus]	1
184	2	13,740	6,044	gi|157951672	fructose-bisphosphate aldolase B [Gallus gallus]	2
185	2	4,896	4,896	gi|118094291	PREDICTED: polypyrimidine tract-binding protein 2 [Gallus gallus]	1
186	2	7,724	7,724	gi|57530626	60S ribosomal protein L7 [Gallus gallus]	1
187	2	0,874	0,874	gi|57530349	bifunctional aminoacyl-tRNA synthetase [Gallus gallus]	1
188	2	5,053	5,053	gi|57530169	cleavage stimulation factor subunit 2 [Gallus gallus]	1
189	2	18,540	18,540	gi|57525453	PEST proteolytic signal-containing nuclear protein [Gallus gallus]	2
190	2	3,456	3,456	gi|46048768	alpha-enolase [Gallus gallus]	1
191	2	1,769	1,769	gi|45384406	peroxisomal multifunctional enzyme type 2 [Gallus gallus]	1
192	2	3,295	3,295	gi|45382803	drebrin [Gallus gallus]	1
193	2	5,648	5,648	gi|363740341	PREDICTED: endonuclease G, mitochondrial-like [Gallus gallus]	1
193	0	5,648	5,648	gi|118099296	PREDICTED: endonuclease G, mitochondrial [Gallus gallus]	1
194	2	68,890	68,890	gi|307746908	thymosin beta 15 [Gallus gallus]	2

195	2	4,969	4,969	gi|256017200	probable ATP-dependent RNA helicase DDX6 [Gallus gallus]	2
196	2	2,000	2,000	gi|74723316	Keratin, type I cytoskeletal 25 (Cytokeratin-25) (Keratin-25) (K25) (Type I inner root sheath-25irs1) (Keratin 25A)	1
197	2	3,279	3,279	gi|71895537	cytoplasmic dynein 1 light intermediate chain 2 [Gallus gallus]	1
198	2	11,480	11,480	gi|50808963	PREDICTED: UPF0366 protein C11orf67 homolog isoform 3 [Gallus gallus]	1
198	0	11,480	11,480	gi|363729432	PREDICTED: UPF0366 protein C11orf67 homolog isoform 2 [Gallus gallus]	1
198	0	11,480	11,480	gi|363729430	PREDICTED: UPF0366 protein C11orf67 homolog isoform 1 [Gallus gallus]	1
199	2	6,627	3,012	gi|45384208	L-lactate dehydrogenase A chain [Gallus gallus]	2
200	2	8,721	8,721	gi|45382487	cellular nucleic acid-binding protein [Gallus gallus]	1
201	2	1,353	1,353	gi|363744091	PREDICTED: ubiquitin-associated protein 2 [Gallus gallus]	1
202	2	8,173	8,173	gi|363734468	PREDICTED: tetratricopeptide repeat protein 9A [Gallus gallus]	1
203	2	6,204	6,204	gi|363728297	PREDICTED: adaptin ear-binding coat-associated protein 1 [Gallus gallus]	1
204	2	3,767	3,767	gi|209417930	cyclin-dependent kinase 5 [Gallus gallus]	1
205	2	5,340	5,340	gi|118086182	PREDICTED: mammalian ependymin-related protein 1 [Gallus gallus]	1
206	2	11,400	11,400	gi|71895805	protein-L-isoaspartate(D-aspartate) O-methyltransferase [Gallus gallus]	1
207	2	7,599	7,599	gi|71895311	prostaglandin reductase 1 [Gallus gallus]	1
208	2	15,270	15,270	gi|57525310	coiled-coil-helix-coiled-coil-helix domain-containing protein 2, mitochondrial [Gallus gallus]	1
209	2	13,730	13,730	gi|45384204	10 kDa heat shock protein, mitochondrial [Gallus gallus]	2
210	2	3,082	3,082	gi|363741398	PREDICTED: erythrocyte membrane protein band 4.1-like 1 [Gallus gallus]	1
211	2	7,895	7,895	gi|363732614	PREDICTED: non-histone chromosomal protein HMG-14A [Gallus gallus]	1
211	0	16,670	16,670	gi|118405162	non-histone chromosomal protein HMG-17 [Gallus gallus]	1
212	2	8,368	8,368	gi|363732539	PREDICTED: microtubule-associated protein RP/EB family member 3-like [Gallus gallus]	2
213	2	11,900	11,900	gi|363728332	PREDICTED: protein C10 [Gallus gallus]	1
214	1,85	7,558	5,814	gi|71897075	beta-adrenergic receptor kinase 1 [Gallus gallus]	3
215	1,78	12,070	9,770	gi|46048798	alpha-2-macroglobulin receptor-associated protein precursor [Gallus gallus]	2
216	1,73	4,406	2,682	gi|363732984	PREDICTED: LOW QUALITY PROTEIN: disks large homolog 3 [Gallus gallus]	2
217	1,7	3,431	3,431	gi|363727927	PREDICTED: synapsin-3 isoform 2 [Gallus gallus]	2
217	0	3,436	3,436	gi|363727925	PREDICTED: synapsin-3 isoform 1 [Gallus gallus]	2
218	1,64	5,696	3,481	gi|50731161	PREDICTED: ester hydrolase C11orf54 [Gallus gallus]	1
219	1,64	3,038	3,038	gi|57524826	dual specificity mitogen-activated protein kinase kinase 1 [Gallus gallus]	1

220	1,54	6,696	6,696	gi|45383702	superoxide dismutase [Mn], mitochondrial precursor [Gallus gallus]	1
221	1,53	7,547	7,547	gi|118094519	PREDICTED: ERI1 exoribonuclease 3 [Gallus gallus]	2
222	1,49	15,050	15,050	gi|118101449	PREDICTED: nucleolysin TIA-1 isoform p40 isoform 2 [Gallus gallus]	4
222	0	8,616	8,616	gi|363742174	PREDICTED: nucleolysin TIA-1 isoform p40 [Gallus gallus]	3
223	1,39	16,810	16,810	gi|363743798	PREDICTED: UPF0449 protein C19orf25 homolog [Gallus gallus]	1
224	1,35	15,110	11,560	gi|50730713	PREDICTED: ES1 protein homolog, mitochondrial isoform 2 [Gallus gallus]	2
224	0	20,860	15,950	gi|363729154	PREDICTED: ES1 protein homolog, mitochondrial isoform 1 [Gallus gallus]	2
225	1,3	4,412	4,412	gi|71895031	peptidyl-prolyl cis-trans isomerase F, mitochondrial [Gallus gallus]	1
226	1,3	7,285	7,285	gi|319655747	cystatin precursor [Gallus gallus]	1
227	1,28	6,207	6,207	gi|326633233	ubiquitin-conjugating enzyme E2 variant 1 [Gallus gallus]	1
228	1,22	9,932	9,932	gi|118104237	PREDICTED: isochorismatase domain-containing protein 1-like [Gallus gallus]	2
229	1,17	2,786	2,786	gi|56606150	amphiphysin [Gallus gallus]	1
230	1,16	0,859	0,859	gi|148727317	cortactin binding protein 2 [Gallus gallus]	1
231	1,15	13,110	7,767	gi|363746026	PREDICTED: partner of Y14 and mago-like [Gallus gallus]	1
232	1,14	10,870	9,269	gi|61098206	YTH domain family protein 1 [Gallus gallus]	2
233	1,14	3,927	3,927	gi|363736886	PREDICTED: calponin-3 [Gallus gallus]	1
234	1,12	9,189	3,514	gi|363744581	PREDICTED: phosphoserine aminotransferase [Gallus gallus]	1
235	1,07	1,777	1,015	gi|363729863	PREDICTED: tyrosine-protein phosphatase non-receptor type 23-like [Gallus gallus]	1
236	0,99	8,943	8,943	gi|363728395	PREDICTED: neuromodulin [Gallus gallus]	2
237	0,95	11,560	11,560	gi|363747283	PREDICTED: peptidyl-prolyl cis-trans isomerase-like 1-like [Gallus gallus]	1
238	0,92	2,638	2,638	gi|45384486	phosphoglycerate kinase [Gallus gallus]	1
239	0,9	28,000	28,000	gi|363746305	PREDICTED: NEDD8-like [Gallus gallus]	1
240	0,87	2,673	2,673	gi|363730192	PREDICTED: uncharacterized protein LOC420634 [Gallus gallus]	1
241	0,85	2,137	2,137	gi|72535134	cytoplasmic aconitate hydratase [Gallus gallus]	1
242	0,84	6,400	2,600	gi|118098116	PREDICTED: 4-aminobutyrate aminotransferase, mitochondrial [Gallus gallus]	1
243	0,82	3,125	3,125	gi|57525201	short-chain specific acyl-CoA dehydrogenase, mitochondrial [Gallus gallus]	1
244	0,77	2,537	2,537	gi|61098378	aspartyl aminopeptidase [Gallus gallus]	1
245	0,77	10,670	10,670	gi|118097879	PREDICTED: uncharacterized protein C17orf39 homolog [Gallus gallus]	1
246	0,75	3,490	1,595	gi|47825387	trifunctional purine biosynthetic protein adenosine-3 [Gallus gallus]	2
247	0,72	21,370	21,370	gi|363738397	PREDICTED: GABA(A) receptor-associated protein-like 2 isoform 2 [Gallus gallus]	2

247	0	21,370	21,370	gi|118096668	PREDICTED: GABA(A) receptor-associated protein-like 2 isoform 1 [Gallus gallus]	2
248	0,7	0,454	0,454	gi|363739654	PREDICTED: periplakin [Gallus gallus]	1
249	0,7	2,455	2,455	gi|45384168	protein kinase C and casein kinase substrate in neurons protein 2 isoform 2 [Gallus gallus]	1
249	0	2,268	2,268	gi|226958424	protein kinase C and casein kinase substrate in neurons protein 2 isoform 1 [Gallus gallus]	1
250	0,57	13,980	10,170	gi|386848	keratin	3
251	0,47	15,540	6,081	gi|50053682	stathmin [Gallus gallus]	1
252	0,44	5,818	3,636	gi|363745006	PREDICTED: keratin, type II cytoskeletal 75 [Gallus gallus]	2
253	0,42	2,760	2,760	gi|118099921	PREDICTED: NADPH:adrenodoxin oxidoreductase, mitochondrial [Gallus gallus]	1
254	0,41	2,621	2,621	gi|363742282	PREDICTED: MAP7 domain-containing protein 1 [Gallus gallus]	1
255	0,39	5,882	5,882	gi|50810900	PREDICTED: coiled-coil domain-containing protein 124 [Gallus gallus]	1
256	0,35	1,591	1,591	gi|113951717	serine/threonine-protein kinase STK11 [Gallus gallus]	1
257	0,31	1,961	1,961	gi|363742810	PREDICTED: ubiquitin associated protein 2-like [Gallus gallus]	1
258	0,29	0,848	0,848	gi|363745869	PREDICTED: anoctamin-8-like [Gallus gallus]	1
259	0,29	1,651	1,651	RRRRRgi|36372	REVERSED PREDICTED: uncharacterized protein LOC100858131 [Gallus gallus]	1

UNIVERSITAS
Miguel
Hernández

7. CONCLUSIONS

UNIVERSITAS
Miguel
Hernández

1. Highly sensitive esterases to OPs were detected in soluble and in membrane fractions of chicken brain with unknown functions.

2. Kinetic models have been successfully applied to kinetically characterize these complex biological preparations considering multiple enzymatic systems, spontaneous reactivation, ongoing inhibition and/or chemical hydrolysis of the inhibitor.

3. Seven esterase components have been discriminated in soluble and membrane fractions of brain with paraoxon, mipafox and PMSF with varying kinetic behavior. **Eα**, **Eβ** and **Eγ** in the soluble fraction and **EPα, EPβ, EPγ** and **EPδ** in the membrane fraction.

4. Components **Eα** and **EPα** can be time progressively inhibited by paraoxon with time, but they are spontaneously reactivated. They can be related with toxic OPs long-term low-level toxicity.

5. Preincubation to PMSF, paraoxon or mipafox at non inhibitory concentrations diminishes sensitivity to mipafox, PMSF or paraoxon in components **Eα** and **Eγ**, probably by an irreversible modification of other sites different to the catalytic center.

6. The chromatography of the soluble brain fraction in the molecular exclusion BioSep s-3000 shows three different peaks (S1, S2 AND S3) of phenyl valerate esterase activity and when they were fractionated by ion exchange chromatography they were separated in 12 different fractions enriched with the different enzymatic components.

7. The Tandem-Mass Spectrometry analysis of one of the separated fractions, called S1D1, allows the identification of 259 proteins present in the sample according to the genomic data of Gallus gallus. The cholinesterase precursor was identified in this sample, with 19.9% coverage and six peptides identified, as the only protein present in the sample with potential serine esterase activity according to the proteomic data.

UNIVERSITAS
Miguel
Hernández

8. REFERENCES

UNIVERSITAS
Miguel
Hernández

Abdel Rasoul GM, Abou Salem ME, Mechael AA, Hendy OM, Rohlman DS, Ismail AA. Effects of occupational pesticide exposure on children applying pesticides. Neurotoxicology. 2008;29:833–8.

Akassoglou K, Malester B, Xu J, Tessarollo L, Rosenbluth J, Chao MV. Brain-specific deletion of neuropathy target esterase/swisscheese results in neurodegeneration. Proc Natl Acad Sci U S A. 2004 Apr 6;101(14):5075-80.

Aldridge WN. A method for the characterization of two similar B-esterases present in the chicken central nervous system. Biochem J. 1964. Dec;93(3):619-23.

Aldridge WN. Postscript to the symposium on organophosphorus compound induced delayed neuropathy.V Chem Biol Interact. 1993 Jun; 87(1-3):463-6.

Aldridge, W.N., and Reiner E. Acylated amino acids in inhibited B-esterases. In: Neuberger A., Tatum E.L., (Eds), Enzyme inhibitors as substrates. 1972. North-Holland Publishing Company, Amsterdam, pp:170-175.

Aprea C, Betta A, Catenacci G, Lotti A, Magnaghi S, Barisano A, Passini V, Pavan I, Sciarra G, Vitalone V, Minoia C. Reference values of urinary 3,5,6-trichloro-2-pyridinol in the Italian population--validation of analytical method and preliminary results (multicentric study). J AOAC Int. 1999. Mar-Apr;82(2):305-12.

Atkins J, Glynn P. Membrane association of and critical residues in the catalytic domain of human neuropathy target esterase. J Biol Chem. 2000 Aug 11;275(32):24477-83.

Baireddy P, Liu J, Hinsdale M, Pope C. Comparative effects of chlorpyrifos in wild type and cannabinoid Cb1 receptor knockout mice. Toxicol Appl Pharmacol.2011 Nov 1;256(3):324-9.

Baker EL Jr, Warren M, Zack M, Dobbin RD, Miles JW, Miller S, Alderman L, Teeters WR. Epidemic malathion poisoning in Pakistan malaria workers. Lancet.1978 Jan 7;1(8054):31-4.

Barglow KT, Cravatt BF. Activity-based protein profiling for the functional annotation of enzymes. Nat Methods. 2007 Oct;4(10):822-7.

Barr DB, Bravo R, Weerasekera G, Caltabiano LM, Whitehead RD Jr, Olsson AO, Caudill SP, Schober SE, Pirkle JL, Sampson EJ, Jackson RJ, Needham LL. Concentrations of dialkyl phosphate metabolites of organophosphorus pesticides in the U.S. population. Environ Health Perspect. 2004 Feb;112(2):186-200.

Barril J, Estévez J, Escudero MA, Céspedes MV, Níguez N, Sogorb MA, Monroy A, Vilanova E. Peripheral nerve soluble esterases are spontaneously reactivated after inhibition by paraoxon: implications for a new definition of neuropathy target esterase. Chem Biol Interact. 1999 May 14;119-120:541-50.

Barril J, Vilanova E. Reversible inhibition can profoundly mislead studies on progressive inhibition of enzymes: the interaction of paraoxon with soluble neuropathy target esterase. Chem Biol Interact. 1997 Dec 12;108(1-2):19-25.

Bazylewicz-Walczak B, Majczakowa W, Szymczak M. Behavioral effects of occupational exposure to organophosphorous pesticides in female greenhouse planting workers. Neurotoxicology. 1999 Oct;20(5):819-26.

Behra M, Etard C, Cousin X, Strähle U. The use of zebrafish mutants to identify secondary target effects of acetylcholine esterase inhibitors. Toxicol Sci. 2004 Feb;77(2):325-33.

Bomser JA, Casida JE. Diethylphosphorylation of rat cardiac M2 muscarinic receptor by chlorpyrifos oxon in vitro. Toxicol Lett. 2001 Feb 3;119(1):21-6.

Borhan B, Hammock B, Seifert J, Wilson BW. Methyl and phenyl esters and thioesters of carboxylic acids as surrogate substrates for microassay of proteinase K esterase activity. Anal Bioanal Chem. 1996 Feb;354(4):490-2.

Brown MA, Brix KA. 1998. Review of health consequences from high-, intermediate- and low-level exposure to organophosphorus nerve agents. J Appl Toxicol. 1998 Nov-Dec; 18(6):393-408.

Carrington CD, Abou-Donia MB. Axoplasmic transport and turnaround ofneurotoxic esterase in hen sciatic nerve. J Neurochem. 1985 Feb;44(2):616-21.

Carrington CD, Abou-Donia MB. The correlation between the recovery rate of neurotoxic esterase activity and sensitivity to organophosphorus-induced delayed neurotoxicity. Toxicol Appl Pharmacol. 1984 Sep 15;75(2):350-7.

Casida JE, Durkin KA. Anticholinesterase insecticide retrospective. Chem Biol Interact. 2013 Mar 25;203(1):221-5.

Casida JE, Quistad GB. Organophosphate toxicology: safety aspects of nonacetylcholinesterase secondary targets. Chem Res Toxicol. 2004. Aug;17(8):983-98.

Casida JE, Quistad GB. Serine hydrolase targets of organophosphorus toxicants. Chem Biol Interact. 2005 Dec 15;157-158:277-83. Epub 2005 Oct 21.

Céspedes MV, Escudero MA, Barril J, Sogorb MA, Vicedo JL, Vilanova E. Discrimination of carboxylesterases of chicken neural tissue by inhibition with a neuropathic, non-neuropathic organophosphorus compounds and neuropathy promoter. Chem Biol Interact. 1997 Oct 24;106(3):191-200.

Changeux JP. [Effects of ionic forces and curarizing agents on the acetylcholine esterase properties of the electric tissue of Torpedo marmorata]. CR Acad Sci Hebd Seances Acad Sci D. 1966 Feb 21;262(8):937-40.

Chatonnet F, Boudinot E, Chatonnet A, Taysse L, Daulon S, Champagnat J, Foutz AS. Respiratory survival mechanisms in acetylcholinesterase knockout mouse. Eur J Neurosci. 2003 Sep;18(6):1419-27.

Chemnitius JM, Dewald K, Kreuzer H, Zech R. Computerized analysis of covalent inhibition kinetics for identification of heart muscle cholinesterase and brain carboxylesterase isoenzymes. Design of differential inhibition assays. Chem Biol Interact. 1993 Jun;87(1-3):239-44.

Chemnitius JM, Haselmeyer KH, Zech R. Neurotoxic esterase. Identification of two isoenzymes in hen brain. Arch Toxicol. 1983 Jul;53(3):235-44.

Chemnitius JM, Zech R. Inhibition of brain carboxylesterases by neurotoxic and nonneurotoxic organophosphorus compounds. Mol Pharmacol. 1983 May;23(3):717-23.

Colosio C, Fustinoni S, Birindelli S, Bonomi I, De Paschale G, Mammone T, Tiramani M, Vercelli F, Visentin S, Maroni M. Ethylenethiourea in urine as an indicator of exposure to mancozeb in vineyard workers. Toxicol Lett. 2002 Aug 5;134(1-3):133-40.

Colosio C, Tiramani M, Brambilla G, Colombi A, Moretto A. Neurobehavioural effects of pesticides with special focus on organophosphorus compounds: which is the real size of the problem? Neurotoxicology. 2009 Nov;30(6):1155-61.

Costa LG. Current issues in organophosphate toxicology. Clin Chim Acta. 2006 Apr;366(1-2):1-13.

COT report, 1999. Organophosphates. A report of the commitee on Toxicology of Chemicals in Food, Consumer Products and the Environment. UK Department of Health, London.

Cravatt BF, Giang DK, Mayfield SP, Boger DL, Lerner RA, Gilula NB. Molecular characterization of an enzyme that degrades neuromodulatory fatty-acid amides. Nature. 1996 Nov 7;384(6604):83-7.

Darvesh S, Walsh R, Kumar R, Caines A, Roberts S, Magee D, Rockwood K, Martin E. Inhibition of human cholinesterases by drugs used to treat Alzheimer disease. Alzheimer Dis Assoc Disord. 2003 Apr-Jun;17(2):117-26.

Davis CS and Richardson RJ. Organophosphorus compounds. In: Spencer P.S. y Schaumburg H.H., Eds., 1980. Experimental and Clinical Neurotoxicology, Baltimore, pp:527-44.

Davison AN. Some observations on the cholinesterases of the central nervous system after the administration of organophosphorus compounds. 1953. Brit. J. Pharmacol. 8, 212.

Degroot A, Nomikos GG. In vivo neurochemical effects induced by changes in endocannabinoid neurotransmission. Curr Opin Pharmacol. 2007 Feb;7(1):62-8.

Deutsch DG, Omeir R, Arreaza G, Salehani D, Prestwich GD, Huang Z, Howlett A. Methyl arachidonyl fluorophosphonate: a potent irreversible inhibitor of anandamide amidase. Biochem Pharmacol. 1997 Feb 7;53(3):255-60.

Doorn JA, Schall M, Gage DA, Talley TT, Thompson CM, Richardson RJ.Identification of butyrylcholinesterase adducts after inhibition with isomalathion using mass spectrometry: difference in mechanism between (1R)- and(1S)-stereoisomers. Toxicol Appl Pharmacol. 2001 Oct 15;176(2):73-80.

Dubois KP, Doull J, et al. Studies on the toxicity and mechanism of action of p-nitrophenyl diethyl thionophosphate. J Pharmacol Exp Ther. 1949. Jan;95(1):79-91.

Dubois KP. New rodenticical compounds. J. Am. Pharm. Assoc. 1948. 37, 307-310.

Duysen EG, Li B, Xie W, Schopfer LM, Anderson RS, Broomfield CA, Lockridge O. Evidence for nonacetylcholinesterase targets of organophosphorus nerve agent:supersensitivity of acetylcholinesterase knockout mouse to VX lethality. J Pharmacol Exp Ther. 2001 Nov;299(2):528-35.

Duysen EG, Li B, Xie W, Schopfer LM, Anderson RS, Broomfield CA, Lockridge O. Evidence for nonacetylcholinesterase targets of organophosphorus nerve agent: supersensitivity of acetylcholinesterase knockout mouse to VX lethality. J Pharmacol Exp Ther. 2001 Nov;299(2):528-35.

Duysen EG, Stribley JA, Fry DL, Hinrichs SH, Lockridge O. Rescue of the acetylcholinesterase knockout mouse by feeding a liquid diet; phenotype of the adult acetylcholinesterase deficient mouse. Brain Res Dev Brain Res. 2002 Jul 30;137(1):43-54.

Eaton DL, Daroff RB, Autrup H, Bridges J, Buffler P, Costa LG, Coyle J, McKhann G, Mobley WC, Nadel L, Neubert D, Schulte-Hermann R, Spencer PS. Review of the toxicology of chlorpyrifos with an emphasis on human exposure and neurodevelopment. Crit Rev Toxicol. 2008;38 Suppl 2:1-125.

Ecobichon D.J., 2010. Anticholinesterase pesticides. Metabolism, Neurotoxicity and Epidemiology. In Anticholinesterase pesticides, 2006. Vol. 2, Agents, 2nd ed. (Satoh and Gupta., Ed.) pp, Academic Press, San Diego.

Ecobichon DJ. Toxic effects of pesticides. En: Casarett & Doull's Toxicology. The basic Science of poisons. 1996. CD Klaasen (ed), McGraw-Hill, New York, pp:643-689.

Ehrich M., and Jortner BS. Organophosphorus-induced delayed neuropathy. In Handbook of Pesticide Toxicology, 2001. Vol. 2, Agents, 2nd ed. (Krieger, R. I., Ed.) pp 987-1012, Academic Press, San Diego.

Escudero MA, Barril J, Tormo N, Vilanova E. Separation of two forms of neuropathy target esterase in the soluble fraction of the hen sciatic nerve. Chem Biol Interact. 1995 Aug 18;97(3):247-55.

Escudero MA, Céspedes MV, Vilanova E. Chromatographic discrimination of soluble neuropathy target esterase isoenzymes and related phenyl valerate esterases from chicken brain, spinal cord, and sciatic nerve. J Neurochem. 1997. May;68(5):2170-6.

Escudero MA, Vilanova E. Purification and characterization of naturally soluble neuropathy target esterase from chicken sciatic nerve by HPLC and western blot. J Neurochem. 1997 Nov;69(5):1975-82.

Eskenazi B, Marks AR, Bradman A, Harley K, Barr DB, Johnson C, Morga N, Jewell NP. Organophosphate pesticide exposure and neurodevelopment in young Mexican-American children. Environ Health Perspect. 2007 May;115(5):792-8.

Estevan C, Vilanova E, Sogorb MA. Chlorpyrifos and its metabolites alter gene expression at non-cytotoxic concentrations in D3 mouse embryonic stem cells under in vitro differentiation: considerations for embryotoxic risk assessment. Toxicol Lett. 2013 Feb 13;217(1):14-22.

Estévez J, Barril J, Vilanova E. Inhibition with spontaneous reactivation and the "ongoing inhibition" effect of esterases by biotinylated organophosphorus compounds: S9B as a model. Chem Biol Interact. 2010 Sep 6;187(1-3):397-402.

Estévez J, Barril J, Vilanova E. Kinetics of inhibition of soluble peripheral nerve esterases by PMSF: a non-stable compound that potentiates the organophosphorus-induced delayed neurotoxicity. Arch Toxicol. 2012 May;86(5):767-77.

Estévez J, García-Pérez A, Barril J, Vilanova E. Inhibition with spontaneous reactivation of carboxyl esterases by organophosphorus compounds: paraoxon as a model. Chem Res Toxicol. 2011 Jan 14;24(1):135-43.

Estévez J, García-Pérez AG, Barril J, Pellín M, Vilanova E. The inhibition of the high sensitive peripheral nerve soluble esterases by mipafox. A new mathematical processing for the kinetics of inhibition of esterases by organophosphorus compounds. Toxicol Lett. 2004 Jun 15;151(1):171-81.

Estévez J, Mangas I, Sogorb MÁ, Vilanova E. Interactions of neuropathy inducers and potentiators/promoters with soluble esterases. Chem Biol Interact. 2013 Mar 25;203(1):245-50.

Estevez J, Vilanova E. Model equations for the kinetics of covalent irreversible enzyme inhibition and spontaneous reactivation: esterases and organophosphorus compounds. Crit Rev Toxicol. 2009;39(5):427-48.

FAO report: FAO/PL:1968/M/9/1/WHO/FOOD ADD./69.35 Joint Meeting of the FAO Working Party of Experts and the WHO Expert Committee on Pesticide Residues. Food and Agriculture Organization of the United Nations. World Health Organization. Geneva, 9-16 December,1969

Farahat TM, Abdelrasoul GM, Amr MM, Shebl MM, Farahat FM, Anger WK. Neurobehavioural effects among workers occupationally exposed to organophosphorous pesticides. Occup Environ Med. 2003;60:279–286.

Fukuto TR. Mechanism of action of organophosphorus and carbamate insecticides. Environ Health Perspect. 1990 Jul;87:245-54.

Garcia-Pérez AG, Barril J, Estévez J, Vilanova E. Properties of phenyl valerate esterase activities from chicken serum are comparable with soluble esterases of peripheral nerves in relation with organophosphorus compoundsinhibition. Toxicol Lett. 2003 Apr 30;142(1-2):1-10.

Gibney G, Camp S, Dionne M, MacPhee-Quigley K, Taylor P. Mutagenesis of essential functional residues in acetylcholinesterase. Proc Natl Acad Sci U S A. 1990 Oct;87(19):7546-50.

Glynn P, Holton JL, Nolan CC, Read DJ, Brown L, Hubbard A, Cavanagh JB. Neuropathy target esterase: immunolocalization to neuronal cell bodies and axons. Neuroscience. 1998 Mar;83(1):295-302.

Glynn P, Read DJ, Guo R, Wylie S, Johnson MK. Synthesis and characterization of a biotinylated organophosphorus ester for detection and affinity purification of a brain serine esterase: neuropathy target esterase. Biochem J. 1994 Jul 15;301 (Pt 2):551-6.

Glynn P, Read DJ, Lush MJ, Li Y, Atkins J. Molecular cloning of neuropathy target esterase (NTE). Chem Biol Interact. 1999 May 14;119-120:513-7.

Glynn P. Neural development and neurodegeneration: two faces of neuropathy target esterase. Prog Neurobiol. 2000 May;61(1):61-74.

Glynn P. Neuropathy target esterase and phospholipid deacylation. Biochim Biophys Acta. 2005 Sep 15;1736(2):87-93.

Goldstein DA, McGuigan MA, Ripley BD. Acute tricresylphosphate intoxication in childhood. Hum Toxicol. 1988 Mar;7(2):179-82.

Greenspan RJ, Finn JA Jr, Hall JC. Acetylcholinesterase mutants in Drosophila and their effects on the structure and function of the central nervous system. J Comp Neurol. 1980 Feb 15;189(4):741-74.

Grigoryan H, Schopfer LM, Peeples ES, Duysen EG, Grigoryan M, Thompson CM, Lockridge O. Mass spectrometry identifies multiple organophosphorylated sites on tubulin. Toxicol Appl Pharmacol. 2009 Oct 15;240(2):149-58.

Grigoryan H, Schopfer LM, Thompson CM, Terry AV, Masson P, Lockridge O. Mass spectrometry identifies covalent binding of soman, sarin, chlorpyrifos oxon, diisopropyl fluorophosphate, and FP-biotin to tyrosines on tubulin: a potential mechanism of long term toxicity by organophosphorus agents. Chem Biol Interact. 2008 Sep 25;175(1-3):180-6.

Grube A, Donaldson D, Kiely T, Wu L. Pesticides Industry Sales and Usage 2006 and 2007 Market Estimates. 2011. Biological and Economic Analysis Division Office of Pesticide Programs. Office of Chemical Safety and Pollution Prevention U.S. Environmental Protection Agency, Washington.

Guillozet AL, Smiley JF, Mash DC, Mesulam MM. Butyrylcholinesterase in the life cycle of amyloid plaques. Ann Neurol. 1997 Dec;42(6):909-18.

Gupta RC. Classification and uses of organophosphates and carbamates. In Toxicology of Organophosphate and Carbamate compounds,2006. pp.5-25 ed by Gupta. Academic Press.

Guttman M, Betts GN, Barnes H, Ghassemian M, van der Geer P, Komives EA. Interactions of the NPXY microdomains of the low density lipoprotein receptor-related protein 1. Proteomics. 2009 Nov;9(22):5016-28.

Harel M, Sussman JL, Krejci E, Bon S, Chanal P, Massoulié J, Silman I. Conversion of acetylcholinesterase to butyrylcholinesterase: modeling and mutagenesis. Proc Natl Acad Sci U S A. 1992 Nov 15;89(22):10827-31.

Haux JE, Lockridge O, Casida JE. Specificity of ethephon as a butyrylcholinesterase inhibitor and phosphorylating agent. Chem Res Toxicol. 2002. Dec;15(12):1527-33.

Haux JE, Quistad GB, Casida JE. Phosphobutyrylcholinesterase: phosphorylation of the esteratic site of butyrylcholinesterase by ethephon [(2-chloroethyl)phosphonic acid] dianion. Chem Res Toxicol. 2000. Jul;13(7):646-51.

Hernández AF, Parrón T, Tsatsakis AM, Requena M, Alarcón R, López-Guarnido O. Toxic effects of pesticide mixtures at a molecular level: Their relevance to human health. Toxicology. 2013 May 10;307:136-45

Herschman Z, Aaron C. Prolongation of cocaine effect. Anesthesiology. 1991. Mar;74(3):631-2.

Hoffman RS, Henry GC, Wax PM, Weisman RS, Howland MA, Goldfrank LR. Decreased plasma cholinesterase activity enhances cocaine toxicity in mice. J Pharmacol Exp Ther. 1992 Nov;263(2):698-702.

Hovanec JW, Broomfield CA, Steinberg GM, Lanks KW, Lieske CN. Spontaneous reactivation of acetylcholinesterase following organophosphate inhibition. I. An analysis of anomalous reactivation kinetics. Biochim Biophys Acta. 1977 Aug 11;483(2):312-9.

Howard MD, Mirajkar N, Karanth S, Pope CN. Comparative effects of oral chlorpyrifos exposure on cholinesterase activity and muscarinic receptor binding in neonatal and adult rat heart. Toxicology. 2007 Sep 5;238(2-3):157-65.

ICGSC. International Chicken Genome Sequencing Consortium. "Sequence and comparative analysis of the chicken genome provide unique perspectives on vertebrate evolution." Nature, 2004. Dec 9;432(7018):695-716

Inestrosa NC, Alvarez A, Pérez CA, Moreno RD, Vicente M, Linker C, Casanueva OI, Soto C, Garrido J. Acetylcholinesterase accelerates assembly of amyloid-beta-peptides into Alzheimer's fibrils: possible role of the peripheral site of the enzyme. Neuron. 1996 Apr;16(4):881-91.

Interactions of the NPXY microdomains of the low density lipoprotein receptor-related protein 1. Proteomics. 2009 Nov;9(22):5016-28.

Iverson F, Grant DL, Lacroix J. Diazinon metabolism in the dog. Bull Environ Contam Toxicol. 1975 May;13(5):611-8.

Jamal GA, Hansen S, Julu PO. Low level exposures to organophosphorus esters may cause neurotoxicity. Toxicology. 2002 Dec 27;181-182:23-33.

James GT. Inactivation of the protease inhibitor phenylmethylsulfonyl fluoride in buffers. Anal Biochem. 1978 Jun 1;86(2):574-9.

Jennings LL, Malecki M, Komives EA, Taylor P. Direct analysis of the kinetic profiles of organophosphate-acetylcholinesterase adducts by MALDI-TOF mass spectrometry. Biochemistry. 2003 Sep 23;42(37):11083-91.

Jett DA, Navoa RV, Beckles RA, McLemore GL. Cognitive function and cholinergic neurochemistry in weanling rats exposed to chlorpyrifos. Toxicol Appl Pharmacol. 2001 Jul 15;174(2):89-98.

Johnson G, Moore SW. The adhesion function on acetylcholinesterase is located at the peripheral anionic site. Biochem Biophys Res Commun. 1999 May 19;258(3):758-62.

Johnson MK, Lauwerys R. Protection by some carbamates against the delayed neurotoxic effects of di-isopropyl phosphorofluoridate. Nature. 1969a Jun 14;222(5198):1066-7.

Johnson MK, Read DJ. Prophylaxis against and promotion of organophosphate-induced delayed neuropathy by phenyl di-n-pentylphosphinate. Chem Biol Interact. 1993 Jun;87(1-3):449-55.

Johnson MK. Improved assay of neurotoxic esterase for screening organophosphates for delayed neurotoxicity potential. Arch Toxicol. 1977 Jun18;37(2):113-5.

Johnson MK. The delayed neurotoxic effect of some organophosphorus compounds. Identification of the phosphorylation site as an esterase. Biochem J. 1969b. Oct;114(4):711-7.

Johnson MK. The primary biochemical lesion leading to the delayed neurotoxic effects of some organophosphorus esters. J Neurochem. 1974 Oct;23(4):785-9.

Johnson, MK.The target for initiation of delayed neurotoxicity by 693 organophosphorus esters: biochemical studies and toxicological applications. Rev. Biochem. Toxicol. 1982. 4, 141–212. 695

Jokanović M. Biotransformation of organophosphorus compounds. Toxicology. 2001. Sep 25;166(3):139-60.

Kam CM, Abuelyaman AS, Li Z, Hudig D, Powers JC. Biotinylated isocoumarins,new inhibitors and reagents for detection, localization, and isolation of serine proteases. Bioconjug Chem. 1993 Nov-Dec;4(6):560-7.

Kam CM, Abuelyaman AS, Li Z, Hudig D, Powers JC. Biotinylated isocoumarins, new inhibitors and reagents for detection, localization, and isolation of serine proteases. Bioconjugate chemistry 1993;

Kamel F, Rowland AS, Park LP, Anger WK, Baird DD, Gladen BC, et al. Neurobehavioral performance and work experience in Florida farmworkers. Environ Health Perspect. 2003;111:1765–1772

Karalliedde L, Baker D, Marrs TC., 2010. Organophosphate-induced intermediate syndrome: aetiology and relationships with myopathy. Toxicol Rev. 2006;25(1):1-14.

Karalliedde L, Henry JA. Effects of organophosphates on skeletal muscle. HumExp Toxicol. 1993 Jul;12(4):289-96.

Karczmar, A. Anticholinesterases: dramatic aspects of their use and misuse. Neurochem. Int. 1998. 32, 401-411.

Kemp JR, Wallace KB. Molecular determinants of the species-selective inhibition of brain acetylcholinesterase. Toxicol Appl Pharmacol. 1990 Jun 15;104(2):246-58.

Kienesberger PC, Oberer M, Lass A, Zechner R. Mammalian patatin domain containing proteins: a family with diverse lipolytic activities involved in multiple biological functions. J Lipid Res. 2009 Apr;50 Suppl:S63-8.

Knaak JB, Al-Bayati MA, Raabe OG. Physiologically based pharmacokinetic modeling to predict tissue dose and cholinesterase inhibition in workers exposed to organophosphorus and carbamate pesticides. 1993. In Health Risk Assessment: Dermal and Inhalation Exposure and absortion of Toxicants (R.G.M.Wang, J.B. Knaak, and H.I. Maibach, Eds), pp. 3-29. CRC Press, Boca Raton, FL.

Kovarik Z, Radić Z, Berman HA, Simeon-Rudolf V, Reiner E, Taylor P. Acetylcholinesterase active centre and gorge conformations analysed by combinatorial mutations and enantiomeric phosphonates. Biochem J. 2003 Jul 1;373(Pt 1):33-40.

Kutty KM, Payne RH. Serum pseudocholinesterase and very-low-density lipoprotein metabolism. J Clin Lab Anal. 1994;8(4):247-50. Review. PubMed PMID:7931819.

The Merck-index: an encyclopedia of chemicals, drugs, and biological. Martha Windholz; Merck and Company. Edited by Rahway, N.J. : Merck, 1983.

Spencer, E.Y. Guide to the Chemicals Used in Crop Protection. 6th ed. Publication 1093, Research Institute, Agriculture Canada, Ottawa, Canada: Information Canada, 1973. 357

Lenfant N, Hotelier T, Bourne Y, Marchot P, Chatonnet A. Proteins with an alpha/beta hydrolase fold: Relationships between subfamilies in an ever-growing superfamily. Chem Biol Interact. 2013 Mar 25;203(1):266-8.

Li B, Schopfer LM, Hinrichs SH, Masson P, Lockridge O. Matrix-assisted laser desorption/ionization time-of-flight mass spectrometry assay for organophosphorus toxicants bound to human albumin at Tyr411. Anal Biochem. 2007 Feb 15;361(2):263-72.

Li B, Stribley JA, Ticu A, Xie W, Schopfer LM, Hammond P, Brimijoin S, Hinrichs SH, Lockridge O. Abundant tissue butyrylcholinesterase and its possible function in the acetylcholinesterase knockout mouse. J Neurochem. 2000. Sep;75(3):1320-31.

Li Y, Dinsdale D, Glynn P. Protein domains, catalytic activity, and subcellular distribution of neuropathy target esterase in Mammalian cells. J Biol Chem. 2003 Mar 7;278(10):8820-5.

Little PJ, Scimeca JA, Martin BR. Distribution of 3H]diisopropylfluorophosphate, [3H]soman, [3H]sarin, and their metabolites in mouse brain. Drug Metab Dispos. 1988 Jul-Aug;16(4):515-20.

Liu X, Yang Q, Nakamura C, Miyake J. Avidin-biotin-immobilized liposome column for chromatographic fluorescence on-line analysis of solute-membrane interactions. J Chromatogr B Biomed Sci Appl. 2001 Jan 5;750(1):51-60.

Liu Y, Patricelli MP, Cravatt BF. Activity-based protein profiling: the serine hydrolases. Proc Natl Acad Sci U S A. 1999 Dec 21;96(26):14694-9.

Lockdridge O, Schopfer LM. Biomarkers of exposure. In Toxicology of Organophosphate and Carbamate Compounds 2006. (Gupta., Ed.) pp703-715, Academic Press, San Diego.

Lockridge O, Duysen EG, Voelker T, Thompson CM, Schopfer LM. Life without acetylcholinesterase: the implications of cholinesterase inhibitor toxicity in AChE-knockout mice. Environ Toxicol Pharmacol. 2005 May;19(3):463-9.

Lockridge O, Schopfer LM. Review of tyrosine and lysine as new motifs for organophosphate binding to proteins that have no active site serine. Chem Biol Interact. 2010 Sep 6;187(1-3):344-8.

Long JZ, Cravatt BF. The metabolic serine hydrolases and their functions in mammalian physiology and disease. Chem Rev. 2011 Oct 12;111(10):6022-63.

Long JZ, Li W, Booker L, Burston JJ, Kinsey SG, Schlosburg JE, Pavón FJ, Serrano AM, Selley DE, Parsons LH, Lichtman AH, Cravatt BF. Selective blockade of 2-arachidonoylglycerol hydrolysis produces cannabinoid behavioral effects. Nat Chem Biol. 2009

Lotti M, Caroldi S, Moretto A, Johnson MK, Fish CJ, Gopinath C, Roberts NL. Central-peripheral delayed neuropathy caused by diisopropylphosphorofluoridate (DFP): Segregation of peripheral nerve and spinal

cord effects using biochemical clinical, and morphological criteria. 1987. Toxicol Appl Pharmacol 88:87-96

Lotti M. Low-level exposures to organophosphorus esters and peripheral nerve function. Muscle Nerve. 2002;25:492–504

Lotti M. Organophosphorus compounds. In Experimental and Clinical Neurotoxicology, 2000. 2nd ed. (Spencer, P. S., Schaumburg, H. H., and Ludolph, A. C., Eds.) pp 897-925, Oxford University Press, New York.

Lotti M. Promotion of organophosphate induced delayed polyneuropathy by certain esterase inhibitors. Toxicology. 2002 Dec 27;181-182:245-8.

Lowit AB. Federal Regulations and Risk assessment of Organophosphate and Carbamate Pesticides In Toxicology of Organophosphate Pesticides Ed. Gupta. Neurochem Int. 2007 Feb;50(3):531-9. Epub 2006 Dec 18.

Macdonald IR, Martin E, Rosenberry TL, Darvesh S. Probing the peripheral site of human butyrylcholinesterase. Biochemistry. 2012 Sep 11;51(36):7046-53.

Mach M, Grubbs RD, Price WA, Nagaoka M, Dubovický M, Lucot JB. Delayed behavioral and endocrine effects of sarin and stress exposure in mice. J ApplToxicol. 2008 Mar;28(2):132-9.

Mackenzie Ross SJ. Cognitive function following *exposure to contaminated air on commercial aircraft. A case series of 27 airline pilots seen for clinical purposes.*Journal of Nutritional & Environmental Medicine*, 2008. 17 (2): 111-126*.

Mamczarz J, Pereira EF, Aracava Y, Adler M, Albuquerque EX. An acute exposure to a sub-lethal dose of soman triggers anxiety-related behavior in guinea pigs:interactions with acute restraint. Neurotoxicology. 2010 Jan;31(1):77-84.

Marks AR, Harley K, Bradman A, Kogut K, Barr DB, Johnson C, Calderon N,Eskenazi B. Organophosphate pesticide exposure and attention in young Mexican-American children: the CHAMACOS study. Environ Health Perspect. 2010 Dec;118(12):1768-74.

Marrs TC. Organophosphate poisoning. Pharmacol Ther. 1993;58(1):51-66.

Marrs, T. C., Maynard, R. L., and Sidell, F. R., Eds. Chemical Warfare Agents: Toxicology and Treatment, 1996. 243 pp,Wiley, New York.

Masoud A, Kiran R, Sandhir R. Impaired mitochondrial functions in organophosphate induced delayed neuropathy in rats. Cell Mol Neurobiol. 2009 Dec;29(8):1245-55.

Masson P, Froment MT, Bartels CF, Lockridge O. Importance of aspartate-70 in organophosphate inhibition, oxime re-activation and aging of human butyrylcholinesterase. Biochem J. 1997 Jul 1;325 (Pt 1):53-61.

Masuda N, Takatsu M, Morinari H, Ozawa T. Sarin poisoning in Tokyo subway. Lancet. 1995 Jun 3;345(8962):1446.

McCauley LA. Organophosphates and the Gulf War Syndrome. In Toxicology of Organophosphate and Carbamate Compounds 2006.. (Gupta., Ed.) pp 69-79, Academic Press, San Diego.

McCormack AL, Schieltz DM, Goode B, Yang S, Barnes G, Drubin D, Yates JR 3rd. Direct analysis and identification of proteins in mixtures by LC/MS/MS and database searching at the low-femtomole level. Anal Chem. 1997 Feb 15;69(4):767-76.

McDaniel KL, Moser VC. Differential profiles of cholinesterase inhibition and neurobehavioral effects in rats exposed to fenamiphos or profenofos. Neurotoxicol Teratol. 2004 May-Jun;26(3):407-15.

Middlemore-Risher ML, Buccafusco JJ, Terry AV Jr. Repeated exposures to low-level chlorpyrifos results in impairments in sustained attention and increased impulsivity in rats. Neurotoxicol Teratol. 2010 Jul-Aug;32(4):415-24.

Millard CB, Kryger G, Ordentlich A, Greenblatt HM, Harel M, Raves ML, Segall Y, Barak D, Shafferman A, Silman I, Sussman JL. Crystal structures of aged phosphonylated acetylcholinesterase: nerve agent reaction products at the atomic level. Biochemistry. 1999 Jun 1;38(22):7032-9.

Moretto A, Bertolazzi M, Capodicasa E, Peraica M, Richardson RJ, ScapellatoML, Lotti M. Phenylmethanesulfonyl fluoride elicits and intensifies the clinical expression of neuropathic insults. Arch Toxicol. 1992;66(1):67-72.

Moretto A, Bertolazzi M, Lotti M. The phosphorothioic acid O-(2-chloro-2,3,3-trifluorocyclobutyl) O-ethyl S-propyl ester exacerbates organophosphate polyneuropathy without inhibition of neuropathy target esterase. Toxicol Appl Pharmacol. 1994 Nov;129(1):133-7.

Moretto A, Capodicasa E, Peraica M, Lotti M. Phenylmethanesulfonyl fluoride delays the recovery from crush of peripheral nerves in hens. Chem Biol Interact. 1993 Jun;87(1-3):457-62.

Moretto A, Gardiman G, Panfilo S, Colle MA, Lock EA, Lotti M. Effects of S-ethyl hexahydro-1H-azepine-1-carbothioate (molinate) on di-n-butyldichlorovinyl phosphate (DBDCVP) neuropathy. Toxicol Sci. 2001 Aug;62(2):274-9.

Moretto A, Gardiman G, Panfilo S, Colle MA, Lock EA, Lotti M. Effects of S-ethyl hexahydro-1H-azepine-1-carbothioate (molinate) on di-n-butyldichlorovinyl phosphate (DBDCVP) neuropathy. Toxicol Sci. 2001 Aug;62(2):274-9.

Moretto A, Lotti M. Peripheral Nervous System Effects and Delayed Neuropathy In Toxicology of Organophosphate and Carbamate Compounds 2006. (Gupta., Ed.) pp361-371, Academic Press, San Diego.

Moretto A, Lotti M. Poisoning by organophosphorus insecticides and sensory neuropathy. J Neurol Neurosurg Psychiatry. 1998 Apr;64(4):463-8.

Moretto A, Nicolli A, Lotti M. The search of the target of promotion: Phenylbenzoate esterase activities in hen peripheral nerve. Toxicol Appl Pharmacol. 2007 Mar;219(2-3):196-201.

Moscioni AD, Engel JL, Casida JE. Kynurenine formamidase inhibition as a possible mechanism for certain teratogenic effects of organophosphorus and methylcarbamate insecticides in chicken embryos. Biochem Pharmacol. 1977 Dec 1;26(23):2251-8.

Moser M, Li Y, Vaupel K, Kretzschmar D, Kluge R, Glynn P, Buettner R. Placental failure and impaired vasculogenesis result in embryonic lethality for neuropathy target esterase-deficient mice. Mol Cell Biol. 2004 Feb;24(4):1667-79.

Moser VC. Animal models of chronic pesticide neurotoxicity. Hum Exp Toxicol. 2007 Apr;26(4):321-31. Review.

Moser VC. Comparisons of the acute effects of cholinesterase inhibitors using a neurobehavioral screening battery in rats. Neurotoxicol Teratol. 1995.Nov-Dec;17(6):617-25. PubMed PMID: 8747743.

Nagase T, Kikuno R, Ishikawa K, Hirosawa M, Ohara O. Prediction of the coding sequences of unidentified human genes. XVII. The complete sequences of 100 new cDNA clones from brain which code for large proteins in vitro. DNA Res. 2000 Apr 28;7(2):143-50.

Nallapaneni A, Liu J, Karanth S, Pope C. Modulation of paraoxon toxicity by the cannabinoid receptor agonist WIN 55,212-2. Toxicology. 2006 Oct 3;227(1-2):173-83.

Nallapaneni A, Liu J, Karanth S, Pope C. Pharmacological enhancement of endocannabinoid signaling reduces the cholinergic toxicity of diisopropylfluorophosphate. Neurotoxicology. 2008 Nov;29(6):1037-43.

Nomura DK, Blankman JL; Simon GM, Fujioka K, Issa RS, Ward AM, Cravatt BF, Casida JE. Activation of the endocannabinoid system by organophosphorus nerve agents. Nat. Chem. Biol. 2008. 4, 373–378.

Nomura DK, Casida JE. Activity-based protein profiling of organophosphorus and thiocarbamate pesticides reveals multiple serine hydrolase targets in mouse brain. J Agric Food Chem. 2011. 59(7):2808-15.

Nomura DK, Durkin KA, Chiang KP, Quistad GB, Cravatt BF, Casida JE. Serine hydrolase KIAA1363: toxicological and structural features with emphasis on organophosphate interactions. Chem Res Toxicol. 2006 Sep;19(9):1142-50.

Nomura DK, Leung D, Chiang KP, Quistad GB, Cravatt BF, Casida JE. A brain detoxifying enzyme for organophosphorus nerve poisons. Proc Natl Acad Sci U S A. 2005. 102(17):6195-200.

Ollis DL, Cheah E, Cygler M, Dijkstra B, Frolow F, Franken SM, Harel M, Remington SJ, Silman I, Schrag J, et al. The alpha/beta hydrolase fold. Protein Eng. 1992 Apr;5(3):197-211.

Ortigoza-Ferado J, Richter RJ, Hornung SK, Motulsky AG, Furlong CE. Paraoxon hydrolysis in human serum mediated by a genetically variable arylesterase and albumin. Am J Hum Genet. 1984 Mar;36(2):295-305.

Osman KA, Moretto A, Lotti M. Sulfonyl fluorides and the promotion of diisopropyl fluorophosphate neuropathy. Fundam Appl Toxicol. 1996. 33(2):294-7.

Ostrea EM, Morales V, Ngoumgna E, Prescilla R, Tan E, Hernandez E, Ramirez GB,Cifra HL, Manlapaz ML. Prevalence of fetal exposure to environmental toxins as determined by meconium analysis. Neurotoxicology. 2002 Sep;23(3):329-39.

Oswal DP, Garrett TL, Morris M, Lucot JB. Low-dose sarin exposure produces long term changes in brain neurochemistry of mice. Neurochem Res. 2013 Jan;38(1):108-16.

Pamies D, Reig JA, Vilanova E, Sogorb MA. Expression of Neuropathy Target Esterase in mouse embryonic stem cells during differentiation. Arch Toxicol. 2010. Jun;84(6):481-91.

Pamies D, Vilanova E, Sogorb MA. Functional pathways altered after silencing Pnpla6 (the codifying gene of neuropathy target esterase) in mouse embryonic stem cells under differentiation. In Vitro Cell Dev Biol Anim. 2013 Oct 19.

Parrón T, Hernández AF, Villanueva E. Increased risk of suicide with exposure to pesticides in an intensive agricultural area. A 12-year retrospective study.Forensic Sci Int. 1996 May 17;79(1):53-63.

Parrón T, Requena M, Hernández AF, Alarcón R. Association between environmental exposure to pesticides and neurodegenerative diseases. Toxicol Appl Pharmacol. 2011 Nov 1;256(3):379-85.

Peeples ES, Schopfer LM, Duysen EG, Spaulding R, Voelker T, Thompson CM, Lockridge O. Albumin, a new biomarker of organophosphorus toxicant exposure,identified by mass spectrometry. Toxicol Sci. 2005 Feb;83(2):303-12.

Peraica M, Capodicasa E, Moretto A, Lotti M. Organophosphate polyneuropathy in chicks. Biochem Pharmacol. 1993 Jan 7;45(1):131-5.

Peraica M, Capodicasa M, Scapellato ML, Bertolazzi M, Moretto A, Lotti M. Organophosphate induced delayed polyneuropathy (OPIDP) in chicks: induction,promotion and recovery. Toxicologist 1991. 11:306

Poet TS, Kousba AA, Dennison SL, Timchalk C. In vitro rat hepatic and intestinal metabolism of the organophosphate pesticides chlorpyrifos and diazinon. Toxicol. Sci. 2003. 72, 193-200.

Poet TS, Kousba AA, Dennison SL, Timchalk C. Physiologically based pharmacokinetic/pharmacodynamic model for the organophosphorus pesticide diazinon. Neurotoxicology. 2004 Dec;25(6):1013-30.

Pope CN, Mechoulam R, Parsons L. Endocannabinoid signaling in neurotoxicity and neuroprotection. Neurotoxicology. 2010 Sep;31(5):562-71.

Pope CN, Padilla S. Potentiation of organophosphorus-induced delayed neurotoxicity by phenylmethylsulfonyl fluoride. J Toxicol Environ Health. 1990. Dec;31(4):261-73.

Pope CN, Tanaka D Jr, Padilla S. The role of neurotoxic esterase (NTE) in the prevention and potentiation of organophosphorus-induced delayed neurotoxicity (OPIDN). Chem Biol Interact. 1993 Jun;87(1-3):395-406.

Pope CN. Central Nervous System Effects and Neurotoxicity. In Toxicology of Organophosphate and Carbamate Compounds 2006. (Gupta., Ed.) pp271-293, Academic Press, San Diego.

Pope CN. Organophosphorus pesticides: do they all have the same mechanism of toxicity? J Toxicol Environ Health B Crit Rev. 1999 Apr-Jun;2(2):161-81.

Poulsen E, Aldridge WN. Studies on esterases in the chicken central nervous system. Biochem J. 1964 Jan;90(1):182-9.

Proctor NH, Casida JE. Organophosphorus and methyl carbamate insecticide teratogenesis: diminished NAD in chicken embryos. Science 1975. 190, 580-582.

Prueitt RL, Goodman JE, Bailey LA, Rhomberg LR. Hypothesis-based weight-of-evidence evaluation of the neurodevelopmental effects of chlorpyrifos. Crit Rev Toxicol. 2011 Nov;41(10):822-903. doi: 10.3109/10408444.2011.616877.

Quistad GB, Sparks SE, Casida JE. Fatty acid amide hydrolase inhibition by neurotoxic organophosphorus pesticides. Toxicol Appl Pharmacol. 2001 May15;173(1):48-55.

RAC report: Research Advisory Commitee on Gulf War veterans´Illnesses, 2008. Gulf War Illness and the Health of Gulf War Veterans. Scientific Findings and Recommendations. U S Goverment Printing Office, Washington D.C. 2008.

Radić Z, Taylor P. Peripheral site ligands accelerate inhibition ofacetylcholinesterase by neutral organophosphates. J Appl Toxicol. 2001 Dec;21Suppl 1:S13-4.

Radic Z, Taylor P. Structure and Functionof Cholinesterase. In Toxicology of Organophosphate and Carbamate Compounds 2006.. (Gupta., Ed.) pp1614-187, Academic Press, San Diego.

Rainier S, Albers JW, Dyck PJ, Eldevik OP, Wilcock S, Richardson RJ, Fink JK. Motor neuron disease due to neuropathy target esterase gene mutation: clinical features of the index families. Muscle Nerve. 2011 Jan;43(1):19-25.

Rainier S, Bui M, Mark E, Thomas D, Tokarz D, Ming L, Delaney C, Richardson RJ, Albers JW, Matsunami N, Stevens J, Coon H, Leppert M, Fink JK. Neuropathy target esterase gene mutations cause motor neuron disease. Am J Hum Genet. 2008. Mar;82(3):780-5.

Ramachandran BV, Agren G. Esterases of rat-liver cell fractions. correlation of df32p-binding capacity to esterase activity. Biochem Pharmacol. 1963. Sep;12:981-8.

Ray DE, Richards PG. The potential for toxic effects of chronic, low-dose exposure to organophosphates. Toxicol Lett. 2001 Mar 31;120(1-3):343-51.

Read DJ, Li Y, Chao MV, Cavanagh JB, Glynn P. Neuropathy target esterase is required for adult vertebrate axon maintenance. J Neurosci. 2009. Sep 16;29(37):11594-600.

Read DJ, Li Y, Chao MV, Cavanagh JB, Glynn P. Organophosphates induce distal axonal damage, but not brain oedema, by inactivating neuropathy target esterase. Toxicol Appl Pharmacol. 2010 May 15;245(1):108-15.

Richards PG, Johnson MK, Ray DE. Identification of acylpeptide hydrolase as a sensitive site for reaction with organophosphorus compounds and a potential target for cognitive enhancing drugs. Mol Pharmacol. 2000 Sep;58(3):577-83.

Richardson RJ, Hein ND, Wijeyesakere SJ, Fink JK, Makhaeva GF. 2013. Neuropathy target esterase (NTE): overview and future. Chem Biol Interact. 2013 Mar 25;203(1):238-44.

Robaire B, Kato G. Acetylcholinesterase and alpha-bungarotoxin: a study of their possible interaction. FEBS Lett. 1974 Sep 15;46(1):218-23.

Roger JC, Chambers H, casida JE. Nicotinic acid analogs: effects on responseof chick embryos and hens to organophosphate toxicants. science. 1964 may. 1;144(3618):539-40.

Rohlman DS, Anger WK, Lein PJ. Correlating neurobehavioral performance with biomarkers of organophosphorous pesticide exposure. Neurotoxicology. 2011 Mar;32(2):268-76.

Roldán-Tapia L, Nieto-Escamez FA, del Aguila EM, Laynez F, Parron T, Sanchez- Santed. F. Neuropsychological sequelae from acute poisoning and long-term exposure to carbamate and organophosphate pesticides. Neurotoxicol Teratol 2006; 28(6):694–703.

Romana MJ, A J, Sheridan R, Sidell FR. Health effects of low-level exposure to nerve agents. CRC Press; Boca Raton: 2001.

Ross SM, McManus IC, Harrison V, Mason O. Neurobehavioral problems following low-level exposure to organophosphate pesticides: a systematic and meta-analytic review. Crit Rev Toxicol. 2013 Jan;43(1):21-44.

Roufogalis BD, Quist EE. Relative binding sites of pharmacologically active ligands on bovine erythrocyte acetylcholinesterase. Mol Pharmacol. 1972 Jan;8(1):41-9.

Rousseaux CG, Dua AK. Pharmacology of HI-6, an H-series oxime. Can J Physiol Pharmacol. 1989 Oct;67(10):1183-9.

Sánchez del Campo LF, Nieto-Cerón S, Morote-García JC, Muñoz-Delgado E, Vidal CJ, Campoy FJ. Butyrylcholinesterase activity and molecular components in thymus of healthy and merosin-deficient Lama2dy mice. Neurochem Int. 2007Feb;50(3):531-9.

Satoh T, Hosokawa M. Organophosphates and their impact on the global environment. Neurotoxicology. 2000 Feb-Apr;21(1-2):223-7.

Satoh T, Hosokawa M. The mammalian carboxylesterases: from molecules to functions. Annu Rev Pharmacol Toxicol. 1998;38:257-88.

Schumacher M, Camp S, Maulet Y, Newton M, MacPhee-Quigley K, Taylor SS, Friedmann T, Taylor P. Primary structure of Torpedo californica acetylcholinesterase deduced from its cDNA sequence. Nature. 1986 Jan 30-Feb 5;319(6052):407-9.

Scremin OU, Shih TM, Huynh L, Roch M, Booth R, Jenden DJ. Delayed neurologic and behavioral effects of subtoxic doses of cholinesterase inhibitors. J Pharmacol Exp Ther. 2003

Segall Y, Quistad GB, Nomura DK, Casida JE. Arachidonylsulfonyl derivatives as cannabinoid CB1 receptor and fatty acid amide hydrolase inhibitors. Bioorg Med Chem Lett. 2003 Oct 6;13(19):3301-3.

Segall Y, Quistad GB, Nomura DK, Casida JE. Arachidonylsulfonyl derivatives as cannabinoid CB1 receptor and fatty acid amide hydrolase inhibitors. Bioorg Med Chem Lett. 2003 Oct 6;13(19):3301-3.

Seifert J, Casida JE. Mechanisms of teratogenesis induced by organophosphorus and methylcarbamate insecticides. In Progress in Pesticide Biochemistry 1981. Hutson, D. H., andRoberts, T. R., Eds.) Vol. 1, pp 219-246, Wiley, New York.

Seifert J; Wilson BW. Solubilization of neuropathy target esterase and other phenyl valerate carboxylesterases from chicken embryonic brain by phospholipase A-2. Comparative Biochemistry and Physiology C Pharmacology Toxicology and Endocrinology, v. 108, n.3. 1994: 337-341.

Senanayake N, Karalliedde L. Neurotoxic effects of organophosphorus insecticides. An intermediate syndrome. N Engl J Med. 1987 Mar 26;316(13):761-3.

Senanayake N. Tri-cresyl phosphate neuropathy in Sri Lanka: a clinical and neurophysiological study with a three year follow up. J Neurol Neurosurg Psychiatry. 1981 Sep;44(9):775-80.

Sigrist CJ, de Castro E, Cerutti L, Cuche BA, Hulo N, Bridge A, Bougueleret L, Xenarios I. New and continuing developments at PROSITE. Nucleic Acids Res. 2013Jan;41(Database issue):D344-7. Lin D, Tabb

DL, Yates JR 3rd. Large-scale protein identification using mass spectrometry. Biochim Biophys Acta. 2003 Mar 21;1646(1-2):1-10.

Skrinjaric-Spoljar, M., Simeon, V., and Reiner, E. Spontaneous reactivation and aging of dimethylphosphorylated acetylcholinesterase and cholinesterase. Biochim. Biophys. Acta 1973. 315:363–369.

Slotkin TA, Tate CA, Ryde IT, Levin ED, Seidler FJ. Organophosphate insecticides target the serotonergic system in developing rat brain regions: disparate effects of diazinon and parathion at doses spanning the threshold for cholinesterase inhibition. Environ Health Perspect. 2006 Oct;114(10):1542-6.

Smith M.I., Elvove E., Uglarer P.J., Frazier W.H., Mallory G.E., (1930). Pharmacological and chemical studies of the cause of so-called ginger paralysis. Preliminary report. Public Health Rep. 45:1.703-1.716.

Sogorb and Vilanova. Detoxication of anticholinesterases pesticides In Anticholinesterases pesticides, 2006. (Satoh and Gupta., Ed.) pp121-133, Academic Press, San Diego.

Sogorb MA, García-Argüelles S, Carrera V, Vilanova E. Serum albumin is as efficient as paraxonase in the detoxication of paraoxon at toxicologically relevant concentrations. Chem Res Toxicol. 2008 Aug;21(8):1524-9.

Sogorb MA, González-González I, Pamies D, Vilanova E. An alternative in vitro method for detecting neuropathic compounds based on acetylcholinesterase inhibition and on inhibition and aging of neuropathy target esterase (NTE).Toxicol In Vitro. 2010 Apr;24(3):942-52.

Sogorb MA, Monroy A, Vilanova E., 1998. Chicken serum albumin hydrolyzes dichlorophenyl phosphoramidates by a mechanism based on transient phosphorylation. Chem Res Toxicol. 1998 Dec;11(12):1441-6.

Sogorb MA, Sánchez I, López-Rivadulla M, Céspedes V, Vilanova E., 1999. EDTA-resistant and sensitive phosphotriesterase activities associated with albumin and lipoproteins in rabbit serum. Drug Metab Dispos. 1999 Jan;27(1):53-9.

Sogorb MA, Vilanova E, Carrera V. Future applications of phosphotriesterases in the prophylaxis and treatment of organophosporus insecticide and nerve agent poisonings. Toxicol Lett. 2004 Jun 15;151(1):219-33.

Sogorb MA, Vilanova E, Quintanar JL, Viniegra S. Bovine chromaffin cells in culture show carboxylesterase activities sensitive to organophosphorus compounds. Int J Biochem Cell Biol. 1996 Sep;28(9):983-9

Sogorb MA, Vilanova E. Enzymes involved in the detoxification of organophosphorus, carbamate and pyrethroid insecticides through hydrolysis. Toxicol Lett. 2002 Mar 10;128(1-3):215-28.

Sogorb MA, Viniegra S, Reig JA, Vilanova E. Partial characterization of neuropathy target esterase and related phenyl valerate esterases from bovine adrenal medulla. J Biochem Toxicol. 1994 Jun;9(3):145-52.

Soreq H, Seidman S. Acetylcholinesterase--new roles for an old actor. Nat Rev Neurosci. 2001 Apr;2(4):294-302..

Spencer EY. Guide to the Chemicals Used in Crop Protection. 6th ed. Publication 1093, Research Institute, Agriculture Canada, Ottawa, Canada: Information Canada, 1973. 357

Srivastava AK, Gupta BN, Bihari V, Mathur N, Srivastava LP, Pangtey BS, Bharti RS, Kumar P. Clinical, biochemical and neurobehavioural studies of workers engaged in the manufacture of quinalphos. Food Chem Toxicol. 2000 Jan;38(1):65-9.

Sultatos LG. Mammalian toxicology of organophosphorus pesticides. J Toxicol Environ Health. 1994 Nov;43(3):271-89.

Sussman JL, Harel M, Frolow F, Oefner C, Goldman A, Toker L, Silman I. Atomic structure of acetylcholinesterase from Torpedo californica: a prototypicacetylcholine-binding protein. Science. 1991 Aug 23;253(5022):872-9.

Suzuki T, Morita H, Ono K, Maekawa K, Nagai R, Yazaki Y. Sarin poisoning in Tokyo subway. Lancet. 1995 Apr 15;345(8955):980.

Taylor, P. Anticholinesterase agents. In Goodman & Gilman's The Pharmacological Basis of Therapeutics, 2001. 10th ed. (Hardman, J. G., and Limbird, L. E., Eds.) pp 175-191, McGraw- Hill, New York.

Terry AV, Stone JD, Buccafusco JJ, Sickles DW, Sood A, Prendergast MA. Repeated exposures to subthreshold doses of chlorpyrifos in rats: hippocampal damage, impaired axonal transport, and deficits in spatial learning. J Pharmacol Exp Ther. 2003;305:375–384.

Thiermann H, Worek F, Kehe K. Limitations and challenges in treatment of acute chemical warfare agent poisoning. Chem Biol Interact. 2013 Sep 30. doi:pii:S0009-2797(13)00240-8.

Tormo N, Gimeno JR, Sogorb MA, Díaz-Alejo N, Vilanova E. Soluble and particulate organophosphorus neuropathy target esterase (NTE) in brain and sciatic nerve of the hen, cat, rat and chick. J. Neurochem 1993. 61:2164-2168

Travers PR .The results of intoxication with orthocresyl phosphate absorbed from contaminated cooking oil, as seen in 4,029 patients in Morocco.Proc R Soc Med. 1962 Jan;55:57-60.

Tsigelny I, Shindyalov IN, Bourne PE, Südhof TC, Taylor P. Common EF-hand motifs in cholinesterases and neuroligins suggest a role for Ca2+ binding in cell surface associations. Protein Sci. 2000 Jan;9(1):180-5.

Uniprot C. "Ongoing and future developments at the Universal Protein Resource". 2010. Nucleic Acids Research 39 (Database issue): D214–D219. doi:10.1093/nar/gkq1020. PMC 3013648. PMID 21051339. edit

USDA, Pesticide Data Program Annual Summary, US Department of Agriculture, 2005, World Health Organization, 1992)

Vicedo JL, Carrera V, Barril J, Vilanova E. Properties of partly preinhibited hen brain neuropathy target esterase. Chem Biol Interact. 1993. Jun;87(1-3):417-23.

Vilanova E, Barril J, Carrera V, Pellin MC. Soluble and particulate forms of the organophosphorus neuropathy target esterase in hen sciatic nerve. J Neurochem. 1990 Oct;55(4):1258-65.

Vilanova E, Barril J, Carrera V. Biochemical properties and possible toxicological significance of various forms of NTE. Chem Biol Interact. 1993. Jun;87(1-3):369-81.

Vilanova E, Escudero MA, Barril J. NTE soluble isoforms: new perspectives for targets of neuropathy inducers and promoters. Chem Biol Interact. 1999. May14;119-120:525-40.

Vilanova E, Johnson MK and Vicedo JL. The interaction of some unsubstituted phosphoramidates analogues of methamidophos (O,S-dimethyl phosphorothioamidate) with acetylcholinesterase and neuropathy target esterase of hen brain. Pestic. Biochem. Physiol. 1987. 28: 224-238

Vilanova E, Sogorb MA. The role of phosphotriesterases in the detoxication of organophosphorus compounds. Crit Rev Toxicol. 1999 Jan;29(1):21-57.

Vilanova E, Vicedo JL. Serum cholinesterase inhibitors in the commercial hexane impurities. Arch Toxicol. 1983 May;53(1):59-69.

Vilanova E. Peripheral nerve soluble esterases are spontaneously reactivated after inhibition by paraoxon: implications for a new definition of neuropathy esterase. Chem Biol. Interac. 1999. 119-120: 541-550

Wadia RS, Ichaporia RN, Karnik VM, Relwani GS, Grant KB. Cholinesterase levels in diazinon poisoning and after atropine treatment. J Indian Med Assoc. 1972 Sep 16;59(6):234-8. No abstract available.

Walter HE In: Bergmeyer HU (ed-in-chief), 1984. Bergmeyer J, Grassl M (eds) Methods of enzymatic analysis, 3rd edn, vol V. Verlag Chemie, Weinheim Deerfield Beach Basel, pp 270–277).

Webb EC. Enzyme nomenclature 1992: recommendations of the Nomenclature Committee of the International Union of Biochemistry and Molecular Biology on the nomenclature and classification of enzymes. San Diego: Published for the International Union of Biochemistry and Molecular Biology by Academic Press. ISBN 0-12-227164-5.

WHO, 1986a. Properties and analytical methods. En: Organophosphorus Insecticides: A general Introduction. World Health Organization, Geneva, pp:23-29.

WHO, 1986b. Effects on animals. In: Organophosphorus Insecticides: A general introduction. World Health Organization, Geneva, pp:56-96.

Winrow, C.J., Hemming, M.L., Allen, D.M., Quistad, G.B., Casida, J.E., Barlow, C., 2003. Loss of neuropathy target esterase in mice links organophosphate exposure to hyperactivity. Nat. Genet. 33 (4), 477–485. 723

Worek, F., Aurbek, N., Koller, M., Becker, C., Eyer, P., Thiermann, H., 2007. Kinetic analysis of reactivation and aging of human acetylcholinesterase inhibited by different phosphoramidates. Biochem. Pharmacol.

Worek, F., Thiermann, H., Szinicz, L., Eyer, P., 2004. Kinetic analysis of interactions between human acetylcholinesterase, structurally different organophosphorus compounds and oximes. Biochem. Pharmacol.68,2237–2248.

Xie W, Stribley JA, Chatonnet A, Wilder PJ, Rizzino A, McComb RD, Taylor P, Hinrichs SH, Lockridge O. Postnatal developmental delay and supersensitivity to organophosphate in gene-targeted mice lacking acetylcholinesterase. J Pharmacol Exp Ther. 2000 Jun;293(3):896-902.

Xie W, Stribley JA, Chatonnet A, Wilder PJ, Rizzino A, McComb RD, Taylor P, Hinrichs SH, Lockridge O. Postnatal developmental delay and supersensitivity to organophosphate in gene-targeted mice lacking acetylcholinesterase. J Pharmacol Exp Ther. 2000 Jun;293(3):896-902.

Wu and Chang in Molecular Toxicology of Neuropathy Target Esterase, 2006. (Gupta., Ed.) pp1614-187, Academic Press, San Diego.

Young JG, Eskenazi B, Gladstone EA, Bradman A, Pedersen L, Johnson C, Barr DB,Furlong CE, Holland NT. Association between in utero organophosphate pesticide exposure and abnormal reflexes in neonates. Neurotoxicology. 2005.

Lin D, Tabb DL, Yates JR 3rd. Large-scale protein identification using mass spectrometry. Biochim Biophys Acta. 2003 Mar 21;1646(1-2):1-10.

UNIVERSITAS
Miguel
Hernández